Optimisation de la digestion anaérobie de la vinasse de canne à sucre : modélisation et expérimentations à l'échelle du laboratoire

Hélène Caillet

Ecole doctorale n°542 : Sciences Technologies et Santé

Section 62 - Spécialité Génie des Procédés

Doctorat Université de La Réunion

THÈSE

pour l'obtention du grade de docteur délivré par l'Université de La Réunion

Présentée et soutenue publiquement par

HÉLÈNE CAILLET

Le 30 novembre 2019

Optimisation de la digestion anaérobie de la vinasse de canne à sucre : modélisation et expérimentations à l'échelle du laboratoire

Jury

Laetitia Adelard	Maître de Conférences HDR, Université de La Réunion	Directrice
Jean Castaing-Lasvignottes	Maître de Conférences HDR, Université de La Réunion	Co-directeur
Hélène Carrère	Directrice de recherche, INRA Narbonne	Présidente et Rapportrice
Kamal El Omari	Maître de Conférences HDR, Université de Pau	Rapporteur
Daniel Madyira	Maître de Conférences HDR, Université de Johannesbourg	Rapporteur
Alain Bastide	Professeur des Universités, Université de La Réunion	Examinateur
Lingai Luo	Professeure des Universités, Université de Nantes	Examinatrice
Thomas Petit	Professeur des Universités, Université de La Réunion	Examinateur

Titre : Optimisation de la digestion anaérobie de la vinasse de canne à sucre : modélisation et expérimentations à l'échelle du laboratoire

Résumé : La digestion anaérobie est un processus naturel où la matière organique est dégradée par des micro-organismes en l'absence d'oxygène générant ainsi un biogaz composé essentiellement de méthane et de dioxyde de carbone. L'industrialisation du procédé et l'intérêt de la production de biogaz en tant qu'énergie renouvelable, poussent au traitement de substrats variés. A l'échelle industrielle, l'agitation mécanique ou la recirculation doivent permettre la diffusion des micro-organismes vers la matière organique à traiter. Ces apports mécaniques constituent un poste important de consommation énergétique. En outre, le couplage et les interrelations entre agitation mécanique à l'intérieur des digesteurs et les transferts de masse ont été peu approchées en méthanisation. Ces recherches proposent une première contribution à cette problématique. Dans cette optique, nous étudions l'impact de l'agitation sur les rendements en biogaz de la digestion anaérobie de la vinasse brute en s'appuyant sur des expérimentations et des simulations numériques basés sur la mécanique des fluides (CFD). Les expérimentations menées portent sur la détermination du potentiel méthanogène de la vinasse ainsi que l'étude dans des conditions réelles à différentes intensités d'agitation, en suivant les propriétés physicochimiques du milieu au cours de la digestion. En parallèle, des simulations CFD sur les écoulements au sein d'un digesteur agité mécaniquement sont effectuées afin d'apporter des éléments de compréhension sur les écoulements. Ces travaux sont en accord avec l'étude bibliographique, notamment sur le fait que l'agitation mécanique ait un impact sur les rendements en biogaz.

Mots-clés : Digestion anaérobie, expérimentation, simulations CFD, hydrodynamique, agitation mécanique, vinasse.

Title: Optimisation of anaerobic digestion of sugar cane vinasse: modelling and experimentation at the laboratory scale

Abstract: Anaerobic digestion is a natural process where organic matter is degraded by microorganisms in the absence of oxygen, generating a biogas composed mainly of methane and carbon dioxide. The industrialisation of the process and the interest of biogas production as a renewable energy source led to the processing of a wide range of substrates. On an industrial scale, mechanical agitation or recirculation must allow the diffusion of microorganisms to the organic matter to be treated. These mechanical contributions are an important factor in energy consumption. In addition, the coupling and interrelationships between mechanical agitation inside the digesters and mass transfers have been poorly addressed in methanisation. This research proposes a first contribution to this problem. In this perspective, the impact of mechanical agitation on biogas yields of anaerobic digestion of raw vinasse using experiments is studied and numerical simulations based on fluid mechanics (CFD) are carried out. The experiments carried out concern the determination of the methanogenic potential of the vinasse as well as the study under real conditions at different agitation intensities, following the physicochemical properties of the medium during digestion. In parallel, CFD simulations on flows in a mechanically stirred digester are performed to provide understanding of flows inside. This work is in line with the literature review, particularly the fact that mechanical agitation has an impact on biogas yields.

Keywords: Anaerobic digestion, experimentation, CFD simulations, hydrodynamic, mechanical stirring, vinasse.

Remerciements

Mes sincères remerciements vont en premier lieu à Madame Laetitia ADELARD, Maître de Conférences Habilitée à Diriger la Recherche à l'Université de la Réunion, qui m'a encadrée durant ces trois années de thèse. Je vous remercie infiniment pour le temps que vous m'avez accordé ainsi que nos nombreuses discussions qui m'ont permis d'avancer tant bien sur le plan professionnel que personnel. Je suis extrêmement reconnaissante d'avoir réalisé cette thèse sous votre direction. Votre humanité, votre rigueur et votre niveau scientifique ont été pour moi les piliers de ce travail. La confiance que vous m'avez accordé tout au long ces travaux en me laissant l'autonomie dont j'avais besoin a également contribué de manière significative au travail produit. Je tiens aussi à remercier Monsieur Jean CASTAING-LASVIGNOTTES, Maître de Conférences Habilité à Diriger la Recherche, co-directeur de cette thèse, pour ses précieux conseils, tout particulièrement en phase de rédaction et pour la préparation de la soutenance. Mes remerciements vont aussi à Monsieur Vincent FONTAINE, Maître de Conférences à l'Université de La Réunion, encadrant de cette thèse pour m'avoir accordé du temps et m'avoir conseillé sur la partie numérique de ces travaux. Je remercie également Monsieur Alain BASTIDE, Professeur à l'Université de La Réunion, pour sa confiance, sa bienveillance, son temps et son aide précieuse sur les aspects numériques de ces travaux ; et grâce à qui j'ai pu continuellement me dépasser et énormément apprendre.

J'adresse mes sincères remerciements à Madame Hélène CARRERE, Directrice de Recherche à l'Institut National de la Recherche Agronomique (INRA), à Monsieur Daniel MADYIRA, Enseignant Chercheur à l'Université de Johannesburg en Afrique du Sud ainsi qu'à Kamal EL OMARI, Maître de Conférences Habilité à Diriger la Recherche à l'Université de Pau, de l'honneur qu'ils m'ont fait en acceptant d'être rapporteurs de cette thèse. Je vous remercie de vous êtes déplacés pour ma soutenance ainsi que pour vos précieux conseils. J'exprime ma gratitude à Madame Lingai LUO, Professeure à l'Université de Nantes, Monsieur Alain BASTIDE et Monsieur Thomas PETIT, Professeurs à l'Université de La Réunion, qui ont bien voulu être examinateurs de ces travaux.

Je remercie Madame Esther AKINLABI, Professeure à l'Université de Johannesburg et Monsieur Daniel MADYIRA pour tous nos échanges et moments partagés enrichissant dans le cadre du projet PROTEA ainsi que nos déplacements

respectifs à l'Université de La Réunion et de Johannesburg. Je remercie également Monsieur Madushele NKOSINATHI, enseignant chercheur à l'Université de Johannesburg et Monsieur Samson MASEBINU, aujourd'hui jeune docteur pour leur accueil et le temps qu'ils m'ont accordé. Je remercie aussi Paul GUILLOU, doctorant du Laboratoire PIMENT avec qui j'ai partagé ce déplacement pour ta présence et tes nombreux conseils. Je vous remercie tous pour avoir pris sur votre temps pour me faire visiter la ville de Johannesburg.

Je remercie Monsieur Teddy BOYER Directeur et Monsieur Patrick MARIMOUTOU Technicien de la Distillerie Rivière du Mât pour avoir fourni la matière première nécessaire à l'ensemble des travaux expérimentaux effectués au cours de cette thèse et également pour nos échanges et votre gentillesse.

Je remercie la Région Réunion pour avoir financé cette thèse ainsi que le Laboratoire PIMENT de l'Université de La Réunion, où j'ai mené ces travaux.

Je remercie également l'équipe administrative avec qui j'ai beaucoup interagi ces dernières années. Je pense à Vanessa DIJOUX, gestionnaire du Laboratoire PIMENT, Fabienne ETHEVE, gestionnaire du département SBE, Patricia FONTAINE, gestionnaire du département Génie Civil de l'IUT, Maria MOSSADAQ également appelée la « maman des doctorants », secrétaire de l'Ecole Doctorale, Jessica VELLAIDON, gestionnaire des Ecoles Doctorales au Pôle Recherche et enfin Marion LE LAY et Fabien HAZERA, membres de Cellule Valorisation du Pôle Recherche.

Je remercie Jérôme VIGNERON, technicien au Laboratoire PIMENT, pour son aide et son avis technique. Je suis également très reconnaissante envers Gwendoline HOAREAU, Véronique CHARI, Ingrid LEBRETON et Eloïse du département Génie Biologique de l'IUT pour leurs conseils avisés au niveau expérimental et bien entendu les nombreux moments d'échanges et de rires. Je remercie également Steven MENARD du département SBE de l'Université du Tampon avec qui j'ai eu l'occasion de travailler dans le cadre de mes activités d'enseignement mais aussi pour nos discussions.

Mes remerciements vont également aux enseignants qui m'ont fait confiance et accompagné pour dispenser des TD et TP et participé aux soutenances au département SBE et à l'IUT. Je remercie donc Laetitia ADELARD, Hubert AMBROIS, Alain BASTIDE, Harry BOYER, Éric FOCK, Vincent FONTAINE, Bruno MALET-

DAMOUR, Olivier MARC, Dominique MORAU, Isabelle NALLET et Jean-Philippe PRAENE.

Je remercie les doctorants de l'Université de La Réunion, sans qui, ces trois années n'auraient pas eu le même goût. Je remercie notamment Sébastien, Jonathan, Stéphane et Mélissa, avec qui nous avons représenté les doctorants à l'Ecole Doctorale pendant deux ans. Je vous remercie pour votre implication sans faille et nos moments d'échanges enrichissants. J'en profite pour remercier Monsieur Christian LEFEBVRE-D'HELLENCOURT et Monsieur Alain BASTIDE, Professeurs à l'Université de La Réunion et Directeurs de l'Ecole Doctorale STS, pour les discussions et l'accompagnement dont nous avons bénéficié en tant que représentants des doctorants. Mes remerciements vont tout naturellement aux doctorants du Laboratoire PIMENT avec qui j'ai tissé des liens particuliers. Je retiens énormément de bons moments de partage, notamment culinaires ou encore autour de sujets d'actualités au sein du Laboratoire. Je suis également très heureuse de la cohésion de groupe dont nous avons bénéficié. C'était un honneur d'avoir pu vous représenter en tant que Présidente du Conseil des Doctorants du Laboratoire PIMENT, je vous suis très reconnaissante de votre confiance et votre bienveillance. Mes sincères remerciements vont encore une fois à Monsieur Alain BASTIDE, mais aussi à Mathieu DAVID, successivement directeurs du Laboratoire et à Monsieur Jean CASTAING-LASVIGNOTTES, codirecteur du Laboratoire, pour les discussions très intéressantes et le soutien sur les projets que j'ai souhaité mener pour les doctorants. Je pense tout particulièrement à l'événement « The RED² PIMENT » qui vise l'insertion professionnelle des doctorants et j'en profite pour remercier Maïté BERNHARD pour son aide précieuse ainsi que tous ceux qui se sont impliqués. Je remercie encore une fois ma directrice de thèse Laetitia ADELARD pour m'avoir laissé m'investir sur des projets autres que mes travaux de thèse, qui ont fortement contribué et mon épanouissement et mon intégration au sein du Laboratoire et à l'Université.

Je remercie tout particulièrement Eve et Leslie, doctorantes et très chères amies, pour leur soutien et amitié et nos innombrables moments de complicité qui nous ont permis de se changer les idées. Je remercie également Justie pour son soutien moral et sa bonne humeur. Mes remerciements vont aussi à Edouard qui a pris une place très particulière dans ma vie pendant cette thèse. Je le remercie pour sa bonne humeur continuelle et son soutien sans faille. Je remercie également mes proches, amis et famille,

qui me soutiennent et croient en moi depuis de nombreuses années dans tous mes projets. Je pense principalement à ma meilleure amie Shameema, qui malgré la distance est plus que présente pour me rassurer et m'encourager dans les moments de doutes. Je remercie mes frères et sœurs qui me supportent depuis ma naissance en m'aimant telle que je suis. Enfin, je remercie mes parents pour tout ce que vous faites et avez fait pour moi à tous les niveaux. Chaque pas que je fais est possible grâce à vous, à l'éducation et à l'amour que vous m'avez donné quotidiennement et aux valeurs que vous m'avez inculqué. Vous m'avez porté jusqu'à aujourd'hui et continuez encore. Je vous suis infiniment reconnaissante.

Ce doctorat m'aura certes permis de produire ce travail mais surtout d'apprendre à me connaître et de murir grâce à toutes les personnes, qui de près ou de loin, ont en quelque sorte fait partie de mon parcours de thèse et qui ont fait que ces trois années resteront dans ma mémoire.

Table des matières

Liste des figures

Introduction générale

Chapitre I

Chapitre III

Chapitre IV

Chapitre V

Chapitre VI

Chapitre VII

Liste des tableaux

Introduction générale

Chapitre III

Chapitre IV

Chapitre V

Chapitre VI

Introduction générale

Cette thèse, financée par la Région Réunion, a été menée au sein du Laboratoire PIMENT (Physique et Ingénierie Mathématique pour l'Energie, l'environnemeNt et le bâtimenT) rattaché à l'Université de La Réunion (France). Ces travaux ont porté sur l'étude de la digestion anaérobie de la vinasse de canne à sucre, plus communément appelée méthanisation. La méthanisation permet de répondre à deux enjeux majeurs qui sont la production d'énergie renouvelable et le traitement des déchets organiques. Nous donc allons dans un premier temps présenter le contexte énergétique régional puis dans un deuxième le traitement des déchets à La Réunion. Ce qui nous amènera dans un troisième temps au contexte scientifique. Et enfin dans un quatrième temps nous résumerons l'organisation du manuscrit.

Le contexte énergétique régional :

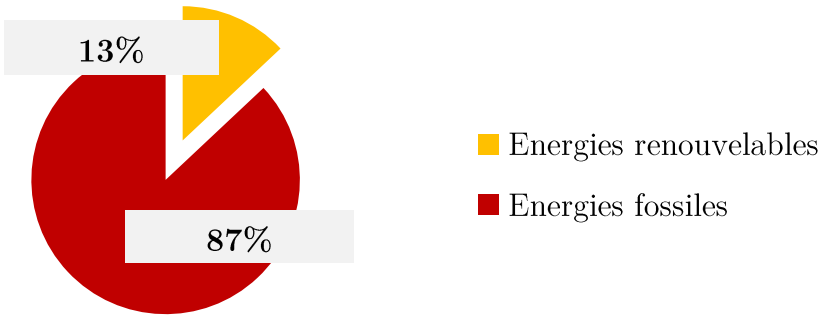

Figure 1: Consommation d'énergie primaire en 2017 à La Réunion (SPL Energies Réunion)

A La Réunion, en termes de consommation d'énergie primaire, les énergies fossiles représentent 87 % des consommations avec le pétrole, le charbon et le butant. En effet, ce territoire insulaire ne dispose pas de centrale nucléaire ainsi ce dernier est fortement dépendant aux énergies fossiles importées. Ceci est un obstacle important pour atteindre une autosuffisance énergétique. Quant aux énergies renouvelables, nous retrouvons l'énergie produite à partir de la combustion de la bagasse (7 %), l'hydraulique (2,5 %),

le solaire PV (panneaux photovoltaïques) et l'éolien (1,6 %), le solaire thermique (1,5 %), le biogaz (0,3 %) et enfin les huiles usagées (0,1 %). Nous constatons que la part d'énergie renouvelable est faible mais les sources d'énergie sont variées. Comme énoncé précédemment, nous travaillerons sur la production de biogaz qui est aujourd'hui peu exploitée mais ayant un fort potentiel de développement notamment par l'utilisation de déchets organiques en intrants.

Le traitement des déchets à La Réunion :

Le gisement réunionnais total représente 4,3 Mt. Nous avons notamment les déchets inertes du BTP (2 Mt), les déchets organiques ou non des activités économiques (DAE) (1,8 Mt) et les déchets ménagers et assimilés (DMA) (0,5 Mt). La production moyenne de DMA est de 618 kg/hab/an.

Les déchets produits peuvent être valorisés selon les voies de traitement choisies. La valorisation organique des déchets consiste à les utiliser en tant qu'amendement organiques sous forme de compost, de digestat ou de déchets organiques transformés par voie biologique. La valorisation énergétique est l'exploitation du gisement d'énergie contenu dans les déchets. Enfin, la valorisation matière est l'utilisation des déchets ou d'une fraction des déchets en remplacement d'un élément ou d'un matériau.

A La Réunion, il y a deux centres d'enfouissement situés à Pierrefonds et à Bel Air, dix-huit stations d'épuration ainsi que trois distilleries industrielles (Savanna, Rivière du Mât et Isauthier). Parmi ces installations, du biogaz est capté au niveau des centres d'enfouissement, la station d'épuration de Grand Prado est équipée d'un digesteur de boues et la distillerie Rivière du Mât possède un digesteur de vinasses. La production totale de biogaz est de 4,2 ktep.

La **Figures 2** présente la répartition des modes de traitement des DAE en 2015 (Espélia). Pour cette catégorie de déchets, 61 % sont déchets sont valorisés organiquement, 36 % sont valorisés énergétiquement et seulement 6 % sont éliminés.

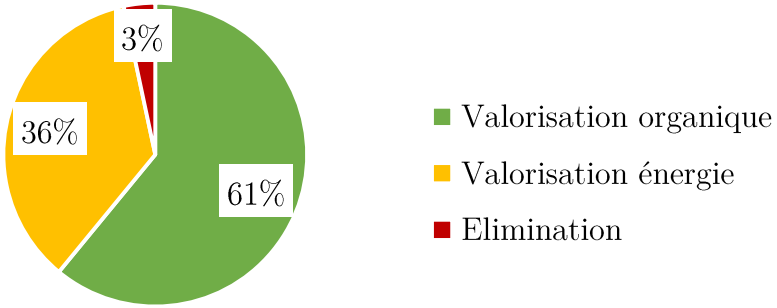

Figure 2: Répartition des modes de traitement des DAE en 2015

La **Figures 3** présente la répartition des modes de traitement des DMA en 2015 (Espélia). 20 % des déchets sont valorisés organiquement, la valorisation matière représente 13 % et la valorisation énergie seulement 1 %. Une grande proportion des déchets sont enfouis avec 66 % du gisement. La fraction biodégradable des déchets enfouis est naturellement méthanisée. Il en résulte la production des biogaz composé essentiellement de méthane et de dioxyde de carbone. A La Réunion, ce biogaz est capté afin de produire de l'énergie, cependant des pertes subsistent et la production n'est pas optimisée.

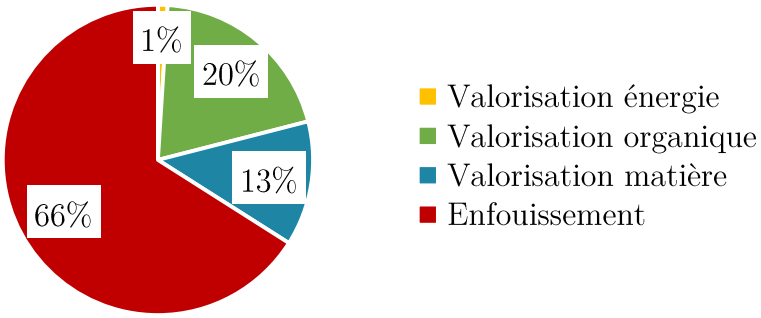

Figure 3: Répartition des modes de traitement des DMA en 2015

En France, d'après l'ADEME (2011), 2,6 % des émissions des gaz à effet de serre (GES), soit 12,9 million $t_{eq,CO2}$ sont attribués au traitement des déchets (hors valorisation énergétique). Le méthane non capté émis par les installations de stockage, naturellement produit par le processus de la méthanisation, représente la principale source d'émission (ADEME). La digestion anaérobie est un processus naturel au cours duquel la matière organique est dégradée par quatre groupes de micro-organismes en l'absence d'oxygène. En fin de réactions bio-physico-chimiques, les produits obtenus sont un biogaz ainsi qu'un digestat pouvant être valorisé en amendement organique. L'industrialisation de la

méthanisation et l'intérêt de la production de biogaz en tant qu'énergie renouvelable, poussent au traitement de substrats variés ayant des comportements physiques différents. De surcroît, les déchets organiques sont une ressource inépuisable pour la digestion anaérobie. Le tonnage de biodéchets produits par les gros producteurs est conséquent, doit réglementairement être traité pour éviter l'enfouissement en ISDND (Installations de Stockage de Déchets Non Dangereux) (articles L. 541-21-1 et R. 543-225 du code de l'environnement, Arrêté du 12 juillet 2011 fixant les seuils définis à l'article R. 543-225 du code de l'environnement). Nous retrouvons les résidus agricoles, les boues de stations d'épuration urbaines (STEP), les eaux usées, les déchets verts et la Fraction Fermentescible des Ordures Ménagères (FFOM). Il est donc indispensable d'adapter la stratégie de l'unité de méthanisation selon les déchets traités pour optimiser les rendements. Les paramètres industriels influents sont notamment la température, le pH, le brassage du milieu, la nature du substrat organique, le chargement organique et le temps de séjour hydraulique du digesteur. Compte-tenu des déchets pouvant être traités par méthanisation, nous observons une augmentation de l'intérêt de la digestion par voie sèche.

Dans ce travail, nous nous concentrons sur la digestion anaérobie de la vinasse de canne à sucre. En effet, la superficie consacrée à la culture cannière (22 664 ha) représente environ 52,94 % de la superficie agricole à La Réunion (DAAF Réunion, 2015). En 2015, 1 896 656 tonnes de canne ont été produites, générant ainsi 80 000 Hectolitres d'Alcool Pur (DAAF Réunion). Les vinasses de canne à sucre sont les eaux résiduaires générées lors de la phase de distillation. Les vinasses sont des déchets liquides, récalcitrants (difficilement biodégradables) et ayant une forte teneur en matières organiques. Il y a donc une nécessité de les traiter afin de les dépolluer avant leur rejet dans le milieu naturel. La méthanisation est donc une solution conciliant les enjeux : énergétique et le traitement de ce déchet. C'est d'ailleurs pour cette solution que la distillerie Rivière du Mât a opté. L'énergie produite est directement utilisée par le site. Nous avons ainsi une valorisation énergétique avec la production de biogaz et la valorisation organique avec l'amendement organique. Nous explicitons dans la partie suivante le contexte scientifique de ces travaux.

Le contexte scientifique :

Dans ce contexte, le laboratoire PIMENT a déjà encadré quatre thèses portant sur l'analyse du gisement de déchets sur La Réunion (Hatik, 2015), et la méthanisation de déchets tels que les boues de STEP (Morau, 2006), les déchets fermiers en cométhanisation (Rakotoniaina, 2012), et la recherche de prétraitements optimisés pour la méthanisation de biomasse récalcitrante comme les vinasses issues de l'industrie sucrière (Chupa Tostain, 2016) [1]. Une cinquième thèse est actuellement en cours sur la problématique de la méthanisation par voie sèche des déchets ménagers (Lebon, 2019). La suite logique de ces recherches est l'optimisation de la codigestion des déchets et l'optimisation de la digestion anaérobie. La thèse présentée apporte ainsi une contribution à cette problématique.

Le processus de digestion anaérobie est gouverné par cinq réactions biologiques qui sont : l'hydrolyse, l'acidogenèse, l'acétogenèse, l'homoacétogenèse et enfin la méthanogenèse. Le processus est détaillé sur la **Figure 4**. Chaque réaction a lieu sous l'action d'un groupe de micro-organismes spécifiques. Il est ainsi indispensable qu'il y ait une population bactérienne diversifiée et suffisante pour permettre la production du biogaz.

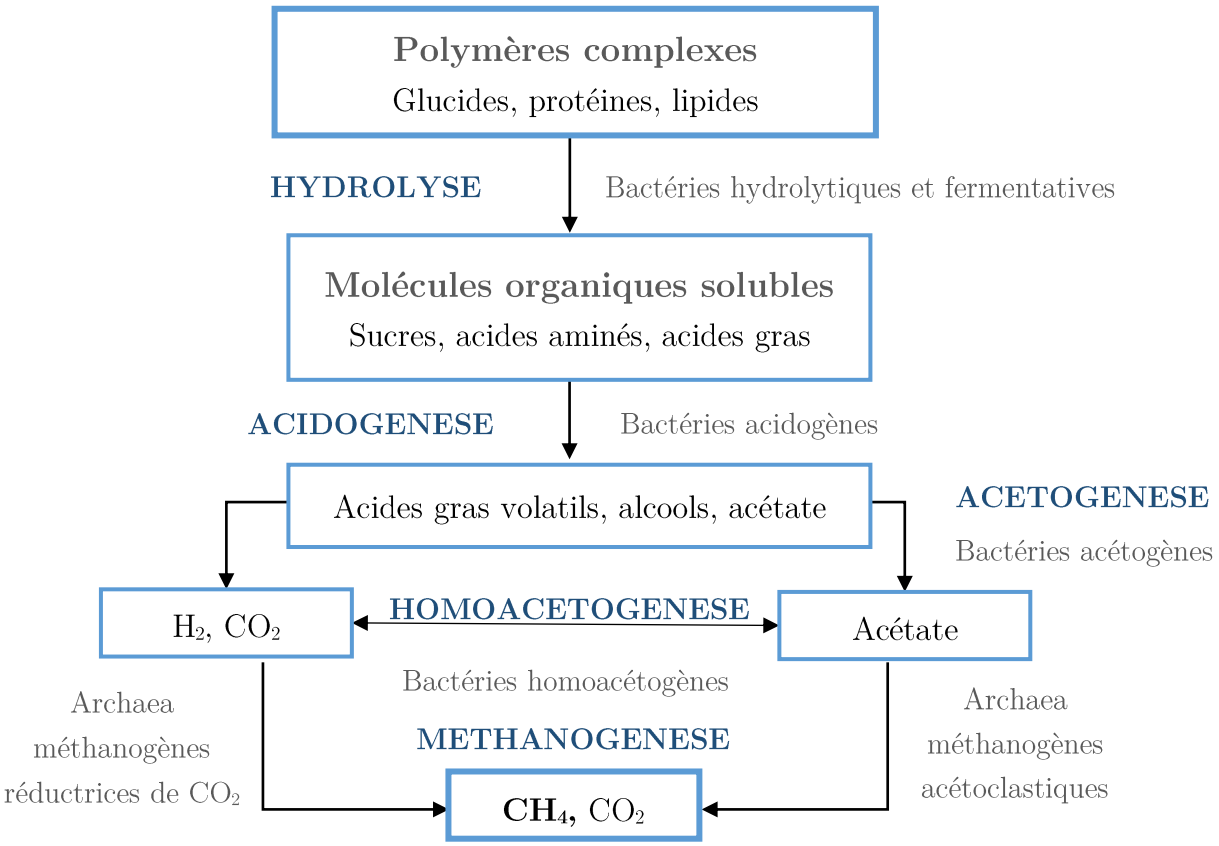

Figure 4: La digestion anaérobie

L'agitation du milieu facilite le contact entre les bactéries, les enzymes et les substrats à digérer, empêchant l'accumulation de substrats et intermédiaires dans le milieu et garantissant des conditions homogènes [2]. En effet, l'accumulation de produits intermédiaires conduit à des inhibitions et des zones mortes existent dans le cas d'un brassage insuffisant. Les inhibitions du milieu sont principalement dues à l'apparition de zones acides (acidose), l'excès d'ammoniac (alcalose), le sulfure d'hydrogène, les métaux lourds et les antibiotiques. Par ailleurs, les bactéries acétogènes et archaea méthanogènes vivant fixées les unes aux autres, une agitation trop vigoureuse risquerait de détruire ce lien d'où la recommandation d'un brassage lent [3]. L'agitation du milieu est ainsi une problématique majeure pour la digestion anaérobie. Il faut garantir le contact entre les micro-organismes et les substrats et homogénéiser le milieu sans déstabiliser les réactions bio-physico-chimiques. La question se pose autant dans le cas de la digestion par voie humide que par voie sèche. La compréhension des écoulements au sein des digesteurs pour ces deux cas de digestion est un atout pour optimiser l'agitation du milieu. La

Figure 5 décrit de manière qualitative les effets de la vitesse d'écoulement sur le rendement en biogaz.

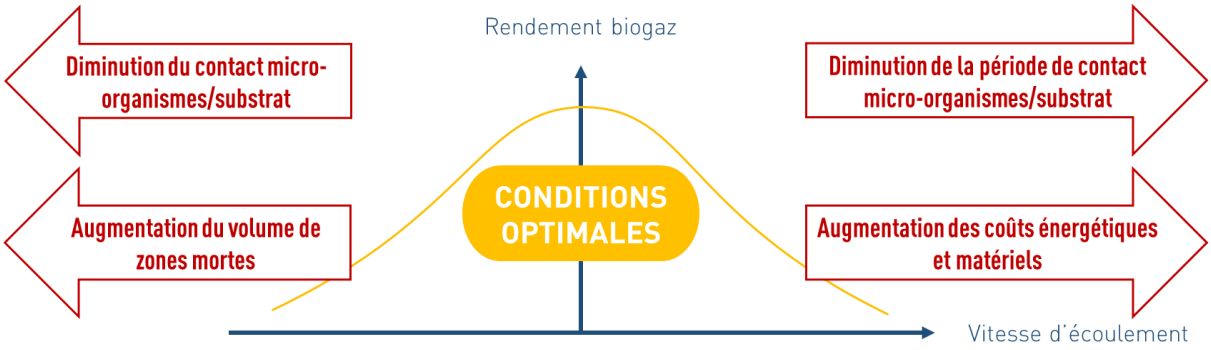

Figure 5: Description qualitative des effets de la vitesse d'écoulement sur le rendement en biogaz

D'un point de vue modélisation, le modèle de la digestion anaérobie n°1 (ADM1) prend en compte la composition des substrats, la cinétique des réactions bio-physico-chimiques ainsi que les réactions d'inhibition. Cependant le mode d'agitation (fréquence et intensité) n'est pas pris en compte dans ce modèle. Or il a été prouvé expérimentalement que ce paramètre influe largement sur la digestion anaérobie [4, 5]. En effet une agitation adaptée permet de conserver les centres méthanogènes lors du lancement d'un digesteur mais aussi leur extension au sein du digesteur [6]. De plus, l'agitation optimale dépend également de la réaction limitante [6]. En outre, l'évaluation de l'impact de l'intensité d'agitation montre l'existence d'un seuil de gradient de vitesse au-dessus duquel un mélange accru devient contre-productif induisant la diminution de la production de biogaz [7]. De même, d'autres expérimentations montrent que les conditions de mélange ont une incidence sur la production de méthane due à l'accumulation d'acides gras volatils (AGV) [8]. Tous ces aspects, y compris le besoin croissant de simulations d'écoulement précises, justifient le recours à la CFD (Computational Fluid Dynamics) [8]. En effet, ces simulations permettent de caractériser les écoulements au sein des digesteurs en prenant en compte le comportement du milieu de digestion, notamment grâce aux modèles rhéologiques. Dans cette optique, la vitesse d'agitation optimale, pour le lancement d'un digesteur, peut être déterminée en fonction du volume de zones mortes [9]. En comparant les rendements en biogaz et l'homogénéisation du milieu grâce à la simulation des écoulements pour différentes

intensités d'agitation, il est possible de déterminer l'agitation nécessaire pour homogénéiser le milieu [10]. Ces résultats réaffirment l'existence d'une intensité d'agitation optimale pour la production de méthane [10]. L'agitation mécanique a donc un effet non négligeable sur les rendements de la méthanisation. De plus, le brassage est nécessaire pour homogénéiser le milieu, favoriser les transferts de chaleur, empêcher la stratification, maintenir les particules en suspension et réduire le volume des zones mortes. L'agitation du milieu doit être adaptée en fonction du taux de matière sèche du substrat [11] qui est lié à la viscosité. En effet, les phénomènes de diffusion sont fortement réduits dans le cas de la digestion par voie sèche car la viscosité de ces substrats est plus importante et la teneur en eau, qui favorise les écoulements, est réduite [11].

La **Figure 6** présente les principales entrées et sorties des modèles de la digestion anaérobie et des modèles locaux basés sur la mécanique des fluides. La modélisation des écoulements est un outil adapté pour l'optimisation de la digestion par voie liquide et par voie sèche. Elle permet d'avoir une compréhension fine et locale de la digestion anaérobie contrairement aux modèles biochimiques globaux. En effet, les entrées des modèles biochimiques sont la composition et les propriétés physico-chimiques des effluents ainsi que les constantes cinétiques et d'inhibitions et les sorties sont le volume est la composition du biogaz avec les propriétés physico-chimiques du milieu. Tandis que les entrées des modèles CFD sont les données permettant de décrire le comportement rhéologique des substrats (par exemple la viscosité) ainsi que les conditions physiques, et les sorties sont le champ de vitesse, le champ de température ou encore les zones mortes et turbulente. Nous voyons ainsi que les résultats obtenus par les modèles CFD sont

locaux et permettent d'avoir une description précise alors que les résultats des modèles de digestion anaérobie sont globaux.

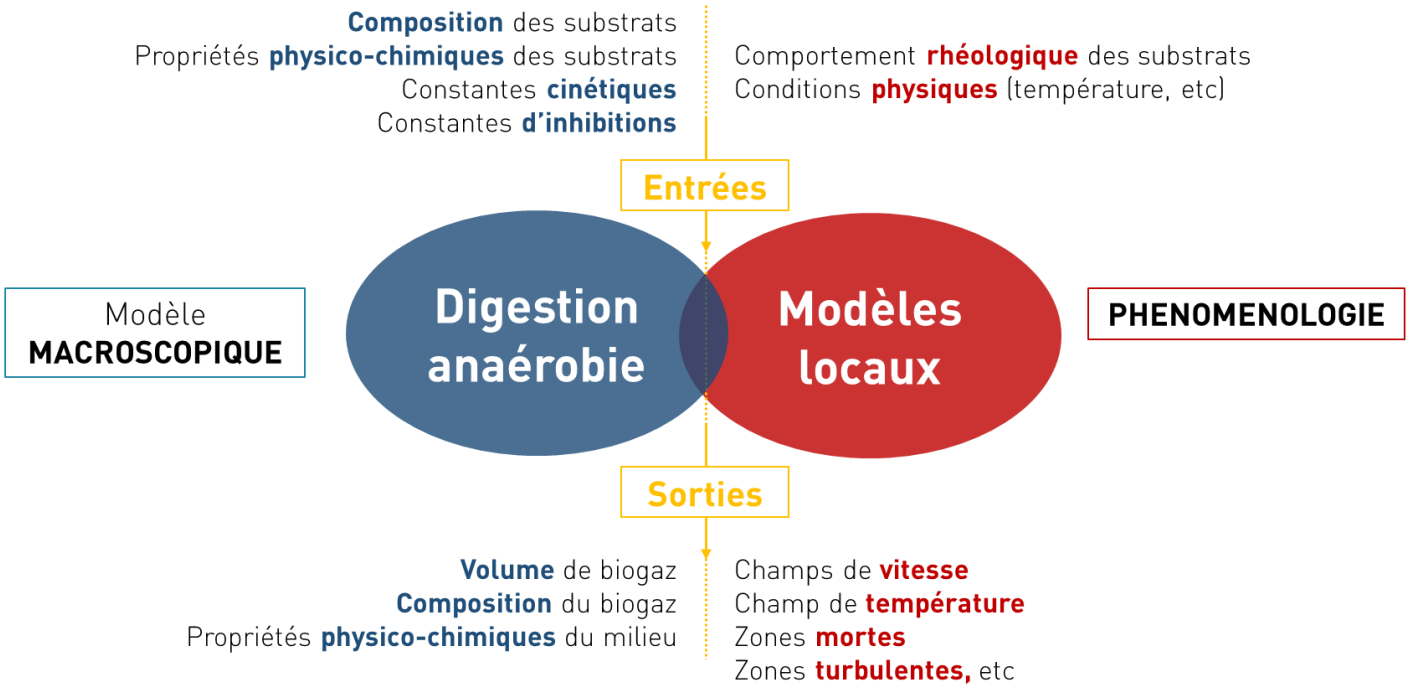

Figure 6: Les entrées et sorties des modèles de la digestion anaérobie et locaux

De plus, selon le ou les déchets à traiter, la digestion peut se dérouler aussi bien par voie liquide que par voie sèche. Cependant, la teneur en eau et la viscosité corrélées aux écoulements au sein des digesteurs ne sont pas pris en compte dans les modèles biochimiques classiques. En résumé, la viscosité impacte les écoulements, qui à leur tour ont un effet sur les rendements du processus. Par conséquent, nous nous proposons dans ce travail, d'évaluer l'impact de l'agitation mécanique sur les rendements en biogaz, expérimentalement et en ayant recours à la modélisation basée sur la dynamique des fluides numérique (CFD).

Ces travaux de thèse consistent dans un premier temps à confirmer ou infirmer que l'agitation mécanique impacte les rendements de la digestion anaérobie de la vinasse qui est un déchet liquide présentant des suspensions solides. Dans un second temps, nous chercherons à expliquer cet impact par la compréhension des écoulements. Nous utilisons le dispositif AMPTS pour l'étude du potentiel méthanogène de la vinasse (conditions optimales) et un digesteur pilote de 16 L pour celle de la méthanisation de ce déchet à une plus grande échelle dans des conditions réelles. Après avoir lancé le pilote en

respectant un protocole précis, nous testons de manière successive différentes intensités d'agitation mécanique afin d'évaluer son impact sur les rendements en biogaz, sur les propriétés physicochimiques du milieu ainsi que sur l'homogénéisation du milieu en effectuant des mesures en différents points du pilote. En parallèle, nous réalisons des simulations numériques basées sur la mécanique des fluides d'un milieu monophasé agité mécaniquement. Les simulations à différentes intensités d'agitation permettent d'obtenir le taux d'homogénéisation du milieu ainsi que le pourcentage de zones mortes. Les simulations CFD apportent des informations supplémentaires, à un niveau local, permettant d'apporter des connaissances supplémentaires sur l'impact de l'agitation sur les rendements en biogaz. L'agitation du milieu est en effet nécessaire pour l'homogénéiser, cependant, une agitation excessive pourrait inhiber le processus en limitant la durée de contact entre le substrat et les micro-organismes ou encore en déstabilisant les centres de la méthanogénèse. C'est pour cela qu'il est crucial de comprendre d'une part l'impact de l'agitation à la fois sur l'homogénéisation du milieu grâce aux simulations CFD et aux mesures expérimentales locales des propriétés physicochimiques du milieu ; et d'autre part l'impact de l'agitation sur les rendements en biogaz du processus. Ces études couplées permettent de déterminer le degré d'homogénéisation optimal et ainsi le champ de vitesse optimal pour la digestion anaérobie. Ces conclusions sont bien évidemment valables uniquement dans le cas de la vinasse de canne à sucre.

Organisation du manuscrit :

Le manuscrit de thèse est divisé en sept chapitres. Le premier chapitre bibliographique ainsi que le chapitre sur les conclusions et perspectives générales de la thèse sont rédigés en français. Les autres chapitres sont rédigés en anglais sous forme d'articles scientifiques. Afin de faciliter la lecture du manuscrit, chaque chapitre en anglais comporte un en-tête en français afin d'introduire les articles. Nous récapitulons sur la **Figure 7** l'organisation et le contenu du manuscrit.

Nous exposons dans les **chapitres I et II** la synthèse bibliographique du projet de thèse. Le **chapitre I** aborde le contexte scientifique général avec les technologies de digesteurs, les équations de réaction de la méthanisation, les équations de conservation, le modèle de RANS, les modèles de turbulence et les modèles rhéologiques. Le **chapitre II** (format article) porte sur la rhéologie des substrats de digestion et les lois de comportements ; les modèles biochimiques ; ainsi que les modèles basés sur la mécanique des fluides. Cet article sur la revue de littérature a été soumis au journal « Renewable & Sustainable Energy Reviews » (juillet 2019). La bibliographie relative à l'étude expérimentale est explicitée dans les chapitres concernés.

Nous présentons dans les **chapitres III, IV et V** l'étude expérimentale de la digestion anaérobie de la vinasse brute en régime mésophile. Dans le **chapitre III**, nous présentons l'étude pour la détermination du potentiel méthanogène de la vinasse brute. Ces travaux ont été présentés lors du congrès SMPM en Afrique du Sud (mars 2019). Le **chapitre IV** expose le lancement du pilote expérimental avec le protocole et le suivi des paramètres physicochimiques du milieu de digestion. Le chargement organique est augmenté progressivement et la stabilisation des propriétés physicochimiques du milieu a permis de conclure sur la durée de la phase de lancement. Ces travaux ont été présentés au congrès ICEECC à l'île-Maurice (juillet 2019) et l'article est également soumis au journal « Waste and Biomass Valorization » (juillet 2019). Enfin, le **chapitre V** concerne l'étude de l'impact de l'agitation mécanique sur les rendements de la digestion anaérobie de la vinasse brute et les propriétés physicochimiques du milieu de digestion. Les résultats expérimentaux sont produits sur une durée d'étude de 6 mois au cours desquels l'agitation mécanique a varié de 20 à 60rpm. Cet article sera soumis à la suite de l'article précédent. Les travaux de la partie 2 ont mis en exergue l'impact non négligeable de l'agitation sur

les rendements. Ainsi, il est nécessaire d'avoir une analyse fine de la digestion anaérobie dans les modèles pour comprendre l'impact de l'hydrodynamique sur les cinétiques de réactions afin d'optimiser le procédé. Les modèles biochimiques étant des modèles globaux, nous ne pouvons pas prendre en compte ces effets de manière précise.

Ainsi, le **chapitre VI** présente les premiers travaux sur la simulation des écoulements basée sur la mécanique des fluides. Ce chapitre comporte des éléments d'un article présenté au congrès WasteEng à Prague (2018) dont l'objectif était de montrer l'importance de la prise en compte de l'hydrodynamique du milieu de digestion dans les modèles ainsi que l'état de l'art sur les objectifs des modèles CFD. Ensuite les premiers résultats des simulations numériques d'un digesteur agité mécaniquement dans le cas d'un fluide Newtonien. Ces résultats seront valorisés ultérieurement.

Enfin, le manuscrit est clôt avec le **chapitre VII**. Dans un premier temps, les apports et résultats des études expérimentales et numériques sont discutés, puis les conclusions et perspectives générales de ces travaux de thèse sont exposées.

Comment **améliorer** la digestion anaérobie par une meilleure maîtrise de l'**hydrodynamique** ?

CHAPITRE I et II :

Etat de l'art sur la digestion anaérobie, les digesteurs anaérobies, la rhéologie des substrats, les modèles de cinétiques et la modélisation des écoulements.

Approche expérimentale

CHAPITRE III :

Détermination du **potentiel méthanogène** de la vinasse en adaptant le protocole à la vinasse, qui est un substrat récalcitrant.

CHAPITRE IV :

Etude du **démarrage du pilote** du laboratoire et suivi de la digestion anaérobie de la vinasse en régime mésophile.

CHAPITRE V :

Etude en pilote de laboratoire de **l'impact de l'intensité d'agitation** sur la production de biogaz et les propriétés physico-chimiques du milieu lors de la digestion anaérobie de la vinasse.

Les intensités d'agitation testées sont : 20, 30, 40, 50 et 60 tr/min.

Analyses du milieu de digestion avant et après agitation à différentes profondeurs du pilote.

Dynamique des fluides numérique (CFD)

CHAPITRE VI :

Compréhension locale du milieu de digestion.

Mise en œuvre d'un maillage adapté à l'étude de l'agitation mécanique.

Modélisation et simulations des écoulements au sein d'un digesteur agité mécaniquement (modèle RANS monophasé et fluide Newtonien) : 20, 40, 60 et 100 tr/min.

CHAPITRE VII :

Discussions des résultats, conclusion et perspectives générales de la thèse

Figure 7: Schéma récapitulatif du travail de thèse

Chapitre I

La digestion anaérobie et la modélisation des écoulements

Dans ce chapitre, nous allons exposer les différents éléments bibliographiques nécessaires à la compréhension du travail mené. Une première partie est dédiée à la digestion anaérobie et une deuxième partie à la modélisation des écoulements.

Tout d'abord, il est important d'expliquer le processus complexe de la digestion anaérobie. Il découle de cette complexité l'importance de caractériser les substrats (intrants) destinés à la méthanisation mais aussi le milieu de digestion afin de contrôler le procédé, notamment à l'échelle industrielle. A cette échelle, différentes technologies ont vu le jour, nous explicitons donc leurs caractéristiques. Enfin, la modélisation de la digestion anaérobie a été l'objet de nombreux travaux, nous présentons donc dans ce chapitre le modèle global de la digestion anaérobie (ADM1).

Les écoulements au sein des digesteurs anaérobies peut causer des inhibitions et est au sein des réflexions dans le développement des technologies de méthanisation. Nous utilisons dans cette thèse le modèle de RANS (Range Averaged Navier Stokes) qui signifie en français, les équations de Navier-Stokes moyennées. Pour cela, nous présentons les lois de comportement, les équations de conservation, les équations de Navier-Stokes, les modèles de turbulence (k-epsilon et k-omega). Et enfin, nous explicitons la décomposition de Reynolds qui nous permet d'écrire le modèle de RANS.

I-1. La digestion anaérobie

I-1.1. Le processus de la digestion anaérobie

La digestion anaérobie est un processus gouverné par cinq réactions biochimiques qui sont : l'hydrolyse, l'acidogenèse, l'acétogenèse, l'homoacétogenèse et enfin la méthanogenèse. La disponibilité des réactifs et l'accumulation de produits intermédiaires sont à l'origine de diverses inhibitions voire de la défaillance du procédé. Nous présentons donc les différentes étapes, les réactifs et les produits dans les lignes suivantes.

De manière globale, la méthanisation est décrite par la réaction :

$$C_6H_{12}O_6 \rightarrow 3CO_2 + 3CH_4 \quad (1)$$

Avec $C_6H_{12}O_6$ une molécule de sucre, CO_2 le dioxyde de carbone, CH_4 le méthane, C le carbone, H l'hydrogène et O l'oxygène.

L'hydrolyse est la première étape de la digestion anaérobie, durant cette étape, les biopolymères (protéines, lipides, hydrates de carbone, polysaccharides, cellulose…) sont hydrolysés en monomères et oligomères hydrosolubles (acides aminés, Sucres acides gras, glycérol…) grâce à des enzymes extracellulaires excrétées par des micro-organismes (bactéries hydrolytiques) [12, 13].

En considérant la dégradation de cellulose en glucose sous l'action d'enzymes, les réactions d'hydrolyse enzymatique sont représentées ainsi :

$$(C_6H_{10}O_5)_n + nH_2O \rightarrow nC_6H_{12}O_6 \quad (2)$$

Dans le **Tableau 1**, nous présentons les temps de croissance, la gamme de pH optimal, les réactifs et la sensibilité de chaque groupe de micro-organismes. Les bactéries hydrolytiques ont un temps de croissance rapide (de l'ordre de 1 à 5 heures) et agissent dans des gammes de pH comprises entre 4,5 et 6,3 [3, 14]. De plus ce sont des bactéries relativement résistantes et tolérantes à l'oxygène [3]. Le temps de croissance des bactéries hydrolytiques est le plus court avec quelques heures, tandis que celui des bactéries acétogènes est de 80 à 90 heures et celui des bactéries méthanogènes est de 5 à 16 jours [3, 14, 15]. En outre, les bactéries acétogènes et archaea méthanogènes sont également

les plus sensibles [3, 14, 15]. Il est donc nécessaire de garantir des conditions optimales pour ces bactéries mais également de conserver les micro-organismes au sein du réacteur.

Tableau 1 : Tableau récapitulatif des caractéristiques des micro-organismes intervenant dans le processus de digestion anaérobie [3, 14, 15]

Bactéries/ Archaea	Temps de croissance	pH optimal	Réactifs	Sensibilité
B. hydrolytiques	1-5 heures	4,5-6,3	Matière organique	-
B. acidogènes	36 heures	4,5-6,3	Monomères	Excès d'ammoniac, sulfure d'hydrogène, sels minéraux, antibiotiques
B. acétogènes	80-90 heures	6,8-7,5	AGV	Oxygène, excès de dihydrogène, sulfure d'hydrogène, d'ammoniac, sels minéraux, antibiotiques, variations de température
A. méthanogènes acétotrophes	5-16 jours	6,8-7,5	Acide acétique	Oxygène, variation de pH et de température, chargement hydraulique et organique, composition de l'influent, cuivre, sels minéraux
A. méthanogènes hydrogénotrophes			Dihydrogène Dioxyde de carbone	

L'acidogenèse est réalisée par des bactéries dites acidogènes, c'est l'étape durant laquelle les produits de l'hydrolyse (molécules simples de matière organique : monomères) sont transformés en AGV (tels que l'acétate, le propionate, le butyrate), en acides organiques (lactique, succinique,...), en alcools, en hydrogène, en dioxyde de carbone (CO_2), et en ammonium [12, 13].

La cinétique de l'acidogenèse étant la plus élevée, une accumulation d'éléments intermédiaires tels que l'acétate et le dihydrogène peut survenir en conditions de surcharge organique, conduisant à l'inhibition des activités des bactéries acétogènes et méthanogènes intervenant dans les étapes suivantes, pouvant aller jusqu'à l'arrêt de la digestion anaérobie [16].

Tableau 2 : Réactions de fermentation du glucose (Dolfing, 1988 ; Angelidaki & Ellegaard, 2002 ; Rodriguez 2006) [13]

Produits	**Réactions**
Acétate	$C_6H_{12}O_6 \rightarrow 2CH_3COOH + 2CO_2 + 4H_2$
Propionate + acétate	$3\ C_6H_{12}O_6 \rightarrow 4CH_3CH_2COOH + 2CH_3COOH + 2CO_2 + 2H_2O$
Butyrate	$C_6H_{12}O_6 \rightarrow CH_3CH_2CH_2COOH + 2CO_2 + 2H_2$
Lactate	$C_6H_{12}O_6 \rightarrow 2CH_3CHOHCOOH$
Éthanol	$C_6H_{12}O_6 \rightarrow 2CH_3CH_2OH + 2CO_2$

Les bactéries concernées, appelées bactéries acidogènes ou fermentaires, sont nombreuses et sensibles notamment à l'ammoniac (NH_3), au sulfure d'hydrogène (H_2S), aux sels minéraux et antibiotiques [3]. Les bactéries acidogènes sont sensibles à l'oxygène [3]. Elles participent en général à l'étape d'hydrolyse également [3]. Ces bactéries ont un temps de croissance relativement court, d'une durée inférieure à 36 heures [14]. La gamme de pH optimale est de 4,5 à 6,3 tout comme celle de l'étape d'hydrolyse [3].

L'acétogenèse transforme les produits de l'hydrolyse et de l'acidogenèse (sauf l'acétate) en acétate et dioxyde de carbone sous l'action des bactéries acétogènes [12, 13]. Il y a les bactéries acétogènes syntrophes productrices d'hydrogène et les bactéries acétogènes non-syntrophes avec les bactéries fermentatives acétogènes et les acétogènes hydrogénotrophes ou homoacétogènes. Les réactions de l'acétogénèse avec production de dihydrogène et de formate sont présentées dans le **Tableau 3** :

Tableau 3 : réactions de l'acétogénèse avec production de dihydrogène et de formate [17]

Produits	**Réactions**
Propionate	$CH_3CH_2COOH + 2H_2O \rightarrow CH_3COOH + 3H_2 + CO_2$
	$CH_3CH_2COOH + 2H_2O + 2CO_2 \rightarrow 2CH_3COOH + 2H_2$
Butyrate	$CH_3CH_2CH_2COOH + 2H_2O \rightarrow 2CH_3COOH + 2H_2$
	$CH_3CH_2CH_2COOH + 2H_2O + 2CO_2 \rightarrow 2CH_3COOH + 2H_2 + 2HCOOH$
Lactate	$CH_3CH_2OH + 2H_2O \rightarrow CH_3COOH + 2H_2$
Éthanol	$CH_3CHOHCOOH + H_2O \rightarrow CH_3COOH + 2H_2 + CO_2$

La méthanogenèse, dernière étape du processus de dégradation, forme le méthane suivant deux métabolismes. Les méthanogènes acétotrophes transforment l'acétate en méthane et dioxyde de carbone alors que les méthanogènes hydrogénotrophes combinent l'hydrogène et le dioxyde de carbone pour former du méthane et de l'eau [12, 13].

L'homoacétogenèse combine l'hydrogène et le dioxyde de carbone en acétate [12].

Les réactions de la méthanogénèse, de l'oxydation de l'acétate et de l'homoacétogenèse sont présentées dans le **Tableau 4** :

Tableau 4 : Réactions de la méthanogénèse (acétoclaste et hydrogénotrophe) [18]

Réactions	**Equations**
Méthanogénèse acétoclaste	$CH_3COOH + H_2 \rightarrow CO_2 + CH_4$
Méthanogénèse hydrogénotrophe	$CO_2 + 4H_2 \rightarrow 2H_2O + CH_4$
Oxydation d'acétate	$CH_3COOH + 2H_2O \rightarrow 4H_2 + 2CO_2$
Homoacétogénèse	$2HCO^{-3} + 4H_2 + H^- \rightarrow CH_3COO^- + 4H_2O$
Homoacétogénèse	$4H_2 + CO_2 \rightarrow CH_3COOH + 2H_2O$

La méthanogenèse est influencée par les conditions de fonctionnement du digesteur, telles que la température, le taux de chargement hydraulique, le taux de chargement organique ainsi que la composition du substrat influent [15].

Dans les digesteurs anaérobies, environ 60 à 70% du méthane est produit par les méthanogènes acétoclastes [19].

Les archaea sont des micro-organismes proches des bactéries [3]. Ces micro-organismes se développent en condition anaérobie stricte et sont totalement intolérantes à l'oxygène [3]. Elles nécessitent également la présence de nickel (Ni) pour se développer [3]. Les archaea sont également sensibles aux variations de pH et de température ainsi qu'au cuivre (Cu) et sels minéraux [3]. Elles évoluent dans une gamme de pH de 6,8 à 7,5 [3]. Elles se régénèrent en 5 à 16 jours, ce qui est le temps de régénération le plus long [14]. Deux groupes de méthanogènes interviennent durant la digestion anaérobie : les archaea acétotrophes et hydrogénotrophes [3]. Les acétoclastes produisent du méthane à partir

de l'acide acétique [3]. Les archaea hydrogénotrophes produisent du méthane à partir de dihydrogène (H_2) et de dioxyde de carbone (CO_2) [3].

Selon la nature du substrat, l'étape limitante et les conditions de réaction ne seront pas les mêmes, en effet :

- Avec des substrats contenant de la cellulose (qui sont difficilement dégradables), l'étape limitante est l'hydrolyse [14].
- Avec des substrats riches en protéines, le pH optimal identique dans toutes les étapes du processus anaérobie, donc un seul digesteur est suffisant pour une bonne performance [14].
- Avec des substrats riches en matières grasses, la vitesse d'hydrolyse augmente avec une meilleure émulsification, l'acétogenèse est ainsi l'étape limitante [14].

I-1.2. La caractérisation des substrats et du milieu de digestion

Plusieurs paramètres permettent de caractériser un substrat, le digestat et le milieu au cours de la digestion. En effet, compte tenu des coûts importants résultants de la défaillance d'un réacteur, des mesures physico-chimiques sont réalisées afin d'anticiper les inhibitions du processus. Dans le cadre de ces travaux de thèses, nous réalisons une étude expérimentale à l'échelle du pilote de laboratoire (16 L). La durée de démarrage d'un pilote étant de l'ordre de plusieurs mois, il est nécessaire d'anticiper les dysfonctionnements. De plus, il est intéressant de produire des données complètes sur le suivi expérimental d'un digesteur, dans ce sens des mesures physico-chimiques du milieu seront réalisées. C'est pour cela que nous présentons les intérêts des mesures couramment réalisées.

Les tests BMP (Biochemical Potential Test) ont pour objectif de déterminer le potentiel méthanogène d'un substrat, c'est-à-dire le volume de méthane maximum que l'on peut produire à partir d'une quantité donnée de substrat. Cette mesure est réalisée dans des conditions contrôlées (limitation des inhibitions, présence des nutriments essentiels, conditions optimales) de manière à obtenir la quantité maximale de méthane. La valeur du BMP est généralement exprimée en Litres de CH_4 par gramme de Matière Volatile (MV) en condition standard (0°C, 1013 mbar), ce qui correspond à des m^3 par kg. La production de méthane peut aussi être exprimée en fonction de la DCO de

l'intrant. Il existe une relation intéressante entre le potentiel méthane et la DCO. En effet, un kg de DCO dégradé produit toujours la même quantité de méthane (0,35 m^3). Il est donc possible d'estimer la biodégradabilité d'un produit selon la formule suivante : Biodégradabilité = BMP / (DCO x 0,35). Cette relation est intéressante car elle permet d'estimer la quantité de méthane qu'il est possible d'obtenir avec un déchet donné, et la quantité de matière organique résiduelle qui n'aura pas été dégradée et qui se retrouvera donc dans le digestat. Et enfin de vérifier que le réacteur fonctionne convenablement, en comparant le méthane réellement produit avec le BMP.

Les teneurs en MS et en MV sont des paramètres incontournables pour la caractérisation du substrat. En outre, les propriétés du substrat telles que le pH, les AGV, l'azote total de Kjeldahl, l'ammonium (ou azote ammoniacal) et l'alcalinité méritent d'être déterminées car elles peuvent être utilisées pour prévoir les phénomènes d'inhibition lors des tests BMP (Biochemical Methane Potential) [20].

Les matières volatiles sont assimilées à la matière organique, en effet, seule la matière organique pourra être éliminée par la méthanisation, à condition d'être biodégradable [21]. De plus, une faible part de la matière organique dégradée sera convertie en biomasse microbienne (entre 5 et 10%) [21]. Notons que dans le cas de déchets tels que les déchets ménagers, des matières volatiles non biodégradables (plastiques) sont prises en compte dans la mesure et peuvent la fausser de manière significative.

Le Carbone Organique Total (COT) et la composition élémentaire (CNHX) peuvent-être des paramètres utiles. Un autre paramètre intéressant à analyser est la DCO. Il est suggéré d'utiliser des procédures analytiques spéciales pour résoudre les problèmes liés à la détermination de la DCO [22, 23].

Les AGV sont les produits de l'acidogénèse, qui seront ensuite convertis en méthane ou en hydrogène au cours de l'acétogénèse. L'accumulation d'AGV au sein des digesteurs provoque des dysfonctionnements [24]. La concentration en AGV a un impact sur les cinétiques de réaction [25]. Il est donc essentiel de suivre les concentrations en AGV.

L'alcalinité mesure le pouvoir tampon dans le digesteur et donc sa capacité à maintenir un pH stable. L'alcalinité du milieu dépend principalement de la concentration

en bicarbonate, en AGV et en ammonium [25]. La mesure de l'alcalinité due au bicarbonate permet d'évaluer l'état biologique des digesteurs [25].

La détermination de la teneur en fibre, par la méthode de Van Soest (1963), a pour objectif d'évaluer la complexité de la matière organique présente dans le déchet. En effet, les composés complexes, tels que la lignine, ne peuvent pas être dégradés par les micro-organismes. Les déchets riches en lignine seront donc difficilement biodégradables (récalcitrants).

Une revue de littérature porte sur les inhibitions dues à l'**ammoniac** [26]. En effet, en cas de trop fortes concentrations, la méthanogénèse est inhibée [26]. L'ammoniac est produit suite à la dégradation des matières azotées [26]. L'ammoniac et l'ion ammonium sont les deux principales formes de l'azote ammoniacal inorganique, toutes deux peuvent être à l'origine d'inhibitions, directement ou indirectement. L'augmentation du pH du milieu de digestion entraine une augmentation du ratio NH_3/NH_4^+ [27].

La présence de **métaux lourds** dans le processus de digestion anaérobie peut provoquer des effets indésirables, ce qui entraîne une toxicité pour les activités microbiennes et provoquer une perturbation ou une défaillance du processus. Dans une étude approfondie de la performance du digesteur anaérobie, il a été constaté que la toxicité des métaux lourds est l'une des principales causes de défaillance du digesteur [28]. Les métaux lourds ne sont pas biodégradables, ils peuvent donc s'accumuler jusqu'à atteindre des concentrations potentiellement toxiques pour le processus de digestion anaérobie [29].

I-1.3. Les technologies de traitement des effluents par méthanisation

A l'échelle industrielle, la digestion anaérobie se déroule dans un environnement contrôlé : les digesteurs anaérobies. Nous présentons dans cette partie les digesteurs destinés à la digestion anaérobie par voie liquide (taux de MS inférieur à 15%). En effet, l'effluent étudié au cours de cette thèse est liquide.

Différentes technologies de traitement par méthanisation ont ainsi été développées en vue d'améliorer les rendements et la stabilité du procédé mais aussi pour s'adapter à

plusieurs types d'effluents. Comme le souligne Moletta, une installation de méthanisation doit répondre aux caractéristiques suivantes [24] :

- La digestion anaérobie se déroule en absence d'oxygène ;
- La vitesse de croissance des micro-organismes est lente ;
- Le milieu de digestion doit être homogène : distribution des micro-organismes, concentration en matière organique et température ;
- Les conditions hydrodynamiques, régies par l'agitation, doivent être adéquates ;
- Le biogaz est composé de méthane, de dioxyde de carbone et parfois de dihydrogène.

Pour répondre à ces exigences, les digesteurs doivent être clos. Il faut également conserver les populations de micro-organismes au sein du réacteur [24]. Le choix de l'agitation employée est également important [24] et doit être fait en fonction du type de réacteur et des substrats à traiter. Enfin un système de récupération du biogaz doit être mis en place [24].

La digestion anaérobie peut être réalisée avec un procédé à une ou deux étapes. Dans le premier cas, l'ensemble des réactions chimiques se déroulent dans une cuve unique. Dans le deuxième cas, l'hydrolyse et l'acidogénèse se déroulent dans une première cuve et l'acétogénèse et la méthanogénèse dans une deuxième cuve. Des conditions particulières sur le temps de séjour hydraulique (quelques heures) et le pH (autour de 6) de la première cuve permettent la séparation du procédé en deux phases [24]. Les intérêts du procédé à deux étapes sont de traiter dans la deuxième cuve les déchets ayant une charge organique plus importante, d'augmenter la stabilité du processus et enfin c'est une stratégie adaptée à la digestion par voie sèche [24].

I-.1.3.i. Les procédés mettant en œuvre des micro-organismes libres [24]

Les procédés mettant en œuvre des micro-organismes libres (ou en flocs) ont été qualifié de « première génération ». Les micro-organismes étant dans le milieu de digestion et ainsi dans le digestat, il est nécessaire de mettre en place des solutions pour les conserver dans le milieu réactionnel. Ceci est possible soit en maîtrisant l'hydrodynamique du réacteur et donc en limitant la perte de micro-organismes lors du

retrait du digestat ; soit en récupérant les micro-organismes directement en sortie à l'aide d'un décanteur. Les différentes technologies, illustrées dans la **Figure 6**, sont :

- Le **réacteur mélangé** et le **contact anaérobie** ont été conçus pour la digestion des boues aérobies. Ce sont ainsi des réacteurs agités mécaniquement ou par recirculation. Dans le cas du contact anaérobie, un système de décantation est mis en place pour récupérer une partie des micro-organismes. Ces réacteurs sont adaptés aux effluents chargés en matières en suspension.

- Le **réacteur à lit de boues** est développé pour mieux conserver les micro-organismes au sein du réacteur. La décantation est réalisée au sein même du réacteur, on a donc une séparation boue/liquide. Les micro-organismes sont ainsi sous forme de flocs. L'effluent à traiter traverse le lit de boue, il est donc nécessaire de maitriser l'hydrodynamique afin de maintenir une bonne rétention des boues.

- Le **réacteur à compartiments** où, comme son nom l'indique, l'effluent passe par différents compartiments en séries ayant des lits de boues anaérobies. Ce type de réacteur est souvent utilisé dans le cas de la digestion solide. L'intérêt de cette technologie est la possibilité de récupérer l'hydrogène produit en phase acidogène pour limiter les inhibitions de l'acétogénèse et de la méthanogénèse acétoclaste.

- Le **bassin de méthanisation** qui est un bassin couvert contenant un lit de boues pouvant faire plusieurs dizaines de milliers de m^3. Des effluents chauds sont souvent utilisés, ce type de réacteur ne possédant pas de système de régulation de température. La répartition des micro-organismes est faite grâce à un brassage séquentiel ou par un garnissage à l'intérieur des lagunes anaérobies. Enfin, le biogaz est récupéré à l'aide d'un dispositif de couverture flottante.

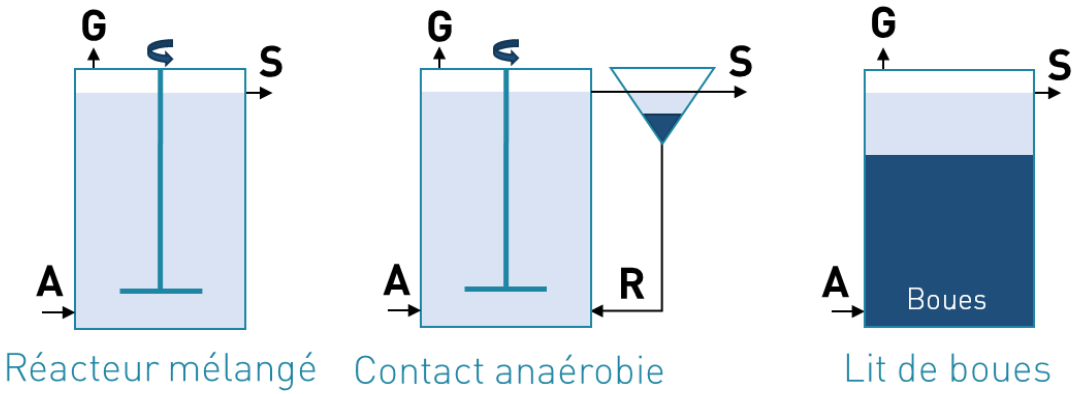

Figure 1: Procédés mettant en œuvre des micro-organismes libres ou en flocs (réacteurs de première génération) (A : Alimentation, G : Biogaz, R : Recirculation, S : Sortie de l'effluent)

I-.1.3.ii. Les procédés mettant en œuvre des micro-organismes formant un biofilm [24]

Il existe deux types de biofilms, ceux formés sur un support minéral ou organique (fixe ou mobile) et les granules (agglomération naturelle de micro-organismes de quelques dizaines de microns à plusieurs millimètres de diamètre). La particularité de ces granules est qu'ils sédimentent plus facilement que les flocs. Ces réacteurs permettent d'avoir des concentrations en micro-organismes plus importantes et ainsi de meilleures performances. Au niveau des supports fixes, ils peuvent être positionnés de manière aléatoire ou de manière ordonnée. Les réacteurs à supports fixes sont qualifiés de « deuxième génération ». Les technologies, illustrées sur la **Figure 7**, sont :

- Le **réacteur UASB** (Up-flow Anaerobic Sludge Blanket) est caractérisé par son lit de boues, essentiellement constitué de granules mais aussi de flocs de micro-organismes. Le système de piégeage du biogaz, permettant la réalisation d'un décanteur intégré, est placé en partie supérieure du réacteur.

- Le **filtre anaérobie** est composé d'un support fixe (en vrac ou orienté) colonisé par des micro-organismes formant un biofilm [24]. L'effluent entrant dans le réacteur traverse ainsi ce filtre, favorisant le contact entre le substrat et les micro-organismes. Afin de conserver un filtre homogène, il est nécessaire de remettre les micro-organismes en suspension momentanément à l'aide de la recirculation de biogaz [24].

• Le **lit fluidisé** est un réacteur possédant un support particulaire continuellement en suspension grâce à un système de recirculation. La vitesse de recirculation est donc suffisamment importante pour maintenir le lit de particules, de 5 à 10 $m.h^{-1}$. Par conséquent, le temps de séjour est court. Ce type de réacteur permet d'appliquer des charges volumiques et organiques élevées grâce à sa forte concentration en micro-organismes et aux faibles risques de colmatage et d'encombrement.

• Le **réacteur à recirculation interne** utilise la production de biogaz pour agiter le milieu de digestion. En remontant, le biogaz entraine également une fraction de boue de liquide. Le biogaz est récupéré tandis que le mélange boue et liquide redescend dans le digesteur, ce qui participe à l'agitation du milieu.

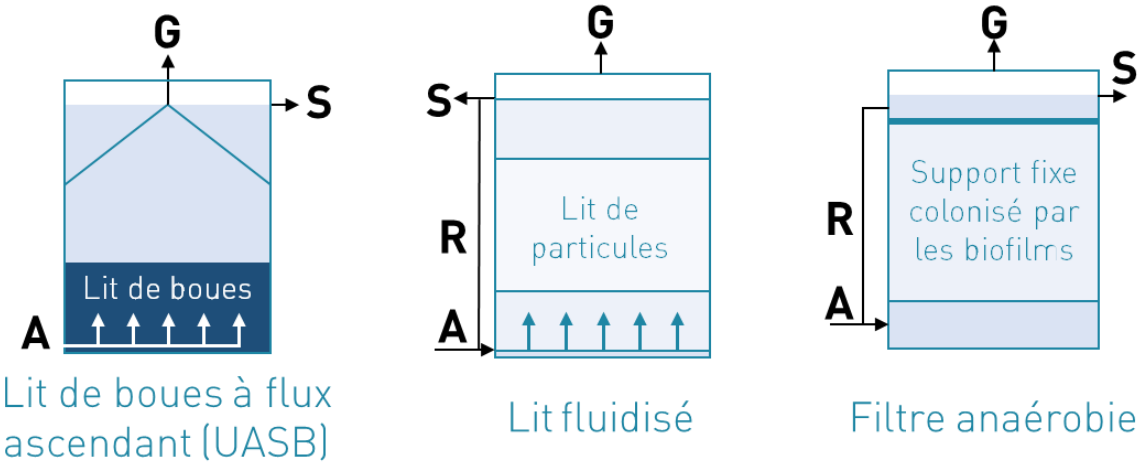

Figure 2: Procédés mettant en œuvre des micro-organismes formant un biofilm (A : Alimentation, G : Biogaz, R : Recirculation, S : Sortie de l'effluent)

Les modifications apportées aux réacteurs anaérobies ont pour objectif principal la conservation des micro-organismes au sein des réacteurs. En effet, leurs concentrations diminuaient lors du retrait du digestat. L'enjeu est important car les temps de croissance des micro-organismes sont longs. De plus, il est d'autant plus important de conserver la biomasse active puisqu'elle s'acclimate aux conditions du milieu avec l'âge du digesteur.

D'autres modifications visent à réduire les inhibitions du processus avec notamment la séparation des réactions chimiques pour que les produits des premières réactions n'inhibent pas les réactions suivantes. Dans le cas des réacteurs à compartiments,

l'hydrogène formé lors de l'acidogénèse est capté, réduisant les risques d'inhibition de l'acétogénèse et de la méthanogénèse acétoclaste.

I-1.4. La modélisation de la digestion anaérobie

Le modèle ADM1 (Anaerobic Digestion Model No 1) développé par D.J.Bastone et al., en 2002, permet de modéliser les processus biochimiques et physico-chimiques mis en jeu en méthanisation. Ce modèle repose sur le fractionnement de la DCO en considérant 3 phases (solide, liquide, gazeuse), 5 étapes de la digestion anaérobie, 7 populations de micro-organismes, 19 processus biochimiques et 3 processus cinétiques de transfert gaz-liquide. Les étapes biochimiques comprennent la désintégration des particules homogènes en glucides, protéines et lipides ; l'hydrolyse extracellulaire de ces substrats particulaires en sucres, acides aminés et acides gras à longue chaîne, respectivement ; l'acidogénèse des sucres et des acides aminés en AGV et hydrogène ; l'acétogénèse des acides gras à longue chaîne et AGV en l'acétate ; et des étapes distinctes de méthanogénèse à partir de l'acétate et de l'hydrogène / CO_2. Les échanges physico-chimiques avec les équilibres acide/base et les transferts entre les phases liquides et gazeuses sont également pris en compte [30]. Les voies métaboliques et les processus modélisés dans le modèle ADM1 sont récapitulés dans la **Figure 3**.

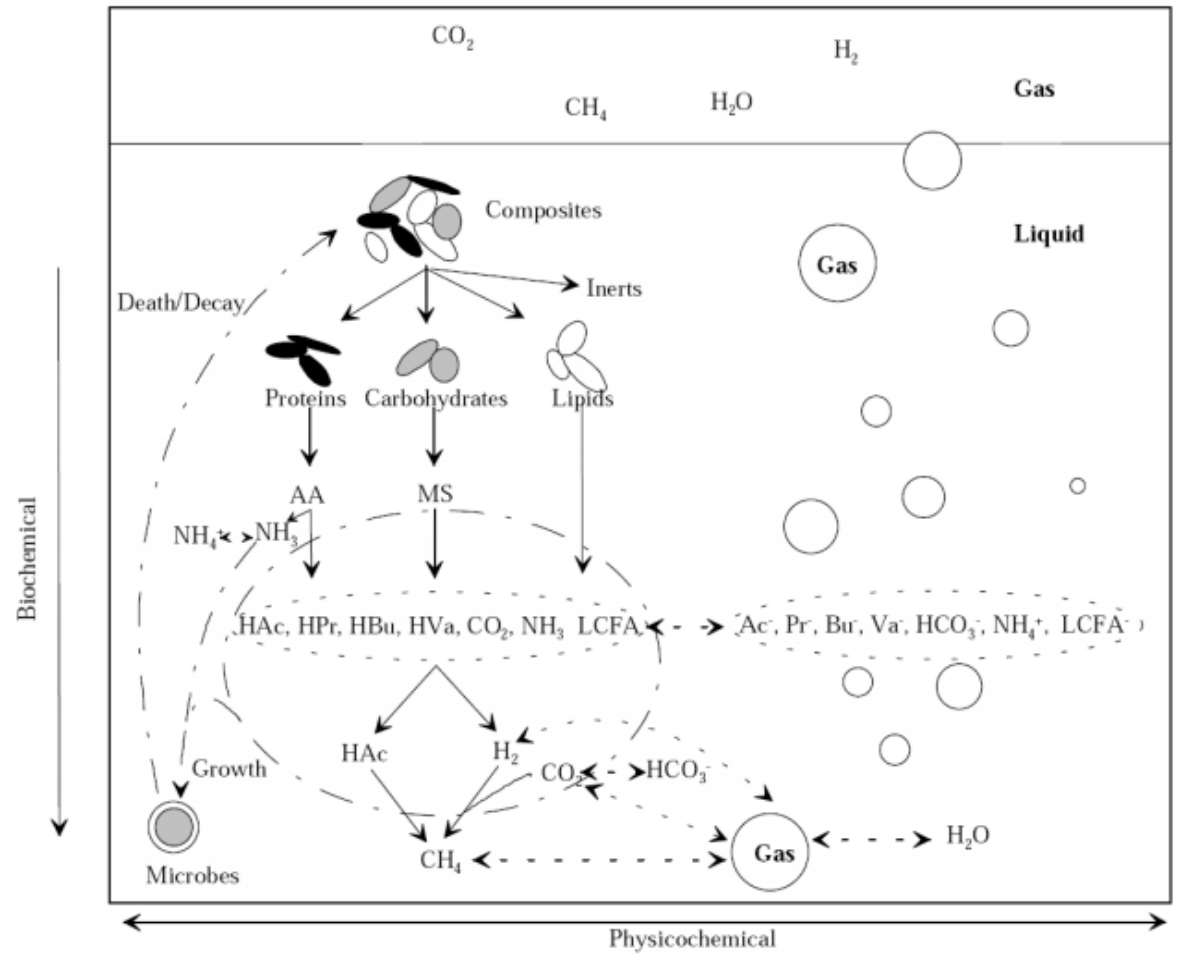

Figure 3: Processus bio-physico-chimiques considérés dans le modèle ADM1 (Source : IWA Task Group for Mathematical Modelling of Anaerobic Digestion Processes, 2002)

Le domaine de la méthanisation se développe rapidement, avec l'apparition de nouvelles technologies. En effet les nouveaux procédés tendent à comporter des teneurs en MS plus importantes. Les défis liés à ces nouveaux processus ainsi que l'optimisation des processus existants, nécessitent la considération de la variance spatiale et l'amélioration de la caractérisation des intrants. De plus, les processus microbiens émergents remettent en question la compréhension du rôle du métabolisme central du carbone catabolique dans la digestion anaérobie. En effet, Batstone et al., relèvent une importance accrue du phosphore, du soufre et des métaux en tant que source et puits d'électrons, et la prise en compte de l'hydrogène et du méthane comme sources potentielles d'électrons. Les nouveaux processus ne sont généralement pas compatibles

avec la structure existante du modèle ADM1. D'où la nécessité du modèle ADM2 [31]. Ainsi Flores Alsina et al., en 2015 proposent des extensions de modèle qui décrivent les interactions entre le phosphore (P), le soufre (S), le fer (Fe) et leurs effets sur la production totale de biogaz (CO_2, CH_4, H_2 et H_2S) [32].

Les différentes modifications apportées aux modèles de la digestion anaérobie seront détaillées dans le chapitre suivant.

I-2. La modélisation des écoulements : les équations de Navier-Stokes et le modèle de RANS

L'étude bibliographique a clairement montré que les écoulements ont un impact sur les rendements de la digestion anaérobie et sur la stabilité du procédé. La modélisation des écoulements est ainsi digne d'intérêt dans le domaine de la méthanisation. Une partie de ces travaux y est donc consacrée.

Nous présentons donc les lois de comportement décrivant les écoulements des fluides Newtoniens et non-Newtoniens ; les équations de conservation ; puis les équations de Navier-Stokes ; les modèles de turbulence ; la décomposition de Reynolds qui nous permet d'aboutir au modèle de RANS.

La turbulence est modélisée avec différentes méthodes :

- DNS (Direct Numerical Simulation) : cette méthode est la plus coûteuse en termes de calculs. En effet, toutes les échelles de la turbulence sont calculées. Les résultats sont ainsi extrêmement précis et le maillage doit-être très fin. Dans notre cas, nous souhaitons modéliser les écoulements au sein d'un digesteur qui est un domaine grand. Cette méthode n'est donc pas adaptée à nos besoins.

- LES (Large Eddy Simulation) : cette méthode reste couteuse en temps de calcul même si une partie des échelles de turbulence n'est pas calculée (les échelles de turbulence de taille inférieure à la plus petite des mailles du maillage). Les échelles non calculées sont modélisées. Les résultats obtenus sont précis mais le maillage nécessaire reste conséquent. Cette méthode restant couteuse ne sera pas utilisée dans ces travaux de thèse.

• RANS (Reynolds Averaged Navier-Stokes) : c'est la méthode la moins couteuse en calcul et qui permet l'utilisation d'un maillage moins fin. En effet, la turbulence est modélisée mathématiquement. On s'intéresse dans ce cas aux quantités moyennes. Pour cela, on applique l'opérateur de moyenne d'ensemble sur les équations instantanées en pratiquant la décomposition de Reynolds sur les inconnues du problème. Les méthodes de RANS sont moins précises que les méthodes DNS et LES. Cependant ces méthodes ont l'avantage de calculer des configurations complexes à grand nombre de Reynolds [33]. Nous utilisons cette approche dans ces travaux de thèse (Chapitre VI).

I-2.1. Les équations de conservation et de Navier-Stokes

I-.2.1.i. La conservation de la masse

D'après le principe physique, la masse se conserve, à l'exception des réactions nucléaires. L'équation de la conservation de la masse s'écrit :

$$\frac{d}{dt}\iiint_V \rho \, dV = -\iint_S \rho \vec{u}.\vec{n} \, dS \tag{3}$$

Avec ρ la masse volumique du fluide, $\vec{u}$ le champ de vitesse du fluide, V le volume, S la surface et $\vec{n}$ est un vecteur normal unitaire défini localement sur S.

Le principe de conservation de la masse conduit à l'équation de continuité :

$$\frac{\partial \rho}{\partial t} + \nabla.(\rho \vec{u}) = 0 \tag{4}$$

Dans le cas d'un fluide incompressible, cette équation devient :

$$\nabla.\vec{u} = 0 \tag{5}$$

I-.2.1.ii. La conservation de la quantité de mouvement

L'équation de la conservation de mouvement vient de la loi de Newton qui dit que la somme des forces et égale à l'accélération suivant le mouvement du fluide. La forme générale de l'équation de la conservation de la quantité de mouvement dans le cas d'un écoulement incompressible est :

$$\frac{d}{dt}\iiint_V \rho\vec{u}\ dV = -\iint_S \rho\vec{u}\left(\vec{u}.\vec{n}\right)\ dS + \sum \vec{F}_{ext} \tag{6}$$

Avec ρ la masse volumique du fluide, $\vec{u}$ le champ de vitesse du fluide, V le volume, S la surface et $\vec{F}_{ext}$ les forces extérieures.

L'équation de conservation de la quantité de mouvement s'écrit [33] :

$$\frac{\partial}{\partial t}\left(\rho\vec{u}\right) + \nabla.\left(\rho\vec{u}\otimes\vec{u}\right) + \nabla.\left(pI - \tau\right) = \vec{F}_{ext} \tag{7}$$

I-.2.1.iii. L'équation de conservation de l'énergie

L'énergie totale massique est la somme de l'énergie cinétique et de l'énergie inerme massique. L'équation de la conservation de l'énergie est :

$$\frac{d}{dt}\int_V \rho E = \int_V \left(\frac{\partial}{\partial t}\left(\rho E\right) + \nabla.\left(\rho\vec{u}E\right)\right) = \int_V \vec{u}.\vec{F}_{ext} + \int_S \left(\vec{u}\left(\tau - pI\right) - q\right)\vec{n} \tag{8}$$

Avec E l'énergie, $\vec{u}$ le champ de vitesse, q la densité de flux d'énergie transporté par conduction thermique, ρ la masse volumique, F_{ext} les forces extérieures, τ la contrainte totale, $\vec{n}$ est un vecteur normal unitaire défini localement sur S.

En utilisant la formule de Stokes, la relation devient :

$$\frac{\partial}{\partial t}\left(\rho E\right) + \nabla.\left(\vec{u}\left(\rho E + pI\right)\right) = \nabla.\left(\vec{u}\tau + q\right) + \vec{u}.\vec{F}_{ext} \tag{9}$$

I-.2.1.iv. Les équations de Navier-Stokes

Sous l'hypothèse d'un fluide Newtonien et celle d'incompressibilité, les équations du mouvement prennent la forme des équations dites de « Navier-Stokes ».

A coefficients de viscosité constants, l'équation devient :

$$\frac{\partial\rho\vec{u}}{\partial t} + \rho\left(\vec{u}.\nabla\right)\vec{u} = -\nabla p + \mu\left[\Delta\vec{u} + \frac{1}{3}\nabla\left(\nabla.\vec{u}\right)\right] + \rho\vec{F}_{ext} \tag{10}$$

Avec ρ la masse volumique du fluide, u le champ de vitesse du fluide, p la pression, $\vec{F}_{ext}$ les forces extérieures, μ la viscosité dynamique.

En considérant un fluide incompressible, l'équation devient :

$$\frac{\partial \rho \vec{u}}{\partial t} + \rho(\vec{u}.\nabla)\vec{u} = -\nabla p + \mu \Delta \vec{u} + \rho \vec{F}_{ext} \tag{11}$$

Cette équation s'associe à l'équation d'incompressibilité pour former les équations de Navier-Stokes. De plus, en supposant que le système n'est soumis à aucune force extérieure, nous obtenons les équations de Navier-Stokes. Le développement complet est détaillé dans la thèse [33].

$$\frac{\partial \rho}{\partial t} + \nabla.(\rho \vec{u}) = 0 \tag{12}$$

$$\frac{\partial \rho \vec{u}}{\partial t} + \nabla.(\rho \vec{u} \otimes \vec{u}) = \nabla.\sigma \tag{13}$$

$$\frac{\partial \rho E}{\partial t} + \nabla.(\rho \vec{u} E) = \nabla.(\vec{u}\sigma) - \nabla q \tag{14}$$

Avec $\sigma = -pI + \tau$

I-2.2. Les lois de comportement des fluides Newtoniens et non-Newtoniens [34], [35]

Le comportement rhéologique d'un fluide a une importance non négligeable sur les écoulements au sein d'un digesteur. En effet, les modèles rhéologiques décrivent la manière dont un fluide s'écoule en fonction des contraintes de cisaillement qui lui sont appliquées. Dans le cas d'un digesteur anaérobie, les substrats sont soumis à des contraintes de cisaillement. Selon le comportement rhéologique des déchets, les écoulements seront différents. Il est donc nécessaire de modéliser avec précision leurs comportements. C'est pour cela que différents auteurs ont étudié le comportement rhéologique de différents fluides. Ces études ne sont pas uniquement concentrées sur les déchets. Nous retrouvons notamment des études sur la boue, dues aux enjeux industriels pétroliers mais également sur les lisiers dans le cadre de la digestion anaérobie, ou encore sur les légumes et fruits nécessaires pour l'optimisation des industries agroalimentaires. Ainsi nous présentons les modèles rhéologiques retenus par les auteurs pour décrire le comportement rhéologique d'un ensemble de substrats, car ces modèles seront utiles pour la modélisation des écoulements au sein d'un digesteur.

Les fluides Newtoniens obéissent à la relation linéaire suivante :

$$\tau = \mu\dot{\gamma} = \mu\frac{\partial u}{\partial y} \tag{15}$$

Avec τ la contrainte de cisaillement, μ est la contrainte intrinsèque appelée viscosité (dynamique) à température donnée et $\dot{\gamma}$ le taux de cisaillement.

Cette loi expérimentale se généralise :

$$\sum = -p1 + 2\mu D \tag{16}$$

Avec $\sum$ le tenseur des contraintes et $D = \frac{1}{2}\left(\nabla u + \nabla u^T\right)$ le tenseur des taux de déformation.

Les fluides non-Newtoniens sont regroupés dans trois classifications :

- Les fluides non-Newtoniens indépendants du temps, où le taux de cisaillement est unique mais est une fonction non-linéaire de la contrainte de cisaillement [35].

- Les fluides non-Newtoniens dépendants du temps, où la relation entre la contrainte de cisaillement et le taux de déformation est plus complexe. Le taux de cisaillement n'est pas une valeur unique fonction de la contrainte de cisaillement. Le taux de cisaillement dépend de la durée du cisaillement ou des précédents taux de cisaillement subis par le fluide [35].

- Dans le cas de fluides viscoélastiques, la déformation de cisaillement ainsi que le taux de déformation sont en relation avec la contrainte de cisaillement. Contrairement à un fluide visqueux dans lequel la totalité de l'énergie de déformation est dissipée, une partie de l'énergie de déformation d'un fluide viscoélastiques peut être récupérée comme lors de la déformation d'un solide élastique [35].

D'après la revue de littérature, le comportement rhéologique des différents déchets recensés est décrit par les modèles de Bingham, d'Hershel-Bulkley, d'Ostwald et de Sisko.

Le modèle plastique de Bingham est adapté aux fluides viscoplastiques qui se comportent comme un fluide parfait à de faibles contraintes puis comme un fluide

visqueux au-delà d'une contrainte seuil. Les fluides plastiques de Bingham présentent une contrainte d'élasticité à un taux de cisaillement nul, suivies d'une relation linéaire entre la contrainte de cisaillement et le taux de cisaillement. Les équations qui régissent le comportement d'un fluide plastique de Bingham sont :

$$\frac{\partial u}{\partial y} = \begin{cases} 0 & ,\tau < \tau_0 \\ (\tau - \tau_0)/\mu_p & ,\tau \geq \tau_0 \end{cases} \tag{17}$$

Avec $\partial u/\partial y$ la vitesse de déformation, τ_0 la contrainte d'écoulement, τ la contrainte de cisaillement, et μ_p la viscosité plastique ou viscosité de Bingham.

Les modèles d'Hershel-Bulkley et d'Ostwald (loi de puissance) permettent de modéliser le comportement des fluides pseudo-plastiques. Ces derniers ne possèdent pas de contrainte d'élasticité. Ils sont également caractérisés par une diminution progressive de la pente de la contrainte de cisaillement en fonction du taux de cisaillement. Cette pente est définie comme la viscosité apparente :

$$\mu_a = \frac{\tau}{\dot{\gamma}} \tag{18}$$

À un taux de cisaillement élevé, la viscosité apparente devient constante et égale à μ_∞ et la contrainte de cisaillement par rapport au taux de cisaillement devient linéaire. Il existe un certain nombre de relations empiriques qui ont été utilisées pour décrire les fluides pseudo-plastiques. La loi de puissance d'Ostwald est la plus simple :

$$\tau = k\dot{\gamma}^n \tag{19}$$

Avec τ la contrainte de cisaillement, k la consistance du fluide ($k = \mu$ pour un fluide Newtonien), $\dot{\gamma}$ le taux de cisaillement et n l'indice de structure (ou d'écoulement). $n<1$ dans le cas d'un fluide rhéofluidifiant (ou pseudoplastique), $n>1$ dans le cas d'un fluide rhéoépaississant (ou dilatant) et $n=1$ dans le cas d'un fluide Newtonien).

Malgré sa relative simplicité, la loi de puissance d'Ostwald n'est pas idéale du fait que la consistance k n'a aucun sens physique, sa dimension étant liée à la valeur de l'exposant

n . Pour cette raison, on essaie de se raccrocher à la notion de viscosité en introduisant une « viscosité apparente » :

$$\mu_a = k\dot{\gamma}^{n-1} \tag{20}$$

Et enfin, l'équation qui régit le comportement d'un fluide d'Herschel-Bulkley développée en 1926 s'énonce de la manière suivante :

$$\tau = \tau_0 + k\dot{\gamma}^n \tag{21}$$

Avec τ_0 le seuil de contrainte.

I-2.3. Le modèle de RANS et le modèle de turbulence k-epsilon standard

I-.2.3.i. La décomposition de Reynolds et le modèle de RANS

Nous expliquons dans cette partie le principe de la décomposition de Reynolds. Elle consiste à décomposer les grandeurs physiques (le champ de vitesse et la pression) en la somme de leur valeur moyenne et d'une fluctuation aléatoire centrée :

$$u_i = \bar{u}_i + u_i' \text{ avec } \bar{u}_i' = 0 \tag{22}$$

Avec u' la composante turbulente.

Nous introduisons donc la décomposition du champ de vitesse et la pression dans les équations de Navier-Stokes.

Dans le cas d'un fluide incompressible et Newtonien, l'équation de conservation de la masse devient :

$$\frac{\partial u_i}{\partial x_i} = \frac{\partial\left(\overline{u_i} + u_i'\right)}{\partial x_i} = 0 \tag{23}$$

$$\frac{\overline{\partial u_i}}{\partial x_i} = \frac{\overline{\partial\left(\overline{u_i} + u_i'\right)}}{\partial x_i} = 0 \tag{24}$$

$$\frac{\partial \overline{u}_i}{\partial x_i} = \nabla . \vec{\overline{u}} = 0 \text{ avec } \frac{\partial u_i'}{\partial x_i} = 0 \tag{25}$$

L'équation de conservation de la quantité de mouvement devient :

$$\frac{\partial u_i}{\partial t} + u_j \frac{\partial u_i}{\partial x_j} = g_i - \frac{1}{\rho}\frac{\partial p}{\partial x_i} + \nu \frac{\partial^2 u_i}{\partial x_j^2} \tag{26}$$

$$\frac{\partial \left(\overline{u}_i + u_i'\right)}{\partial t} + \left(\overline{u}_j + u_j'\right)\frac{\partial \left(\overline{u}_i + u_i'\right)}{\partial x_j} = g_i - \frac{1}{\rho}\frac{\partial \left(\overline{p} + p'\right)}{\partial x_i} + \nu \frac{\partial^2 \left(\overline{u}_i + u_i'\right)}{\partial x_j^2} \tag{27}$$

$$\overline{\frac{\partial \left(\overline{u}_i + u_i'\right)}{\partial t} + \left(\overline{u}_j + u_j'\right)\frac{\partial \left(\overline{u}_i + u_i'\right)}{\partial x_j}} = \overline{g_i - \frac{1}{\rho}\frac{\partial \left(\overline{p} + p'\right)}{\partial x_i} + \nu \frac{\partial^2 \left(\overline{u}_i + u_i'\right)}{\partial x_j^2}} \tag{28}$$

$$\frac{\partial \overline{u}_i}{\partial t} + \overline{u}_j \frac{\partial \overline{u}_i}{\partial x_j} + \overline{u_j' \frac{\partial u_i'}{\partial x_j}} = g_i - \frac{1}{\rho}\frac{\partial \overline{p}}{\partial x_i} + \nu \frac{\partial^2 \overline{u}_i}{\partial x_j^2} \tag{29}$$

Ainsi dans cette expression, le terme $\overline{u_j' \frac{\partial u_i'}{\partial x_j}}$ représente l'influence de l'agitation turbulente sur le bilan moyen de la quantité de mouvement.

$$\overline{u_j' \frac{\partial u_i'}{\partial x_j}} = \frac{\partial}{\partial x_j}\left(\overline{u_i' u_j'}\right) \tag{30}$$

On obtient donc :

$$\frac{\partial \overline{u}_i}{\partial t} + \overline{u}_j \frac{\partial \overline{u}_i}{\partial x_j} = g_i - \frac{1}{\rho}\frac{\partial \overline{p}}{\partial x_i} + \frac{1}{\rho}\frac{\partial}{\partial x_j}\left[\mu\left(\frac{\partial \overline{u}_i}{\partial x_j} + \frac{\partial \overline{u}_j}{\partial x_i}\right) - \rho\overline{u_i' u_j'}\right] \tag{31}$$

Avec $\overline{u_i' u_j'}$ un nouveau terme inconnu appelé le tenseur des contraintes de Reynolds τ_{ij}, apportant 6 inconnues supplémentaires au système.

Dans le cas d'un problème turbulent, nous avons 4 équations avec l'équation de continuité et les équations de Reynolds (issues de Navier-Stokes) et 10 inconnues $\left(\overline{p},\ \overline{u},\ \overline{v},\ \overline{w} \text{ et } -\rho\overline{u_i' u_j'}\right)$. Le système est donc ouvert. La fermeture du système est assurée par un modèle de turbulence.

La fermeture du système est basée sur l'hypothèse de Boussinesq, qui suppose que le tenseur des contraintes de Reynolds a la même forme qu'un tenseur des contraintes visqueuses :

$$-\overline{u_i' u_j'} = \nu_t \left(\frac{\partial \overline{u}_i}{\partial x_j} + \frac{\partial \overline{u}_j}{\partial x_i} \right) - \frac{2}{3} \overline{k} \delta_{ij} \tag{32}$$

Les équations de Navier-Stokes Moyennées sont donc :

$$\begin{cases} \dfrac{\partial \overline{u}_i}{\partial x_i} = 0 \\ \dfrac{\partial \overline{u}_i}{\partial t} = \dfrac{\partial \overline{u}_j \overline{u}_i}{\partial x_j} = -\dfrac{1}{\rho} \dfrac{\partial p^*}{\partial x_i} + \left(\nu + \nu_t \right) \left(\dfrac{\partial^2 \overline{u}_i}{\partial x_j \partial x_j} \right) \end{cases} \tag{33}$$

Avec $p^* = \overline{p} + \frac{1}{3} \rho \overline{k}$ la pression modifiée.

I-.2.3.ii. Le modèle de turbulence k-epsilon standard

Comme énoncé précédemment, la décomposition de Reynolds est utilisée dans le modèle de RANS. Ceci a pour conséquence l'ajout d'inconnues. Il y a faut donc fermer le problème avec un modèle de turbulence. Il existe deux grandes classes de modèles :

- Les modèles à viscosité turbulente (modèles de premier ordre) basés sur l'hypothèse de Boussinesq ;

- Les modèles du deuxième ordre où les tensions de Reynolds sont directement calculées et la modélisation porte sur les moments d'ordre supérieur.

Les modèles de premier ordre, que nous utilisons dans cette thèse, sont classés selon le nombre d'équations. Il existe ainsi des modèles à 0 équation (longueur de mélange), des modèles à 1 équation (énergie cinétique turbulente k) et des modèles à 2 équations (tels que les modèles $k-\varepsilon$ et $k-\omega$).

La qualité des résultats est liée au choix du modèle de turbulence choisi. D'un point de vue industriel, les modèles du premier ordre à deux équations permettent d'obtenir

des résultats satisfaisants. Nous présentons dans le Chapitre II les modèles de turbulence utilisés pour la modélisation des écoulements au sein des réacteurs agités.

Nous présentons dans ce chapitre le modèle $k-\varepsilon$ standard, un modèle fréquemment utilisé dans la littérature. Les simulations numériques présentées dans le Chapitre VI sont effectuées en utilisant le modèle $k-\varepsilon$ standard.

Il est possible de relier, en se basant sur une analyse dimensionnelle, l'énergie cinétique turbulente k, la dissipation de l'énergie cinétique ε et l'échelle de longueur de la turbulence l par la relation :

$$l \approx \frac{k^{3/2}}{\varepsilon} \tag{34}$$

Prandtl et Kolomgorov ont ensuite dérivé la relation pour obtenir la viscosité turbulente :

$$\mu_t = C_\mu \rho \frac{k^2}{\varepsilon} \tag{35}$$

Avec C_μ une constante adimensionnelle à déterminer.

L'équation de l'énergie cinétique turbulente k s'écrit :

$$\frac{\partial k}{\partial t} + U_k \frac{\partial k}{\partial x_k} = \frac{\partial}{\partial x_k}\left[\left(\nu + \frac{C_\mu k^2}{\sigma_k \varepsilon}\right)\frac{\partial k}{\partial x_k}\right] + \frac{C_\mu k^2}{\varepsilon}\left(\frac{\partial U_i}{\partial x_k} + \frac{\partial U_k}{\partial x_i}\right)\frac{\partial U_i}{\partial x_k} - \varepsilon \tag{36}$$

Avec σ_k l'équivalent d'un nombre de Prandtl turbulent (constante).

L'équation de la dissipation ε est :

$$\frac{\partial \varepsilon}{\partial t} + U_k \frac{\partial \varepsilon}{\partial x_k} = \frac{\partial}{\partial x_k}\left[\left(\nu + \frac{C_\mu k^2}{\sigma_\varepsilon \varepsilon}\right)\frac{\partial \varepsilon}{\partial x_k}\right] + C_{\varepsilon 1} C_\mu k\left(\frac{\partial U_i}{\partial x_k} + \frac{\partial U_k}{\partial x_i}\right)\frac{\partial U_i}{\partial x_k} - C_{\varepsilon 2}\frac{\varepsilon^2}{k} \tag{37}$$

Avec $C_{\varepsilon 1}$, $C_{\varepsilon 2}$ et σ_ε les constantes adimensionnelles à déterminer.

Dans le modèle k-epsilon standard, les valeurs des constantes sont : $C_\mu = 0.09$, $C_{\varepsilon 1} = 1.44$, $C_{\varepsilon 2} = 1.92$, $\sigma_k = 1$ et $\sigma_\varepsilon = 1.22$.

I-3. Conclusion

Nous avons présenté les éléments de base nécessaires à la compréhension des travaux menés. La partie sur la digestion anaérobie, la caractérisation des substrats et les technologies de traitement des effluents liquides par méthanisation seront utiles pour les chapitres III, IV, V qui portent sur les expérimentations. La partie sur la modélisation des écoulements a présenté les grandes étapes pour obtenir le modèle de RANS, utilisé pour les simulations numériques présentées dans le chapitre VI.

Nous nous intéresserons dans le chapitre suivant à la revue de littérature des modèles développés, notamment les modèles de la digestion anaérobie et les modèle basés sur la mécanique des fluides pour la simulation des écoulements.

Chapitre II

Anaerobic digestion modelling and waste rheology: a review

Nous avons vu dans le chapitre précédent le procédé de la méthanisation ainsi que technologies de digesteurs dans un premier temps. La nécessité de maitriser l'hydrodynamique des digesteurs est clairement apparu. Ainsi, dans un deuxième temps, nous avons exposé les équations de base des modèles basés sur la mécanique des fluides (CFD) pour la modélisation des écoulements au sein des digesteurs.

Ce chapitre est une revue de littérature rédigée au format d'article scientifique. L'objectif est de relater l'ensemble des travaux menés pour la modélisation du procédé et des écoulements des réservoirs/digesteurs agités ou non pour différents types de déchets.

La première partie concerne la rhéologie des substrats de digestion avec les modèles rhéologiques et les données de la littérature utilisées dans les modèles rhéologiques de divers substrats (vinasse, eaux usées, boues, fumiers et biodéchets). Dans une seconde partie, une revue de littérature sur les objectifs et les avancées des modèles biochimiques et CFD est développée, en passant en revue les objectifs du modèle, les méthodes numériques, la modélisation de la turbulence et le maillage. Puis les modèles thermiques sont présentés. Enfin, la contribution et les intérêts de CFD dans la modélisation numérique seront discutés.

Abstract

Anaerobic digestion is widely used for waste treatment and energy production. Anaerobic digestion is a complex process which involved both physico-chemical reactions driven by four microbial groups and hydrodynamics phenomena. Consequently, many researches have been carried out on the process modelling. Research firstly focused on the development of various models based on kinetics. The different developed models are adapted to a specific waste or mix of waste. Moreover, parameters such as mass transfer and temperature influence the physicochemical and biological reactions. These latter are modelled with computational fluid dynamic (CFD). The knowledge of waste rheology is unavoidable for CFD modelling. In this paper, we present a literature review on waste rheology, mathematical models based on kinetics, and CFD models with the studies aims, numerical methods and turbulence modelling and lastly the thermal models. Finally, all these aspects are discussed. The general conclusion of this literature review is firstly, that rheological behaviour of manure and sludge are best described, however the rheological of behaviour a mix of biowaste is poorly known. Secondly, modified ADM1 will be used for the development of ADM2 and more research are needed. Thirdly, the aim of CFD modelling are numerous. In particular, it allows to provide knowledge and helps with the dimensioning of anaerobic digestion units. Fourthly, the thermal modelling are mainly useful in cold countries and those experiencing significant temperature variations. Few studies concerned the coupling of biochemical and CFD models. This strategy is of interest depending on the objectives of the study. It allows, however, to take into account both the biochemical aspects of the environment and the flows.

Highlights:

- The rheological behaviour of a mix of biowaste is poorly known.
- Modified ADM1 will be used for the development of ADM2 and more research are needed.
- CFD modelling allows to provide knowledge and help with the dimensioning of anaerobic digestion units.
- The thermal modelling are mainly useful in cold countries and those experiencing significant temperature variations.
- Few studies concerned the coupling of biochemical and CFD models. This strategy allows to take into account both the biochemical aspects of the environment and the flows.

Keywords: Anaerobic digestion, kinetic models, CFD, rheology, waste, thermal model

Abbreviations:

ADM1	Anaerobic Digestion Model n°1
ASM	Activated Sludge Model
CARPT	Computer Automated Radioactive Particle Tracking
CFD	Computational Fluid Dynamics
FIW	Food Industry Waste
HRT	Hydraulic Retention Time
KET	Kinetic Energy Transport
KTGF	Kinetic Theory Of Granular Flow
LDA	Laser Doppler Anemometry
LES	Large Eddy Simulation
MRF	Multiple Reference Frame
OFMSW	Organic fraction of municipal solid waste
RANS	Reynolds-averaged Navier-Stokes
RF	Reference Frame
RNG	Re-Normalisation Group
RSM	Reynolds stress model
SGS	Subgrid-scale
SHW	Slaughter house waste
SL	Smagorinsky-Lilly
SM	Sliding Mesh
SRT	Solid retention time
T	Temperature (°C)
Thix	Thixotropy ($Pa.s^{-1}$)
TDS	Total Dissolved Solid
TS	Total Solid (% or $g.L^{-1}$)
TSS	Total Suspended Solid (%)
UI	Uniformity Index
VFA	Volatile Fatty Acids
WALE	Wall-Adapting Local Eddy-Viscosity
WV	Working volume (m^3)
R^2	Coefficient of determination
k	Consistency index ($Pa.s^n$)
$\dot{\gamma}_c$	Critical shear rate (s^{-1})
ρ	Density ($kg.m^{-3}$)
η_{dyn}	Dynamic viscosity (Pa.s or mPa.s))
FCI	Flow consistency index (s)
τ_H	Hershel-Bulkley yield stress (Pa)
α_0	High shear rate viscosity or Bingham viscosity ($Pa.s^n$)
η_{IR}	Infinite-rate viscosity ($Pa.s^n$)
$\eta_{\lim}$	Limit viscosity (mPa.s)
$\eta_{\max}$	Maximum viscosity ($Pa.s^n$)
$\eta_{\min}$	Minimum viscosity ($Pa.s^n$)
n	Power law index

η_p	Pseudoplastic viscosity (Pa.s^n)
$\dot{\gamma}$	Shear rate (s^{-1})
τ	Shear stress (Pa)
C_p	Specific heat (J.kg^{-1}.K^{-1})
λ	Thermal conductivity (W.m^{-1}.K^{-1})
τ_0	Yield stress (Pa)
τ_{dyn}	Yield stress obtained by dynamic measurements (Pa)
τ_{flow}	Yield stress obtained by flow measurements (Pa)
η	Viscosity (Pa.s^n)

1. Introduction

The development of renewable and sustainable energies is generally growing in relation to the current context, particularly the depletion of fossil fuels and the need to limit the negative effects on the environment. Anaerobic digestion is one of the existing options. Indeed, this process makes it possible to produce a biogas rich in methane while respecting the natural carbon cycle. In addition, the raw material required is none other than organic waste. This solution also allows to manage a whole category of waste and thus to promote it energetically. This permits to solve two problems at the same time. The digesters, units necessary for anaerobic digestion have been existing for a long time. Originally, they were mainly used for the treatment of agricultural waste (manure and green waste) and wastewater, but they are nowadays studied for the treatment of other wastes such as food remains but also for cases of co-digestion of different waste. In addition, the current interest is mainly to guarantee both the quality and the quantity of biogas produced. Thus, numerical models are developed in order to understand the existing digesters but also to optimise future digester configurations. The general model for the conversion of biomass into biogas is the IWA ADM1 [30] which is based on mass transfers. Some authors proposed modified ADM1 and ADM2 models will probably be developed [31], based on modifications provided to the ADM1 model. However, given the industrialisation of this process, parameters such as mixing and pumping strategies, which require energy, must be optimised. These parameters are all the more important since solid-state digestion is gaining importance considering the treated waste, and whose interests are savings in water. Zhou and Wen (2019) highlighted that the number of publications with keywords “solid-state anaerobic digestion” has a major increase in interest in this area [36]. All these aspects, including the growing need for accurate flow simulations [8], justify the use of CFD. Indeed, Van Hulle and al. (2014) showed that at pilot scale (120 L), the mixing conditions (mixing and non-mixing conditions) impact the methane production due to VFA accumulation [8]. Indeed, the mixing drives mass and heat transfer through the digestion medium, thus the physicochemical and biological reactions. CFD enables the study of the fluid flow, with greater detail and accuracy [37]. The appropriate model varies according to the waste nature. The knowledge of the waste rheology is necessary for the CFD modelling of all of the type of waste. Moreover, the choice of the turbulence models adapted to the problem dealt with is significant. Indeed, an important condition is the contact between biomass and substrate thanks to mixing [37]. Therefore, turbulence becomes a crucial factor [37].

This paper is thus organised in the following way, the first part concerns the rheological models and the literature data used in rheological models of various waste (vinasse, wastewater, sludges, manures and biowaste). Next, the second part addresses the existing global models on anaerobic digestion with the kinetic models. Then, in the third part, we present a review on the CFD models, going through the model objectives, the numerical methods, the turbulence modelling and the meshing approach of stirred tanks. Hereafter, the thermal models are presented. Lastly, the contribution and future interests of CFD in numerical modelling are discussed.

2. The substrates physical properties used in rheological models

Björn et al. (2018) studied the relationship between the rheological properties of 12 full-scale continuous stirred-tank biogas reactors and operational conditions [38]. Both mono-digestion and co-digestion under mesophilic and thermophilic conditions were studied [38]. They studied various feedstocks: sewage sludge, primary and biological sewage sludge, FIW, whey, fodder residues, manure, starch, fat,

OFMSW, and SHW [38]. The authors found correlation between TVS content and the apparent viscosity (shear rate of 20 s^{-1}) and limit viscosity of reactor with sewage sludge substrate [38]. Moreover, they also found correlation between TS content and limit viscosity, in the case of thermophilic co-digestion reactors [38]. They did not found correlations in the case of mesophilic mono-digestion [38]. Thereby, the authors warn us about the necessary consideration of the operating conditions of continuously stirred digesters in the study of the rheology of digestion media [38]. Consequently, in this section, a review on the modelling of waste rheology is presented. A literature data about various waste (vinasse, sewage sludges, manures and other biowaste) rheological properties are compiled, specifying operational conditions. The data presented are thus valid for specific cases and additional studies must be carried out if the conditions change.

2.1. Wastewater

Some authors characterised the vinasse as a Newtonian fluid [39–41]. We show in the **Table 1** the dynamic viscosity of the vinasse.

Table 1: Dynamic viscosity of vinasse

Source	Substrate	ρ (kg.m^{-3})	η_{dyn} (Pa.s)
[39]	Vinasse	1044.69	0.001 009 7
[42]	Sludge	999.66	0.065

In another study, the vinasse is characterised by the Herschel-Bulkley model [41]. The authors also show that the flow behaviour index approaches the Newtonian behaviour [41]. The **Table 2** presents the yield stress, and the parameters of the models at different temperature.

Table 2: Herschel-Bulkley model parameters of vinasse [41]

T (°C)	τ_0 (Pa)	k (Pa.s^n)	n
20	0.11177	$1.774.10^3$	1.1
25	0.10537	$1.68.10^3$	1.08
30	0.0998	$1.479.10^3$	1.05
35	0.08950	$1.392.10^3$	1.01

In a study conducted by Chacua et al. (2016), it has been shown that vinasse has a pseudoplastic behaviour for temperatures between 10 and 20°C [43]. Indeed, when the temperature is superior to 30°C, the power-law index is close to 1, indicating an approach to the Newtonian model [43]. In the **Table 3**, we show power-law model parameters [43].

Table 3: Power-law model parameters (sugarcane vinasse) [43]

Soluble solids content (°Brix)	T (°C)	k (Pa.s^n)	n
44	20	0.04	0.89
60		0.40	0.74
44	30	0.03	1.09
60		0.18	1.02
44	40	0.02	1.12
60		0.11	1.01

Yu et al. (2013), developed a multiphase model of settling and suspension in anaerobic digester. They made assumptions for the three phases. Concerning the liquid phase (wastewater), they considered the same properties of water at 35°C which is a Newtonian fluid [44]. This assumption is valid when TS is inferior to 1% in the liquid phase [44]. They highlighted that, depending on TS content, the fluid is Newtonian or non-Newtonian [44]. Thus, the shear stress equation for a non-compressive Newtonian fluid could not be suitable for wastewater with high concentration of colloidal solids [44].

2.2. Sludges

In this part, the experimental studies on sludge rheology measurements and models used by various authors are presented. The rheological data used in CFD modelling are also presented.

In 2008, experimental studies were performed to determine the pseudoplastic viscosity and the power-law index [45]. These parameters are related in the **Table 4** [45]. The authors used equations to describe the relationships between the viscosity coefficients and the solid concentration [45]. The two equations describing the relationships are [45]:

$$\mu_p = 0.018e^{0.071X} \quad (38)$$

$$n = 0.68e^{-0.0069X} \quad (39)$$

Table 4: Anaerobic digestion sludge rheological properties in Pseudoplastic model (non-Newtonian)

Data source	Sludge Concentration (kg.m^{-3})	η_p (Pa.s^n)	n
[45]	19	0.085	0.58
	63	1.80	0.43
	72	3.0	0.41

In 2013, Ratkovich et al. did a review on the data collection and modelling of activated sludge [46]. This work consisted in reviewing the measurements and experimental protocols, used to study the rheology of sludge [46]. As the authors pointed out, the quality and validity of the models resulting from rheological measurements depends on the accuracy of the experimental measurements and protocols [46]. Thus the authors did a critical analysis of the protocols and models found in literature [46]. The authors warn us about the precautions to take when using a model, they advise us to verify that the model has been developed properly [46].

Baudez et al. (2013) carried out a study on the impact of temperature on the rheological behaviour of anaerobic digested sludge [47]. The authors did rheological experimental measurements at different temperatures: 10°C, 25°C, 40°C and 60°C [47]. The viscosity and the yield stress decrease with the temperature increasing [47]. They also showed that the rheological behaviour is irreversibly modified by the thermal history [47]. Craig et al. (2013) did CFD simulations of anaerobic digester with variable sewage sludge rheology [48]. The **Table 5** shows the rheological properties used in different models.

Baroutian et al. (2013) carried out rheological measurements on a mixture of primary and secondary sewage sludge with the aim of studying the impact of solid concentration and temperature [49]. They used the Hershel-Bulkley model because it allows to study the rheogram on the complete range of shear rate while the Ostwald model only allows rheogram to be studied in the case of the modelling of the shear-thinning zone [49]. The authors concluded that the Hershel-Bulkley model fits well with the

experimental data [49]. Moreover, the solid concentration and the temperature have a significant impact on the yield stress and the model parameters [49].

Table 5: Sludge rheological properties used in Hershel-Bulkley model

Model using data	T (°C)	TS (%)	Sludge age (days)	k (Pa.s^n)	n	$\dot{\gamma}_c$ (s^{-1})	τ_0 (Pa)
[48]		3-4	0	0.5	0.5	0	0.9
		3-4	0	0.75	0.66	0.01	0.7
		3-4	40	0.0017	1.15	0.01	0.3
[47, 50]	25	1.85	-	0.169	0.308	0.01-30	0.092
[47]		2.55	-	0.436	0.308	0.01-30	0.293
		3.25	-	0.905	0.308	0.01-q30	0.711
		4.90	-	2.769	0.308	0.01-30	2.300

Lotito and Lotito (2014) carried out rheological measurements on sewage sludge in the aim to design pump [51]. The measurements were done at different solid concentrations (1.69 to 9.35% for anaerobically digested sludge, 3.37 to 12.16% for raw mixed sludge and 1.30 to 7.55% for return activated sludge) and different temperature (10 to 30°C) [51]. The Bingham model was used and the Ostwald model provided good correlation coefficients [51]. The authors concluded that the yield stress and consistency coefficient increased with TS concentration and decreased with temperature [51]. Moreover, they suggested that the raw mixed sludge would be pumped most easily and the return activated sludge the less easily [51]. The coefficients of the three sludge studied at 30°C are shown in the **Table 6** [51].

Table 6: Bingham coefficients and thixotropy at 30°C [51]

Sludge	TS (%)	τ_0 (Pa)	k (Pa.s^n)	Thix (Pa.s^{-1})
Anaerobically digested sludge	1.69	0.518	0.0065	22.18
	3.48	4.365	0.0185	95.67
	5.07	11.04	0.0500	153.3
	6.39	28.87	0.0841	315.3
	7.96	44.92	0.1165	1197
	9.35	85.30	0.1129	2260
Raw mixed sludge	3.37	0.920	0.0084	6.416
	5.07	4.103	0.0189	51.06
	7.43	9.140	0.0253	147.6
	9.02	24.46	0.0362	506.4
	9.66	36.92	0.0619	864.8
	12.16	62.10	0.0663	2311
Return activated sludge	1.30	1.195	0.0092	5.446
	3.50	13.97	0.0547	308.0
	4.88	34.88	0.0913	633.8
	5.88	48.56	0.1193	1620
	7.55	120.5	0.1524	3990

Jiang et al. (2014) published a paper on the characteristics of highly concentrated anaerobic digested sludge with TS upper to 8% [52]. The impact of TS (8 to 16%) and temperature (35, 55 and 70°C) were studied [52]. The Hershel-Bulkley model was used to model the sludge rheology [52]. The authors

concluded that the sludge rheology is more impacted by the TS than the temperature [52]. The **Table 7** presents the yield stress obtained by flow and dynamic measurements [52].

Table 7: Yield stress obtained by flow and dynamic measurements [52]

TS (%)	τ_{flow} (Pa)	τ_{dyn} (Pa)
8	25.3	35
10	81	91
13	171	300
16	319.2	420

Dai et al. (2014) studied the rheology evolution of sludge through high-solid anaerobic digestion [53]. The influence of the SRT and the temperature were studied [53]. The authors also used the Hershel-Bulkley model [53]. In conclusion, shear stress, viscosity, yield stress, consistency index are lower and flow index is higher with longer SRT [53]. Furthermore, the TS of the thermophilic digester is higher than the TS of the mesophilic digester, but has a better flowability [53]. The authors said that the sludge rheology could be a controlling parameter of anaerobic digestion process [53].

Table 8: Rheological properties and models [54]

Digested substrate	TS (%)	Viscosity curve behaviour	η_{dyn} (mPa.s)	$\eta_{\lim}$ (mPa.s)
Slaughter house waste	3.9	Viscoplastic	18	6
Biosludge paper mill industry1	3.8	Thixotropic	436	8
Biosludge paper mill industry2	3.7	Viscoplastic	267	29
Wheat stillage	3.0	Pseudoplastic or viscoplastic	33	6
Cereal residues	7.7	Viscoplastic	443	36

Table 9: Obtained results from mathematical modelling of rheogram data [54]

Digested substrate	Herschel-Bulkley				Ostwald			Bingham	
	τ_0 (Pa)	n	k (Pa.s^n)	R^2	n	k (Pa.s^n)	R^2	τ_0 (Pa)	R^2
Slaughter house waste	0.24	1.06	0.003	0.93	0.69	0.35	0.8	0.21	0.92
Biosludge paper mill industry1	2.57	3.40	5.10^{-10}	0.45	0.08	2.28	0.002	1.88	0.12
Biosludge paper mill industry2	2.89	0.59	0.42	0.99	0.44	1.23	0.99	6.36	0.95
Wheat stillage	0	0.65	0.04	0.88	0.64	0.04	0.87	0.33	0.95
Cereal residues	2.38	0.49	0.98	0.96	0.39	1.98	0.96	8.31	0.91

Farno et al. (2014) studied the impact of temperature and thermal history (20°C to 80°C, then to 20°C) on the sludge rheology [55]. The authors concluded that the changes in temperature, previously cited, affect irreversibly the rheology and the yield stress [55]. Moreover, a proportionality was found between the soluble COD and the yield stress and infinite viscosity [55]. Next, Farno et al. (2015) studied the impact of temperature and duration of thermal treatment on anaerobic digested sludge [56]. The authors used a modified Hershel-Bulkley model by coupling the Herschel–Bulkley and Bingham model, developed by [47, 56]:

$$\tau = \tau_{HO} + \alpha_0 \dot{\gamma} + k\dot{\gamma}^n \quad (40)$$

Where τ / τ_{HO} is dimensionless shear stress. A new model for the prediction of yield stress and apparent viscosity at various temperatures and thermal histories is proposed [56]. Moreover, the variation of the yield stress and the apparent viscosity of the digested sludge (in the case of thermal treatment) can be estimated by the soluble COD measurement [56].

In the CFD model developed by López-Jiménez et al. (2015), according to the sludge treated in a Wastewater treatment plant anaerobic digester, different TDS contents sludge were used in simulations: 2.5, 5.4 and 9.1 TDS. At the beginning, the fluid was considered Newtonian. The physical parameters are given in the **Table 1** [42]. This hypothesis was supported by viscosity measurements from a rotating viscometer [42]. The physical parameters are given in the **Table 5**. As a second assumption, the sludge was considered non-Newtonian, the rheological properties used in the CFD model are those of liquid manure given in the **Table 17** [42].

According to the study conducted by Hong et al. (2015), the solid concentration, the temperature, and the sludge age affect the viscosity, the yield stress, the flow index and the flow consistency [57]. The authors also noted that a low temperature storage (4°C), thus the sludge age, affected the sludge rheology [57]. Moreover, they tested various rheological models: Bingham, power law (Ostwald), Herschel-Bulkley, Casson, Sisko, Careau and Cross models [57]. They concluded that the Bingham plastic and Sisko models best fitted with experimental data [57]. The yield stress and viscosity (Bingham model), and the infinite-rate viscosity, flow consistency index and flow index (Sisko model) for different temperature are shown in the **Table 10**. The **Table 11** presents the rheological parameters of sludge for different sludge age. The **Table 12** presents the yields and the viscosity for varying TS.

Table 10: Yield stress and viscosity (Bingham model), and the infinite-rate viscosity, flow consistency index and flow index (Sisko model) for different temperature [57]

T (°C)	Bingham model		Sisko model		
	τ_0 (Pa)	η (Pa.s)	η_{IR} (Pa.s)	FCI (s)	FI
25	6.8	0.02	0.02	3	0.2
30	7.9	0.02	0.02	5	0.1
35	8	0.02	0.01	3	0.2
40	5.8	0.02	0.02	4	0.1
55	4.5	0.01	0.01	2	0.2

Table 11: Yield stress and viscosity (Bingham model), and the infinite-rate viscosity, flow consistency index and flow index (Sisko model) for different sludge age [57]

Days	TS (g.L^{-1})	VS (g.L^{-1})	Bingham model		Sisko model		
			τ_0 (Pa)	η (Pa.s)	η_{IR} (Pa.s)	FCI (s)	FI
1	29	25.4	5.8	0.020	0.02	3.9	0.3
15	28	24.9	6.1	0.019	0.01	1.9	0.1
32	25	21.65	4.9	0.016	0.01	2.2	0.2

Table 12: Yield stress and viscosity for different TS [57]

TS (g.L^{-1})	Rheological model	τ_0 (Pa)	η (Pa.s)	n	R^2
30	Casson	4.6	0.010	-	0.99
	Bingham	7.4	0.021	-	0.98

	Power	-	1.100	0.46	0.94
25	Casson	0.8	0.017	-	0.99
	Bingham	2.1	0.024	-	0.97
	Power	-	0.154	0.73	0.99
20	Casson	0.3	0.015	-	0.98
	Bingham	1.1	0.018	-	0.98
	Power	-	0.061	0.83	0.99

Seyssiecq et al. (2015) carried out in situ rheological characterisation of wastewater sludge in order to compare stirred bioreactor (helical ribbon impeller equipped with a rheometer) and pipe flow configurations [58]. The use of the two configurations is discussed in the paper [58]. The authors concluded that the Hershel-Bulkley model best fits with the experimental data obtained with the helical ribbon impeller [58]. Nonetheless, the measurements on suspensions were not consistent, and thus required an adjustment du to wall slip effect [58]. The model parameters are given in function of TSS concentration [58]. The principal interest of in situ characterisation is to overcome the effects of the study of a sample, especially since it will not necessarily be representative of the medium in the case of heterogeneous fluid. Moreover, this method facilitates the study of the medium during digestion process in real time.

Cheng and Li (2015) studied the rheological behaviour of sewage sludge with TS content ranging from 2 to 15% [59]. They found that the influence of organic content was non-significant at low TS (inferior to 6%) [59]. A new model was developed, combining the exponential model and power model in order to describe the relation between TS, shear rate and viscosity of the high solids sludge [59].

Eshtiaghi et al. (2016) carried out a study on the prediction of apparent viscosity and yield stress of digested and secondary sludge mixtures [60]. The sludge studied (1.4 to 7% TS) were chosen because it can be treated in anaerobic digester [60]. A master curve was developed in order to predict the sludge flow behaviour independently of TS concentration [60].

Feng et al. (2016) studied the rheological behavior of the sludge in an anaerobic digester (105 days) [61]. The Herschel-Bulkley model, the Bingham Law equation and the Power-Law equation were compared [61]. The Herschel-Bulkley model best fitted [61]. The authors observed that the TSS concentration influenced the viscosity [61].

Al-Dawery (2016) studied the effects of suspended solid and polyelectrolyte on the settling and the rheological properties of municipal activated sludge [62]. The authors used the Bingham model [62]. They concluded that yield stress and limit viscosity increased with the increase of TS and the limit viscosity is strongly dependent on TS [62].

Zhang et al. (2016) studied the variation of the rheological characteristics of high-solid (15-20% TS) municipal sludge during the anaerobic digestion process [63]. The two-part Hershel-Bulkley model was used to characterise the rheological behaviour of the sludge [63]. The model parameters at different stage of digestion are given in the paper [63]. The authors observed that the yield stress, viscosity, and critical shear rate decreased with the digestion [63].

Cao et al. (2016) studied the rheology of municipal sewage sludge (with and without anaerobic digestion) [64]. The authors performed rheological measurements at 20, 35 and 55°C, and at TS concentration from 4 to 10% [64]. In this study, the authors compared three rheological models (Ostwald

de Waele, Herschel-Bulkley and Bingham), and found that Ostwald de Waele model best fitted with experimental data [64]. The authors concluded that the TS concentration and temperature impacted sludge rheology critically [64].

Markis et al. (2016) established an equation to predict the viscosity in function of the pH [65]. The authors worked on various mixtures of primary, secondary and anaerobically digested sewage sludge [65]. The equation developed is [65]:

$$\eta = -0.0135pH^2 + 0.1965pH - 0.667 \quad (41)$$

The authors [65] used a dimensionless Hershel-Bulkley form, developed by Markis et al. (2014) [66]. In this paper, the authors studied the impact of TS content on the viscosity of the sludge [66]. The study showed that the apparent viscosity, the yield stress and the fluid consistency increased with the increasing of TS concentration [66].

Hong et al. (2017) showed that the yield stress and the viscosity of digested sludge increased with the increasing of TS and VS concentration [67]. Moreover, Hii et al. (2017) showed that the treated sludge viscosity and the yield stress decrease linearly with temperature [68]. Furthermore, the soluble COD has linear correlation with yield stress and apparent viscosity [68]. The authors used the Hershel-Bulkley model and gave the calculated parameters [68].

Liang et al. (2017) proposed a protocol of uniaxial compression test for studying the transition between solid and fluid behaviour of sludge (TS around 20%) [69]. They studied various samples: raw sludge, six days aging sludge, 5 min mixing sludge and 20 min mixing sludge [69]. It was found that the viscosity and yield stress are the most sensitive rheological factors to operational conditions [69]. The impact of the aging and the mixing of sludge is a decrease of the viscosity and the yield stress with an increase of the adhesive effect [69].

Abbà et al. (2017) studied the rheology and microbiology of sludge from a thermophilic aerobic membrane reactor [70]. The Hershel-Bulkley model fitted with experimental data [70]. In this work, the authors studied the influence of pH, aeration, temperature and suspended solid concentration (biomass concentration) on rheological behaviour of sludge [70].

Bobade et al. (2017) studied the impact of gas injection on the apparent viscosity and viscoelastic property of waste activated sewage sludge [71]. In another study published in 2018, the authors proposed a linear relationship between the change of viscoelastic properties and the change of other physiochemical properties [72].

Gienau et al. (2018) carried out study on the rheological characterisation of 16 anaerobic sludge from agricultural and bio-waste biogas plants [73]. The power-law equation was used to describe the rheological behaviour and the Arrhenius law was used for the temperature dependency [73]. The authors highlighted that the temperature-dependent rheology is essential for engineering utilisations such as pressure drops, agitators and pumps design [73].

Cao et al. (2018) studied the effect of TSS content and heat and anaerobic digestion treatments on the rheological properties of municipal sludge [74]. They found that the sludge exhibits shear-thinning behaviour [74]. The viscosity of the anaerobically digested sludge is the lowest, then it is fresh mixed sludge and the most viscous is the thermal hydrolysed sludge [74]. The Hershel-Bulkley model fits well with the experimental results [74].

Björn et al. (2018) studied the rheology of sewage sludge [38]. They found that the Bingham model, the Ostwald model and the Hershel-Bulkley model fitted with experimental data, depending on the sample [38]. The rheological models and parameters are shown in the **Table 13**.

Table 13: Rheological models and parameters of primary and biological sewage sludge [38]

TS (%)	TVS (%)	T (°C)	WV (m^3)	Rheological model	τ_0 (Pa)	k (Pa.s)	n	R^2
2.4	1.6	51-53	1.70	Ostwald	-	0.1900	0.4627	0.48
				Bingham	0.6404	0.0047	-	0.90
3.0	1.8	36-38	2.00	Ostwald	-	0.3377	0.4448	0.98
				Hershel-Bulkley	0.9130	0.0372	0.7479	0.96
3.9	2.4	36-38		Ostwald	1.8640	0.1559	0.6128	0.97
				Hershel-Bulkley	1.5385	0.0913	0.6862	0.98

2.1. Manure

Achkari-Begdouri and Goodrich (1992) carried out rheological measurements on Moroccan dairy cattle manure at different TS content and temperature [75]. They studied this fluid between 2.5 and 12.1% TS and from 20 to 60°C [75]. We present in the **Table 17** the rheological parameters k and n for different TS content at 35°C [75]. The consistency coefficient k and the power-law index n of liquid manure are expressed [75–77]:

$$k = \left[8.722e^{\left(4830/T + 0.58319 \times TS\right)} \right] \times 10^{-10} \tag{42}$$

$$n = 0.6894 + 0.0046831 \times \left(T - 273\right) - 0.042813 \times TS \tag{43}$$

The density, the specific heat and thermal conductivity are expressed [75, 76, 78, 79]:

$$C_p = 4187.5 - 28.9 \times TS \tag{44}$$

$$\lambda = 0.6173 - 0.0069 \times TS \tag{45}$$

$$\rho = 0.0367 \times TS^3 - 2.38 \times TS^2 + 14.6 \times TS + 1000 \tag{46}$$

Rheological properties of liquid manure are dependent on TS [79]. Moreover, viscosity and shear stress increase exponentially with the increase of TS [79]. The authors used non-linear regression technique to get the following relations [79]:

$$\eta = 0.001e^{0.462TS} \tag{47}$$

$$\tau = 0.157e^{0.462TS} \tag{48}$$

The rheological properties used in this study are shown in the **Table 17**. (Bakker et al., 2009) carried out numerical modelling of non-Newtonian slurry, using Hershel-Bulkley and Bingham models [80]. We show in the **Table 14**, the rheological properties used in the models for the simulations [80].

Table 14: Bindura nickel ore slurry rheological properties used in Hershel-Bulkley and Bingham models [80]

Model	wf %	k (Pa.s)	n	ρ ($kg.m^{-3}$)	τ_0 (Pa)
Hershel-Bulkley	40	0.439	0.34	1364	0.456

	50	2.130	0.323	1500	2.130
	50	3.774	0.565	1667	3.774
Bingham	40	$6.79.10^{-3}$	-	-	1.945
	50	$1.47.10^{-2}$	-	-	8.189
	50	$7.42.10^{-2}$	-	-	52.180

Thota Radhakrishnan et al. (2018) studied the rheology of two types of slurries using a narrow gap couette rheometer: black water (consisting of human faecal waste, urine, and flushed water from vacuum toilets) (sample 1) and black water with ground kitchen waste (sample 2) [81]. Depending on the percentage of TSS, the slurry rheological behaviour is described by the Hershel-Bulkley model, the Bingham model or the linear model [81]. The viscosity increases with increase in TSS concentration and decreases with increase of temperature [81]. The authors concluded that the Hershel-Bulkley model best suits. The physical properties (at 30°C) are related in the **Tables 15** and **16**. In their model, Wu (2010) considered that the manure slurry exhibits non-Newtonian pseudo-plastic fluid behaviour when TS is superior to 2.5% [82]. The rheological properties of liquid manure are presented in the **Table 17.**

Table 15: Slurry rheological properties at 30°C (sample 1) [81]

Model	TSS (%)	k (Pa.s^n)	n	τ_0 (Pa)
Hershel-Bulkley	11.2	0.9462	0.45	1.07
	10	0.28666	0.56	0.803
	7.2	0.08741	0.65	0.325
	5	0.02123	0.78	0.135
	3.9	0.01187	0.82	0.073
	3.2	0.00764	0.87	0.053
Bingham	2.6	0.00293	1	0.052
	1.8	0.00223	1	0.011
Linear	1.4	0.00204	1	0
	0.7	0.00152	1	0
	0.4	0.00125	1	0

Table 16: Slurry rheological properties at 30°C (sample 2) [81]

Model	TSS (%)	k (Pa.s^n)	n	τ_0 (Pa)
Hershel-Bulkley	3	0.01021	0.85	0.054
Bingham	2.6	0.00343	1	0.074
	2.1	0.00303	1	0.061
	1.8	0.00278	1	0.044
	1.2	0.00244	1	0.035
	1	0.00227	1	0.023
Linear	0.8	0.00159	1	0

Table 17: Liquid manure rheological parameters used in Pseudoplastic model [10, 42, 75, 76, 78, 79, 82–84]

TS (%)	Manure type	T (°C)	k (Pa.s^n)	n	$\dot{\gamma}$ (s^{-1})	ρ (kg.m^{-3})	η_{min} (Pa.s)	η_{max} (Pa.s)	C_p (J/kg.K)	λ (W/(m.K)
2.5	DC	35	0.042	0.710	226-702	1000.36	0.006	0.008	4186.78	0.6171
5.4		35	0.192	0.562	50-702	1000.78	0.01	0.03	4185.94	0.6169
7.5		35	0.525	0.533	11-399	1001.00	0.03	0.17	4185.33	0.6168
8.9		17-24	2.6	0.42	-	-	-	-	-	-
9.1		35	1.052	0.467	11-156	1001.31	0.07	0.29	4184.87	0.6167
12.1			5.885	0.367	3-149	1001.73	0.25	2.93	4184.00	0.6165
10	DC	17-24	5.3	0.11	0.90-23.90	999.6	-	-	-	-
	S		2.7	0.33	0.90-23.90	1008.3	-	-	-	-
	P		8.9	0.29	0.96-24.14	1036.5	-	-	-	-
	Pi		2.2	0.21	0.90-23.90	1025.7	-	-	-	-
	DC	35	16.1	0.348	-	-	-	-	-	-
		40	16.7	0.325	-	-	-	-	-	-
		50	13.0	0.332	-	-	-	-	-	-
14.2	DC	17-24	22.9	0.41	-	-	-	-	-	-
15	DC	17-24	31.3	0.3	0.61-24.37	973	3.35	44.24	4183.17	0.6163
	S		19.4	0.29	0.70-23.90	965.1	2.04	24.99	4183.17	0.6163
	P		2.4	0.38	0.80-23.90	1063.6	0.34	2.76	4183.17	0.6163
	Pi		2.4	0.38	0.96-23.90	967.7	0.34	2.46	4183.17	0.6163
20	P		35.4	0.29	0.64-24.14	1091.8	3.69	48.6	4181.72	0.6159
	Pi		56.8	0.35	0.24-23.90	1090	7.22	143.62	4181.72	0.6159
	-	35	56.8	0.35	0.24-23.90	1090	34.47	172.5	-	-

(DC=dairy cattle, S=sheep, P=poultry, Pi=pig).

2.2. Other types of biowaste

There is very little research on the rheology of solid waste such as food waste. However anaerobic digestion of biowaste is worthwhile. (Diamante and Umemoto, 2015) presented a review on the rheological properties of fruits and vegetables [85]. The corresponding models and source to specific categories of waste are presented in the **Table 18.**

Table 18: Rheological models of fruits and vegetables

Model	Waste	Source
Hershel-Bulkley	Berry fruits products	[86–90]
	Stone fruits	[90–97]
	Coriander puree	[98]
	Mint puree	[98]
	Tamarind juice	[99]
	Tomato juice	[100, 101]
Power-Law	Citrus fruit juice	[102, 103]
	Kiwifruit juice	[102]
	Guava products	[104, 105]
	Fenugreek paste	[106]
	Tomato ketchup	[107]
Bingham	Sloe juice	[96]
	Pineapple juice	[108]
Newtonian	Cherry juice	[92]
	Carrot juice	[109]
	Apple juice	[91, 110]
	Pear juice	[103, 110]

A study was conducted in 2017 in order to characterise treated and non-treated putrescible food waste [111]. In this study, the authors worked on anaerobically digested and diluted carbohydrates, vegetables & fruits, and meat samples [111]. Rheological measurements were performed at different temperature (25, 35 and 45°C) using a model ARG2 stress-controlled rotational rheometer (TA Instrument Ltd, US) [111]. They concluded that food waste exhibits shear-thinning flow behaviour; viscosity is a function of temperature and composition; the composition affects the flow properties; at a given temperature, the viscosity decreased as the carbohydrate proportion increased, thus the high water content of vegetable and fruits (or TS) is a key controlling factor of the rheology; and the Hershel-Bulkley model is used to characterise the food waste flow behaviour [111].

Björn et al. (2018) studied the rheology of full-scale digester feedstocks, in mesophilic and thermophilic conditions [38]. The rheological models and parameters are shown in the **Table 19.**

Table 19: Rheological models and parameters [38]

Feedstock	WV (m^3)	TS (%)	TVS (%)	T (°C)	Rheological model	τ_0 (Pa)	k (Pa.s)	n	R^2
OFMSW (62%), SHW (9%), fodder residues (13%), na (16%)	3.20	2.7	1.6	52-55	Ostwald	-	0.0000	2.0831	0.97
					Ostwald	-	0.0000	2.2345	0.89
		3.6	1.8		Ostwald	-	0.0000	1.8681	0.99
					Ostwald	-	0.0000	2.0276	0.94
SHW (45%), Manure (29%), whey (14%), fat (12%)	1.70	5.0	3.8	51-53	Ostwald	-	0.0001	1.5865	0.92
					Ostwald	-	0.0003	1.4265	0.93
OFMSW (23%), SHW (45%), Manure (32%)	6.50	3.9	2.8	37	Bingham	0.1394	0.0074	-	0.96
					Bingham	0.4527	0.0102	-	0.95
OFMSW/SHW (32%), Manure (68%)	2.25	4.0	2.9	38	Hershel-Bulkley	0.3322	0.0001	1.5581	0.69
		3.5	2.5		Ostwald	-	0.0001	1.6643	0.98
		4.0	2.9		Ostwald	-	0.0007	1.2796	0.70
OFMSW (57%), SHW (12%), starch (21%), na* (10%)	2.90	4.2	2.5	37	Hershel-Bulkley	1.2207	0.0370	0.7618	0.71
					Hershel-Bulkley	0.5489	0.0193	0.8754	0.99
		4.1	2.5		Bingham	3.4542	0.0068	-	0.52
					Hershel-Bulkley	1.0244	0.0227	0.8519	0.91
OFMSW (95%), fat (5%)	1.10	2.1	1.5	53	Ostwald	-	0.0000	1.9554	0.90
SHW (in majority), FIW	na	5.3	3.8	37	Bingham	0.8060	0.0119	-	0.95

* Information not available.

2.3. Gas

The physical properties of the biogas used in the CFD model developed by (Yu et al., 2013) are presented in the **Table 20.**

Table 20: Gas rheological properties

Source	ρ (kg.m^{-3})	η (Pa.s)	Bubble diameter (mm)
[44]	1.139	1.9.10-5	0.1

3. Global models: kinetic models

Anaerobic digesters are subject to various instabilities that can lead to process failure. On an industrial scale, the consequence can go as far as stopping the digester and sludge or chemicals addition to relaunch the unit. As the costs generated are very important, it is essential to put in place strategies to avoid malfunctions. Models are thus developed in order to adapt the industrial parameters (hydraulic residence time, applied organic load, agitation, etc.) according to the composition of the inputs. For this reason, research on the biochemical modeling of anaerobic digestion and the adaptation of models to various substrates are carried out. In this part, we present the evolution of biochemical models of anaerobic digestion. Their improvements, leading to the development of more and more complex models, are possible thanks to measurements of intermediate products and kinetics of reactions.

A review on the modelling of anaerobic digestion was published by Lyberatos and Skiadas (1999). This review addresses the mathematical models developed before 1999 [112]. The first models were limited to the modeling of the rate-limiting step, also called the rate-determining step, which is the slowest [112, 113]. However, depending of parameters, such as hydraulic loading rate, temperature and so on, the rate-limiting step is not always the same [112]. This is how various models are developed, based on different rate-limiting step [112]. Thus, the author pointed out that in considering the limiting-step hypothesis, we obtain simple and readily models, but the models do not describe very well the digester behaviour [112]. The limiting-step considered in literature are the hydrolysis, the acetogenesis and the methanogenesis [112]. Depending of the models, different inhibitions are taken into account, the different key parameters are the unionised VFA, the unionised NH_3, the unionised acetate, the toxic substances, the total VFA, the H_2 partial pressure, the unionised propionate and butyrate and the pH [112]. The different developed models are adapted to various substrates: soluble organics matter, animal waste, easily fermentable substrates, biodegradable organic particulate, glucose and soluble carbohydrates [112].

Andrew and Graef developed a dynamic model of anaerobic digestion [114]. The methanogenesis was considered as the rate-limiting step [114]. They integrated an inhibition function for volatile acids concentration and specific growth rate for methanogens [114]. The unionized acid as the growth limiting substrate and inhibiting agent were considered [114]. Finally, the consideration of the interactions between the liquid phase, the gas and the biological phases was included. Then, Graef and Andrews (1974) added an expression for organism death due to a conservative toxic agent [115]. The unionised VFA inhibition was accounted [112, 115].

Hill and Barth (1977) included a group of hydrolytic bacteria to consider the degradation of the soluble substrate into acetic acid [113]. The model is suitable for animal waste anaerobic digestion [113]. The formation of gases, the carbonate equilibrium and the nitrogen balance were added [113]. The

mathematical model predicted the percent of methane, the percent of carbon dioxide and the percent of ammonia [113]. The authors considered two microbial culture model, composed of the acid-formers (facultative heterotrophs) and the methane-formers (obligate anaerobes) [113]. They took into account the inhibitions due to unionised VFA and unionised NH_3 [112, 113]. Furthermore, the kinetics is in function of process temperature [112, 113].

Thanks to advances in microbiology, Hill (1982) developed a more complete model which considered the acidogenesis; the acetogenesis, the homoacetogenesis and the methanogenesis steps [116]. The H_2 methanogenic archaea and the acetate methanogenic archaea were considered separately [112, 116]. The acetogenesis was the limiting-step [112, 116]. The inhibitions due to total VFAs concentrations were accounted [112, 116]. The model is valid for swine, dairy, beef and poultry manures [116].

Kleinstreuer and Poweigha (1982) developed a transient two-culture anaerobic digestion model [117], suitable for various substrates [112]. The acetogenesis and the methanogenesis were integrated in the model [117]. The mathematical model consisted in 11 coupled, non-linear first-order rate equations based on mass conservation and biochemical reaction kinetics [117]. The unionised acetate and toxic substances were accounted as inhibition at each reactions [112, 117]. Moreover, the kinetics is in function of process temperature and pH [112, 117].

Bryers (1985) considered the four chemical reactions of anaerobic digestion process and the acetogenesis as the limiting-step [112, 118]. The kinetics are modelled with the Monod model and the Monod kinetic is a function of pH for the methanogenesis step [112, 118]. The equations were transformed to a unit mass of COD [118]. His model is suitable to biodegradable organic particulate substrates [112]. Moletta et al. (1986) also considered a two-stages model with acidogenesis and methanogenesis [119]. The model is suitable for the digestion of easily fermentable substrates [112]. Moreover, as [113, 117], the inhibitory effects of the unionised acid concentration on microorganisms growth rate and the methane production from acetate were taken into account separately [119].

Afterwards, models using H_2 as control parameter are developed [112]. We find the model of Mosey (1983) [120] and Costello et al. (1991) [121]. They both modelled the acidogenesis, the acetogenesis and methanogenesis steps [112, 120, 121]. The acetogenesis was the limiting-step [112, 120, 121]. Concerning the bacterial groups, they both took into account the acid-forming bacteria, the propionic acid bacteria, the butyric acid bacteria, the acetoclastic methane archaea and the hydrogen-utilising archaea [112, 120, 121]. Costello et al. regarded in addition the lactic acid bacteria [112, 121].

Angelidaki et al. (1993) accounted more inhibition in their model of anaerobic digestion of cattle manure in continuously stirred tank reactor [122]. The inhibition due to total VFA, the acetate and free ammonia were taken into account [112, 122]. In addition, the pH and the temperature of the process were also accurately predicted because these two parameters strongly impact the free ammonia content [122]. The mathematical model is complex with the account of the enzymatic hydrolytic step, four bacterial steps and 12 chemical compounds [122]. The acetogenesis is the limiting step and the failure of the digester is predicted by the pH drop [112, 122].

Siegrist et al. (1993) developed a mathematical model for the mesophilic anaerobic digestion of sludge [123]. The hydrolysis, the fermentation of aminoacids and sugars anaerobic oxidation of fatty acids, the anaerobic oxidation of propionate, the acetate conversion to methane and the hydrogen conversion to methane were included in the model [112, 123]. The limiting step was the acetogenesis step [123] as

[122]. Furthermore, the inhibitions due to the H_2 partial pressure, the acetate, the pH and the free ammonia were considered in this model [112, 123].

Batstone et al. (2002) developed the ADM1, with the aim of developing a generalised anaerobic digestion model. The ADM1 considers the substrate composition, the kinetic of micro-organisms, the biochemical (cellular step: acidogenesis, acetogenesis of both VFAs and LCFAs and methanogenesis; extracellular step: disintegration and hydrolysis) and physico-chemical (ion association/dissociation, and gas-liquid transfer) processes and the inhibition phenomena. Precipitation phenomenon is not included in this model [30].

Keshtkar et al. (2003) developed a kinetic model for cattle manure which takes into account the mixing conditions of the digester [124]. Indeed, the authors highlighted that existing models consider optimum mixing conditions while imperfect mixing patterns are more common [124]. The authors are able to evaluate the effects of the hydraulic retention time, the composition of feed, the initial conditions of the reactor and the degree of mixing on process performance [124]. They concluded that mixing had significant effect on the reactor performance [124].

Wu et al. (2006) developed a three-dimensional model for the prediction of the biogas production of liquid manure [125]. The authors neglected the momentum and turbulence, considering very low flow rate [125]. The model is based on the mass conservation equation, the energy equation, the species transport equations and the chemical reaction equations [125]. The simulations results are validated with experimental data [125].

Lübken et al. (2007) used and modified the ADM1 for simulating the energy production from cattle manure and renewable energy crops [126]. The simulations showed that a continuous feeding has a negative effect on the net energy yield [126]. Moreover, the ratio of co-substrate to liquid manure impacted the energy production when the inflow load was split [126].

Yasui et al. (2008) proposed a modified ADM1 structure for the modelling of municipal primary sludge hydrolysis [127]. They considered a more elaborate particle disintegration/hydrolysis model for considering the degradation of large-sized particles, which requires disintegration before hydrolysis [127].

Ramirez et al. (2009) developed a modified ADM1 disintegration and hydrolysis structures for modelling batch thermophilic anaerobic digestion of thermally pre-treated waste activated sludge. The Contois model (1959) [128] was first introduced for the disintegration and the hydrolysis steps instead of first-order kinetics and the Hill function was used for modelling the ammonia inhibition of aceticlastic methanogens instead of a non-competitive function [129].

Fezzani and Ben Cheikh (2009) proposed an extension of ADM1 for including phenolic compounds biodegradation processes to simulate the anaerobic co-digestion of olive mill waste at thermophilic temperature. The general structure of the ADM1 was unchanged except for the modifications related to the inclusion of phenolic compounds degradation processes into acetate and into methane and CO_2. The impact of soluble phenolic compounds on the pH was considered in the pH simulation equations. The inhibitory effect of phenolic compounds on the fermenting process and methanogenic sub-populations was considered by the use of non-competitive inhibition functions [130].

Galí et al. (2009) developed a modified version of ADM1 for agro-waste [131]. Astals et al. (2011) proposed a modified ADM1 to model the co-digestion of pig manure and glycerine. It appeared useful to predict the methane production and the limitations related to the lack or excess of nitrogen [132]. Soda (2011) applied the modified ADM1 to long-term experiments for methane and hydrogen production from organic waste [133]. Antonopoulou et al. (2012) modelled the fermentative hydrogen production from sweet sorghum extract based on modified ADM1 which included lactate and ethanol among the metabolites [134].

Abbassi-Guendouz et al. (2012) studied anaerobic digestion at TS content ranging from 10 to 35% [135]. They noted a decrease in methane yields with the increase of the dry matter content from 10 to 25% [135]. Then, they noticed two different behaviours when increasing from 25 to 35% [135]. One of the digesters saw its production identical while the other encountered inhibitions of the process [135]. Thus, the authors take into account in the ADM1 model mass transfers, which explain the inhibitions of anaerobic digestion at significant dry matter levels [135]. The effect of the reduction of mass transfer is the reduction of the microbial hydrolysis rate [135]. A mass transfer coefficient was integrated, taking into account the difference between the diffusivity coefficient in the digestate and in water [135]. The authors recommended to carried more studies to understand the impact of TS content on the microbial community for both wet and dry anaerobic digestion [135].

Mottet et al. (2013) proposed a new model structure for the hydrolysis step [136] as (Yasui et al., 2008) [127]. They introduced the new model in the ADM1 to improve the representation of the bioaccessibility of particulate organic matter [136]. Two particulate organic matter fractions were determined: a readily hydrolysable fraction and a slowly hydrolysable fraction [136].

Hinken et al. (2014) developed a modified ADM1 to model an up-flow anaerobic sludge blanket reactor laboratory plant treating starch wastewater. Lactic acid fermentation (formation, degradation and inhibition processes) was added to ADM1 [137].

Batstone et al. (2015) presented a review on the application and future needs concerning the mathematical modelling of anaerobic digestion processes. They observed an increased demand on mathematical modelling in terms of complexity, particularly in anabolic processes, need to consider complex behaviour (distributed parameter and non-linear characteristics in space) and the need to better characterise inputs and their primary conversion processes, as well as supporting models such as the chemistry models [31].

Flores Alsina et al. (2015) proposed extensions to the ADM1 in order to describe the interactions among phosphorus, sulphur, iron and their potential effect on total biogas production (CO_2, CH_4, H_2 and H_2S) during sludge stabilisation processes in wastewater treatment plants [32].

Barrera et al. (2015) developed a modified ADM1 for the modelling of the anaerobic digestion of cane molasses vinasse, extending the ADM1 with sulphate reduction for a very high strength and sulphate rich wastewater [138]. The authors included volatile fatty acids (propionic and acetic acids) in the sulphate degradation reactions, hereby including an accurate prediction of the concentrations of total aqueous sulphide, free sulphides and gas phase sulphides [138].

Bai et al. (2015) developed a modified ADM1 to simulate substrate degradation and the influence of pH on VFAs production. They found that the Monod model best simulated the soluble protein and

carbohydrate degradation, whereas the Contois model best simulated the particle protein and carbohydrate degradation [139].

Xie et al. (2016) published a critical review of mathematical modelling on anaerobic co-digestion [140]. Compared to anaerobic digestion models, the transient variation in pH and inhibitory intermediates must be considered in the anaerobic co-digestion model [140]. Moreover, the conversion and distribution of sulphur, phosphorus, and nitrogen need to be developed in anaerobic co-digestion model [140].

Bai et al. (2017) developed a modified ADM1 for modelling free ammonia inhibition in anaerobic acidogenic fermentation with high-solid sludge [141]. The modification made to the model allows to simulate the VFA (acetate, propionate, butyrate and valerate) generation in batch, semi-continuous and full scale sludge [141]. The authors tested simple inhibition, Monod and non-inhibition forms [141]. The VFA accumulation were successfully simulated with the three models [141]. They concluded that the simple inhibition model provides accurate outcomes on VFA generation [141]. The predictions of the VFA production with the non-inhibition model are lower than in the experiments [141]. The Monod model was the better model in case of semi-continuous fermentation [141].

4. Local models: CFD modelling

4.1. Work Contributions

In this part, we expose the work contributions of CFD modelling studies. Indeed, this tool has been widely used for anaerobic digester or stirred tank flow modelling and process optimisation. The contributions are manifold. The **Figure 2** presents a histogram showing the number of work per contributions. Most of the work have been done on the mixing mode or design, the multiphase study and the effect of rheology and TS content. Other studies also include the dead zone study, the turbulent flow modelling, the bioreactor configuration, the settling and suspensions modelling and the scale-up effect. The **Table 21** shows the objectives of the CFD simulations carried out between 2005 and 2019 and the corresponding papers.

The mixing mode and design was the most studied aspect, with 34 papers between 2005 and 2019. It regroups the choice of mixing system (mechanical mixing, gas mixing or mechanical pumping) [142–147], the choice of technology (for instance the type of impeller) [83, 142, 146, 148–155], the optimum impeller rotational velocity [9, 10, 82, 144, 147, 150, 151, 155–166] or liquid/gas velocity inlet [50, 147, 154, 167–172] and the position of stirring system [144, 154]. The aims of these studies were the reduction of energy consumption. In the same context, studies have also been carried out on the bioreactor configurations [82, 143, 146, 149, 151, 165, 167, 169, 172, 173].

The study if the effect of substrate rheology and TS content on the flow pattern was also carried out by many authors. In fact, the choice of mechanical system is linked to the substrate rheology. Therefore, these works allowed to evaluate the impact of the substrate on the power input. It is useful for engineering applications. As detailed in the previous part on waste rheology, the choice of rheological model and waste characterisation are essential for flow modelling.

Furthermore, the turbulent modelling study is worth of interest. In fact, turbulent flow generally appears with stirring. Hence, many works have focused on the choice of the turbulent model such as [77, 162, 174]. Details on the different approaches are specified in a dedicated section.

The dead zones volume is a typical result from CFD simulations in anaerobic digestion tank. Indeed, it informs the non-agitated areas within the reactor. Thus, based on this, it is possible to evaluate and compare agitation strategies and different configurations. We report 16 studies that have produced this outcome [9, 42, 45, 79, 82, 149, 153, 158, 160, 163, 167, 169, 170, 172, 174, 175].

Many works concerned the multiphase study. Multiphase flow modelling is necessary for gas mixing [145, 152] and mechanical pumping modelling [144, 176]. In addition, it is also used to model the settling phenomena's, such as [44]. These works are detailed in a subsequent section.

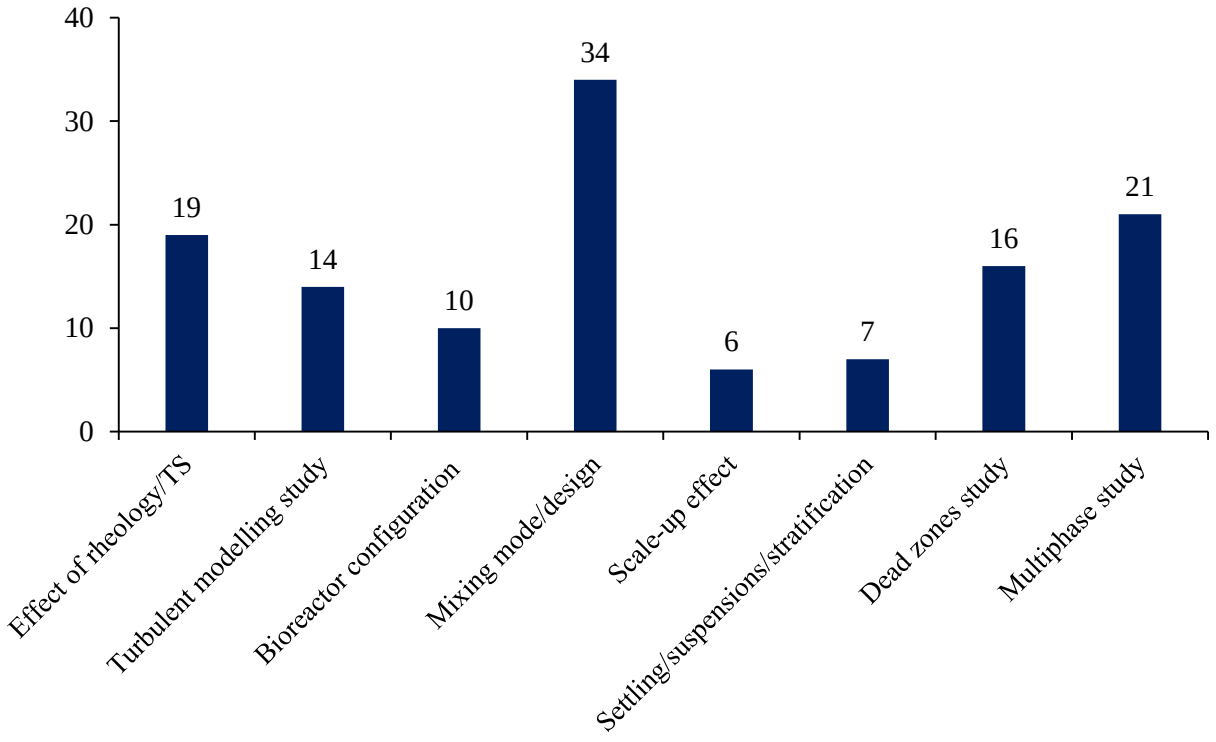

Figure 2: Contributions of work using CFD modelling in stirred tank

Table 21: Objectives of the CFD simulations

Sources	Authors	Date	Objectives
[167]	Vesvikar and Al-Dahhan	2005	Visualisation of flow pattern, proxy of hydrodynamic parameters and study of mixing time
[157]	Zadghaffari et al.	2009	
[177]	Wu	2010	
[42]	López-Jiménez et al.	2015	
[162]	Cheng et al.	2017	
[178]	Alcamo et al.	2005	Computation of the turbulent flow in a stirred tank
[156]	Zhengming	2006	
[79]	Wu and Chen	2007	
[179]	Zadghaffari et al.	2010	
[180]	Coughtrie et al.	2013	
[162]	Cheng et al.	2017	
[181]	Madhania et al.	2018	
[155]	Wiedemann et al.	2018	
[79]	Wu and Chen	2007	Characterisation of the mixing and dead zones/ Reduction the percentage of poorly mixing zone
[172]	Karim et al.	2007	
[175]	Mendoza et al.	2010	
[170]	Sajjadi et al.	2016	
[153]	Mohammadrezaei et al.	2017	
[163]	Lebranchu et al.	2017	
[169]	Leonzio	2018	
[79]	Wu and Chen	2007	Study of the effect of TS content on rheological properties, on the mixing time or on the required impeller torque
[177]	Wu	2010	
[77]	Wu	2012	
[158]	Bridgeman	2012	
[48]	Craig et al.	2013	
[182]	Ryma et al.	2013	
[145]	Dapelo et al.	2015	
[176]	Zhang et al.	2016	
[159]	Wang et al.	2017	
[111]	Mishra and Ein-Mozaffari	2017	
[146]	Meister et al.	2018	
[50]	Dapelo and Bridgeman	2018	
[181]	Madhania et al.	2018	
[165]	Rasouli et al.	2018	

[166]	Xie et al.	2019	
[168]	Wei et al.	2019	
[148]	Jahoda et al.	2007	Study of the liquid homogenisation in stirred tank
[172]	Karim et al.	2007	
[149]	Meroney and Colorado	2009	
[169]	Leonzio	2018	Test of different configurations of the bottom of the digester or of the tank
[165]	Rasouli et al.	2018	
[173]	Foukrach et al.	2019	
[45]	Terashima et al.	2009	Addition of 3D pseudoplastic laminar model in the CFD model in order to describe the rheological properties of sludge
[142]	Wu	2009	
[152]	Wu	2014	
[144]	Trad et al.	2015	
[145]	Dapelo et al.	2015	
[176]	Zhang et al.	2016	
[159]	Wang et al.	2017	
[183]	Zhang et al.	2017	
[160]	Rasool et al.	2017	
[153]	Mohammadrezaei et al.	2017	
[163]	Lebranchu et al.	2017	Study of mixing designs in anaerobic digesters
[146]	Meister et al.	2018	
[50]	Dapelo and Bridgeman	2018	
[169]	Leonzio	2018	
[154]	Zhang et al.	2018	
[164]	Xinxin et al.	2018	
[10]	Zhai et al.	2018	
[165]	Rasouli et al.	2018	
[155]	Wiedemann et al.	2018	
[166]	Xie et al.	2019	
[83]	Yu et al.	2011	
[170]	Sajjadi et al.	2016	CFD study in high solid anaerobic digester
[146]	Meister et al.	2018	
[175]	Mendoza et al.	2011	
[44]	Yu et al.	2013	
[183]	Zhang et al.	2017	Study of the stratification, settling, suspension or granulation in anaerobic digester
[147]	Fan et al.	2018	
[154]	Zhang et al.	2018	
[166]	Xie et al.	2019	

[44]	Yu et al.	2013	Evaluation of the biomass retention physical process
[79]	Wu and Chen	2007	Study of the scale effect
[177]	Wu	2010	
[150]	Wu	2011	
[44	Yu et al.	2013	
[174]	Vesvikar and Al-Dahhan	2015	
[159]	Wang et al.	2017	
[184]	Okiyama et al.	2017	Study of the species concentration profiles

4.2. Reactors and mixing systems

Various reactors have been studied in literature. First of all, a distinction is made between laboratory, pilot and full-scale reactors.

Then, three mixing systems are used in stirred tanks (anaerobic or aerobic): gas mixing, mechanical pumping and mechanical mixing. The **Figure 1** presents the proportion and the numbers of studies of each mixing systems from 2005 and 2019. Mechanical mixing is the most studied with 36 papers (58%). Then, gas mixing and mechanical pumping were studied in 12 (19%) and 14 papers (23%) respectively.

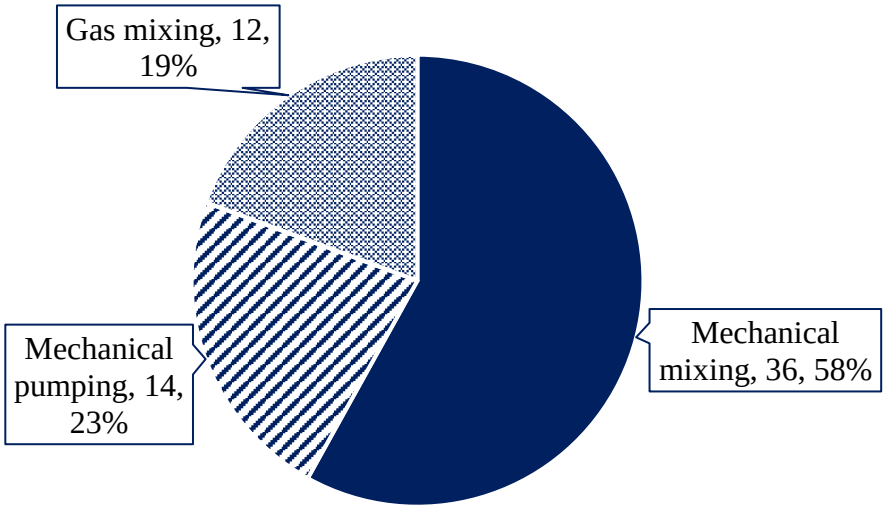

Figure 1: Proportion and number of studies of each mixing systems: Gas mixing, Mechanical pumping and Mechanical mixing

Furthermore, we have different types of digesters with different stirring modes and shapes. Details on agitation mode, reactor type, diameter, agitation speeds or flow rate and exact agitation technology are shown in the **Table 23**. Various stirring technologies have been tested such as the six-blade Rushton turbine, the Lightnin A310 and draft tube with different diameters. The aim was to determine the most efficient technology and the appropriate stirring velocity or flow rate to achieve the desired agitation and homogenisation of the medium.

The modelling of the mechanical stirring can be carried out by different methods. We report in the **Table 22** the approaches chosen in the different studies and specify the interests of each method. In the case of stirred digesters or tanks, two main methods were frequently used: the Moving Reference Frames (MRF) and the Sliding Mesh (SM). In the case of SM, two zones are defined. A mobile zone where the mechanical agitator is located, and a stationary zone. The interface between the zones must be identical for the two regions. Regarding the MRF, we consider a multi-fluid flow. Indeed, a speed rotation is assigned to the moving volume.

Cortada-Garcia et al. did experimental and CFD studies of power consumption in the agitation of highly viscous shear thinning fluids. The two main approaches for modelling stirred tanks are the MRF and the SM [185]. The MRF converged fast, but it was suitable only for steady-state flows [185]. In a stationary

frame of reference (stationary relative to the laboratory) the flow in the stirred tank is unsteady [185]. In contrast, SM was suitable also for unsteady flows, for which it provided a time dependent solution, but at the expense of significant computational effort and time [185]. In the SM approach, the geometry should have at least two connected non-deforming sections that slide in relation to each other [185].

The SM technique was more accurate, but it was also much more time consuming than the MRF [148]. Wu (2010) also compared the two techniques [177], the authors preferred the MRF approach in terms of prediction accuracy and computing time [177].

In conclusion, two meshing approaches exist for the modelling of mixing. Both MRF and SM are used by many authors. The SM approach provided more accurate results but it was more time-consuming. Furthermore, the SM approach should be used in case of transient simulations.

Table 22: Mechanical stirred tank meshing approach

Multiple Reference Frames (Steady-state simulations)	Sliding Mesh (Transient simulations)
Jahoda et al., 2007 [148]	
Zadghaffari et al., 2009 (MRF at the start and then SM) [157]	
Zadghaffari et al., 2010 (MRF at the start and then SM) [179]	
Wu, 2010 [177]	
Wu, 2012 [77]	
Cortada-Garcia et al., 2017 [185]	
Madhania et al., 2018 [181]	
Wu, 2009 [142]	Hartmann et al., 2004 [187]
Wu, 2010 [82]	Jian and Zhengming, 2006 [156]
Wu, 2011 [150]	Mishra and Ein-Mozaffari, 2017 [161]
Yu et al., 2011[83]	Lebranchu et al., 2017 [163]
Craig et al., [48]	Fan et al., 2018 [147]
Ryma et al., 2013 [182]	
Trad et al., 2015 [144]	
Zhang et al., 2017 [183]	
Ri et al., 2017 [186]	
Rasool et al., 2017 [160]	
Wang et al., 2017 [159]	
Cheng et al., 2017 [162]	
Mohammadrezaei et al., 2017 [153]	
Mohammadrezaei et al., 2018 [9]	
Xinxin et al., 2018 [164]	
Rasouli et al., 2018 [165]	
Meister et al., 2018 [146]	
Wiedemann et al., 2018 [155]	
Foukrach et al., 2019 [173]	

4.3. Multiphase flow modelling

There is different ways to model the digestion medium. First, we can consider one liquid phase, regrouping the both liquid part and particles, neglecting the biogas. This assumption is largely used for the study of mechanical mixing. Second, liquid-solid two-phase flow [161, 183] or liquid-gas-solid three-phase flow [44] can be used to study the settling and suspensions phenomena. Third, we can consider two-phase flow: liquid-liquid or liquid-gas. These approaches are used for the study of mechanical pumping and gas mixing respectively.

We summarise in **Table 24** the multiphase studies with the considered phases, the mixing system, the mathematical model the turbulent model, the fluids and the multiphase approach. Three multiphase approaches to describe the fluid motion have been used: the Euler-Euler approach [44, 143, 147, 152, 154, 159, 161, 165, 166, 183], the Lagrange-Lagrange approach [174] and the Euler-Lagrange approach [50, 145, 168, 180].

In an Eulerian approach, each phase is mathematically considered as follows interpenetrating continua. Each phase volume is defined. The sum of all volume fractions is equal to one. The fluid properties are written in function of space and time. In the Lagrangian approach, the fluid flow is modelled by following the motion and the properties of the particles. The computational cost of the Lagrangian model is more expensive than the Eulerian model.

The three methods provided good results. The Euler-Euler approach is the most used for the multiphase modelling of anaerobic digesters.

Table 23: Agitation mode, reactor type, diameter, agitation speeds or flow rate and exact agitation technology

Sources	Authors	Date	Mixing system	Reactor	Reactor diameter	Intensity / Inlet velocity / flow rate	Stirring technology
[167]	Vesvikar and Al-Dahhan	2005	Gas mixing	Mimic anaerobic digester	0.2032 m	0.027, 0.048, 0.072 cm/s	Draft tube
[178]	Alcamo et al.	2005	Mechanical mixing	Stirred tank	0.19 m	200 rpm	6-blade Rushton turbine
[156]	Jian and Zhengming	2006	Mechanical mixing	Stirred tank	0.476 m	150, 180, 260, 300 rpm	3-narrow blade hydrofoil CBY impeller
[79]	Wu and Chen	2007	Gas mixing	Stirred anaerobic digester	0.12, 1, 1.26, 1.44, 1.6, 1.72 m	2, 5 m/s	Draft tube
[148]	Jahoda et al.	2007	Mechanical mixing	Stirred tank	0.29 m	300 rpm	Six-blade 45° pitched blade turbine, standard Rushton turbine
[172]	Karim et al.	2007	Gas mixing	Gas-lift digester	0.2032 m	28.32, 56.64, 84.96 l/h (superficial gas velocities: 0.02, 0.05, 0.07 cm/s)	Draft tube (4.4 cm internal diameter)
[149]	Meroney and Colorado	2009	Mechanical pumping	Full-scale circular anaerobic digester tank	13.7, 21.3, 30.5, 33.5 m	395 l/min	Single and multiple draft impeller tube mixers (jet mixing)
[45]	Terashima et al.	2009	Mechanical pumping	Egg-shaped anaerobic digester	11 m	0.2 m3/min	Draft tube mechanical mixer
[142]	Wu	2009	Mechanical mixing & Mechanical pumping	Full-scale anaerobic digester	12 m		(1) Mechanical pumping by two 10 hp propellers in two external draft tubes, (2) mechanical stirring by two 10 hp side-entry propellers, (3) mechanical pumping by one 20 hp propeller in an internal draft tube, and (4) mechanical stirring by one 20 hp top-entry propeller.
[157]	Zadghaffari et al.	2009	Mechanical mixing	Fully baffled stirred vessel	0.30 m	225, 300, 400 rpm	Two six-blade Rushton turbines
[179]	Zadghaffari et al.	2010	Mechanical mixing	Baffled tank	0.30 m	250 rpm	Six-blade Rushton turbine

Sources	Authors	Date	Mixing system	Reactor	Reactor diameter	Intensity / Inlet velocity / flow rate	Stirring technology
[171]	Wu	2010	Mechanical pumping	Full-scale anaerobic digester	12, 13.74, 15.12, 16.29, 17.31 m	0.138 to 0.209 m/s	Pumped circulation
[177]	Wu	2010	Mechanical mixing	Full-scale anaerobic digester	0.147 m	600 rpm	Rushton turbine
[82]	Wu	2010	Mechanical pumping	Egg-shaped and cylindrical shape anaerobic digester	20.1 m	400, 450, 500, 550, 600, 650, 700, 750 rpm	Draft tube (pumped recirculation)
[143]	Wu	2010	Gas mixing & Mechanical pumping & Mechanical mixing	Cylindrical tank with conical bottom	12 m	7.6 m/s	Draft tube (0.66 m diameter)
[150]	Wu	2011	Mechanical mixing	Lab-scale and full-scale (model application) anaerobic digester	0.9 m and 12 m	60, 150, 250, 350, 800 rpm	Pitched blade turbine (Lightnin A310 and PMSL 3LS39)
[175]	Mendoza et al.	2011	Mechanical pumping	Full-scale anaerobic digester	30.5 m	-	2 nozzles DINOMIX system (jet)
[83]	Yu et al.	2011	Mechanical mixing	Cylindrical anaerobic digester with conical bottom	0.152 m	500 rpm	A-310 impeller (62 mm diameter) and helical ribbon (120 mm diameter)
[151]	Wu	2012	Mechanical mixing	Cylindrical tank and rectangular lagoon	Cylindrical tank: 40.844, 64.618, 71.932, 86.564, 65, 120 m	400, 416, 425, 420, 440 rpm	6 impellers (3 blades)
[188]	Wu	2012	Mechanical pumping	Egg-shaped plug-flow anaerobic digester	-	-	-
[77]	Wu	2012	Mechanical mixing	Cylindrical anaerobic digester with conical bottom	0.152 m	500 rpm (model validation)	Lightnin A310

Sources	Authors	Date	Mixing system	Reactor	Reactor diameter	Intensity / Inlet velocity / flow rate	Stirring technology
[158]	Bridgeman	2012	Mechanical mixing	Lab-scale cylindrical vessel	0.160 m	30, 50, 100, 200 rpm	2 six-blades paddles
[180]	Coughtrie et al.	2013	Gas mixing	Bench-scale anaerobic gas-lift digester	0.2032 m		Central draft-tube
[44]	Yu et al.	2013	Gas mixing	Lab-scale and pilot-scale anaerobic digester with conical bottom	0.0762 m and 0.117 m	1.24 m/s	Jet agitation
[48]	Craig et al.	2013	Mechanical mixing	Full-scale anaerobic digester	13.5 m	500 rpm	Impeller situated in a centrally-located draft tube (0.61 m diameter)
[182]	Ryma et al.	2013	Mechanical mixing	Stirred tank	0.36 m	250 rpm	six-blade Rushton turbine (0.1243 m diameter)
[152]	Wu	2014	Gas mixing	Cylindrical tank	10 m	7.6 and 8.0 m/S	Unconfined mixing by 2 bottom diffusers, confined mixing by one draft tube, unconfined mixing by 2 cover mounted lances, confined mixing by 2 bubble guns
[42]	López-Jiménez et al.	2015	Mechanical pumping	Ontinyent Wastewater Treatment Plant anaerobic digester	15 m		"HEATMIX": 2 tubes (31 mm internal diameter)
[144]	Trad et al.	2015	Mechanical mixing & Mechanical pumping	Anaerobic submerged membrane bioreactor	0.170 m	100, 150, 200, 400 rpm	Four-blade disk Rushton turbine (56 mm) & three-blade, 45° pitched blade turbine (82 mm)
[145]	Dapelo et al.	2015	Mechanical mixing & Gas mixing	Lab-scale digester	0.20 m (experiment)	2.05, 5.30, 8.63 ml/s	-
[174]	Vesvikar and Al-Dahhan	2015	Gas mixing	Gas-lift loop anaerobic digester (lab-scale & pilot-scale)	6 & 18 inches	2.74 & 4.5 mm/s respectively	Draft tube

Sources	Authors	Date	Mixing system	Reactor	Reactor diameter	Intensity / Inlet velocity / flow rate	Stirring technology
[176]	Zhang et al.	2016	Mechanical mixing	Stirred tank reactor (STR)	0.20 m	80 rpm	Three-layered 45° pitched blade (0.17 m diameter)
[170]	Sajjadi et al.	2016	Mechanical pumping	Cylindrical tank	0.19 m	0.6, 1.3, 2.6 l/min	Jet agitation
[159]	Wang et al.	2017	Mechanical mixing	Continuously stirred tank reactor (CSTR)	0.25 m	20, 60, 100, 140 rpm	Six-blade radial Rushton turbines
[183]	Zhang et al.	2017	Mechanical mixing	Stirred tank	0.20 m	80 rpm	4 two-blade impellers
[160]	Rasool et al.	2017	Mechanical mixing	Fully baffled stirred tank	0.30 m	60 to 135 rpm (step 15 rpm)	three-blade impeller
[184]	Okiyama et al.	2017	Mechanical pumping	Lab-scale up-flow anaerobic packed bed reactor (APBR)	0.08 m	4.6 l/day	Pumped circulation
[161]	Mishra and Ein-Mozaffari	2017	Mechanical mixing	Stirred tank (experiment: cylindrical vessel)	0.40 m	180 to 600 rpm	Maxblend impeller (250 mm diame+A42:I42ter)
[162]	Cheng et al.	2017	Mechanical mixing	Stirred tank	0.24 m	170, 220, 300, 400, 425, 440, 500, 540 rpm	Rushton turbine (0.08 m diameter)
[153]	Mohammadrezaei et al.	2017	Mechanical mixing	Full-scale anaerobic digester (1200 l)	-	30 rpm	Six-blade turbine, four-blade turbine, six-flat-blade disc turbine
[163]	Lebranchu et al.	2017	Mechanical mixing	Stirred tank	0.136 m	10, 50, 90 rpm & 22, 66, 110 rpm	Double helical ribbon & six-blade Rushton turbine
[146]	Meister et al.	2018	Mechanical mixing & Mechanical pumping	Cylindrical & egg-shaped digesters	20.10 m	840 rpm	Impeller (helical & 4PBT 45) rotating within a mechanical draft tube.
[50]	Dapelo and Bridgeman	2018	Gas mixing	Full-scale unconfined anaerobic digester	14.63 m	4.717.10-3 m3/s per nozzle	12 nozzles

Sources	Authors	Date	Mixing system	Reactor	Reactor diameter	Intensity / Inlet velocity / flow rate	Stirring technology
[9]	Mohammadrezaei et al.	2018	Mechanical mixing	Full-scale anaerobic digester (1200 l)	1 m	0, 40, 80, 120 rpm	45° six-blade turbine (0.3 m diameter)
[181]	Madhania et al.	2018	Mechanical mixing	Stirred tank with conical bottom	0.28 m	1000 rpm	Side-entry Marine propeller (0.036 m diameter)
[147]	Fan et al.	2018	Mechanical mixing & Gas mixing	Aerobic stirred tank	0.165 m	100, 250, 300 rpm & 450, 925 L/h	Plastic cuboid baffle agitator & diffuser (3 cm diameter)
[169]	Leonzio	2018	Mechanical pumping	Anaerobic continuously stirred digester	8 m	Inlet velocity: 0.5 to 1 m/s	External pumps
[154]	Zhang et al.	2018	Mechanical mixing	Spiral symmetry stream anaerobic bioreactor (SSSABR)	0.08 m	Inlet velocity: 2.0*10-3 m/min	cutting angle set to 30°, 45°, 60°
[164]	Xinxin et al.	2018	Mechanical mixing	Full-scale anaerobic digester	16 m	200, 250, 300, 400, 450 500 rpm	Side-entering agitator
[10]	Zhai et al.	2018	Mechanical mixing	Cylindrical pilot-scale anaerobic digester (1m3)	1.2 m	50, 100, 150 rpm	Double disc 45° six pitched-blade turbine impeller (6PBT-45)
[165]	Rasouli et al.	2018	Mechanical mixing	Novel prototype radial mixed semi-continuous plug-flow reactor (PFR)	0.73 m	20, 50, 100 rpm	32 blades impeller
[155]	Wiedemann et al., 2018	2018	Mechanical mixing	Cylindrical anaerobic digester	18 m (CFD), 1.5 (experiments)	60, 80 rpm	3 types of mechanical mixers (propeller and paddle)
[173]	Foukrach et al.	2019	Mechanical mixing	Cylindrical, polygon (without/with baffles), circular tanks	0.6 m	-	Six-blade Rushton turbine
[166]	Xie et al.	2019	Mechanical mixing	Stirred tank	0.146 m	100, 200, 250, 300 rpm	Stirring paddle

Sources	Authors	Date	Mixing system	Reactor	Reactor diameter	Intensity / Inlet velocity / flow rate	Stirring technology
[168]	Wei et al.	2019	Gas mixing	Gas-lift anaerobic digester (7.2 l)	0.2032 m	28.32, 56.64, 84.96 l/h (superficial gas velocities: 0.02, 0.05, 0.07 cm/s)	Gas injection pipe (0.5 cm diameter) & draft tube (4.4 cm diameter)

Table 24: Multiphase CFD studies

Sources	Authors	Date	Mixing system	Phases	Fluids	Multiphase approach
[167]	Vesvikar and Al-Dahhan	2005	Gas mixing	Liquid-Gas	Dilute slurry (physical properties of water); air	-
[143]	Wu	2010	Mechanical mixing	Liquid-Gas	Liquid manure	Euler-Euler
[180]	Coughtrie et al.	2013	Gas mixing	Liquid-Gas	Slurry	Euler-Lagrange
[44]	Yu et al.	2013	Mechanical mixing	Liquid-Gas-Solid	Wastewater	Eulerian approach for each phases
[182]	Ryma et al.	2013	Gas mixing	Liquid-Gas	Addition of variable quantity of CMC (carboxymethylcellulose) in water	Euler-Euler
[152]	Wu	2014	Mechanical pumping	Liquid-Gas	Power-law fluid	Euler-Euler
[144]	Trad et al.	2015	Mechanical mixing & Gas mixing	Liquid-Liquid		Euler-Euler
[145]	Dapelo et al.	2015	Gas mixing	Liquid-Gas	Addition of variable quantity of CMC in water	Euler-Lagrange
[174]	Vesvikar and Al-Dahhan	2015	Mechanical mixing	Liquid-Gas	Slurry (water density)	Lagrange-Lagrange
[176]	Zhang et al.	2016	Mechanical pumping	Liquid-Liquid	Cattle manure & corn stover (incompressible, pseudo-plastic)	-
[170]	Sajjadi et al.	2016	Mechanical mixing	Liquid-Liquid	Highly viscous xanthan gum solution for simulating municipal wastewater (power-law model)	-
[159]	Wang et al.	2017	Mechanical mixing	Liquid-Gas	Mixture of food waste and activated sludge (homogeneous & incompressible)	Euler-Euler
[183]	Zhang et al.	2017	Mechanical mixing	Liquid-Solid-Solid	Distilled water, floating particles & sinking particles	Eulerian approach for each phases

Sources	Authors	Date	Mixing system	Phases	Fluids	Multiphase approach
[161]	Mishra and Ein-Mozaffari	2017	Mechanical mixing	Liquid-Solid	Slurry (water is used in experiment)	Euler-Euler
[162]	Cheng et al.	2017	Mechanical mixing	Liquid-Liquid-Gas	Water, immiscible kerosene oil & air	Eulerian approach for each phases
[50]	Dapelo and Bridgeman	2018	Mechanical mixing	Liquid-Gas	Wastewater sludge	Euler-Lagrange
[181]	Madhania et al.	2018	Mechanical mixing & Gas mixing	Liquid-Liquid	Water, molasses (miscible liquids with high viscosity difference)	-
[147]	Fan et al.	2018	Mechanical pumping	Liquid-Gas	Water, air bubbles	Euler-Euler
[154]	Zhang et al.	2018	Mechanical mixing	Liquid-Gas-Solid	Wastewater (primary phase), gas & sludge granules (second phase)	Eulerian approach for each phases
[165]	Rasouli et al.	2018	Mechanical mixing	Liquid-Gas	Cow dung, biogas	Euler-Euler
[166]	Xie et al.	2019	Gas mixing	Liquid-Solid	PPD (pphenylenediamine) solution (liquid phase), solid PMDA (pyromellitic dianhydride anhydride) (solid phase)	Euler-Euler
[168]	Wei et al.	2019		Liquid-Gas	Liquid phase (water, sludge1, sludge2), Gas phase (air)	Euler-Lagrange

4.4. Turbulence modelling

Turbulence phenomena occur in anaerobic digesters. Different turbulence models exist. Both RANS and LES turbulence models were used. In the following part, we specify the choice of turbulence model of the different authors for these two categories of turbulence models. In the **Table 25**, the turbulence model studied and chosen and the respective sources are presented.

In general, the main RANS and LES turbulence models studied in the literature were:

- Standard k-epsilon, Realisable k-epsilon, Re-Normalisation-Group (RNG) k-epsilon, Reynolds Stress Model (RSM), Standard k-omega, SST k-omega;
- Smagorinsky-Lilly, Smagorinsky-Van Driest, Wall-Adapting Local Eddy-Viscosity (WALE), Kinetic Energy Transport (KET).

In the following sub-sections, we first detail the studies that used a RANS approach, and then those that used an LES approach.

4.4.1. RANS approach

RANS approach was widely used by many authors for turbulent flow modelling. In fact, this approach requires less fine meshes and is therefore less time-consuming.

In the case of the settling and suspension model, the standard k-epsilon turbulence model wad used for suspension process [44]. Just as the previous model, the CFD models [42, 79] employed the standard k-epsilon turbulence model. Indeed, this turbulence model has been successfully used by many researches for similar problems as we can see in **Table 25** [42]. The k-epsilon model was also used for the liquid phase modelling of the mimic anaerobic digester [167]. The realisable k-epsilon model was used for mixing simulations in anaerobic digesters realised by Wu (2009), Wu (2010) and Zhai et al. (2018) [10, 82, 142]. The model [83] which concerned the high solid anaerobic digesters did not consider turbulent flow but laminar flow, assuming that the turbulent flow was suppressed by high viscosity. In [83], the standard k-epsilon model was used when the Reynolds number was upper to 1000, the low-Re-k-epsilon model was used when the Reynolds number was comprised between 10 and 1000, and the laminar model was used when the Reynolds number was inferior to 10 [83].

The RNG k-epsilon turbulence model was used also used in many studies as specified in **Table 25**, such as for studying the effect of the impeller on sinking and floating behaviour of suspending particles and the effect of impeller rotational speed and velocity field [183].

Wu (2011) conducted a study on turbulence models. The studied turbulent models were the standard k-epsilon model, the RNG k-epsilon model, the realisable k-epsilon model, the standard k-omega model, the SST k-omega model and the RSM. It was found that the realisable k-epsilon model and the standard k-omega model were the most appropriate models through comparing power and flow numbers [150].

Craig et al. (2013) used the SST k-omega turbulence model for the turbulent closure [48]. This choice was based on previous authors experiences and recommendations [48, 80, 171]. In this study, the results from the RSM and SST k-omega turbulence model were compared. The authors concluded that the outcomes were adequately closed for justifying the use of the cheaper SST k-omega turbulence model

[48]. In addition, the turbulent flow of the CFD model developed by Wu (2014) [152] was also modelled by the SST k-omega model, as proposed in a previous work [143].

Coughtrie et al. (2013) tested four RANS turbulence models (RNG k-epsilon, k-omega SST, Linear RSM, and SST Transition) for a gas-lift loop reactor modelling [180]. They concluded that the turbulence model had an impact on the flow predictions [180]. Moreover, the SST transition turbulence model provided the most accurate predictions for velocity, separation and reattachment and overall flow-field, whereas the k-omega SST and RSM provided the most accurate results with inaccuracies with velocity and separation and reattachment predictions [180].

In 2016, a study was carried out to compare different models of turbulence (Spalart-Allmaras, transition SST k-omega, k-epsilon, realisable k-epsilon, and RSM) for low Reynolds flow [37]. The authors concluded that isotropic models could underestimate the turbulence phenomenon and that the RSM model provided the most accurate predictions [37].

In their review, Karpinska and Bridgeman (2016) presented a comparison between the standard k-epsilon model, the RNG, the realisable k-epsilon model, the standard k-omega model, the SST k-omega model and the RSM [189]. The standard k-epsilon model was more stable than RNG model [189]. The different turbulence models were adapted to different case studies, for instance, the realisable k-epsilon model was suitable for planar and rounded jet [189]. Moreover, the SST k-omega model was less suitable for free shear flows [189]. The RSM provided accurate results but was computationally expensive [189]. They concluded that RANS/URANS closed by the standard k-epsilon model was the most computationally efficient scenario for the modelling of activated sludge tanks [189].

4.4.2. LES approach

Different authors explored the LES approach in order to compare the two approaches and to improve the simulations precision. In addition, compared to the available numerical resources, we can use methods that require more computing time. Therefore, the studies presented below compared LES and RANS approaches in different case studies.

Hartmann et al. (2004) carried out LES and RANS simulations on the flow in a baffled stirred tank [187]. They used Smagorinsky and Voke (modified Smagorinsky) subgrid-scale (SGS) models in LES simulations, and numerical Lattice-Boltzmann scheme for Navier-Stokes equation discretisation [187]. The simulations results were compared with experimental data from LDA [187]. Both models provided an accurate representation of the flow field compared to experimental data [187]. The authors concluded from the comparison of simulations and experiments that LES provided better results than RANS in terms of the structure and levels of the turbulent kinetic energy in the impeller discharge flow [187]. The upward directed radial impeller outflow was well represented by the LES model but not found with the RANS model [187]. Thereby, LES provided more accurate results than RANS simulations.

Jian and Zhengming (2006) performed LES with Smagorinsky-Lilly SGS model of mixing process in a stirred tank [156]. They found better results (power demand and mixing time) with this approach than with RANS approach (with the standard k-epsilon model) compared with experimental predictions [156]. Moreover LES was a good tool to investigate the unsteady and quasi-periodic behaviour of the turbulent flow in stirred tanks [156].

Jahoda et al. (2007) also compared RANS with standard k-epsilon model (with MRF and SM techniques) and LES with SL SGS model (with SM technique) approaches [148]. They concluded that LES was the most time-consuming method but the results on flow patterns and liquid homogenisation were closer to reality [148].

By comparing results from LES and RANS simulations and experimentations, Zadghaffari et al. (2010) concluded that the predictions can be substantially improved with LES [179]. The authors used an eddy diffusivity scalar SGS model [179].

Jiang et al. carried out CFD simulations and compared three turbulent models: Standard k-epsilon, Realisable k-epsilon and Smagorinsky-Lilly [181]. They also recommended the LES approach with the Smagorinsky-Lily SGS model [181].

In a study conducted by Wu in 2012, the free SGS models investigated were SL model, WALE model and KET model [77]. The three models gave very similar results for flow fields [77]. The comparison between simulated and measured axial velocities showed that the LES shapes were in general agreement with the experimental data but they differed clearly in velocity magnitudes [77]. Concerning the impeller power and flow numbers, the SGS models gave excellent predictions, with the KET model provided the best results [77]. The author also compared the results with six RANS turbulence models (realisable k-epsilon model with SM, standard k-omega model with SM, Reynolds stress model with SM, realisable k-epsilon model with MRF, standard k-omega model with MRF, Reynolds stress model with MRF) [77].

Table 25: Turbulence modelling approach

Sources	Dimension	Mathematical model	Turbulence model	Recommended turbulent model
[167], [174]	3D	RANS	Zero-equation model (gas phase)	-
[45], [44], [163]	3D	Laminar flow model	Laminar	-
[79], [176], [170], [159], [153], [42], [182], [166], [173], [147], [169], [161], [9], [149], [175], [167]	3D	RANS	Standard k-epsilon	-
[183], [160], [168], [165], [154], [164]	3D	RANS	RNG k-epsilon	-
[142], [82], [10], [151]	3D	RANS	Realisable k-epsilon	-
[145]	3D	RANS	Reynolds stress model (RSM)	-
[48], [152]	3D	RANS	SST k-omega	-
[178]	3D	LES	Smagorinsky-Van Driest	-
[157], [179]	3D	LES	Smagorinsky-Lilly	-
[156]	3D	RANS & LES	Standard k-epsilon Smagorinsky-Lilly	LES Smagorinsky-Lilly
[148]	2D	RANS & LES	Standard k-epsilon Smagorinsky-Lilly	LES Smagorinsky-Lilly
[171], [143]	3D	RANS	Three high-Reynolds-number k-epsilon Six low-Reynolds-number k-epsilon Two k-omega RSM	Chang-Hsieh-Chen low-Reynolds-number k-epsilon and standard k-omega [171] 3 low-Reynolds-number k-epsilon (Abid, Abekondoh-Nagano, Chang-Hsieh-Chen) for TS=2.5 % [143] Chang-Hsieh-Chen for TS=5.4 % [143]
[177]	3D	RANS	Standard k-epsilon RNG k-epsilon Realisable k-epsilon RSM	Realisable k-epsilon
[150]	3D	RANS	Standard k-epsilon RNG k-epsilon Realisable k-epsilon Standard k-omega SST k-omega RSM	Realisable k-epsilon and Standard k-omega

Sources	Dimension	Mathematical model	Turbulence model	Recommended turbulent model
[83]	3D	RANS	Standard k-epsilon (Re>1000) Low-Reynolds-k-epsilon (10<Re<1000) Laminar (Re<10)	-
[77]	3D	LES & RANS	Smagorinsky-Lilly Wall-Adapting Local Eddy-Viscosity (WALE) Kinetic Energy Transport (KET) 6 RANS turbulence models	LES KET
[158]	3D	RANS	Standard k-epsilon Realisable k-epsilon RNG k-epsilon Standard k-omega RSM	RSM (MRF)
[180]	3D	RANS	SST k-omega RNG k-epsilon Linear RSM Transition-SST	Transition-SST
[144]	1D & 3D	RANS	Standard k-epsilon RNG k-epsilon Chen-Kim k-epsilon	Chen-Kim k-epsilon
[174], [155]	3D	RANS	Standard k-epsilon Standard k-omega	-
[146]	3D	RANS	Realisable k-epsilon Standard k-omega	Realisable k-epsilon
[162]	3D	RANS	Standard k-epsilon model RSM	RSM
[181]	3D	RANS & LES	Standard k-epsilon Realisable k-epsilon Smagorinsky-Lilly	LES Smagorinsky-Lilly

5. Thermal modelling

Anaerobic digestion proceeds at a precise optimal temperature, thus some models have been developed in order to provide temperature profiles in digesters. These models allow several thermal digester optimisation.

Gebremedhin et al. (2004) carried out simulation of heat transfer for biogas production. The mathematical model developed described the heat exchange between the digester and the environment during the year [190].

Gomez et al. (2007) developed a two-phase (liquid-gas) mathematical model of autothermal thermophilic aerobic digesters. The biochemical and physico-chemical transformations are similar to those proposed in ADM1 of IWA. The authors added an energy balance in order to predict the temperature of the system [191].

Perrigault et al. (2012) developed a one-dimensional, time-dependent heat transfer model in order to optimise tubular digester in cold climates. In this model, Radiative, convective and conductive heat transfer phenomena were considered. The model was validated with experimental data, with a standard error of 2% [192].

Merlin et al. (2012) developed a steady-state heat transfer model based on energy balance for forecasting the biogas production depending on ambient air and dairy wastewater temperatures variations in a continental climate context. The uncertainty of the model predictions compared to experimental measurements was about 10%. They concluded that the heat transfer must be taken into account for the biogas plant design and unheated digester are very sensitive to external temperature conditions [193].

Wu (2012) carried out simulations which include mixing (with CFD), heat transfer, and biochemical reaction kinetics in anaerobic methane fermentation. The main hurdle for coupling these phenomena is to solve the physical–biological interactions concurrently using the small time interval required for the mixing and heat transfer. Thus the chosen approach was to develop a two-stage simulation strategy that predicts the temporal biological process using a large time step based on steady fluid flow and heat transfer, in which a computational cell is physically treated as an individual bioreactor with its own residence time and temperature. In conclusion, the temperature was the most important physical condition for bacterial growth, residence time determined the duration of digestion by anaerobes, and pH regulated the microbiological process [188].

Terradas-Ill et al. (2014) developed a thermal model to predict biogas production in unheated fixed-dome digesters buried in the ground. The authors used a one-dimensional thermal model. In conclusion; this model could be used for assessing the methane production and for improving the digesters during cold period [194].

Hreiz et al. (2017) developed a zero-dimensional transient thermal model is proposed for predicting temperature variations in semi-buried anaerobic digesters as a function of climatic conditions (ambient temperature, solar irradiation, rain intensity). This model provides the identification of phenomena leading to major energy losses from the reactor, and thus to propose technical solutions to reduce these heat losses. The thermal model was written in Fortran 90. The fourth order Runge-Kutta scheme was used for time integration. The model is presented by the authors as a powerful predictive tool for assisting engineers in determining optimal design and in studying the influence of materials type on the

reactor heating requirements. Furthermore, it may be coupled with the ADM1 for predicting biogas production as a function of environmental conditions[89][88]. Indeed, ADM1 provides data like biogas composition and production rate that are needed for an accurate modelling of some heat transfer terms. Moreover, digestate and biogas temperature, calculated in the thermal model, are required for determining the biochemical reactions rates and gas-liquid mass transfer rates [195].

The model results [195] revealed that the required heat to warm the inputs and radiations to the cover constitute the major heat losses, each one accounting for about 30% of the total thermal energy lost by the digestate. Besides, heat transfer to the ground and to the biogas constitute each one for about 15% of the heat lost by the digestate [195]. Regarding the cover heat losses, it may be noticed that average heat gains from solar irradiance are considerable in spring and summer [195].

Singh et al. (2017) studied a fixed type anaerobic digester. They studied the temperature distribution around the digester using CFD simulations. The ANSYS software was used with the SIMPLE algorithm and the standard k-epsilon model [196].

6. Discussions

6.1. Rheological properties

Many studies have been carried out on the rheological characterisation of various waste. The authors agree on the rheological models to be used to characterise each waste. The appropriate model depends on the type of waste, the temperature, and the total solid content.

The vinasse is mostly characterised by a Newtonian model at temperatures above 30 °C, even if the Hershel-Bulkley model or the power-law model are also suitable. The rheological behaviour of sludge has been well studied, the models used were the Hershel-Bulkley model, the modified Hershel-Bulkley model, the Bingham model and the Sisko model. The rheological behaviour of the manure is modelled by the Hershel-Bulkley model or the Bingham model, depending of the study. In CFD modelling, the authors used the rheological data of sludge for the modelling of manure rheology. Concerning the biowaste, rheological measurements have been done only on fruits and vegetables, some are Newtonian and others non-Newtonian. Most of the studies have been done on one fruit or vegetable, and not on a mixture. Hershel-Bulkley model, power-law model and Bingham models are used to model the rheological behaviour of fruits and vegetables. However, because of the diversity of biowaste, only specific studies of biowaste rheological behaviour have been done, thus we have few literature data on a mix of biowaste. It is important to note that the rheological properties depend on the mix of biowaste, the total solid and volatile solid contents. Thus, the data available in the literature are a basis, they allow us to have a general idea of the rheological behaviour of some biowaste: manure, vinasse, sludge, fruits, vegetables, mix of OFMSW, SHW, starch, fat, whey, fodder residues. However, in the case of anaerobic digestion of specific biowaste or biowaste mixture, we should perform rheological measurements on the waste mixture.

Moreover, some authors highlighted relation between soluble COD, pH and the viscosity of the sludge. These relations allow us to estimate the viscosity from these parameters. The highlighted relationship are only valid for the studied waste. Moreover, the studies on the impacts of temperature, or thermal treatment have shown that it impact the viscosity of the fluid.

The choice of the rheological model is crucial for the modelling of hydrodynamics (CFD model). Indeed, the flows depend on the rheological behaviour of the fluid. In CFD modelling, we can use literature data if the rheological behaviour of the studied fluid is known. Otherwise, it is possible to use the data of a similar fluid or we have to carry out rheological measurements.

6.2. Biochemical modelling

Anaerobic digestion of waste faces various inhibitions. The latter are related to the operating conditions, such as hydraulic loading rate, temperature, mixing conditions and pH. In order to control digesters and avoid malfunctions, biochemical models of anaerobic digestion have been developed and adapted to various substrates.

The first models were simple. Indeed, only the limiting step was taken into account. However, the results obtained were not precise enough, nor valid for all the waste. Thanks to a better understanding of the chemical reactions involved and the process microbiology, it is possible to develop more complex models. Thus, all the chemical reactions are gradually integrated into the biochemical models, but also the inhibitions of the reactions of the process. All these models, more and more complete and precise, led to the development of a generalised model, the ADM1 model, which takes into account the main reactions of anaerobic digestion. Nevertheless, this model is not suitable for the digestion of all waste. Several modifications are therefore still necessary to adapt the model. Any changes made to the ADM1 model will contribute to the realisation of the ADM2 model.

However, these are one-dimensional models based on mass transfer. Thus, these models rarely consider the fluid dynamics of the digester [42], while the mixing conditions, the pH and the temperature impact the digestion process [4, 5]. Keshtkar et al. (2003) developed a kinetic model which takes into account the mixing inside the digester and concluded that it affects the methane yield [124]. Lindmark et al. (2014) published a review on the effect of mixing on the anaerobic digestion process [197]. The literature review on experimentations showed that mixing mode and mixing intensity have direct effects on the biogas production [197]. Moreover, the authors recommended to carried out research on the effect of mixing on chemical and microbial level and on different steps of the process [197]. Furthermore, more studies are needed to understand the effect of TS content on the microbial community [135]. CFD is a powerful tool for optimising the process [197]. Therefore, local models using CFD are developed by many authors. Their applications and interests are manifold.

6.3. CFD modelling

CFD have been used in several tank and digester studies. Indeed, the mixing conditions impact the anaerobic digestion process, which gives a major interest for the study of the flows within the digesters. CFD simulations provide precise description of the flow around the tank. Indeed, most of the studies have been carried out on stirring. Moreover, as CFD models are local models, the characterisation of the fluid is crucial, thereby, some studies concern simulations on different substrate (Newtonian and non-Newtonian). For each substrate, different rheological models are tested in order to choose the better one for each case. The turbulence modelling is also important in CFD, it has been shown that LES models give more precise outcomes with more simulations time than RANS models. Then, the last point of interest is the meshing approach. The appropriate mesh is chosen depending of the study. Studies of different types of mesh have been carried out on mechanical stirred tank, the three studied meshes are the moving frame of reference, the multiple reference frame and the moving mesh. The moving frame

of reference is the least used mesh. Both the multiple reference frame and the moving mesh give accurate predictions. The moving mesh can be used to model unsteady flows contrary to multiple reference frame.

The literature review shows that more studies have been carried out with RANS approach than with LES approach. This is explained by the fact that simulations of models based on RANS equations are faster than simulations of models based on LES. Nevertheless, LES provides more accurate outcomes. In conclusion, the choice of the approach must be done according to the expected accuracy of the results and the computation time.

Various RANS turbulence models have been studied. The turbulence model must be chosen in function of the study. It has been shown that some models are more suitable for some studies. Indeed, all the models have their advantages and disadvantages. The standard k-epsilon model and the realisable k-epsilon model are used by many authors, both the models provide accurate results. Moreover, the SST k-omega model is recommended by others authors. The RSM provides the more accurate results but with the more computation-time. Therefore, choice of the turbulence model must be done according to the aim of the study, the expected accuracy of the results and the computation-time.

Some studies are accompanied of experimental studies on pilot digesters. These studies demonstrated the interest of the choice of appropriate mixing in anaerobic digestion optimisation. These papers reinforce the interest of CFD. However, more studies are needed to fully understand the impact of flows on anaerobic digestion process. Actually, the numerical models allow to understand why a given mixing among several agitations tested, is the more efficient. Contrariwise, we do not choose a proper stirring solely from CFD simulations outcomes but considering experimental studies on pilot digester. Many authors recommend that biochemical phenomena be taken into account in numerical simulations of flows. The coupling of CFD models and biochemical models could be a solution to make possible to choose the appropriate mixing from simulations.

6.4. Thermal modelling

Thermal models have been developed essentially in the case of cold climates. Indeed, as the temperature affects the digestion process, variations of process temperature are avoided. The simulations have shown that the environmental conditions affect the process temperature, especially during winter period. The authors agree on the hypothesis that thermal transfers due to chemical reactions are negligible. Moreover, some thermal models are coupled with biochemical models or CFD models. Thermal models can be used to optimise digesters.

7. Perspectives of the bibliographic study and the objectives of the thesis work

Considering the exposed elements, this thesis focuses on both the experimental aspect with the launch and follow-up of a pilot as well as the modelling of the flows of a mechanically stirred digester. Indeed, we propose to optimise anaerobic digestion with a view to the local behaviour of the digestion medium. Global models, such as ADM1, predict biogas production and composition based on waste composition and chemical reaction kinetics. However, the literature review clearly showed that yields are impacted by flows. However, this aspect is still not very well considered in numerical models and requires additional work to understand the impact of hydrodynamics on reaction kinetics. From an experimental point of view, it is difficult to explain the variations in biogas production observed during changes in

agitation. Indeed, the mixing of the medium is partly responsible for the differences in the efficiency of laboratory and industrial digesters. A detailed analysis of the digestion medium is essential to understand its differences and optimise agitation. The objective of this thesis is to provide elements of understanding on the impact of flows on anaerobic digestion, based on biogas production and the physicochemical properties of the digestion medium. The literature review also revealed that CFD is a proven tool for the characterisation of flows in agitated reactors. Applications to anaerobic digesters are recent but multiple. CFD is used in particular to compare the geometric configurations of digesters and agitators based, for example, on dead zone volumes. The authors also compare simulation results from different numerical models or different types of substrates. In CFD models, substrates are characterised by their rheological behaviour which is closely related to their water content. This tool is therefore very interesting and has a high potential to study agitation parameters in the case of wet and dry digestion. The integration of the equations of biochemical models into a CFD model is an interesting research area despite the significant computation times for this type of simulation.

First, the anaerobic digestion of the raw vinasse, a Newtonian fluid, is studied in a mechanically agitated pilot digester. The protocol for the pilot launch is first proposed. The impact of mechanical agitation on biogas yields is explored through the monitoring of physico-chemical parameters of the digestion medium over a year. In a second step, CFD simulations are performed for different agitation regimes to compare experimental results and flows.

Acknowledgements

This work was supported by the Region of Reunion Island (France) as part of the funding of a research thesis in the PIMENT (Physics and Mathematical Engineering for Energy, Environment and Building) laboratory at the University of Reunion Island.

Chapitre III

Influence of inoculum to substrate ratio on methane production in Biochemical Methane Potential (BMP) tests of sugarcane distillery waste water

Ce chapitre, rédigé au format d'article scientifique, présente les premiers travaux expérimentaux menés sur la vinasse de canne à sucre. En effet, la première étape est la détermination du potentiel méthanogène d'un déchet, c'est-à-dire la production de méthane qui nous pouvons produire dans des conditions optimales pour un déchet donné. Les tests sont effectués en régime mésophile (37°C). La vinasse étant un déchet récalcitrant, il est nécessaire d'adapter le protocole classique du test de potentiel méthanogène à ce substrat. Dans cette étude, le test est réalisé avec différents rapports inoculum (boue contenant les micro-organismes) sur substrat (I / S). Les résultats sont notamment le potentiel méthanogène (production maximale de méthane par unité de matière organique) et des constantes de cinétiques essentiels pour la modélisation de la digestion anaérobie.

Available online at www.sciencedirect.com

ScienceDirect

Procedia Manufacturing 00 (2016) 000–000

Procedia MANUFACTURING

www.elsevier.com/locate/procedia

International Conference on Sustainable Materials Processing and Manufacturing, SMPM 2019, Sun City Resort, South Africa, 08 – 10 March 2019

Helene Caillet[a], Edouard Lebon[a], Esther Akinlabi[b], Daniel Madyira[b], Laetitia Adelard[a1]

[a]Laboratoire de Physique et Ingénierie Mathématique pour l'Energie et l'Environnement (PIMENT), Université de la Réunion, UFR Sciences de l'Homme et de l'Environnement, 117 rue Général Ailleret, 97430 Le Tampon, France

[b]Department of Mechanical Engineering Science, University of Johannesburg, Auckland Park, Kingsway Campus, Johannesburg 2006, South Africa

III-1. Abstract

The sugarcane distillery wastewater (vinasse) are generated throughout sugarcane molasses fermentation and distillation respectively. Regarding the vinasse, a part of the production is treated by anaerobic digestion process. However, the remaining part is diluted then discharged into the sea 900 m of the coast. In this study, the mesophilic biochemical methane potential (BMP) test, with different inoculum to substrate (I/S) ratios, are presented in this paper as well as the methane production and kinetic results. The BMP is modelled by both the first order linear regression and the modified Gompertz model. In a future study, we will propose an alternative solution in order to treat both wastes simultaneously while producing energy with the co-digestion of the vinasse and the activated sludges in semi-industrial scale.

Peer-review under responsibility of the organizing committee of SMPM 2019.

Keywords: anaerobic digestion; biochemical potential test; I/S ratio; modified Gompertz model; sugarcane vinasse

III-2. Introduction

Anaerobic digestion is an extensive process for waste treatment. Moreover, it allows the production of renewable energy. In this context, many studies have been carried out in order to characterise the methanogenic potential of waste and to model the anaerobic process. This led to the publication of standardised protocol for the biochemical potential (BMP) tests to increase the probability of obtaining validated and reproducible results [198]. The I / S ratio is a point of interest as the obtained methane production of the BMP depends on this parameter. Moreover, the optimal I/S ratio depends on the tested substrate. For instance, the optimal I/S (based on VS) ratio of microalgae BMP is 2 in order to avoid volatile fatty acids (VFAs) accumulation [199]. In the case of the BMP of maize, the authors noticed only slight variations of methane yield with different I/S (based on VS) ratios (1, 1.5, 2 and 3) and the optimal ratio is 1 [200]. In a study on okara, S/I (based on VS) ratios in the range of 0.1 to 3 are tested [201]. The authors highlighted that the methane yield reaches its maximum at S/I values of 0.6 to 0.9, and inhibitions occur when the ratio exceeds 1, due to VFAs accumulations [201]. Other authors recommend to test different ratios, based on a study on piggery slaughterhouse waste [202]. Moreover, they recommend an S/I (based on VS) ratio inferior to 0.1 [202]. In the latest study, the recommended ratios based on VS contents are between 2 and 4 [198]. However, it is also mentioned that for easily degradable substrates where rapid accumulation of fermentation intermediates such as VFAs could lead to inhibition of anaerobic digestion, a ratio greater than or equal to 4 should be applied; and for less degradable substrates, such as lignocellulosic organic matter, a ratio less than or equal to 1 can be applied [198]. Regarding the BMP modelling, linear or non-linear regression can be used [203].

This paper deals with the study of the BMP tests of vinasse from sugarcane with vinasse sludge as inoculum. First, we present the BMP tests methods and results for four I/S

ratios, indeed this ratio is a key parameter of BMP tests [198]. Second, the BMP is modelled with both linear and non-linear regressions and the results are compared to literature data.

III-3. Nomenclature

TS	total solid
VS	volatile solid
B	biodegradability
Y_{max}	methane production potential ($Nl_{CH4}.kg_{COD}^{-1}$)
t	time (days)
Y(t)	cumulative methane production ($Nl_{CH4}.kg_{COD}^{-1}$)
k	kinetic constant (day^{-1})
R	methane production rate ($Nl_{CH4}.kg_{COD}^{-1}.days^{-1}$)
λ	lag-phase time (days)
$Y_{m,i}$	measured cumulative methane production ($Nl_{CH4}.kg_{COD}^{-1}$)
$Y_{c,i}$	calculated cumulative methane production potential ($Nl_{CH4}.kg_{COD}^{-1}$)
n	number of measurements during the experiment

III-4. Materials and methods

III-4.1. The Inoculum and substrate

The vinasse and the inoculum come from the active mesophilic biogas plant of the sugar-cane distillery Rivière du Mât (Saint-Benoit, Reunion Island). They come from the same industrial plant, thereby the sludge is already acclimatised to the vinasse. The inoculum is stored at ambient temperature and incubated at 37°C before the BMP tests, which is the process temperature (mesophilic conditions). Regarding the vinasse, it is stored at -20°C and then at 4°C before the tests.

III-4.2. The physico-chemical characterisation

The substrate and inoculum are homogenised with the Ultra turrax IKA T25 digital at 12,000 rpm for 10 min before the characterisation tests. We carried out TS, VS, pH, chemical oxygen demand (COD), total organic carbon (TOC), VFA, ammonium (Am), alkalinity (Alk) and Kjeldahl nitrogen (Ni) measurements. The TS content is obtained after drying 20 g of the samples for 24 h at 105 °C and the VS content after burning the

dried samples for 4h at 550°C. The chemical tests were conducted on the Hach Lange DR5000 Spectrophotometer, using the Hach Lange tests LCK 914 (COD), LCK 381 (TOC), LCK 365 (VFA), LCK 303 (Am), LCK 362 (Alk) and LCK 338 (Ni). The physico-chemical characteristics of the vinasse and the sludge are given in the **Table 1.** The C/N ratio is 15.20, which is in the range of optimum C/N ratio from the study, i.e. 10-30, carried out by (Yadvika et al.) [204]. Nevertheless, other authors reported upper ranges, i.e. 16-25 and 25-35 [205].

Table 1: Physico-chemical characteristics of vinasse and inoculum

Characteristics	TS %	VS %	pH	COD $g.L^{-1}$	TOC $g.L^{-1}$	VFA $g.L^{-1}$	Am $mg.L^{-1}$	Alk $mg_{CaCO3}.L^{-1}$	Ni $g.L^{-1}$	C/N ratio
Inoculum	2.25	0.97	7.57	9.93	-	-	517.67	-	-	-
Vinasse	6.64	4.04	4.84	79.67	27.65	3.05	239.00	3651.25	1.82	15.2

III-4.3. The BMP tests

The BMP tests are carried out using the Automatic Methane Potential Test System II (AMPTS II - Bioprocess Control). The experimental system is presented in the **Figure 1**. We refer to the last recommendations for the BMP test organisation [198]. The digestion is carried out in mesophilic regime at 37°C.

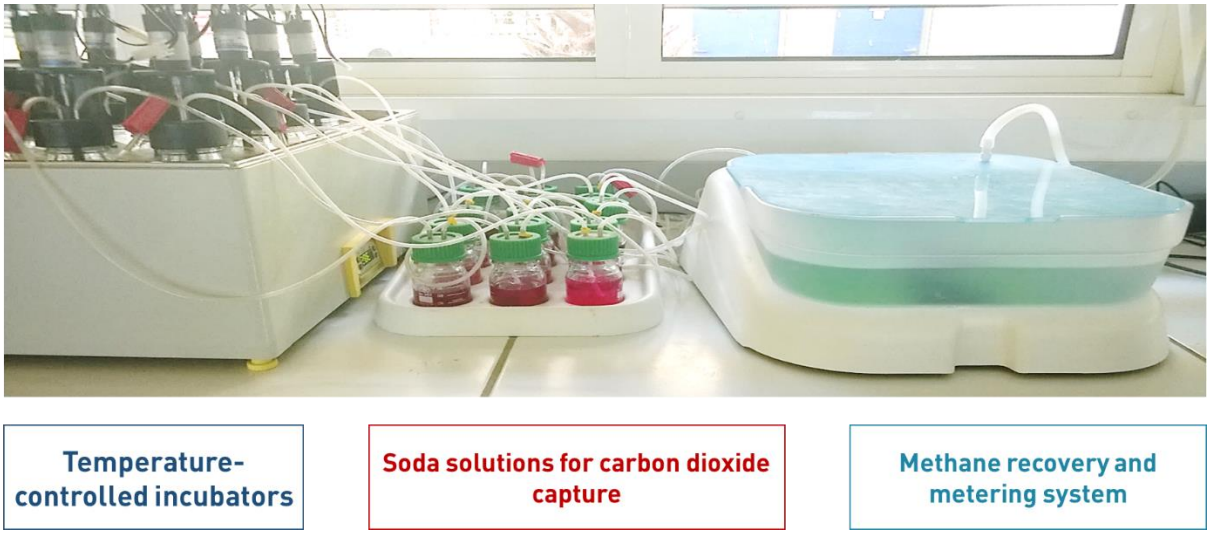

Figure 1: Automatic Methane Potential Test System II (AMPTS II - Bioprocess Control)

The total volume of the digesters is around 590 mL. The operating volume is 400 mL. The digesters volume is adjusted with distilled water in order to have the same test

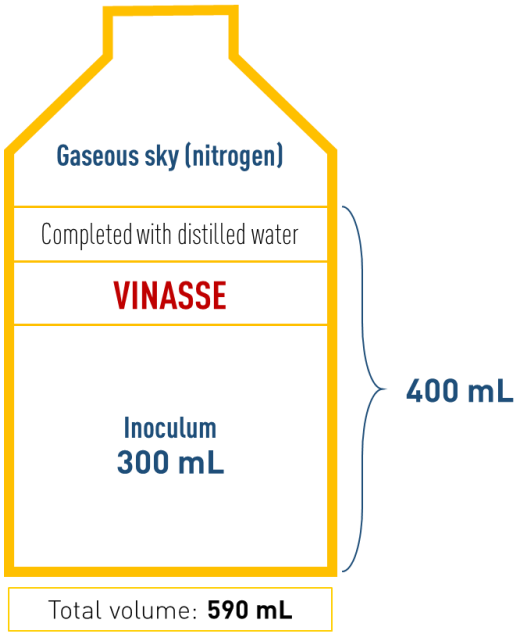

volumes. Then, the headspace is flushed with nitrogen gas. The experiment includes the substrate tests, the positive tests and the blank tests. All the tests are carried out in triplicates. The BMP value is expressed in the volume of methane produced per gram of organic matter which is expressed in COD as the vinasse is liquid. The schematic of a reactor filler is shown on **Figure 2.**

Figure 2: Schematic of a reactor filler

The studied substrate to inoculum ratios (g_{COD}/g_{VS}) are 0.5 (A), 0.75 (B), 1 (C) and 2 D). These ratios correspond to inoculum to substrate ratios (g_{VS}/g_{VS}) of 3.9, 2.6, 2.0 and 1.0. The digesters preparation is summarised in the **Table 2.**

Table 2: Digesters preparation for BMP tests

Ratio	Inoculum volume ml	Inoculum VS g	Substrate	Substrate COD g	Substrate VS g	I/S ratio VS/VS	S/I ratio COD/VS
A	300	2.91	Vinasse	1.46	0.74	3.9	0.50
B	300	2.91	Vinasse	2.18	1.11	2.6	0.75
C	300	2.91	Vinasse	2.91	1.47	2.0	1.0
D	300	2.91	Vinasse	5.82	2.95	1.0	2.0

III-4.4. The biodegradability

The biodegradability is estimated by the following equation:

$$B = \frac{Y_{max}}{350} \quad (49)$$

Where 350 represent the theoretical maximum biodegradability of methane expressed in litters of methane per kilogram of COD.

III-4.5. Regression analysis

In accordance with Kim et al. (2003) anaerobic degradation after initial lag time is limited by the terms associated with substrate and kinetics, which generally could be represented by a first order kinetic law with some assumptions [203]. According to the approach reported by Llabres-Luengo and Mata-Alvarez (1987), the first order linear regression is [206]:

$$Y(t) = -Y_{max}\left(e^{-kt} - 1\right) \quad (50)$$

It has been shown that the BMP fits with the modified Gompertz equation in case of mono-digestion is [203, 207]:

$$Y(t) = Y_{max} * \exp\left[-\exp\left(R * \frac{\exp(1)}{Y_{max}} * (\lambda - t) + 1\right)\right] \quad (51)$$

The root mean square error (RMSE) and determination coefficient R^2 are used to evaluate the model results. The RMSE is expressed as follows:

$$RMSE = \sqrt{\frac{1}{n}\sum_{i=1}^{n}\left(Y_{m,i} - Y_{c,i}\right)^2} \quad (52)$$

III-5. Results and discussion

III-5.1. BMP tests performances

The **Table 3** shows that the highest methane production is obtained with the ratio D followed by the ratio C, then the ratio B and the ratio A with the lowest production.

The methane production increases when the I / S ratio decreases. The methane potential of the vinasse (ratio D) is 109.58 $Nl_{CH4}.kg_{COD}^{-1}$ after 16 days with a biodegradability of 0.31. Consequently, in the case of BMP vinasse test, we should use an I(VS) / S(VS) of 1. As previously said, this ratio (inferior or equal to 1) is recommended for less degradable substrates. Moreover, the maximum methane production is reached between 12 and 19 days for the four ratios.

Table 3: Experimental performances of BMP tests at different I/S ratios

Ratio	S/I ratio COD/VS	Methane yield			Maximum production	Biodegradability
		$Nl_{CH4}.kg_{VS}^{-1}$	$Nl_{CH4}.kg_{COD}^{-1}$	$Nl_{CH4}.l_{sample}^{-1}$	Days	
A	0.50	93.96	47.60	3.86	12	0.14
B	0.75	162.28	82.64	6.67	15	0.24
C	1.0	169.17	85.46	6.72	19	0.24
D	2.0	216.18	109.58	8.74	16	0.31

III-5.2. Results from regression analysis

The **Figure 3** shows the comparison between the measured data, the calculated data with the first order regression and calculated data with modified Gompertz model for each ratio, and the **Table 4** shows the coefficients for the two models. The results from the first order regression don't fit exactly with the measured data, indeed, the determination coefficient for the four ratios are comprised between 0.82 and 0.91 and the RMSE between 4.547 and 15.210. However, the outcomes from the modified Gompertz fit very well with the measured data, this time, the determination coefficient for the four ratios is upper than 0.99 and the RMSE is lower than 2.6.

Regarding the kinetic constant, the first order regression gives values between 0.1137 and 0.1629 $days^{-1}$ for the ratios A, B and D. The kinetic constant for the ratio C is lower than the others with 0.0883 $days^{-1}$. This value is lower due to a higher lag-phase of 6.247 days. Indeed, the minimum lag-phase for the BMP with ratios A, B and D are respectively 2.232, 3.728 and 4.110 days. This time is due to the fact that the inoculum is already acclimatised to the vinasse.

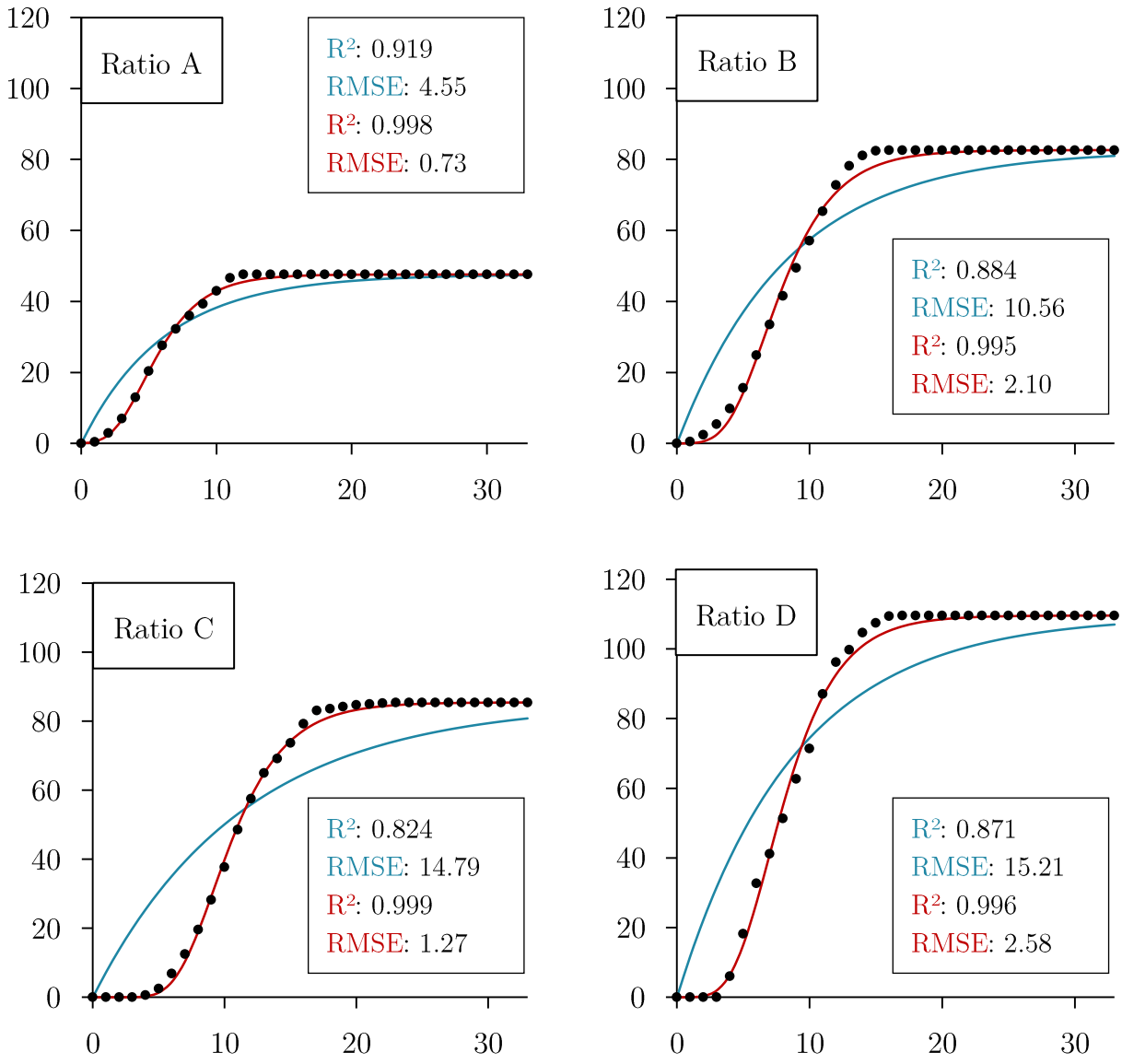

Figure 3: Cumulative methane production ($L_{CH4}.kg_{COD}^{-1}$) in function of time (days): comparison between measured data (point), calculated data with the first order regression (blue full line) and calculated data with modified Gompertz model (red full line) for cumulative methane production at different I/S ratios.

Table 4: First-order regression and modified Gompertz model coefficients

Model		Unit	Coefficients at different I/S ratios			
			A	B	C	D
First-order regression	Kinetic constant k	Day^{-1}	0.1629	0.1189	0.0883	0.1137
	Y_{max}	$Nl_{CH4}.kg_{COD}^{-1}$	47.60	82.64	85.46	109.58
	Correlation factor R^2		0.9196	0.8844	0.8246	0.8715
	RMSE	$Nl_{CH4}.kg_{COD}^{-1}$	4.547	10.560	14.790	15.210
	R	$Nl_{CH4}.kg_{COD}^{-1}.days^{-1}$	7.35	10.50	10.65	14.23
Modified Gompertz model	λ	Days	2.232	3.728	6.247	4.110
	Y_{max}	$Nl_{CH4}.kg_{COD}^{-1}$	47.60	82.64	85.46	109.58
	Correlation factor R^2		0.998	0.9954	0.9987	0.9963
	RMSE	$Nl_{CH4}.kg_{COD}^{-1}$	0.734	2.100	1.268	2.582

III-5.3. Comparison of kinetic constant and methane yield with literature data

From the **Table 5**, we notice that the methane yield obtained in our study (ratio D) is low compared to the methanogenic potential of vinasse found in literature. This difference can be explained by a different of chemical compounds concentrations, resulting from different vinasse treatment. Indeed, as previously said, the C/N ratio may not be optimal.

Table 5: Comparison of kinetic constant and methane yield of crude vinasse with literature data (mesophilic regime) (B: Biodegradability)

Reference	Kinetic constant	Lag-phase	COD	Inoculum source	Methane yield	B
	$Days^{-1}$	Days			$Nl_{CH4}.kg_{COD,Fed}^{-1}$	
Ratio D	0.1137	4.110	79.67 $g_{O2}.L^{-1}$	Sugarcane distillery waste water	109.58	0.31
[208]	0.30	1.99	62.63 $g_{O2}.kg^{-1}$	Pig and cow manure digestate	240	0.69
[209]	0.17	-	20.73 $mg_{O2}.L^{-1}$	reactors used for hydrogen production from sucrose based synthetic wastewater	255.4	0.73
[210]	-	-	68.56 $g_{O2}.L^{-1}$	Brewery wastewater reactor	250	0.71
[211]	-	-	120.221 $g_{O2}.L^{-1}$	Wastewater plant	264.83	0.77

The kinetic constant obtained in this study is 0.1137 $days^{-1}$ and the kinetic constants in literature are 0.17 day^{-1} [209] and 0.30 $days^{-1}$ [208]. Regarding the biodegradability, it is 0.31 in this study, and the maximum biodegradability is 0.73 in another study [209].

III-6. Conclusion

This study focused on the variation of the substrate to inoculum ratio in BMP tests. We studied four ratios ranging from 1 to 4 (I_{VS}/S_{VS}). Based on the experimental results, the production of methane increases with the decrease of this ratio, thus the maximum production was obtained with the ratio 1. The methanogenic potential of vinasse is thus 109.58 $Nl_{CH4}.kg_{COD}^{-1}$. This production is obtained in 16 days. The regression analysis showed that the modified Gompertz model is suitable for the methane production of BMP tests with a coefficient of determination greater than 0.99 and an RMSE less than 2.6. Moreover, the first order regression allowed us to determine the hydrolysis constant of vinasse, which varies from 0.0883 to 0.1629 $days^{-1}$.

Compared to the literature, the methane production of vinasse obtained in this study is lower. Future studies will focus on pre-treatment of the vinasse for the optimisation of methane production.

III-7. Acknowledgements

The authors are grateful to the FEDER and the Region Reunion who supported this work.

Chapitre IV

Start-up strategy and process performance of semi-continuous anaerobic digestion of raw sugarcane vinasse

Nous avons étudié dans le chapitre précédent le potentiel méthanogène de la vinasse (conditions optimales). Nous allons donc étudier la digestion anaérobie de la vinasse dans des conditions réelles en pilote de laboratoire. Ce chapitre, rédigé au format d'article scientifique, présente les travaux réalisés pour le démarrage du pilote de laboratoire. En effet, c'est une phase sensible durant laquelle le procédé est instable avec des phénomènes d'inhibition fréquents.

Le potentiel méthanogène de la vinasse pouvant varier d'une campagne sucrière à l'autre est dépendante des conditions de stockage. Les tests de potentiel méthanogènes sont donc effectués sur le nouvel échantillon de vinasse selon le protocole du précédent chapitre.

Une étude en laboratoire est menée sur la production de méthane de vinasse brute sur une période de 130 jours. La stratégie de démarrage du projet pilote de 16 L est proposée, avec notamment l'augmentation progressive du taux de chargement organique. L'analyse physicochimique du milieu est nécessaire pour prévenir et expliquer les dysfonctionnements du processus. Ainsi, la production de biogaz et les mesures physicochimiques lors de la digestion sont présentées et discutées dans ce chapitre.

Start-up strategy and process performance of semi-continuous anaerobic digestion of raw sugarcane vinasse

Hélène Caillet*[1], Laetitia Adelard[1]

[1] PIMENT laboratory, Reunion Island University, 117 rue Général Ailleret, 97430 Le Tampon, France

*Corresponding Author: helene.caillet@univ-reunion.fr Tel: +06 92 08 68 02

IV-1. Abstract

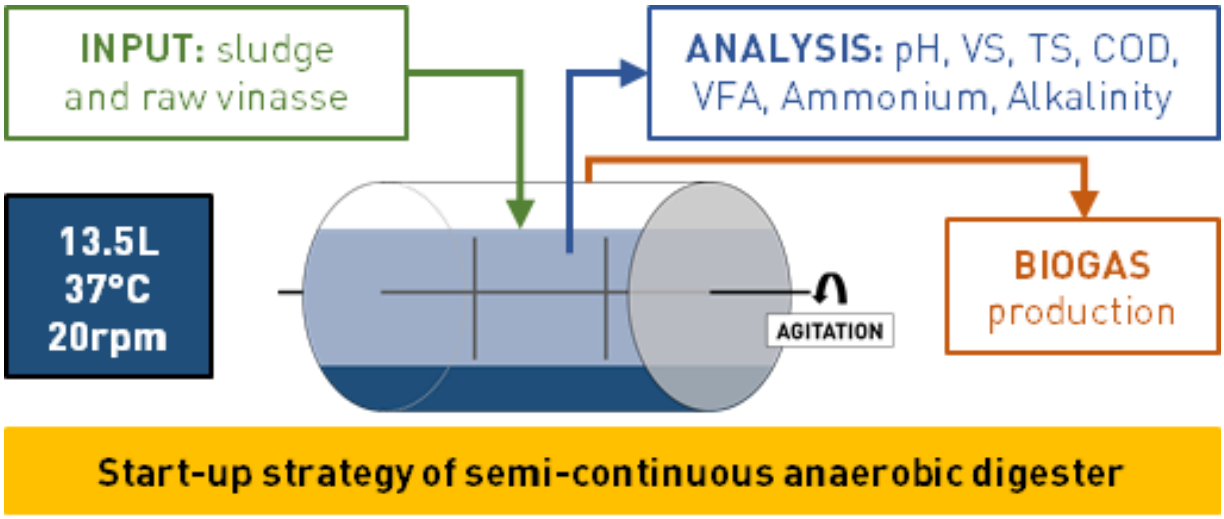

The sugarcane distillery waste water is generated throughout the sugarcane molasses fermentation and distillation. In Reunion Island, a part of the vinasse production is treated by anaerobic digestion process. However, the remaining part is diluted then discharged into the sea. The aim of this study is to propose an alternative solution in order to treat the vinasse while producing energy through anaerobic digestion. Nonetheless, vinasse pollutant load is difficult to treat.

Regarding the experimentations, the biochemical potential (BMP) test is used for the determination of the methanogen potential. The BMP is then modelled with the modified Gompertz model, and first order regression. Furthermore, a laboratory study is carried out for studying the methane production of raw vinasse in semi-industrial scale over a period of 130 days. The start-up strategy of the 16 L pilot is proposed, in particular the gradual increase of organic loading rate. The physico-chemical analysis of the medium is needed to prevent and explain the failure of the process. Indeed, the biogas production and physico-chemical measurements during the digestion are presented and discussed. The maximum methane yield of the BMP is 185.59 $NL_{CH4}.kg_{COD}^{-1}$, obtained with I / S ratio in terms of volatile solids of 0.7. The outcomes showed that the first-order regression and modified Gompertz model fit well with the BMP test curves. Concerning the pilot, the launching period lasted 45 days the maximum specific production was 151.00 $NL_{CH4}.kg_{COD}^{-1}$ (232.31 $NL_{biogas}.kg_{COD}^{-1}$). In further studies, different mixing strategies will be studied.

Keywords: Anaerobic digestion; Sugar cane vinasse; Pilot scale; BMP; Process performance

IV-2. Introduction

Anaerobic digestion is a widely used process for waste treatment and energy production with the biogas. This natural process consists in the degradation of organic materials by microorganisms in absence of oxygen, unlike aerobic digestion. Anaerobic digestion respects the natural cycle of carbon. The biogas produced is mainly composed of methane and carbon dioxide, with traces of hydrogen sulphide and water vapour. The five modes of biogas valorisation are [212]:

- Heat production: energy efficiency is interesting if the heat requirement of the outlets is high enough to allow the maximum use of the available energy to be exploited. In addition, nearby outlets are needed to limit the costly transport of heat or biogas.

- Electricity production: lower energy efficiency due to the energy yield of the electricity, ranging for motors from around 33%.

- The combined production of electricity and heat, also called cogeneration: this is the most common biogas recovery system. Besides the electricity produced by a generator, heat is recovered, mainly from the cooling system. The valorisation of heat requires a nearby outlet.

- Fuel for vehicles: The biogas follows a series of purification/compression steps to be used as a vehicle fuel.

- The injection of clean biogas into the natural gas network: in some European countries, the injection of biomethane into dedicated or non-dedicated networks are more common: Sweden, Germany, Switzerland, Netherlands, etc. The injection of purified biogas into the natural gas network is the most efficient method of valorisation.

Anaerobic digestion is very interesting for an insular territory such as Reunion Island, which is dependent on imported fossil energies. The ambition to achieve energy self-sufficiency by 2025-2030 was initiated by the Region in 2000 through its Regional Plan for the Development of Renewable Energies and Rational Use of Energy (PRERURE) [213]. Following the environment Grenelle, this ambition was relayed by the government with the GIP Project GERRI and it also materialised in 2009 with the program STARTER (Strategy of Energy Autonomy for the Recovery and Transition of the Reunionese economy) [213]. The PETREL report, prepared by the ARER (the regional energy agency of Reunion Island), presents an initial assessment of the Reunion energy mix in the horizons of 2020 and 2030 [213]. The demand and the electricity production are evaluated according to two scenarios, one of them following STARTER [213]. The valorisation of biomass is preponderant in the latter scenario, especially as it provides a so-called "base" energy because it is permanently available [213]. Different ways of biomass valorisation exist, such as the extraction of nanocrystalline cellulose [214–216]. The methanisation biomass is composed by all putrescible organic matter, animal manure, wastewater, wood waste and green waste. According to a study conducted by ADEME in 2010, the methanisation of waste in Reunion Island corresponds to the production of 34.3 million m3 of biogas per year from 853,000 tons of waste, of which: 44% of effluents from farming, 21% of agro-industrial effluents, 21% of sewage sludge, 11% of bio-waste and 3% of wet green waste [213]. The assumptions made are

that 25% of the livestock effluents produced to date on the island will be valorised by anaerobic digestion by 2020 and 50% by 2030 [213]. The sewage sludge would be 91% mobilised, 44% wet green waste and 100% agro-industrial and biowaste effluents [213].

In addition, the waste in Reunion are currently landfilled, however, this method is not sustainable because it is land consuming, not adapted to insular territories. The vinasses (sugarcane distillery waste water generated throughout alcohol production) are treated and then discarded on the high seas via an emissary at 80 m depth. The sugarcane vinasse is treated by anaerobic digestion process in many countries on an industrial scale especially in Brazil, India and South Africa by adapted processes and a simple acclimation of the microbial flora to the conditions of the vinasse. In Reunion Island, the first major biogas unit was built at the Rivière du Mât distillery in 2011. Its implementation was directly linked to the drastic increase in energy costs over the last 5 years [213], and the need of vinasse treatment. The distillery produces 8,000 m3 of pure alcohol per year and the production of vinasse is around 600 m3.d-1 during the sugarcane crop season [213]. Experimental results showed particular difficulties for anaerobic digestion process, given high salinity and high organic matter content (80-120 kgCOD.m-3) [213]. The first phase of the project of anaerobic digestion of the vinasse (2011) concerned only half of the vinasse, which is treated in a 5,800 m3 digester. The organic load is reduced by 80% and the biogas produced is used in a steam boiler, ensuring the energy autonomy of the process distillation [213].

Vinasse is characterised as a highly polluting effluent, containing high levels of organic compounds and nutrients (mainly potassium but also nitrogen and phosphorous) [40, 217]. Furthermore, vinasses are recalcitrant effluents with high pollutant content. The direct discard of vinasse to environment leads to severe environmental impact like salinity, sodicity, phytotoxicity, anoxia, eutrophication, death of aquatic life, and many severe health problems [40, 217]. Moreover, the Rivière du Mât distillery in Reunion Island is constrained to treat a diluted vinasse to guarantee its anaerobic digestion while avoiding inhibitions of the process. The drawback is therefore the massive use of water for the anaerobic digestion of the vinasse. This is why this study focuses on the anaerobic digestion of raw vinasse on a laboratory scale.

Before the industrial treatment of a specific waste, the process must be studied on a laboratory and pilot scale. Indeed, biochemical potential test (BMP) are broadly used for evaluating the methanogenic potential of organic materials. The protocol of this test have been recently standardised because the outcome can vary significantly between laboratories [198]. Nevertheless, a key parameter of this test, the ratio of volatile solid (VS) from inoculum to VS from the substrate (I / S ratio) depends on the substrate [198]. The ratio should be between two and four for most applications [198]. However, for less degradable substrates, a ratio less than or equal to one can be applied, and only if two ISRs lead to the same BMP, one can assume that there was no overload or inhibition [198]. Concerning unknown substrates, the authors recommend to test several ratios [198]. Thereby, in this study, different ratios were tested in order to evaluate the methane yield of the sugarcane vinasse.

There is no standardised method for the pilot experiments. Studies have recently been carried out on pilot tests on sugarcane vinasse, mainly in co-digestion. Among these studies, we find the work led in 2015 on start-up strategies of anaerobic co-digestion of sugarcane filter cake and bagasse [218]. At the beginning of the pilot start-up phase, the load increase is done gradually and the steady conditions were obtained after 70 days [218]. The effect of total solid was studied with the addition of water [219]. The result showed that vinasse / water ratio of 1 / 3 (TS 7.015%) produced the maximum total biogas (37.409 mL.gCOD-1) however vinasse / water ratio of 1 / 2 (TS 9.310%) had the biggest COD removal (23.580%) than others [219]. Moreover, in a study published in 2015, the authors said that biogas production failed when sugar beet vinasse alone was fed to the reactor [205]. For this reason, they studied the addition of cow manure during digestion, which has the consequence of increasing the C / N ratio, which is low in the case of vinasse substrate [205]. Anaerobic digestion was the most stable when cow manure was supplied to digestion of vinasse [205]. The steady conditions were obtained after 50 days [205]. Another study has been carried out on vinasse in 2016 in order to evaluate the anaerobic conversion of vinasse into biomethane with gradual increase in organic loading rate (OLR) in two up flow anaerobic sludge blanket (UASB) reactors of 21.5 L (R2) and 40.5 L (R1), in mesophilic conditions [220]. The OLR values applied in the reactors were 0.2–7.5 gCOD.L-1.d-1 in R1 and 0.2–11.5 gCOD.L-1.d-1 in R2 [220]. The average COD removal efficiencies ranged from 49% to 82% [220]. In 2017, co-digestion of sugarcane press mud with vinasse was studied in order to improve the digestion of

press mud [208]. The methane yield was 64% higher in case of co-digestion compared to mono-digestion of press mud and the process was more stable [208]. All these studies show that co-digestion of vinasse improves yields and stabilises the process. Nevertheless, in this study, we will not carry out experiments in co-digestion. We present the outcomes for the case of vinasse in mono-digestion and slowly increase the OLR to avoid destabilisation of the process as [205].

Furthermore, these studies previously mentioned presented examples of pilot start-up. We retain from these articles that the pilot digester must be started with inoculum (such as manure or sludge), followed by the micro-organisms acclimation and then a gradual increase in load. In this paper, we present the methodology and outcomes for the vinasse and sludge characterisation especially the BMP test of vinasse, the pilot start-up and the monitoring of experimentation over a period of 130 days. The aim of this study is firstly to propose a protocol for start-up a pilot with raw vinasse as substrate. Secondly, we study the increase of OLR of the pilot while following the physico chemical properties of the medium to avoid dysfunctions of the process in case of an increase of OLR too fast. Finally, we study the pilot in steady-state conditions while following the physico chemical properties. In this work, we choose not to add chemicals to adjust the physico-chemical parameters, and not to dilute the vinasse. Indeed, we want to obtain data without interfering with the process and let the process stabilise alone. This case has not been studied yet. The data produced will allow us to create an experimental database to study the impact of mechanical agitation on the anaerobic digestion of raw vinasse in further studies.

IV-3. Methodology

IV-3.1. Substrate and inoculum

The vinasse and the sludge come from the active mesophilic biogas plant of the sugarcane distillery Rivière du Mât (Saint-Benoit, Reunion Island). The sludge is used as the inoculum in the biochemical potential (BMP) tests and the start-up of the pilot digester. It is then stored at ambient temperature and incubated at 37°C before the BMP tests, which is the process temperature (mesophilic conditions). Regarding the vinasse, it is stored in cold storage at 4°C before the tests in order to avoid the degradation of

the substrate before the digestion in the pilot. The vinasse is stored in the cold storage for a maximum of two months before being used. In this study, the vinasse is not frozen because the freezing has the effect of breaking up the cells, which improves the digestion of the latter.

IV-3.2. Physicochemical analysis

The substrate and inoculum are homogenised with the Ultra turrax IKA T25 digital at 12,000 rpm for 10 min before the characterisation tests. We carried out total solid (TS), volatile solid (VS), pH, chemical oxygen demand (COD), total organic carbon (TOC), volatile fatty acids (VFA), ammonium (Am), alkalinity (Alk) and Kjeldahl nitrogen (Ni) measurements. The TS content is obtained after drying 20 g of the samples for 24 h at 105°C and the VS content after burning the dried samples for 4 h at 550°C. The chemical tests were conducted on the Hach Lange DR5000 Spectrophotometer, using the Hach Lange tests LCK 914 (COD), LCK 381 (TOC), LCK 365 (VFA), LCK 303 (Am), LCK 362 (Alk) and LCK 338 (Ni). The physico-chemical characteristics of the vinasse and the sludge are given in the **Table 1.**

Table 1: Physico-chemical characteristics of vinasse and sludge

Characteristics	Sludge	Vinasse
TS %	1.99	6.64
VS %	0.72	4.04
MES $g.L^{-1}$	-	10.0
pH	7.57	4.84
COD $g_{O2}.L^{-1}$	11.60	86.70
TOC $mg.L^{-1}$	-	29 875
VFA $g.L^{-1}$	16.34	19.36
Am $mg.L^{-1}$	-	37.40
Alk $mg_{CaCO3}.L^{-1}$	2,361.9	1,080.6
N $mg.L^{-1}$	1070	1120
Phosphorus $mg.L^{-1}$	-	190
Alk/COD	0.204	0.013
VFA/alk	6.92	17.91
C / N ratio	-	26.67

The BMP tests are carried out using the Automatic Methane Potential Test System II (AMPTS II - Bioprocess Control). We refer to the last recommendations for the BMP

test organisation [198]. The tests are carried out in mesophilic conditions in 50 days. As the substrate is unknown, we must test different inoculum to substrate ratios [221]. The ratios of COD from the substrate to VS from the inoculum tested are 1, 2, 2.5 and 3, which corresponds to a ratio of VS from the inoculum to VS from the substrate of 1.8, 0.9, 0.7 and 0.6. The total volume of the digesters is 650 mL. The operating volume is 400 mL. The digesters volume are adjusted with distilled water in order to have the same test working volumes. The experiment includes substrate tests, the positive tests and the blank tests. All the tests are carried out in triplicates. The BMP value is expressed in the volume of methane produced per gram of organic matter which is expressed in COD as the vinasse is liquid.

IV-3.3. The biodegradability and the COD removal

The biodegradability of the substrate in the BMP test is estimated by the following equation:

$$B = \frac{Y_{max}}{350} \tag{53}$$

Where 350 represents the theoretical maximum biodegradability of methane expressed in litters of methane per kilogram of removal COD at normal temperature and pressure.

The COD removal is calculated by the following equation:

$$R = \frac{M_{COD,digested}}{M_{COD,added}} * 100 = \frac{M_{COD,added} - M_{COD,pilot}}{M_{COD,added}} * 100 = 100 - \frac{M_{COD,pilot}}{M_{COD,added}} * 100 \tag{54}$$

Where, $M_{COD,added}$ is the cumulated mass added in terms of COD, $M_{COD,digested}$ is the cumulated digested mass in terms of COD and the $M_{COD,pilot}$ is the COD measured on the sample collected from the pilot.

IV-3.4. Kinetic models

IV-.3.4.i. First-order model

According to Kim et al. (2003), anaerobic degradation after initial lag-phase time is limited by the terms associated with substrate and kinetics, which are generally

represented by a first order kinetic law [203]. According to the approach reported by Llabres-Luengo and Mata-Alvarez (1987), the first order model is expressed by [206]:

$$Y(t) = -Y_{max}\left(e^{-kt} - 1\right) \quad (55)$$

Where Y is the volume of produced methane ($NL_{CH4}.kg_{COD}^{-1}$) at digestion time t (seconds), Y_{max} is the maximum volume of methane accumulated at an infinite digestion time ($NL_{CH4}.kg_{COD}^{-1}$) and k the kinetic constant (d^{-1}). Nielfa et al. (2015), assumed that k is the specific microorganisms growing speed [222] (d^{-1}).

IV-.3.4.ii. Modified Gompertz model

It has been shown that the BMP fits with the modified Gompertz equation in case of mono-digestion [203, 207]. This model assumed that the biogas production is proportional to the microbial activity [207, 222].

$$Y(t) = Y_{max}\exp\left[-\exp\left(\frac{R_m(\lambda - t)\exp(1)}{Y_{max}} + 1\right)\right] \quad (56)$$

Where Y_{max} is the maximum volume of methane accumulated at an infinite digestion time ($NL_{CH4}.kg_{COD}^{-1}$), R_m is the specific rate constant ($NL_{CH4}.kg_{COD}^{-1}.d^{-1}$) and λ is the lag-phase time constant (d).

IV-.3.4.iii. Statistical analysis

The root mean square error (RMSE) and the determination coefficient R2 are used to evaluate the model results. The RMSE is expressed as follows:

$$RMSE = \sqrt{\frac{1}{n}\sum_{i=1}^{n}\left(Y_{m,i} - Y_{c,i}\right)^2} \quad (57)$$

Where n is the number of measurements, Σ is the sum operator, $Y_{m,i}$ is the measured cumulated methane production ($NL_{CH4}.kg_{COD}^{-1}$) and $Y_{c,i}$ is the calculated cumulated methane production ($NL_{CH4}.kg_{COD}^{-1}$).

As mentioned in the last recommendations for the BMP tests, test results must be rejected if the standard deviation is upper than 10% [198]. The standard deviation is calculated with the following equation:

$$\sigma = \sqrt{\frac{1}{N}\sum_{i=1}^{n}\left(x_i - \bar{x}\right)^2} \quad (58)$$

Where N is the number of assays, x_i are the maximum volume of methane produced of each assays ($NL_{CH4}.kg_{COD}^{-1}$) and $\bar{x}$ is the average value of the maximum volume of methane produced ($NL_{CH4}.kg_{COD}^{-1}$).

IV-3.5. Pilot tests

IV-.3.5.i. Degradation index

The degradation index is calculated according to the following equation [218]:

$$D_{index} = \frac{SMP}{TMP} \quad (59)$$

Where, SMP is the specific methane production of the pilot ($NL_{CH4}.kg_{COD}^{-1}$) and TMP the theoretical methane production of the biochemical potential tests ($NL_{CH4}.kg_{COD}^{-1}$).

IV-.3.5.ii. The pilot set-up

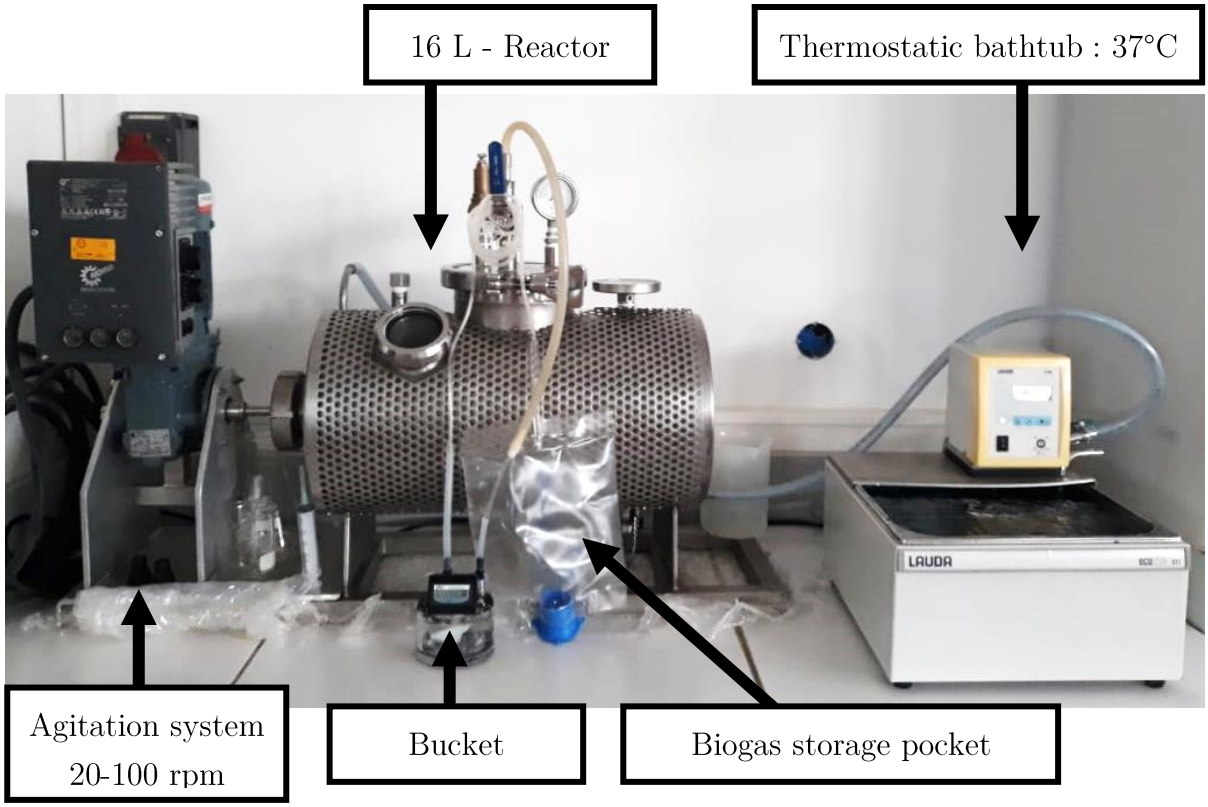

Figure 1: Pilot 16-L set-up

The set-up of the pilot is shown in the **Figure 1.** The total volume of the pilot is 16 L. The operating volume is 14.5 L and the headspace is 1.5 L. The experiment is carried out in mesophilic conditions at 37°C in order to limit energy consumption. The temperature is controlled with water recirculation in the double membrane. The water is maintained at a constant temperature with a thermostatically controlled water bath. The digester is equipped with a mechanical mixing system. Its intensity can vary from 20 rpm to 100 rpm. The mixing mode employed in this work is detailed subsequently in the document. The biogas volume is measured with a bucket counter.

IV-.3.5.iii. Pilot start-up and monitoring

For the start-up of the digester, the digester is filled with 13.5 L of sludge from the sugarcane distillery (which corresponds to 97.20 g_{VS} and 156.60 g_{COD}) for the micro-organisms input and 500 mL of vinasse (which corresponds to 24.40 g_{VS} and 43.35 g_{COD}). The physico-chemical properties of the sludge are presented in the **Table 1**. As the

sludge comes from the same distillery of the vinasse, the sludge is already acclimatised to the vinasse and therefore, acclimatisation period is not needed. Next, the digester is fed with 500 mL of vinasse and a digestate sample of 500 mL is taken once a week during one month. Experimentally, for the digester feeding, we have to open it to recover the digestate and add the substrate. The objective of the launch of the pilot phase, is to gradually replace the sludge by the vinasse. We slowly feed the digester with vinasse in order to avoid inhibitions and failure of the process. The major drawback of the feeding of the digester is the fact of allowing oxygen to enter the medium, which must stay anaerobic.

Physico-chemical tests are carried out on the digestate samples: the pH, the COD, the ammonium concentration, the VFA concentrations, alkalinity and the TS and VS percentages. The biogas volume is measured with a bucket counter and then stocked in a 1500 mL gas storage pocket.

As previously said, if the physico-chemical parameters are not optimal, we do not adjust them with addition of chemical, but change the organic loading rate.

IV-.3.5.iv. Mixing conditions

During the start-up of the pilot, the mixing is minimal: 15 min at 20 rpm before the taking of sample in order to homogenise the medium. This choice is made in the aim to homogenise the medium before taking a sample without destabilising the process or the bacterial centers. Indeed, opening the pilot and allowing oxygen to enter necessarily disrupts the process that can cause the death of methanogenic archaea, and so the reduction of the population of micro-organisms. Moreover, as the growth of methanogenic populations is slow, we must preserve them.

Then the minimal mixing was maintained during two weeks before modification. Indeed we then tested intermittent agitation: 10 hours per day at 20 rpm. As it revealed an absence of biogas production, the mixing was stopped and returned to minimal agitation for the rest of the experiment. We supposed that the continuous stirring prevented the micro-organisms from digesting the substrate. Consequently, the OLR was changed, in order to recover initial physicochemical parameters and biogas production. Indeed, according to Vavilin and Angelidaki (2005), during the start-up of the digester,

the methanogenesis is the limiting-step, consequently, vigorous agitation must be avoided to prevent the dissipation of methanogenic centers [6].

IV-.3.5.v. Organic loading rate (OLR)

The **Table 2** shows the OLR used in literature for vinasse in case of mono and co-digestion. The maximum OLR in terms of volatile solids is 3.0 and 11.5 in terms of COD. During the digestion of the sugar beet vinasse and press mud, the authors made the choice to dilute the vinasse with water. In addition, recirculation allowed to reduce the dilution of the vinasse [220]. Moreover, press mud is used as co-substrate for the digestion of vinasse [208], or cellulose and straw for additional carbon source [205]. Vinasse having a pH lower than the optimal pH of the anaerobic digestion, the authors alkalised the vinasse by adding NaOH solution [208].

With this pilot test, we chose to study the vinasse in mono-digestion, in that respect, no addition of carbon source was made. Moreover, we also chose to not dilute the vinasse as we want to study the anaerobic digestion without consuming water. As these actions would help to stabilise the process, the organic load was increased very gradually to avoid inhibitions of the process.

Table 2: Organic load in literature

Source	Substrate	Remark	OLR range	
			$g_{VS}.L^{-1}.d^{-1}$	$g_{COD}.L^{-1}.d^{-1}$
[223]	Molasses	Mono-digestion	-	1.5-7.5
[205]	Sugar beet vinasse	Dilution of vinasse Addition of cellulose and straw	2.0-3.0	-
[218]	Sugarcane filter cake and bagasse	Co-digestion Addition of water	2.0-3.0	-
[220]	Vinasse	Dilution with water, then recirculation Addition of NaOH	-	0.2-11.5
[208]	Press mud and water Vinasse and press mud	Mono-digestion with addition of water co-digestion	0.5-2.2	-

The organic load and the feeding frequency used in this study are recapitulated in the **Table 3** for the whole study. The initial feeding is 13.5 L of sludge and 0.5 L of vinasse, which corresponds to 14.28 $g_{COD}.L^{-1}$. During the first study phase, the digester is fed with 500 mL of vinasse every two days. The biogas is produced in two days when adding 500 mL, which corresponds to an OLR of 0.85 $g_{VS}.L^{-1}.d^{-1}$ and 1.51 $g_{DCO}.L^{-1}.d^{-1}$. A low initial OLR is chosen because inhibitions due to an accumulation of VFA occur during an excessive OLR during the anaerobic digestion of the vinasse. The latter having a low C / N ratio, the inhibitions are frequent in the case of mono-digestion of vinasse.

The feeding frequency is then changed in order to open the digester less often, to reduce the oxygen input into the digester. Thus 750 mL of vinasse are added every three days, then 1000 mL every 4 days. During the next phase, the OLR is increased from 0.25 $L.d^{-1}$ to 0.38 $L.d^{-1}$.

In case of a drop in biogas production, 250 mL of vinasse and 250 mL of sludge are added instead of 500 mL of vinasse. Sludge is introduced to input micro-organisms.

Table 3: Mixing strategies and organic load

Description	Period (day)	Mixing strategy	Feeding frequency	Average feeding rate		Average OLR	
				Sludge ($L.d^{-1}$)	Vinasse ($L.d^{-1}$)	($g_{VS}.L^{-1}.d^{-1}$)	($g_{COD}.L^{-1}.d^{-1}$)
Initial feeding	0	No mixing	Initial	13.5	0.5	8.69	14.28
Launching of the pilot	1-28	Minimal mixing*	Once a week	-	0.07	0.25	0.45
	29-42	Minimal mixing	Every 2 days	-	0.25	0.85	1.51
Continuous mixing test	43	10h at 20 rpm	Every 2 days	-	0.25	0.85	1.51
Resumption of minimal agitation	44-53	Minimal mixing	Every 2 days	-	0.25	0.85	1.51
Addition of sludge	54-63	Minimal mixing	Every 2 days	0.125	0.125	0.49	0.85
	64-68	Minimal mixing	Every 3 days	-	0.25	0.85	1.51

Modification of feeding frequency	69-72		Every 4 days				
Increase of OLR	73-112	Minimal mixing	Every 4 days	-	0.31	1.06	1.88
	113-130			-	0.38	1.27	2.26

*Minimal mixing: 15 min at 20 rpm before feeding.

IV-4. Results and discussions

IV-4.1. Biochemical potential test performance

The methane production of the vinasse and the blank are represented in **Figure 2.** The maximum production is reached in 12 days for the vinasse and in 43 days for the inoculum. The biochemical potential of vinasse measured with the ratios in terms of VS 0.9, 0.7 and 0.6 are almost the same (181.72 to 185.59 $NL_{CH4}.kg_{COD}^{-1}$). The maximum value is obtained with the ratio 0.7. The potential obtained with the ratio 1.8 is lower with a value of 152.95 $NL_{CH4}.kg_{COD}^{-1}$. As we obtained similar methane yields for different ratios, we can retain the BMP value. The biodegradability (B) for each ratio is given in the **Table 4**. The biodegradability is 0.44 for the S / I ratio 1, 0.52 for the ratios 2 and 2.5, and 0.53 for the ratio 3. Thus, we recommend to use an I / S ratio inferior to 1 for the vinasse BMP and we retain the BMP value of 185.59 $NL_{CH4}.kg_{COD}^{-1}$.

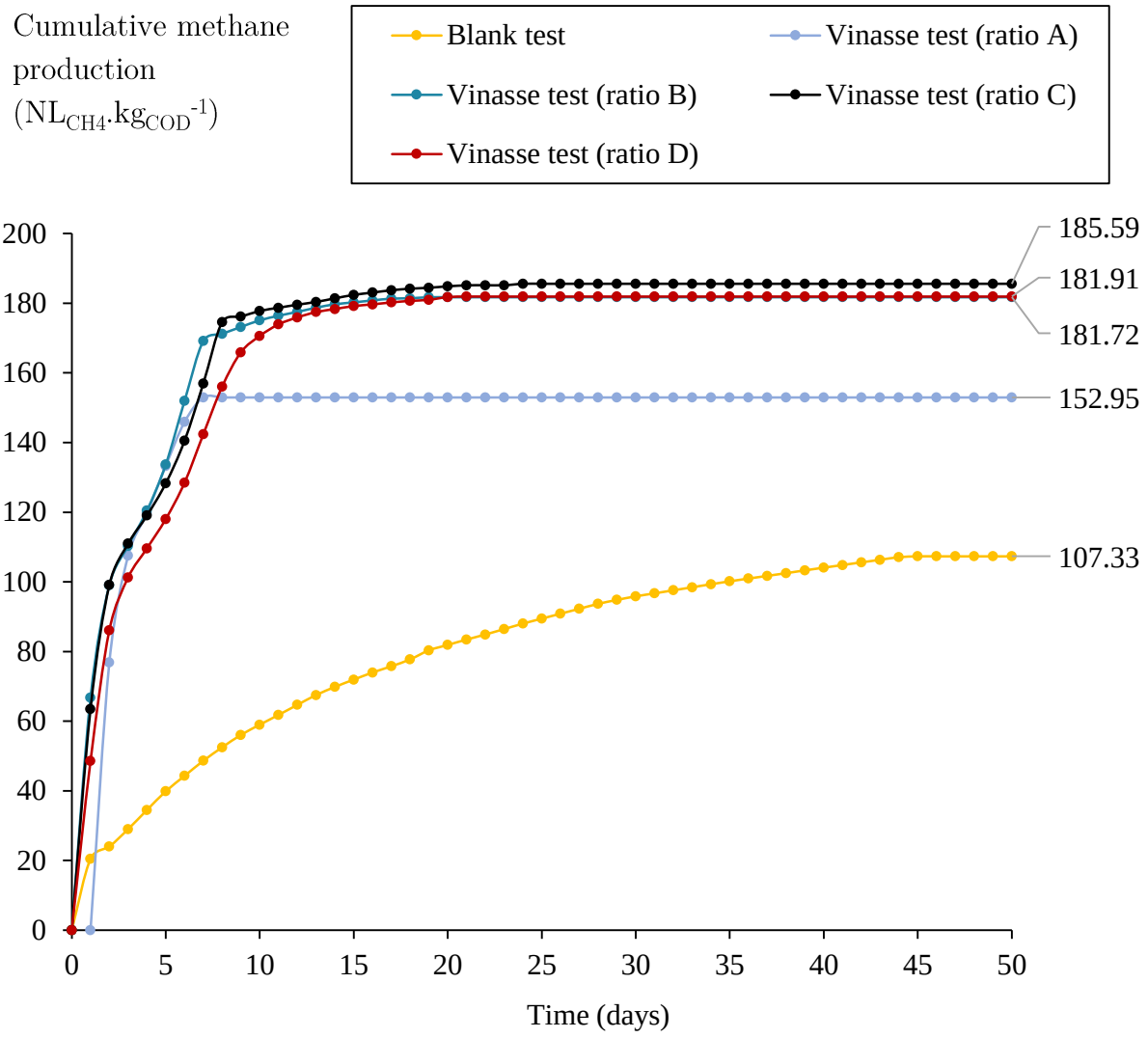

Figure 2: Biochemical potential test results

Table 4: Methane yield and standard deviation

Ratio S / I	B	Methane yield			Standard deviation $NL_{CH4}.kg_{COD}^{-1}$			Standard deviation %		
$g_{COD}.g_{VS}^{-1}$		$NL_{CH4}.kg_{VS}^{-1}$	$NL_{CH4}.kg_{COD}^{-1}$	$NL_{CH4}.L_{sample}^{-1}$	Min	Max	Average	Min	Max	Average
1	0.44	180.53	152.95	8.81	19.51	53.49	42.51	**15**	**38**	**28**
2	0.52	219.93	181.72	16.14	3.80	9.17	5.33	2	13	3
2.5	0.53	251.86	181.59	12.35	7.36	11.10	10.11	5	12	6
3	0.52	322.95	181.91	15.72	0.61	9.19	4.61	1	6	3

The methane yield in terms of COD, VS, sample and the standard deviation are given in the **Table 4**. We clearly see that the methane yield is becoming more important with increasing the ratio S / I. Moreover, we notice that the standard deviation is at least five times more important for ratio 1 than for the other ratios. The maximum standard deviation for the ratio 1 is 53.49 $NL_{CH4}.kg_{COD}^{-1}$ (38 %), which is upper than 10%, thus this test result must be rejected. Since the standard deviation for the ratio 1 is important, this means that the dispersion of the BMP results for this ratio is important, the average BMP results for this ratio is therefore not representative. We interpret this result as follows, for this ratio we put a sample mass too small to be representative of the substrate. Indeed, vinasse being heterogeneous, it requires a sufficiently large sample to be representative of the substrate in terms of methanogenic potential. We free ourselves from the heterogeneity of the vinasse by increasing the ratio S / I, allowing to obtain representative results with standard deviation less than 10 %. A second explanation is that inhibitions occur at this ratio, which would explain that the production of some BMP is lower. Concerning the other tested ratios, the average standard deviation is lower than 6 %, thus the BMP results are acceptable.

IV-4.2. Modelling the kinetics of methane production

Table 5: First-order regression and modified Gompertz model coefficients

	Parameters	Units	Coefficients				
Ratio	S / I	$g_{COD}.g_{VS}^{-1}$	1	2	2.5	3	A*
	I / S	$g_{VS}.g_{VS}^{-1}$	1.8	0.9	0.7	0.6	
First-order regression	Kinetic constant k	Day^{-1}	0.61	0.32	0.29	0.25	0.29
	Maximum methane production Y_{max}	$NL_{CH4}.kg_{COD}^{-1}$	152.9	181.7	185.6	182.5	183.3
	Correlation factor R^2	-	0.97	0.99	0.98	0.99	0.99
	RMSE	$NL_{CH4}.kg_{COD}^{-1}$	4.60	4.01	4.77	3.98	4.25
Modified Gompertz model	Methane production rate Rm	$NL_{CH4}.kg_{COD}^{-1}.day^{-1}$	50.39	28.54	25.44	22.01	25.33
	Lag-phase time λ	Day	0.866	1.483	1.598	1.967	1.683
	Maximum methane production Y_{max}	$Nl_{CH4}.kg_{COD}^{-1}$	150.4	181.2	184.8	181.0	182.3
	Correlation factor R^2	-	0.97	0.97	0.97	0.98	0.97
	RMSE	$Nl_{CH4}.kg_{COD}^{-1}$	4.06	5.65	6.29	5.53	5.83

*Average of BMP (ratio 2, 2.5 and 3)

The coefficients for the first-order regression and the modified Gompertz model for each ratio are given in the **Table 5**. The first-order kinetic model provides the kinetic constant of hydrolysis. The highest value of 0.61 d^{-1} is obtained with the S / I ratio 1. However, the kinetic constant for the ratio 1 is rejected because this BMP was rejected. Then, the kinetic constant decreases with the increasing of S / I ratio. The kinetic constant is 0.32 d^{-1} for S / I ratio 2. The lowest value is therefore obtained with the S / I ratio 3 with a value of 0.25 d^{-1}. Thereby, despite the fact that the kinetic constant is higher for the ratio S / I 1 (I / S of 1.8), the maximum methane production is the lowest. Thus, lower kinetic coefficients led to higher methane yields. Moreover, the average kinetic constant, rejecting the value of the ratio 1, is 0.29 d^{-1}. The kinetic constant values obtained are similar, with a standard deviation of 0.04 d^{-1} (12 %). The kinetic constant will be used in biochemical model as the hydrolysis constant. As the hydrolysis phase is considered as the rate-limiting step, this coefficient is crucial in the anaerobic digestion modelling. The correlation factor is between 0.97 and 0.99 and the RMSE between 3.98 and 4.77 $NL_{CH4}.kg_{COD}^{-1}$. The modified Gompertz model provides the methane production rate and the lag-phase time. The methane production rate decreases with the increasing of S / I ratio from 56.16 to 27.43 $NL_{CH4}.kg_{COD}^{-1}.d^{-1}$. The correlation factor is between 0.97 and 0.98 and the RMSE between 4.06 and 6.29 $NL_{CH4}.kg_{COD}^{-1}$.

The **Figure 3** shows the comparison between measured data, calculated data with the first order kinetic and the calculated data with modified Gompertz model for cumulative methane production at different S / I ratios. The correlation factor of the first-order kinetic is between 0.97 and 0.99. It is similar to the correlation factor of the modified Gompertz model, which is between 0.97 and 0.98. Concerning the RMSE, it is between 3.98 and 4.77 for the first-order kinetic, and between 4.06 and 6.29 for the modified Gompertz model. The first-order kinetic and the modified Gompertz model fit well with the measured data.

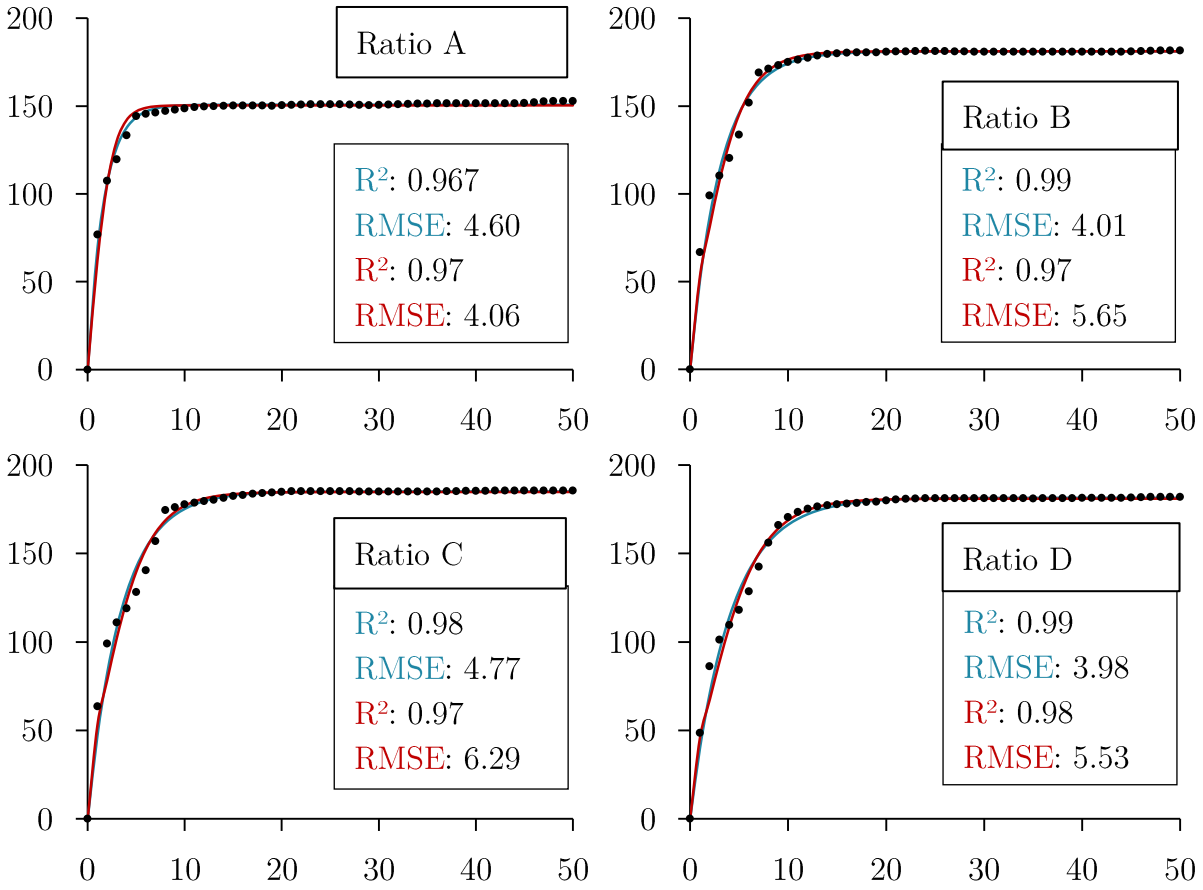

Figure 3: Cumulative methane production ($L_{CH4}.kg_{COD}^{-1}$) in function of time (days): comparison between measured data (point), calculated data with the first order regression (blue full line) and calculated data with modified Gompertz model (red full line) for cumulative methane production at different I/S ratios.

IV-4.3. Comparison of results with the Chapter III and the literature

In the **Table 6**, we present the comparison of kinetic constant (first-order regression) with literature. In this work, we retain the range 0.25-0.32 d^{-1}, we exclude the value 0.61 d^{-1} because the methane production of this BMP has a standard deviation upper to 10%. The average value is therefore 0.29 d^{-1}. Compared to literature, the kinetic constant found in this study is similar to [208] with a value of 0.30 d^{-1} [208] and vinasse with press mud with a range of 0.23-0.33 d^{-1} [208].

In comparison with the Chapter III, the kinetic constant obtained in this study is higher. Indeed, the inoculum was different for the two studies. In this work, we used fresh inoculum. Therefore, it makes sense that the kinetic constant is higher with fresh inoculum. The micro-organisms concentrations might be larger. Consequently, the obtained methane potential is higher with the fresh inoculum. However, the same trend is observed, i.e. the methane potential is obtained when the I_{VS}/S_{VS} value is 1.

Table 6: Comparison of kinetic constant (first-order regression) with literature

Source	Substrate	Kinetic constant range d^{-1}
This chapter	Vinasse + water	0.25 - 0.32
Chapter III	Vinasse + water	0.088 – 0.16
[208]	Vinasse + water	0.30
	Press mud	0.16
	Vinasse + press mud	0.23 - 0.33
[224]	Vinasse + rumen	0.0.73 - 0.210
	Vinasse + rumen + urea	0.087 - 0.206

IV-4.4. Pilot tests performance and physico-chemical analysis

IV-.4.4.i. The specific biogas production and COD removal

The **Figure 4** shows the specific biogas production in litters per kilogram of COD added in the digester and the OLR. The graph illustrates two phases, the start-up phase from day 0 to day 45 and the steady conditions phase from day 46 to day 130. The steady conditions phase begins when the production of biogas stabilises. The duration of the start-up phase is in the same order of magnitude as the duration that the study [205] which is 50 days. During the continuous agitation test (day 43), the production of biogas stopped, so we only tested this stirring for a period of 10 hours and then return to minimal agitation that we maintained until the end of the experiment. Thus, this agitation was tested just before the end of the pilot start-up period. However, as the production of biogas stabilises during the recovery of minimum agitation, we still consider that the steady-conditions phase starts on day 46. We conclude from this test that continuous agitation stops the production of biogas, this may be due to the fact that there is no longer sufficient contact between the microorganisms and the substrate. Stirring the medium only during the filling of the pilot is enough in the case of the

treatment of a liquid waste for the studied volume (16 L). However, it would be interesting to study other intensities of agitation.

During the period 113-130 days, the production of biogas per kilogram of COD is three times higher than in the previous period. It seems that the micro-organisms concentration is larger and the micro-organisms are better acclimated, which would explain this consequent increase in production. In fact, the TS and the VS of the sludge and the liquid phase increase over this period, which means that the biomass concentration increases within the digester. Thus, the physico-chemical conditions at this time are conducive to the anaerobic digestion of the raw vinasse.

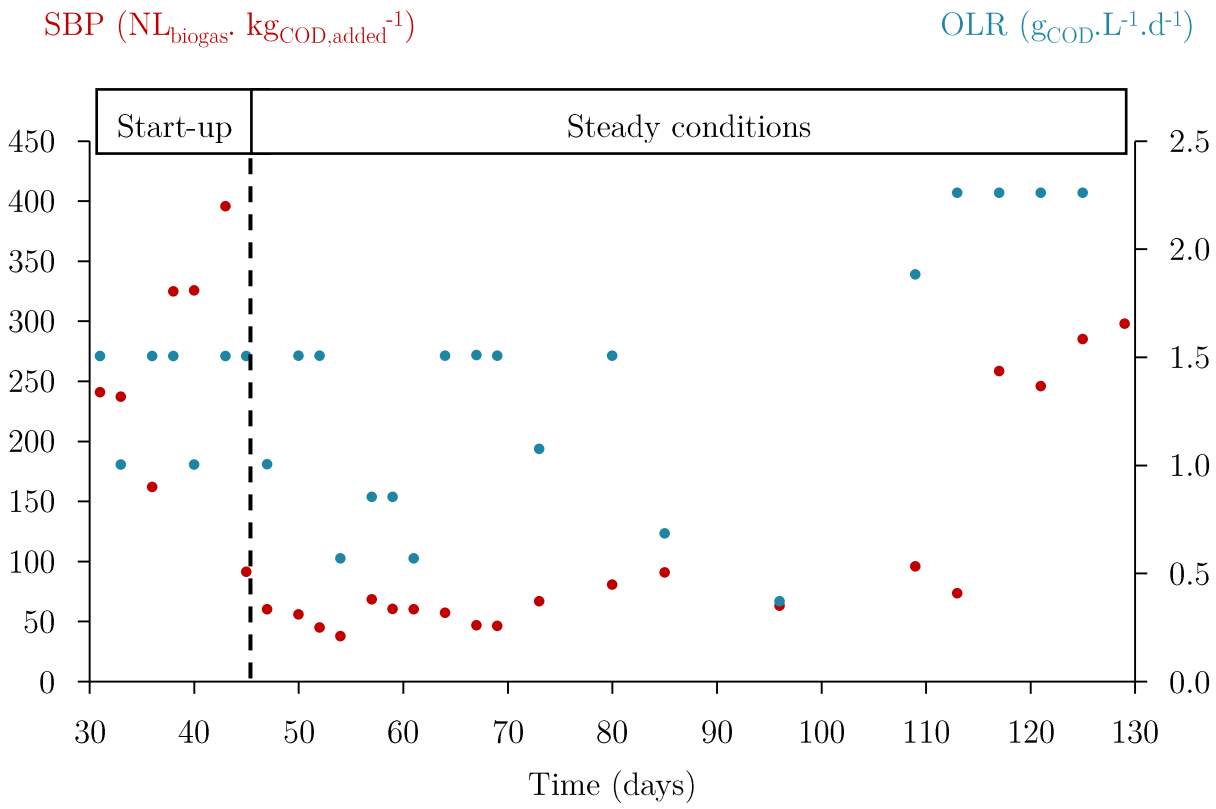

Figure 4: Specific biogas production in $NL.kg_{COD,added}^{-1}$ and organic loading rate (OLR)

The **Table 7** shows the COD removal, the specific methane production (SMP), the specific biogas production (SBP) and the degradation index. The biogas production during the start-up phase is more important than the production during the steady conditions phase. It goes from an average of 182.69 $NL_{CH4}.kg_{COD}^{-1}$ during the period 29-

42 days (start-up phase) to an average of 37.79 $NL_{CH4}.kg_{COD}^{-1}$ during the period 43-53 days (beginning of the steady-conditions phase). Indeed, during the start-up phase, the production of methane is due to the digestion of the vinasse but also to the digestion of the sludge initially introduced into the digester. This is consistent with the BMP blanks assays where only vinasse sludge is inserted into the digesters, we note that the maximum production of methane is reached after days around 45 days, the same duration as the start-up phase.

Table 7: COD removal, specific methane production, specific biogas production and degradation index

Period (day)	COD removal	SMP*	SMP	SBP	D_{index}
	%	$NL_{CH4}.kg_{COD,r}^{-1}$	$NL_{CH4}.kg_{COD}^{-1}$	$NL_{biogas}.kg_{COD}^{-1}$	
1-28	51	-	-	-	-
29-42	49	-	182.69	281.07	0.98
43-53	64	59.64	37.79	58.13	0.20
54-63	68	58.59	40.10	61.68	0.22
64-68	75	40.65	30.32	46.65	0.16
69-72	74	58.50	43.48	66.89	0.23
73-112	79	69.06	52.60	82.74	0.28
113-130	84.3	179.40	151.00	232.31	0.81
Steady conditions 46-130	73	87.54	68.21	104.93	0.37

*COD,r: removal COD

The average production of biogas during the start-up phase is 281.17 $NL_{biogas}.kg_{COD}^{-1}$ and during the steady conditions phase is 104.93 $NL_{biogas}.kg_{COD}^{-1}$. During the steady conditions phase, the minimum and maximum biogas production are respectively 37.90 $NL_{biogas}.kg_{COD}^{-1}$ at day 54 (OLR is 0.85 $g_{COD}.L^{-1}.d^{-1}$) and 298.10 $NL_{biogas}.kg_{COD}^{-1}$ at day 130 (OLR is 2.26 $g_{COD}.L^{-1}.d^{-1}$). We observe that the production of biogas per kilogram of COD added tends to increase: with an average of 58.13 $NL_{biogas}.kg_{COD}^{-1}$ over the period 43-53 days, 61.68 $NL_{biogas}.kg_{COD}^{-1}$ over the period 54-63 days, 66.89 $NL_{biogas}.kg_{COD}^{-1}$ over the period 69-72 days, 82.74 $NL_{biogas}.kg_{COD}^{-1}$ over the period 73-112 days, and 232.31 $l_{biogas}.kg_{COD}^{-1}$ over the period 113-130 days. In the **Table 7**, for the calculation of the production of methane, we assume that the percentage of methane in the biogas is 65% in the results following the analysis of biogas on some samples, all samples must be analysed by chromatography to obtain the proportion of gases for the entire study. Thereby, the specific methane

production has an average of 37.79 $NL_{CH4}.kg_{COD}^{-1}$ over the period 43-53 days and 151.00 $NL_{CH4}.kg_{COD}^{-1}$ over the period 113-130 days (Table 8). The maximum biogas production is obtained with the maximum OLR tested of 2.26 $g_{COD}.L^{-1}.d^{-1}$. The **Table 7** shows also the percentage of COD removal and the degradation index for each period delimited by a change in OLR. During the start-up phase (the first two periods of the **Table 7**), the COD removal has an average of 50%, and during the steady conditions phase, the COD removal gradually increases from 64% to 85% with an average of 73%. Concerning the degradability index, it varies from 0.16 to 0.81 during the steady conditions phase with an average value of 0.37.

IV-.4.4.ii. The follow-up of the physico-chemical properties of the pilot medium and the sludge analysis

Table 8: Physico-chemical properties of the pilot sludge

Day	pH	TS %	VS %	COD $g_{O2}.L^{-1}$	VFA $mg.L^{-1}$	Am $mg.L^{-1}$	Alk $mg_{CaCO3}.L^{-1}$	VFA/alk
109	7.469	5.48	2.85	53.1	10760	312	10685	1.01
117	7.813	5.81	3.92	47.7	18500	226	14868	1.24
129	7.428	-	-	41.3	14900	224	13507	1.10

The **Figure 5** regroups the graphics of the physico-chemical analysis of the effluent: the ammonium, the VFA, the alkalinity, the VFA / Alk ratio, the pH, the COD and COD removal, the TS, the VS and the VS / TS ratio. The **Table 8** shows the maximum, minimum and average values of physico-chemical analysis of the effluent during the start-up period, and the **Table 10** shows the values during the rest of the study. These values must be taken cautiously because of the layer of sedimentation at the bottom of the digester. Thus, the results correspond to the liquid phase of the pilot. As the test progresses, the solid particles sediment and accumulate at the bottom of the pilot, forming a mud. The mud is also present on the side walls as well as on the agitator. The physico-chemical measurements on this mud were carried out. The measurements are given in the **Table 8**. The COD, the VFA and the alkalinity of the sludge are higher than the medium. The pH and the ammonium concentration of the sludge are in the same range as the medium. Thus the recalcitrant COD and VFA accumulate in the bottom of the pilot, but the pH is barely affected thanks to the increasing of the alkalinity. Furthermore, the VFA concentration is two to three times that of the liquid

medium, this means that the products of the acidogenesis accumulate in the mud, and that organic loading is too high compared to the kinetics of acetogenesis reactions. Indeed, under ideal digestion conditions, AGV production rates are compensated for by the rates of consumption and thus there is no accumulation of AGV. Nevertheless, certain conditions can cause imbalances: an organic overload, the presence of organic or inorganic toxins, or temperature fluctuations [11].

Table 9: Maximum, minimum and average values of physico-chemical analysis of the effluent during the start-up period

Parameters	Units	Start-up 0-45 days		
		Min	Max	Average
Ammonium	$mg.L^{-1}$	314	511	425.4
VFA	$mg.L^{-1}$	1980	5270	3751.8
Alkalinity	$mgCaCO_3.L^{-1}$	5594.4	5947.2	5770.8
VFA / Alk	-	-	-	-
pH	-	7.10	7.50	7.32
COD	$g.L^{-1}$	7.66	17.90	14.38
COD removal	%	36.25	62.65	50.96
TS	%	1.69	2.18	1.96
VS	%	0.48	0.80	0.64
VS / TS	-	0.25	0.37	0.32

Table 10: Maximum, minimum and average values of physico-chemical analysis of the effluent at different OLR

Parameters	Units	46-72 days			73-112 days			113-130 days		
		1.51 $g_{COD}.L^{-1}.d^{-1}$			1.88 $g_{COD}.L^{-1}.d^{-1}$			2.26 $g_{COD}.L^{-1}.d^{-1}$		
		Min	Max	A*	Min	Max	A*	Min	Max	A*
Ammonium	$mg.L^{-1}$	297	380	325.6	284	313	297.6	217.0	298	260.0
VFA	$mg.L^{-1}$	3230	5570	4037	3890	4350	4108	4510	6290	5123
Alkalinity	$mg_{CaCO3}.L^{-1}$	5645	6653	6300	6602	7691	6931	6854	7268	6996
VFA / Alk	-	0.49	0.87	0.65	0.56	0.65	0.59	0.65	0.87	0.73
pH	-	7.35	7.51	7.46	7.40	7.59	7.54	7.46	7.60	7.53
COD	$g.L^{-1}$	14.9	18.7	16.9	16.0	21.2	17.8	16.8	19.5	17.9
COD removal	%	62.5	76.5	68.5	71.3	82.3	78.8	82.7	85.0	84.3
TS	%	2.25	2.34	2.29	2.42	2.53	2.47	2.51	3.01	2.79
VS	%	0.75	0.98	0.88	0.89	0.96	0.93	0.82	1.19	1.05
VS / TS	-	0.33	0.42	0.38	0.37	0.38	0.38	0.33	0.43	0.38

*Average value

The **Table 9** shows the maximum, minimum and average values of physico-chemical analysis of the effluent during the start-up period. The **Table 10** shows the maximum, minimum and average values of physico-chemical analysis of the effluent at different OLR.

The ammonium concentration (A) decreases during the start-up phase from 511 to 314 $mg.L^{-1}$, and stabilises during the steady-conditions phase with an average value of 310.45 $mg.L^{-1}$. The VFA (A) increases during the start-up phase from 1,980 to 5,270 $mg.L^{-1}$, and stabilises during the following phase with an average value of 4,279.00 $mg.L^{-1}$. Sludge was added in the digester between days 55 and 65, we note that the VFA decreases from 4,310 to 3,230 $mg.L^{-1}$. Thus, the addition of sludge has the effect of reducing the VFA concentration. The VFA and ammonium concentrations stabilised over the period 46-112 days. However, when we increase the OLR from 1.88 to 2.26 $g_{COD}.L^{-1}.d^{-1}$ (113-125 days), we note an increase in VFA concentration from 4,570 to 7,260 $mg.L^{-1}$ and a decrease in ammonium concentration from 298 to 217 $mg.L^{-1}$. This may lead to inhibitions of digestion, we stop the increase of the OLR until these concentrations stabilise. Despite the increase in the VFA concentration and the decrease in the ammonium concentration, the biogas production increases significantly over this period, from 73.67 to 285.29 $NL_{biogas}.kg_{COD}^{-1}$. We conclude that these concentration variations do not lead to inhibitions of the process, but on the contrary, favour the production of biogas. However, inhibitions may occur if the VFA concentration continues to increase and ammonium to decrease. Indeed the acclimation of the microorganisms and the selection of the populations makes it possible to have a better resistance to the high contents of AGV for a stability of the processes [11]. Compared to literature, the VFA was between 3,570 and 7,850 mg.L-1 in the case of the digestion of vinasse [205].

The alkalinity (B) globally increase over the test period. It varies between 5,594 to 7,691 $mg_{CaCO3}.L^{-1}$. The VFA / Alk ratio (B) varies from 0.49 to 0.87 with an average value of 0.65 over the period 46-72 days. Then, it varies from 0.56 to 0.65 with an average value of 0.59 over the period 73-112 days. Next, the ratio increases over the period 113-130 with the augmentation of the OLR, the ratio varies from 0.65 to 0.87 with an average value of 0.73. The minimum value follows the addition of sludge from day 54 to 63. The VFA / Alk ratio above 0.8 may inhibit methanogenic archaea, of 0.3-0.4 indicates an

unstable system, and a ratio of 0.1-0.2 is appropriate [220, 225]. Compared to the ranges of literature, we have an unstable system. However, the digester has only started for 130 days and the ratio decreases so we could be in appropriate conditions.

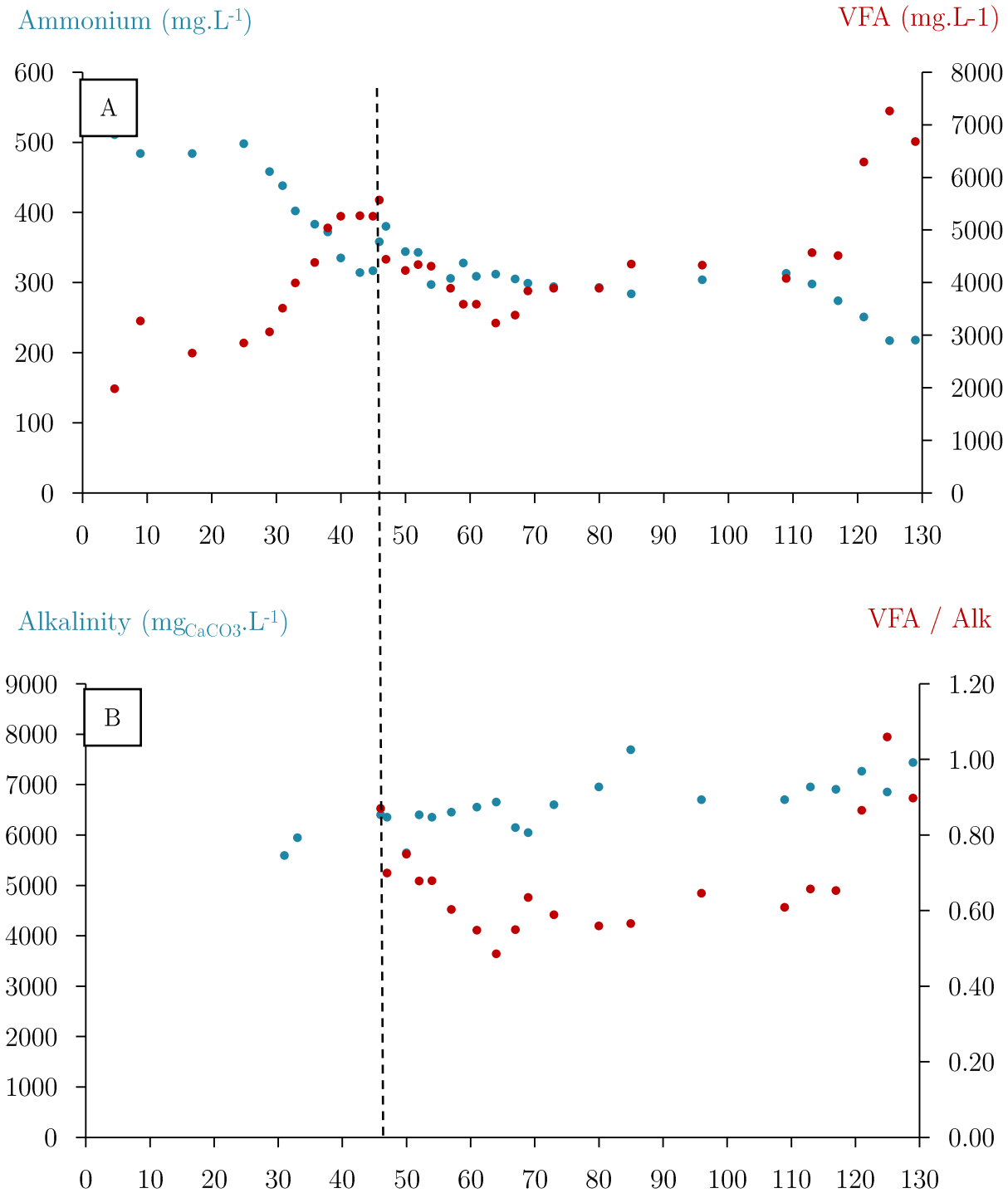

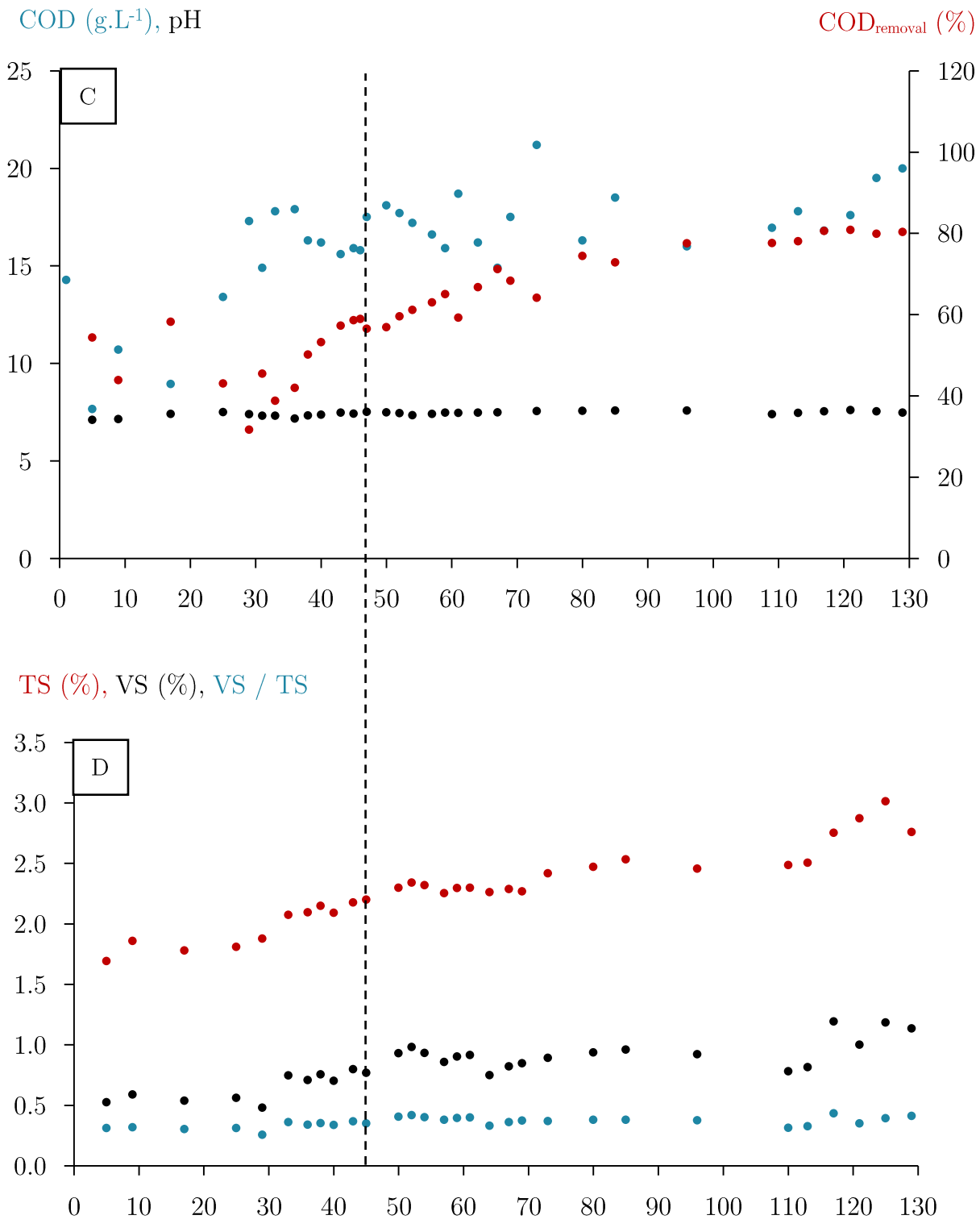

Figure 5: Physico-chemical analysis in function of time (days) of the effluent: (A) Ammonium and VFA, (B) Alkalinity and VFA / Alk ratio, (C) pH, COD and COD removal, (D) TS, VS and VS / TS

The anaerobic digestion process occurs in the pH range of 6.0 to 8.3 [226]. Most methanogens have an optimal pH between 7 and 8 while acid-forming bacteria often have a lower optimum [226]. The pH (Fig. 5-C) of the influents were 7.57 for the sludge and 4.84 for the vinasse. Then, the pH of the medium varies between 7.10 and 7.50 during the start-up phase with an average of 7.31. It varies between 7.35 and 7.60 during the next phase with an average of 7.49. According to the graphic, we see that the pH stabilises during the steady conditions phase. The pH remains stable over the period 113-130 days despite the increase in VFA concentration during this period. Thus, the alkalinity of the digestion medium is sufficiently important to guarantee the stability of the pH. In most digesters, a neutral condition, as indicated by an average pH of 6.8-7.2, is considered normal [225].

Concerning the COD concentration (C), the initial concentration of COD is 14.28 $g.L^{-1}$. During the start-up phase, small amount of vinasse was added, thus, the concentration of COD in the pilot is mainly brought by the sludge. As in the BMP tests, the maximum methane production of the blanks assays (sludge only) is reached in 43 days, we make the assumption that the COD of the sludge is fully consumed after 45 days (steady conditions phase). It slowly decreases between days 1 to 17 from 14.28 to 8.95 $g.L^{-1}$. Then, the COD concentration globally increases during the rest of the test from 8.95 to 19.5 $g.L^{-1}$ with a maximum value of 21.20 $g.L^{-1}$ at day 73. We deduce from this outcomes that the vinasse has a recalcitrant COD which will accumulate in the digestion medium, unlike the sludge. However, this accumulation of organic matter does not seem to affect the production of biogas since it increases over the test period.

In terms of the variation of TS and VS (D), both increase during the assay period. The TS of the samples varies from 1.69% (day 5) to 3.01% (day 125) and the VS from 0.52% to 1.18% (day 125). The averages of TS and VS during start-up phase are respectively 1.96% and 0.64%, and during the steady conditions phase are 2.45% and 0.92%. The ratio VS / TS (E) ranges from 0.25 to 0.42 with an average of 0.32 for the start-up period and ranges from 0.31 to 0.43 with an average of 0.38 for the steady conditions period. The TS and the VS increase on the period 113-130 days, respectively from 2.51 to 3.01% and 0.82 to 1.19%, and the VS / TS ratio remains constant. As previously said, it is the period with the maximum biogas production, which means that

this augmentation of TS is due to the micro-organisms growth. Measures of biological oxygen demand could confirm this hypothesis.

As we see on the graphic (Fig. 5-A), the VFA and ammonium concentrations do not stabilise on the last period. Therefore, we need to continue the test until the stabilisation of these parameters.

IV-5. Perspectives

In this work we obtained the results (biogas production and physicochemical analysis) in the case of mono-digestion of vinasse without any pre-treatment and with constant stirring. Thus, we have data on the physicochemical properties of the digestion medium with the biogas yields. We now have a working pilot. We can vary a selectable parameter to assess its impact on yields and properties of the digestion medium. Thereafter, we will continue the increase of the OLR up to a value of 3 $g_{VS}.L^{-1}.d^{-1}$ as did the authors cited in this article during their pilot studies. The broader perspectives will be to study a pre-treatment of vinasse to improve the biogas yields obtained without diluting the vinasse. The major interest is to limit water consumption in anaerobic digestion plants. In addition, a study will also be performed on different modes of agitation including intermittent agitation and the variation of the stirring intensity.

IV-6. Conclusion

The study showed that the first-order kinetic and the modified Gompertz model fit well with the BMP test curves with a correlation coefficient respectively upper to 0.98 and 0.97. Concerning the I / S ratio, the outcomes demonstrated that a ratio in terms of volatile solids lower than 1 (0.9, 0.7 and 0.6 ratios) gives the maximum methane yield with a value of 185.59 $NL_{CH4}.kg_{COD}^{-1}$ (I / S ratio of 0.7). Moreover, we retain a value of 0.29 $days^{-1}$ for the kinetic constant of the sugarcane vinasse. This parameter is useful for the modelling of the anaerobic digestion process based on reactions kinetics.

In the present study, the biogas production and physico-chemical analysis are given for the pilot test over a period of 130 days. The results showed that the start-up period with vinasse sludge from the same distillery as the vinasse, lasted 45 days. Then the physicochemical parameters and the biogas production were stabilised for each OLR.

That said, although the physicochemical parameters have stabilised, the production of biogas continues to increase. Indeed, with the increase of the pilot's age, the biogas yield improves. The BMP of the vinasse was 185.59 $NL_{CH4}.kg_{COD}^{-1}$ and the average specific biogas production of the last period (OLR of 2.26 $g_{COD}.L^{-1}.d^{-1}$) of the test was 151.00 $NL_{CH4}.kg_{COD}^{-1}$ (232.31 $NL_{biogas}.kg_{COD}^{-1}$), which gave a degradability index of 0.81. The maximum COD removal is 84.3%, it was obtained during the steady-conditions phase (OLR of 2.26 $g_{COD}.L^{-1}.d^{-1}$). We emphasise that the experimental results show that biogas production can be optimised by varying the OLR. It would have been interesting to be able to compare the biogas yields with different pilot start-up strategies, notably by increasing the OLR more or less quickly in order to study the impact of the pilot's loading rise in the start-up phase.

As the biogas yield gradually increased in pilot test, the OLR will be further increased progressively in future studies; in order to avoid inhibitions. The objective is the creation of a database for mesophilic mono-digestion of raw vinasse. The next step will be to test different mixing conditions and pre-treatment on vinasse.

IV-7. Acknowledgements

This work was supported by the Region Reunion (France) as part of the funding of a research thesis in the PIMENT (Physics and Mathematical Engineering for Energy, Environment and Building) laboratory at the University of Reunion Island.

Chapitre V

Study of the impact of mechanical agitation on the performance of semi-continuous anaerobic digestion of vinasse

Dans le chapitre précédent, le démarrage du pilote de laboratoire pour la digestion anaérobie de la vinasse a été effectué avec une agitation minimale de 20 tr/min durant 15 min avant d'extraire le digestat et de nourrir. La consommation électrique de l'agitation des digesteurs industriels étant un pôle de consommation important. L'objectif de ce chapitre, rédigé au format d'article scientifique, est donc de proposer une étude expérimentale sur l'impact de l'intensité du mélange sur la digestion anaérobie de la vinasse brute. Pour cela, des mesures globales et locales des propriétés physicochimiques du milieu de digestion sont effectuées. L'expérimentation est menée pendant 365 jours. Le mélange minimal est employé. Les intensités de mélange testées sont de 20, 30, 40, 50 et 60 tr / min. La relation entre les rendements en biogaz et les propriétés physicochimiques du milieu est étudiée afin de comprendre l'impact de l'agitation mécanique sur la digestion anaérobie.

V-1. Abstract

Sugarcane vinasse is known as a recalcitrant waste in the context of anaerobic digestion on one hand. For this reason, it is typically co-digested or diluted with large amount of water. On the other hand, the electrical consumption of the agitation of industrial digesters is important. Therefore, the aim of this paper is to propose an experimental study on the impact of mixing intensity on the anaerobic digestion of raw vinasse. For this purpose, global and local measurements of the physicochemical properties of the digestion medium are performed. The experimental study is done with a 16 L pilot during 365 days. The mixing mode is a minimal mixing, which consists in 15 min stirring before extraction/feed. The tested mixing intensities are 20, 30, 40, 50 and 60 rpm. The relationship between biogas yields and these properties makes it possible to understand the impact of mechanical agitation. The biogas production gradually increases for stirring intensities ranging from 20 to 60 rpm, with a maximum production of 477 $L_{CH4}.kg_{COD}^{-1}$. Finally, peaks in biogas production are observed during the stirring change. In parallel, variation in VFA and ammonium concentrations are apparent. Nevertheless, the local study allows to understand the impact of mixing on the whole medium and to interpret the yields. Indeed, the homogenisation of the medium is known thanks to these measurements. Furthermore, the local measurements show the location of the acidic zones.

Keywords

Anaerobic digestion, vinasse, mixing conditions, experimental study

V-2. Introduction

The cultivation of sugar cane is predominant in Reunion Island with a cultivated area of 27 000 ha [227]. Reunion Island is a region of France located in the Indian Ocean, in a tropical environment. The molasses are directed to three distilleries for the production of rum, 38% to the Savanna distillery, 59% to the Rivière du Mât distillery and 3% to the Isautier distillery [227]. The vinasse is a waste generated during the alcohol production. In 2000, approximately 150 000 t of the vinasse were produced [227]. All the vinasse was previously diluted due to the potash content, then rejected in sea. However,

the rejection of vinasse may causes environmental pollution such as salinity, sodicity, phytotoxicity, anoxia, eutrophication, death of aquatic life, and many severe health problems due to its high pollutant content [40]. Faced with these risks, the distilleries must treat the vinasse before rejecting it. Anaerobic digestion is an appropriate method for treating this organic waste, as it reduces its pollutant content. This natural process reduces the organic matter content of the waste while producing a biogas. During this process; organic matters are digested by a set of bacteria in the absence of oxygen, producing the digestate and biogas. The biogas produced, rich in methane, which is a source of renewable energy. The biogas production from the vinasse has a large potential [228].Thus the Rivière du Mât (Reunion Island) distillery has developed an industrial anaerobic digester for the treatment of its vinasse with energy recovery. In this context, we wonder how to reduce the consumption of water for the treatment of vinasse while optimising anaerobic digestion.

The sugarcane vinasse is a recalcitrant waste, which means that part of its organic matter is hardly biodegradable. The consequences are that the treated vinasse will keep a polluting organic fraction, and that the production of biogas will depend on its degradation. Studies are therefore needed to optimise the anaerobic digestion of sugar cane vinasse. Janke et al., 2015 assessed the kinetic challenges for biogas production from different types of sugarcane waste [228]. The authors recommended biomass immobilisation system for the anaerobic digestion of vinasse due to it low solid content [228]. At industrial scale, the parameters are mostly: the OLR, the HRT and the stirring conditions. Barros et al. (2016) carried out experimental study on the OLR in UASB reactors [220]. Two pilot digesters were launched (21.5 and 40.5 L), in mesophilic temperature, for 230 days, with different OLR [220]. Cabrera-Díaz et al. (2017) carried out an experimental study on the anaerobic treatment of raw sugarcane vinasse in a combined system [229]. The system consists in two reactors: UASB and APBR reactors with respective working volumes of 4.3 L and 3.5 L [229]. The authors determined that the optimum OLR was 12.5 $kg_{COD}.L^{-1}.days^{-1}$ for the UASB reactor and 4.4 $kg_{COD}.L^{-1}.days^{-1}$ for the APBR [229]. Moreover, it was concluded that the OLR had a major impact on H2S emissions, so on the biogas quality [229]. In addition, the digestion medium is subject to acidification during the anaerobic digestion of the vinasse [209]. For this reason, an experimental study was conducted to compare yields for one- and two-step processes [209].

The choice of the mixing conditions (mode, intensity and frequency) is an important factor. It has been shown that that this parameter largely influences anaerobic digestion [4, 5]. In fact, the process yield depends on the contact between the active microbial community and the substrate. Agitation should be chosen so as to create this contact without destabilising chemical reactions with too vigorous mixing [6]. The agitation of the medium allows this contact and also impacts the physico-chemical parameters of the medium such as the temperature, the pH or VFA concentration. Optimum physico-chemical conditions are necessary to optimise the process and to avoid inhibitions. Van Hulle et al. (2014) showed that at pilot scale (120 L), the mixing conditions (mixing and non-mixing conditions) impact the methane production due to VFA accumulation [8]. The homogenisation of the medium also allows the reduction of dead zones in the digester and promote heat transfer and mass within the digester [9]. Moreover, the agitation of the digestion medium is at the origin of energy consumption which is directly linked to operating costs. Indeed, up to 50 % of the consumption in biogas plant is due to mixing [155]. It must therefore be chosen so as to minimise electric consumption.

The aim of this paper is to study the impact of the mixing intensity on the performances of anaerobic digestion of raw sugarcane vinasse. In addition the effect of mixing on the physico-chemical properties of the digestion medium is studied. This paper follows a first study on pilot scalability where agitation was kept constant. Firstly, a literature data on the experimental study of mixing is presented. Secondly the experimental protocol of the study is presented. Lastly the results are discussed.

V-3. Literature review on experimental study of mixing

It exists three types of mixing: gas lift mixing, impeller mixing and draft tube impeller mixing. As the study is about impeller mixing, the literature review mainly focuses on this mode of mixing. Various authors studied the impact of mixing on process performance.

Stroot et al. (2001) studied the effect the mixing under various OLR during liquid anaerobic digestion of municipal solid waste, primary sludge and waste activated sludge in mesophilic conditions [230]. The authors showed that a reduction of level of mixing

improved the performances [230]. Furthermore, at higher OLR, unstable performance was obtained with continuous mixing contrary to minimal mixing [230]. Lastly, an unstable, continuously mixed digester was quickly stabilised by reducing the mixing level [230]. The authors concluded that a continuous mixing is not the most appropriate mixing for the performance and causes inhibitions at higher OLR [230].

Vavilin and Angelidaki (2005) carried out an experimental study on the effect of mixing on the anaerobic digestion of municipal household solid waste and digested manure in mesophilic conditions. The authors observed that thanks to an agitation described as "weak" (stirring table 58 revolutions per minute with a radius of 17 cm), the initial methanogenic centers were conserved and extend within the digester, whereas in the case of vigorous stirring (stirring table 105 times per minute with a length of 5 cm), these centers were reduced in size and finally dissipated. The authors concluded that when methanogenesis is the limiting step (at the launch of the digester) vigorous stirring must be avoided, but when the hydrolysis step is limiting, greater stirring can improve the production of methane and the degradation of solid particles [6].

Karim et al. (2005) studied the effect of mixing on anaerobic digestion of animal waste. The effect of biogas recycling rates and draft tube height on the performance of the six laboratory reactors were investigated. The authors observed higher methane yield in unmixed reactors and for lower biogas recirculation rate. Moreover, they explained the similar performances for mixed and un-mixed reactors because of the low TS content. They assumed that the natural biogas production was sufficient to mix the medium [231].

A study was conducted on the impact of agitation mode on cow manure methane production in laboratory (5 L) and pilot (800 L) scales. Three stirring strategies were tested in this study: continuous (control), minimal (stirring for 10 min before extraction / feeding), intermittent stirring (stop stirring for 2 h before extraction / feeding). Minimal and intermittent agitation resulted in an improvement in methane production of 12.5 % and 1.3 % respectively compared with continuous agitation in the case of the laboratory pilot. In addition, three stirring intensities were also tested from a laboratory pilot (400 mL working volume): minimal (well shaken by hand for about 1 minute each time a sample was taken), gentle (35 rpm), vigorous (110 rpm). The effect of the mixing intensities showed that when the process was overloaded with a high substrate /

inoculum ratio (40 / 60), a gentle or minimal mixing was advantageous over the vigorous mixing. On the other hand, with a low substrate / inoculum ratio (10 / 90), gentle agitation was better [5].

Sindall et al. (2013) studied the effect of mixing at laboratory scale (working volume of 6 L) during the anaerobic digestion of synthetic sludge. The authors studied various mixing speed in different digesters after the time pilot launch (65 days): 0 rpm, 50 rpm and 200 rpm. The biogas production was recorded for three retention times or until failure. The authors recommended lower mixing speed (50 rpm) for improving biogas production. They observed that a mixing speed of 200 rpm and no mixing led to major reduction of biogas production [7].

Lindmark et al. (2014) carried out a literature review on the effects of mixing on the anaerobic digestion process. In particular, the authors pointed out that the intensity and frequency of agitation affect biogas yields. Moreover, they highlighted problems in experiments due to start-up instabilities. The range of 50-100 rpm resulted in a good gas production. In conclusion, further researches are needed for studying the impact of mixing on a chemical and microbial level and on the different step of the process. In addition, the impact of mixing should be studied on various substrates and mixing modes [197].

Zhai et al. (2018) conducted out experimentations on the effect of mixing during anaerobic digestion of dairy manure. Non-mixing and minimal intermittent mixing (5 min per day during feeding) with intensities of 50, 100 and 150 rpm were tested. The results showed that the intensities of 100 rpm outperformed the other intensities. The authors concluded that it exists a mixing intensity for an optimum methane production [10].

Nguyen et al. (2019) studied the impact of mixing on foaming, substrate stratification, methane production and microbial community, during the anaerobic codigestion of food waste and sewage sludge. Irregular distribution of COD and VS was observed in the case of the lack of mixing. Moreover, the authors did not observe foaming and stratification with internal circulation mixing. Concerning the microbial community, the abundance of methanogens at the top was about four times higher than at the bottom [232].

This work aims to contribute to the understanding of the impact of mixing on reactor performances. The literature showed that the stratification of the substrates due to an inappropriate mixing may cause instabilities. Thus, the mixing strategy depends on the type of substrate. In this paper, the effect of mechanical mixing on the physico-chemical properties of the medium is investigated, during the digestion process.

V-4. Material and methods

V-4.1. Digestion process and pilot digester

We study the mesophilic monodigestion of raw sugarcane vinasse. The operating parameters of the pilot are shown in the **Table 1.**

Table 1: Operating parameters

Parameter	Unit	Value
Temperature	°C	37
Reactor volume	L	16
Operating volume	L	13.5
Fill height	cm	15
Hydraulic retention time	Days	36
Influent flow rate	$L.days^{-1}$	0.375
Influent concentration	-	**Table 4**

The hydraulic retention time HRT is calculated by:

$$HRT = \frac{WV}{Q} \tag{60}$$

Where WV is the working volume (m^3) and Q is the influent flow rate ($m^3 days^{-1}$).

The pilot is horizontal and cylindrical with a total volume of 16 L. It has a double membrane in which water circulates to keep it at a constant temperature. A thermostatically bath with water circulation is used to maintain the water at a given temperature. The mechanical stirring can be set from 20 rpm to 100 rpm with a step of 10 rpm. The pilot is equipped with a security valve and a dial allowing to know the temperature of the medium. The bucket counter MGC-1 V3.1 PMMA is used to measure

the biogas produced volume with a measuring chamber volume of 3.18 mL, a minimum flow of 1 mL/h and a maximum flow of 1 L/h. The pilot set-up and the impeller geometry are shown in the **Figure 1** and their dimensions in the **Table 2.**

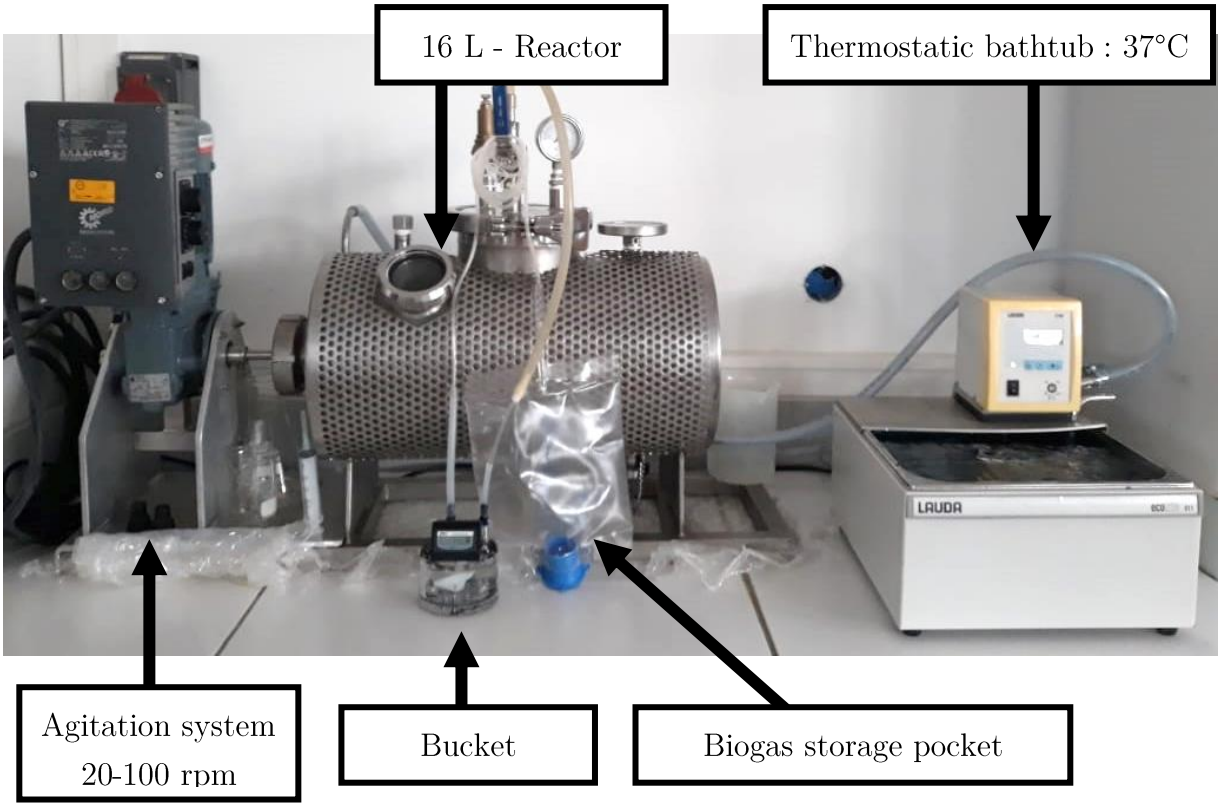

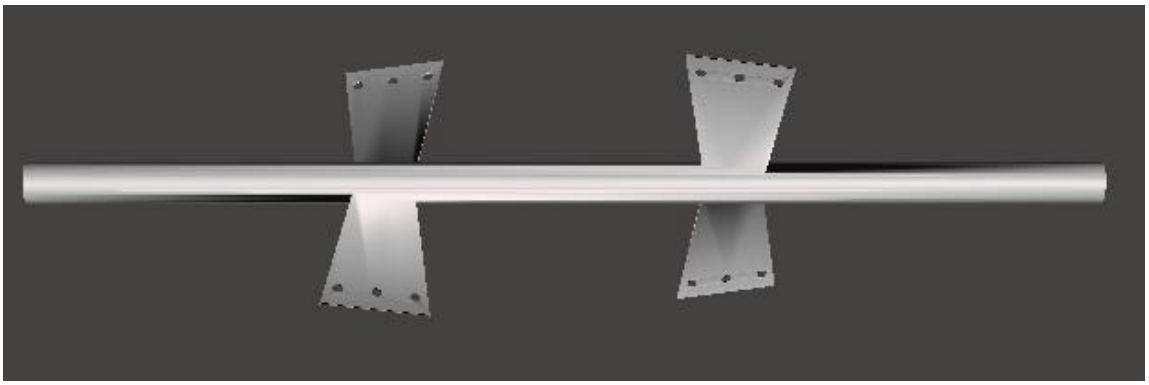

Figure 1: Pilot set-up [ICEECC] and impeller geometry

Table 2: Digester and impeller dimensions

Digester dimensions		
External diameter / internal diameter	cm	27 / 21
Membrane thickness	cm	3
External length	cm	52
Volume	L	16
Impeller dimensions		
Number of blades	-	2*2
Pale spacing	cm	16.5
Axis diameter	cm	1
Length	cm	9
Width	cm	3 to 5
Thickness	mm	1

V-4.2. Substrate, inoculum and physicochemical analysis

The objective is to study the impact of mixing on the performance of the raw vinasse pilot. Therefore, we choose to not add any chemicals to adjust the physicochemical properties. We do not dilute the vinasse as it is done by many authors [205, 218, 220]. However, the vinasse studied in this paper comes from a distillery which processes its vinasse by diluting it to optimise its production of biogas and to avoid the instabilities of the process. In addition, the anaerobic digestion of the vinasse faced to various inhibitions due to is low carbon content. For this reason, press mud [208], cellulose and straw [205] are used as co-substrates. Moreover, the low pH of the vinasse could lead to instabilities, and soda solution is added to alkalise the medium [208].

In this study, the pilot is already been running for 130 days. The experimental data for this period are presented in Chapter IV. The launching of the pilot digester and the increase of the organic load are detailed in Chapter IV. The pilot is already acclimatised to the sugarcane vinasse from the distillery Rivière du Mât (Reunion Island). In this study, we study the same substrate. The vinasse is stocked in a cold chamber at 4°C for limiting the degradation of the substrate. It is stocked for a maximum of four months as the sugarcane campaign does not last all year. Thus, a stock of sugarcane vinasse is collected at the distillery every two months and physicochemical analysis are carried out on each sample. The substrate and the inoculum are homogenised with the Ultra turrax IKA T25 digital at 12,000 rpm for 10 min before the characterisation tests expect for the

BMP test. The TS content is obtained after drying 20 g of the samples for 24 h at 105°C and the VS content after burning the dried samples for 4 h at 550°C. The chemical tests are conducted on the Hach Lange DR5000 Spectrophotometer, using the Hach Lange tests LCK 914 (COD), LCK 381 (TOC), LCK 365 (VFA), LCK 303 (Am), LCK 362 (Alk) and LCK 338 (N).

Physicochemical monitoring is performed during the digestion at the moment of feeding the pilot. At each feeding, 1500 mL of vinasse are added and 1500 mL of the digestion medium are removed. A 60 mL global sample of the removed matter is taken in order to get a sample of the global digester medium. This sample is called "Medium".

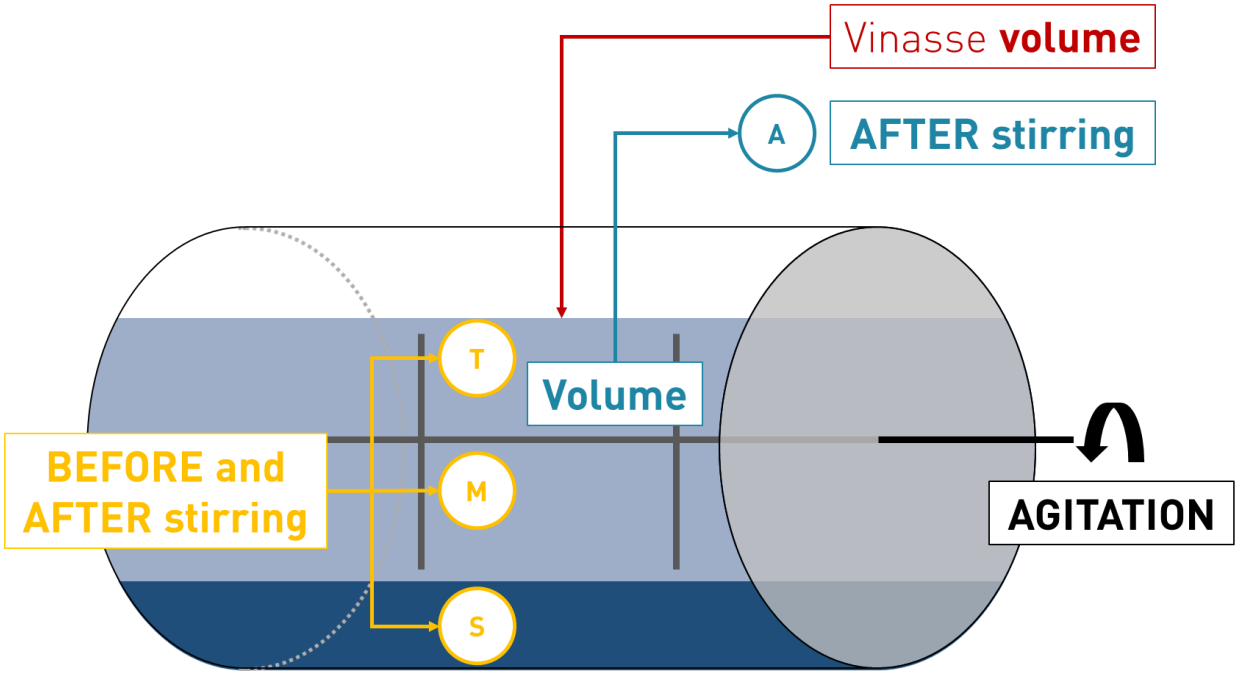

Figure 2: Operating procedure (T: Top, M: Middle, S: Sludge, A: Medium)

Furthermore, another aim is to evaluate the impact of mixing on the physicochemical properties of the medium on the pilot's performance. Therefore, 60 mL local samples are taken from the accumulated sludge at the bottom of the pilot, at the surface of the medium and inside the pilot at 7 cm depth. The samples are respectively named "Sludge", "Top" and "Middle". Samples are withdrawn before and after mixing in order to observe the variation of the physicochemical properties of the fluid before and after the mixing. Samples for local measurements are taken using a 30 mL syringe to control the location of the sample, and to limit the modifications of the medium during the sampling.

However, it remains impossible to perform the sampling at identical locations each time. Taking a sample with a volume of 60 mL allows us to partially overcome this uncertainty.

V-4.3. Organic loading of the pilot

The total volume of the pilot is 16 L and the working volume of the pilot is around 13.5 L. It is fed with 1.5 L of raw vinasse every four days and the same volume of digestate is retired for conserving the working volume. As the COD and TS content of the vinasse vary during the sugar campaign, the OLR also varies but non-significantly. We feed it rarely in order to avoid oxygen input in the digester. We show in the **Table 3** the OLR in function of the sample of vinasse used:

The variation of VS content and COD is between the used sample and the previous substrate sample. We note that the variation of OLR in terms of VS content is negligible (3.15 %) whereas the variation in terms of COD is more remarkable (11.50 %) when we move from vinasse1 sample to the sample vinasse2. Then, when we feed with the vinasse3, the OLR in terms of VS and COD vary respectively by 15.27 % and 6.75 %. Globally, the average values of OLR in terms of VS and COD are respectively 1.36 ± 0.13 $g_{VS}.L^{-1}.d^{-1}$ and 2.38 ± 0.13 $g_{COD}.L^{-1}.d^{-1}$ with the standard deviation which respectively represent 9.55 % and 5.46 % of the average value.

Table 3: Feeding rate and influent concentration

Samples	Vinasse1 08-2018	Vinasse2 10-2018	Vinasse3 12-2018	Average ± standard deviation
Period (days)	0-156	157-197	198-end	-
Volume added / removed (L)	1.5	1.5	1.5	1.5 ± 0
Feeding rate ($L.days^{-1}$)	0.375	0.375	0.375	0.375 ± 0
OLR ($g_{VS}.L^{-1}.d^{-1}$)	1.27	1.31	1.51	1.36 ± 0.13
OLR ($g_{COD}.L^{-1}.d^{-1}$)	2.26	2.52	2.35	2.38 ± 0.13
Variation in terms of VS (%) when changing vinasse feedstock	-	+3.15	-15.27	-
Variation in terms of COD (%) when changing vinasse feedstock	-	+11.50	-6.75	-

As we want to study the impact of stirring on the process yield, we have to identify the cause of the observed variations. Therefore, we do not perform the stirring change at the same time as the vinasse change to separately identify the effects of these two causes of yield variations. Thereby, when changing the vinasse, we expect the production to stabilise before changing the intensity of the mechanical agitation.

V-4.4. Mixing conditions

The literature review showed that the homogenisation of the digestion medium is an important factor in anaerobic digestion factor. The aim of this study is to evaluate the impact of mixing on the biogas yield during the vinasse digestion. For this we have a pilot digester whose characteristics have been exposed previously. Since we have one unit, we must study the agitation regimes one after the other and not in parallel. We expose ourselves to two situations that will impact the results. Firstly, the yield obtained may be due to both the stirring regime applied but also to the previous stirring regime. Secondly, the more the pilot's operating time increases, the more its stability increases, so the improvement of a performance can be due to the agitation and stabilisation of the process over time. It is therefore important to discuss the results carefully taking into account all of these parameters. In order to interpret the produced results, the stirring regimes are studied over a long enough time to allow the process to stabilise at each stirring regime. In addition, we test the different intensities of agitation from the weakest to the strongest. However, the aspect related to the impact of the pilot's age cannot be avoided in this study configuration.

Since the launching of the pilot, the mixing condition applied is 15 min at 20 rpm before the extraction/feed of the pilot (every four days). Therefore, as we change the sample of vinasse, the mixing conditions are maintained for 10 days in order to ensure that the process is not impacted by the variation of OLR. Then, we study the impact of the mixing conditions by modifying only the intensity of mixing, conserving both the mixing time of 15 min and the mixing frequency. The mixing intensity is slowly increased: 10 rpm each time. Furthermore, the duration of each mixing conditions is not defined at the beginning of the experiment, it depends on the stability of the process. When the production volume of biogas per kilogram of added COD is stabilised on the pilot's feed, we change the intensity of the agitation.

V-5. Results and discussions

V-5.1. Physicochemical properties

In the **Table 4**, the physicochemical properties of the inoculum and the vinasse used are presented. The alkalinity, TOC, COD, ammonium and nitrogen concentrations the TS and VS content of the vinasse2 are upper to those of the vinasse1. Nevertheless, the VFA concentration of the vinasse2 is lower to those of the vinasse1. The Alk / COD and C / N ratio of the vinasse samples are closed and the VFA / Alk ratio is more variable with 17.91 for the vinasse1 and 7.59 for the vinasse2. The vinasse3 has the highest value of TS and VS content and VFA concentration. In addition, the vinasse2 has the highest value of COD and ammonium concentration. Globally, the chemical properties of the three vinasse feedstocks are closed but the analysis showed some differences, mostly at the level of VFA concentration and alkalinity with a standard deviation of 3,114 $mg.L^{-1}$ and 637 $mg_{CaCO3}.L^{-1}$ respectively.

Table 4: Physicochemical characteristics of vinasse

Characteristics	Inoculum	Vinasse			
		Vinasse1 08-2018 (Chapter IV)	Vinasse2 10-2018	Vinasse3 12-2018	Average value ± standard deviation
Period (days)		0-156	157-197	198-300	-
BMP ($NL_{CH4}.kg_{COD}^{-1}$)	-	185.59 (Chapter IV)			-
TS %	3.67	7.09	7.97	8.50	7.85 ± 0.71
VS ($\%_{sample}$)	2.21	4.88	5.04	5.78	5.23 ± 0.48
pH	-	4.84	-	4.63	4.74 ± 0.15
COD $g_{O2}.L^{-1}$	37.20	86.70	96.80	90.10	91.2 ± 5.14
TOC $mg.L^{-1}$	12,670	29,875	30,900	-	30,388 ± 725
VFA $mg.L^{-1}$	8,390	19,360	15,237	21,340	18,646 ± 3
Am $mg.L^{-1}$	45.53	37.40	44.93	33.90	38.74 ± 5.64
Alk $mg_{CaCO3}.L^{-1}$	9,107	1,080.86	2,007	2,302	1,796 ± 637
N $mg.L^{-1}$	2,185	1,120.00	1,333	-	1,227 ± 151
Alk / COD	0.25	0.01	0.02	0.03	0.02 ± 0.01
VFA / Alk	0.92	17.91	7.59	9.27	11.59 ± 5.54
C / N ratio	5.85	26.67	23.18	-	24.93 ± 2.47

V-5.2. Performances of the pilot

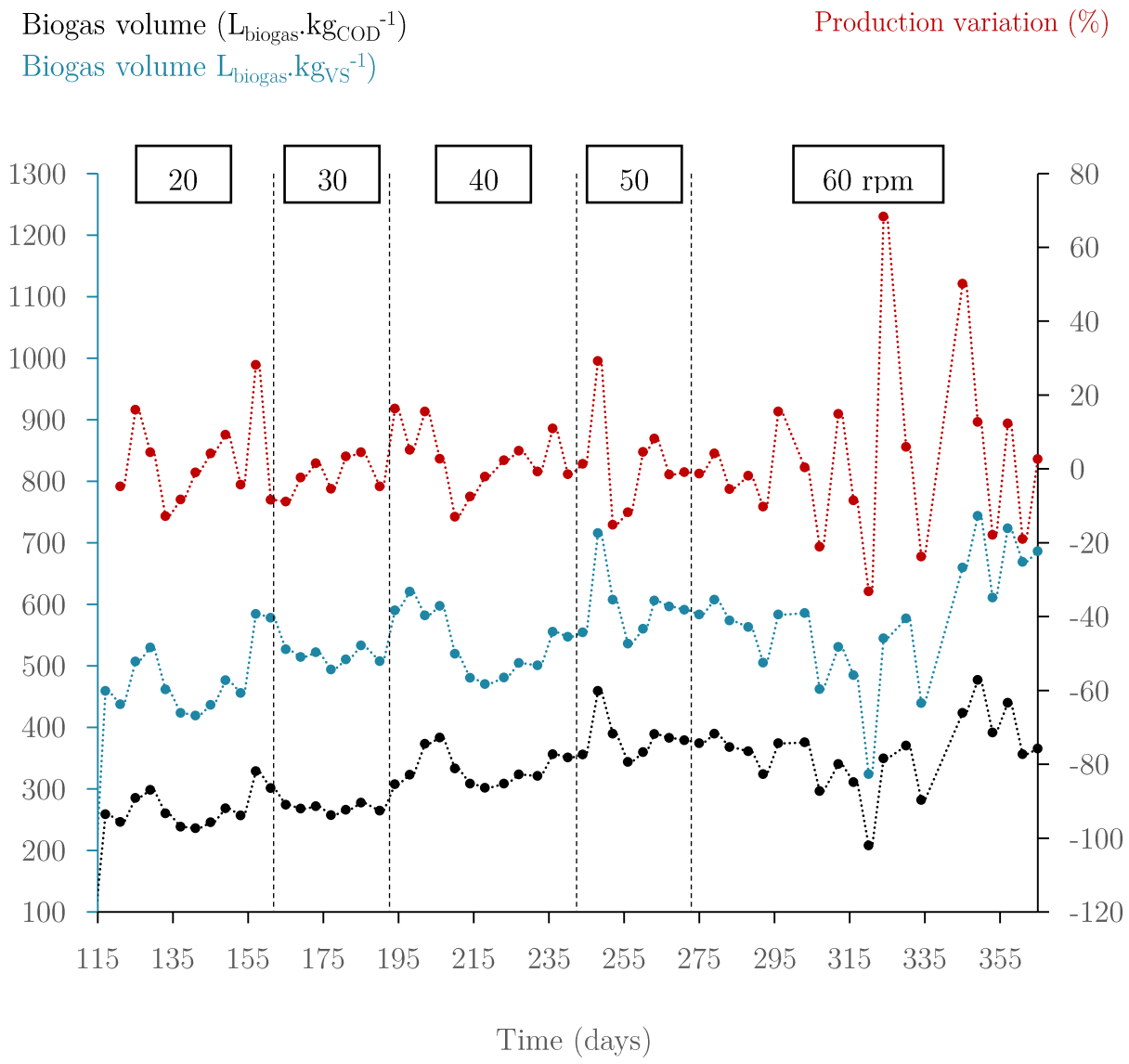

Figure 3: Biogas production, production variation and mixing intensity of the pilot

The semi-continuous pilot is fed every four days. In average, the biogas production is ended in three or four days, thus the biogas production due to the addition of 1.5 L is finished when we feed the digester again. Consequently, we suppose that the obtained biogas production within four days of feeding is due to the 1.5 L of added vinasse. As specified in the materials and method sections, the only parameter modified is the intensity of mixing, indeed the variation of biogas production is related to the change of mixing intensity. However, it is important to note that biogas production also increases

naturally with the age of the pilot. The consequence of the rise of intensity is the increase of the homogenisation of the pilot medium, in particular, biomass, substrates and physicochemical properties.

We show at the **Figure 3**, the biogas production of the pilot at different stirring conditions. Each point corresponds to the production obtained when we feed the pilot with 1500 mL of vinasse. The variation in biogas production from one feeding to another as a percentage of production variation is also shown on the graph.

The period (0-114) days corresponds to the launching of the pilot. The detailed results are presented in a previous chapter. We present in the **Table 5** the minimum, maximum and average production for this period. During this study, the mixing intensity was constant. Therefore, the difference between the minimum and maximum production is substantial. This is reflected in the value of standard deviation of 106 $L_{biogas}.kg_{COD}^{-1}$. Moreover, the maximum production for this period is upper to others, this production was obtained at day 43. Indeed, at this period, the biogas production was due to the anaerobic digestion of both vinasse and sludge.

Table 5: Minimum, maximum and average biogas production ($L_{biogas}.kg_{COD}^{-1}$) in function of mixing intensity

Period	Intensity (rpm)	Duration (days)	Minimum production	Maximum production	A1* ± SD	A2* ± SD
Launching of the pilot						
0-114 (Chapter IV)	20	114	38	396	121 ± 106	-
Study of the impact of mixing intensity						
115-161	20	46	236	329	268 ± 29	270 ± 32
162-190	30	28	257	278	268 ± 7	266 ± 9
191-240	40	49	302	383	332 ± 27	332 ±27
241-271	50	30	344	459	382 ± 35	371 ± 19
272-365	60	93	208	477	359 ± 58	355 ± 63

A1*: Average production; A2*: Average production without the first three values; SD*: Standard deviation

The average biogas production with the mixing intensity of 20 rpm and 30 rpm are 268 $L_{biogas}.kg_{COD}^{-1}$ with a standard deviation of 29 $L_{biogas}.kg_{COD}^{-1}$ and 7 $L_{biogas}.kg_{COD}^{-1}$ respectively. Thus, no remarkable variation in biogas production is observed when

switching the intensity of mechanical agitation from 20 to 30 rpm (day 161). Regarding the standard deviation, the production of biogas is more stable with a stirring of 30 rpm than a stirring of 20 rpm. However, this greater stability can be due to the change of agitation and the stabilisation of the pilot over time. Nevertheless, an increase in biogas production is noted when switching from the agitation intensity of 30 to 40 rpm (day 190). Indeed, the biogas production ranges from 264 to 383 $L_{biogas}.kg_{COD}^{-1}$ from day 190 to 206, which corresponds to an increase of 45 %. Then, the production slowly decreases, but remains higher than the production obtained for stirring at 30 rpm. Thereby, this punctual increase in biogas production following the increase in agitation intensity is due to the return to the digestion medium of accumulated undigested material. The average biogas production for this period is 332 $L_{biogas}.kg_{COD}^{-1}$. Thereby, as the average production with an agitation of 40 rpm is higher than the production with lower agitation, we conclude that the intensity of 40 rpm allows a better homogenisation of the digestion medium allowing an increased production. Likewise, when we switch to 50 rpm, we observe an increase in biogas production from 351 to 459 $L_{biogas}.kg_{COD}^{-1}$ from day 240 to 248, which corresponds to an increase of 31 %. Afterwards, the production slowly decreases to 379 $L_{biogas}.kg_{COD}^{-1}$ with a minimum value of 344 $L_{biogas}.kg_{COD}^{-1}$. The average biogas production for this period is 382 $L_{biogas}.kg_{COD}^{-1}$, which is upper than the average production during the previous period with a mixing intensity of 40 rpm. The last studied mixing intensity is 60 rpm. From the **Figure 3**, we first observe a decrease in biogas production when passing agitation at 60 rpm. Indeed, the biogas production varied from 379 $L_{biogas}.kg_{COD}^{-1}$ at day 271 to 208 $L_{biogas}.kg_{COD}^{-1}$ at day 320, which is the minimum production of this period. Second, the biogas production increased to 440 $L_{biogas}.kg_{COD}^{-1}$ at day 365, with a maximum value of 477 $L_{biogas}.kg_{COD}^{-1}$. The average production is 359 $L_{biogas}.kg_{COD}^{-1}$ with a standard deviation of 58 $L_{biogas}.kg_{COD}^{-1}$. The standard deviation is higher for this period, it reflects the important variations in biogas production. The duration (93 days) for the stabilisation of the biogas production is much longer with the agitation at 60 rpm. However, once the latter has stabilised, the maximum production exceeds the production previously obtained. During the agitation at 60 rpm of the pilot, we notice that the biogas is not yet fully produced. The biogas production was reached after 3 days at most for the preceding agitations whereas it is not yet completed for the agitation at 60 rpm. In addition, during each stirring, biogas is produced. However, the

production of biogas is greater during agitation at 60 rpm with a production of up to half a litter against 200 mL at most for previous agitations.

In conclusion, the biogas production increases with the increase of mechanical mixing intensity of 20 to 60 rpm. Moreover, a peak in biogas production is observed when changing the mixing intensity, followed by a slight decline and the stabilisation of production. Nevertheless, when we increase the stirring intensity to 60 rpm, we observe no peak in the biogas production but a progressive decrease in biogas production with very marked variations, followed by the increase of the production. A phase of stabilisation of the biogas production was necessary before obtaining an improvement of the yields. The initial biogas production reduction could reflect instability of the process that can lead to its failure. In order to confirm or refute this hypothesis, it is necessary to analyse the results on the evolution of the physicochemical parameters during the anaerobic digestion. Thus, from these initial results, we can conclude that we obtain the highest biogas yield for a 60 rpm agitation after thereabouts two months of process stabilisation. In order to confirm these results, it would be interesting to run pilots in parallel with different agitation intensities, to overcome the pilot's age on the results but also the impact of the change of agitation. Indeed, depending on the age of the pilot, the latter may be more resistant to inhibitions. The micro-organisms become more resistant and the pilot's alkalinity increases. Thereby, the response to the change of agitation could be different depending on the age of the pilot. Thus, the observations made depend on the age of the pilot. The gradual increase in mechanical agitation has thus been able to impact the increase in biogas yields. That is why it would be interesting to compare these results with the results of a pilot with constant agitation over the same study period.

The variation of the VS content and removal VS are shown in the **Figure 4.**

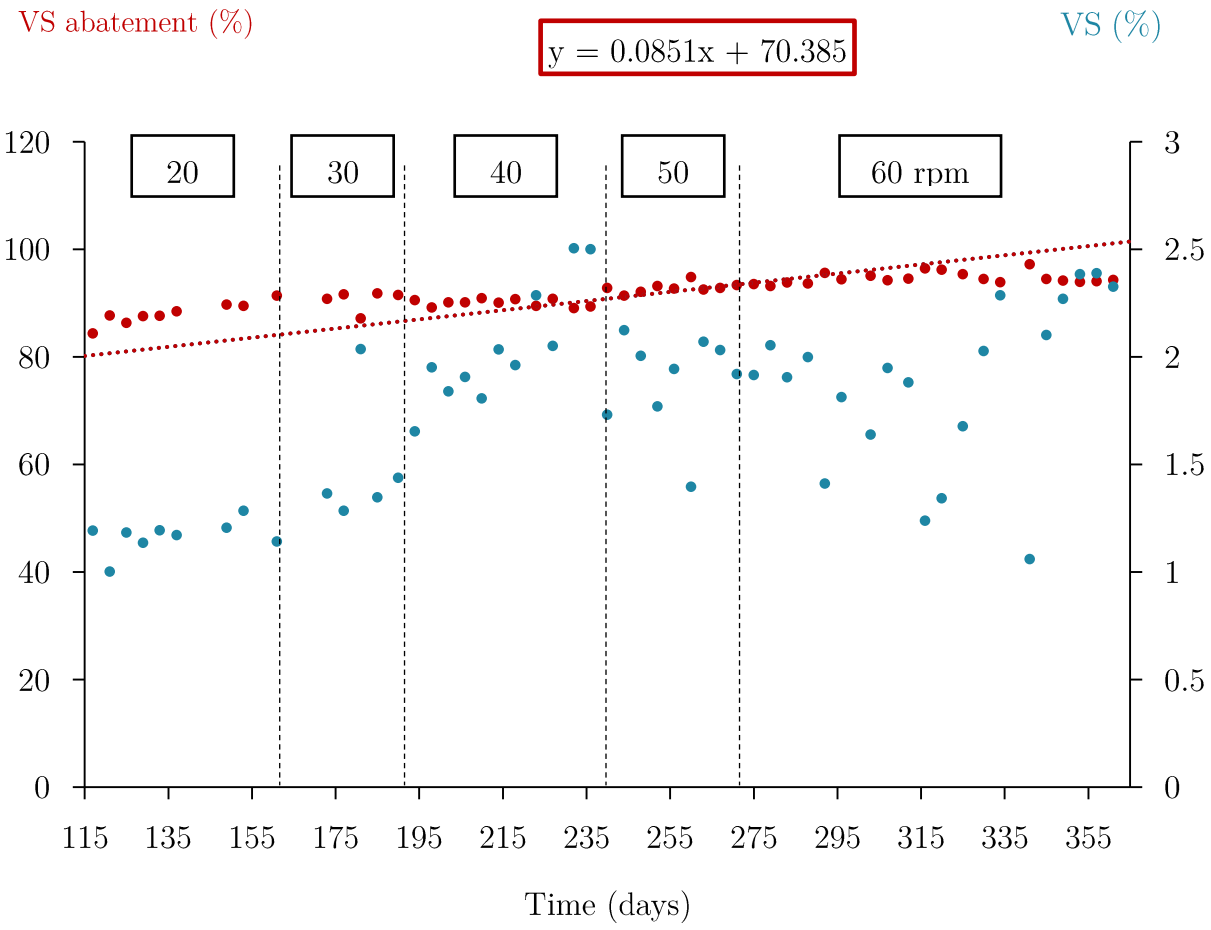

Figure 4: Variation of the VS and removal VS during the process

The removal VS is calculated as follows:

$$VS_{\text{Removal}} = \frac{VS_{digested}}{VS_{added}} * 100 = \frac{VS_{added} - VS_{measured}}{VS_{added}} * 100 \quad (61)$$

Where VS_{added} is the cumulated added VS content in the pilot and $VS_{measured}$ is the VS content of the digestate.

It can be seen that the removal VS is upper than 80 % for the whole study with a maximum value of 97.18 %. Both the removal VS and the VS content gradually increased along the process.

The rest of the study focuses on physicochemical analysis of the medium during digestion. The objective is on the one hand to know the optimal physicochemical properties, and on the other hand to observe the evolution of its properties during

changes in biogas production. Indeed, knowledge of the physicochemical properties of the digestion medium as a function of biogas production makes it possible to anticipate the dysfunctions of the digesters and to optimise the anaerobic digestion process.

V-5.3. Variation of physicochemical properties during the digestion process in the liquid phase

In this section, the variation of physicochemical properties of the digestion medium are presented, in particular, the alkalinity, the pH, the ammonium and VFA concentrations and the VFA to alkalinity ratio. In fact, the first results demonstrated that the mixing intensity has an impact on the biogas yield. In this part, the aim is to study the impact of mixing on the global physicochemical properties of the medium.

V-.5.3.i. VFA and ammonium concentrations

The VFA are the products of the acidogenesis reaction, and the reagents of the acetogenesis. Comparing the VFA concentration of the medium and the treated substrate, we note a decrease in this concentration. From the **Tables 4 and 6**, the average VFA concentration of the vinasse is 18.6 ± 3.1 g.L^{-1} and that of the digestate is 7.80 ± 1.69 g.L^{-1}. Consequently, the high VFA concentration of the medium is due to the substrate VFA concentration and incomplete degradation.

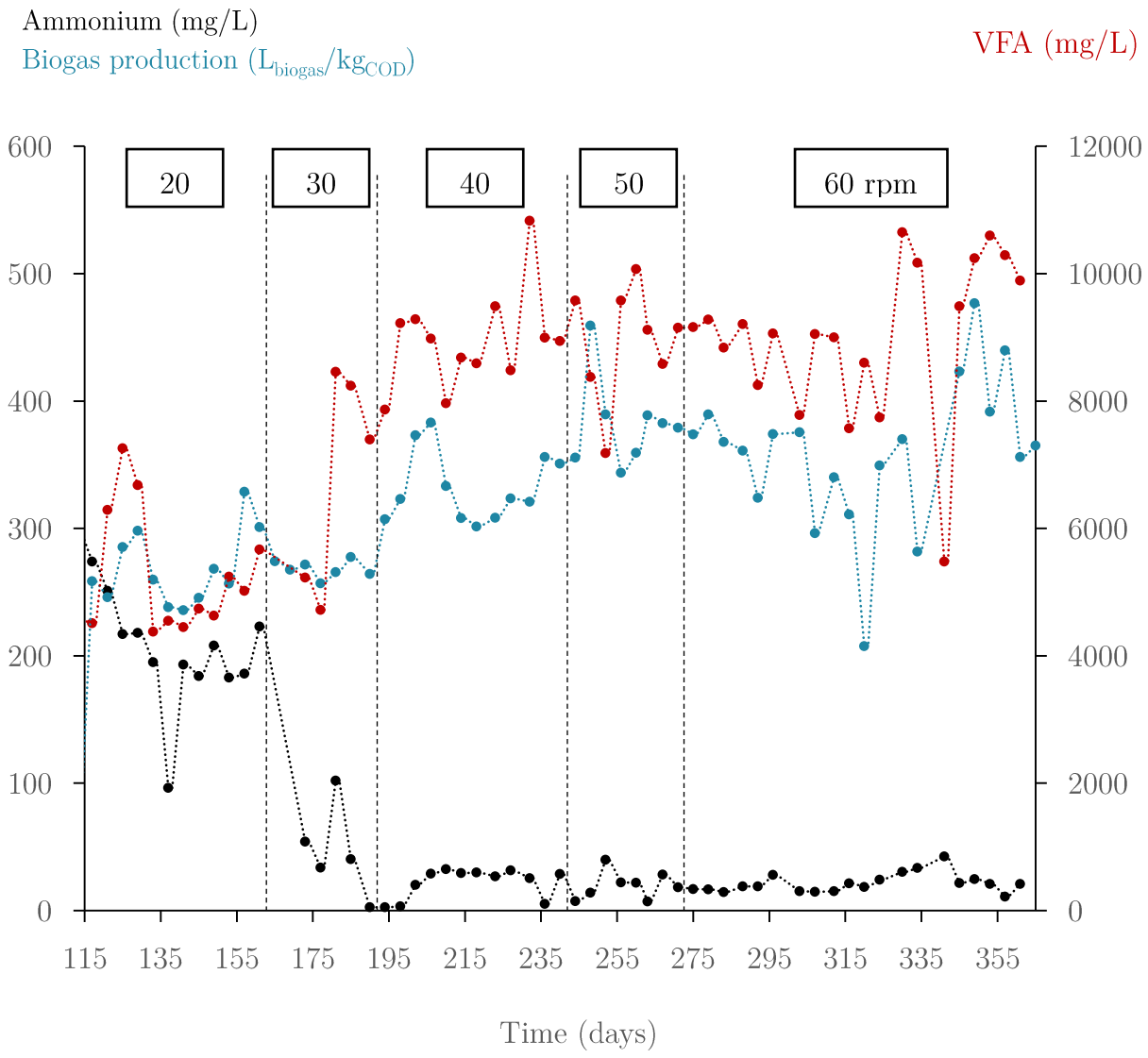

Figure 5: Evolution of VFA and ammonium concentrations during the process

The variation of the VFA and ammonium concentrations are shown in the **Figure 5**. It can be seen that the ammonium concentration is higher and the VFA concentration is lower at the beginning of the study, when the stirring intensity is 20 rpm. Then, when changed it to 30 rpm, a fall in ammonium concentration occurs with an increase in VFA concentration. The two concentrations then stabilised from the moment when the intensity of agitation is 40 rpm. The variations observed when the intensity is 40, 50 and 60 rpm are progressive and not marked at the change. Thus, these measurements give us information on the conditions of the pilot, in the sense that we can compare the concentration ranges in VFA and ammonium concentrations with the performance of

anaerobic digestion. In our study, the VFA concentration is between 8 and 10 $g.L^{-1}$ except at day 341 with a value of 5.48 $g.L^{-1}$. In addition, the ammonium concentration is inferior to 50 $mg.L^{-1}$ for stirring intensity of 40, 50 and 60 rpm. Comparing biogas production with variations in ammonium and VFA concentrations, we do not identify significant variations that would explain variations in biogas production. In addition, despite the increase in VFA concentration and the decrease in ammonium concentration, biogas production is increasing globally.

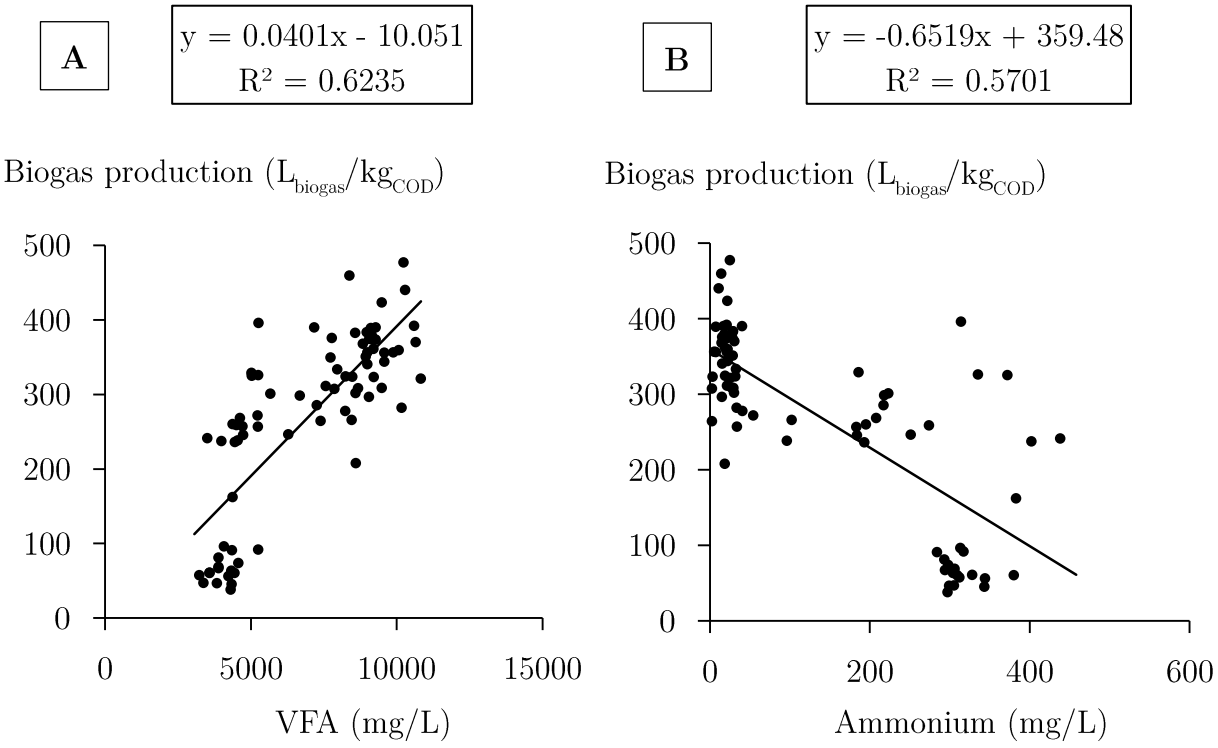

Figure 6: Biogas production in function of VFA concentration (A) and biogas production in function of ammonium concentration (B)

The **Figure 6** shows the biogas production in function of VFA concentration and in function if ammonium concentration. The correlation coefficients are respectively 0.63 and 0.57. The graphs show that the biogas production is more important for higher VFA concentrations and for lower ammonium concentrations.

Janke et al. compared start-up strategies of anaerobic digestion of sugarcane filter cake co-digested with bagasse [218]. Their work lasted 150 days and the physicochemical measurements, including measurement of VFA and ammonium concentrations [218]. During their study, the concentration of VFA tends to decrease to reach a value close to

0 [218]. However, they have VFA concentration peaks that reach at most about 2 $g.L^{-1}$ [218]. Concerning the ammonium concentration, they obtained a similar shape with a progressive decrease of the concentration, which is inferior to 500 $mg.L^{-1}$ at the end of the experiment [218]. The differences between their values of VFA and ammonium concentrations and our values can be explained by the differences between the treated substrates. Souza et al. studied the thermophilic anaerobic digestion of raw vinasse at pilot scale [233]. During their experiment (260 days), the maximum VFA concentration was approximately 3 $g.L^{-1}$ and the mean concentration during the last 50 days of operation was 1.6 $g.L^{-1}$ [233]. Therefore, their values were inferior to ours.

We conclude from the present study that agitation does not directly affect these global concentrations, as there is no remarkable variation in VFA and ammonium concentrations at the time of intensity changes, which are accompanied by a variation in the production of biogas. Moreover, the optimal ranges of VFA and ammonium concentrations are respectively 8 to 10 $g.L^{-1}$ and 0 to 50 $g.L^{-1}$. The optimal range of VFA concentration is higher than those found in literature. It can be explained by the treated substrate and the pilot age. In addition, we do have the nature of VFA. These higher ranges could be explained by a high proportion of propionate.

V-.5.3.ii. Alkalinity and pH

The alkalinity and pH measurements are commonly done on biogas plant to detect instabilities. These two parameters are linked. Indeed, the alkalinity is a measure of the acid-neutralising capacity, which allows to obtain a stable pH. The variation of the alkalinity and pH of the digestion medium are presented in the **Figure 7.**

The pH of the digestion medium is in the range of the anaerobic digestion optimum pH, which is 6.0 to 8.3. In addition, it is also in the range of the methanogens optimum pH, which is 7.0 to 8.0, almost throughout the study. Indeed, we can see that the pH is punctually above 8 for two periods of agitation, 40 and 50 rpm. For the first stirring intensity of 20 rpm, the pH slowly decreased from 7.54 to 7.124 and the alkalinity varied from 6.905 to 8.568 $g_{CaCO3}.L^{-1}$. Then, when we changed the intensity to 30 rpm, the pH decreased to 6.99 and then increased to 7.70. In parallel, the alkalinity significantly increased to 14.011 $g_{CaCO3}.L^{-1}$. As a result of the increase in the intensity of agitation, the pH of the medium has increased, without reaching an inhibitory value for anaerobic

digestion. This is consistent with the variation of the alkalinity, indeed it also increases, which is favourable to the process and allows the pH stabilisation. Indeed, for the rest of the study, the pH stabilises between 7.5 and 8. Whereas the alkalinity oscillates between 10.8 and 17.5 $g_{CaCO3}.L^{-1}$ from day 180. A consequence of the increase in pH is an increase in carbonate CO_3^{2-} ions and thus an increase in the chemical capacity of the medium to absorb CO_2. The solubilisation of CO_2 is therefore higher as the pH increases. Consequently, the CO_2 content of the biogas is expected to decrease

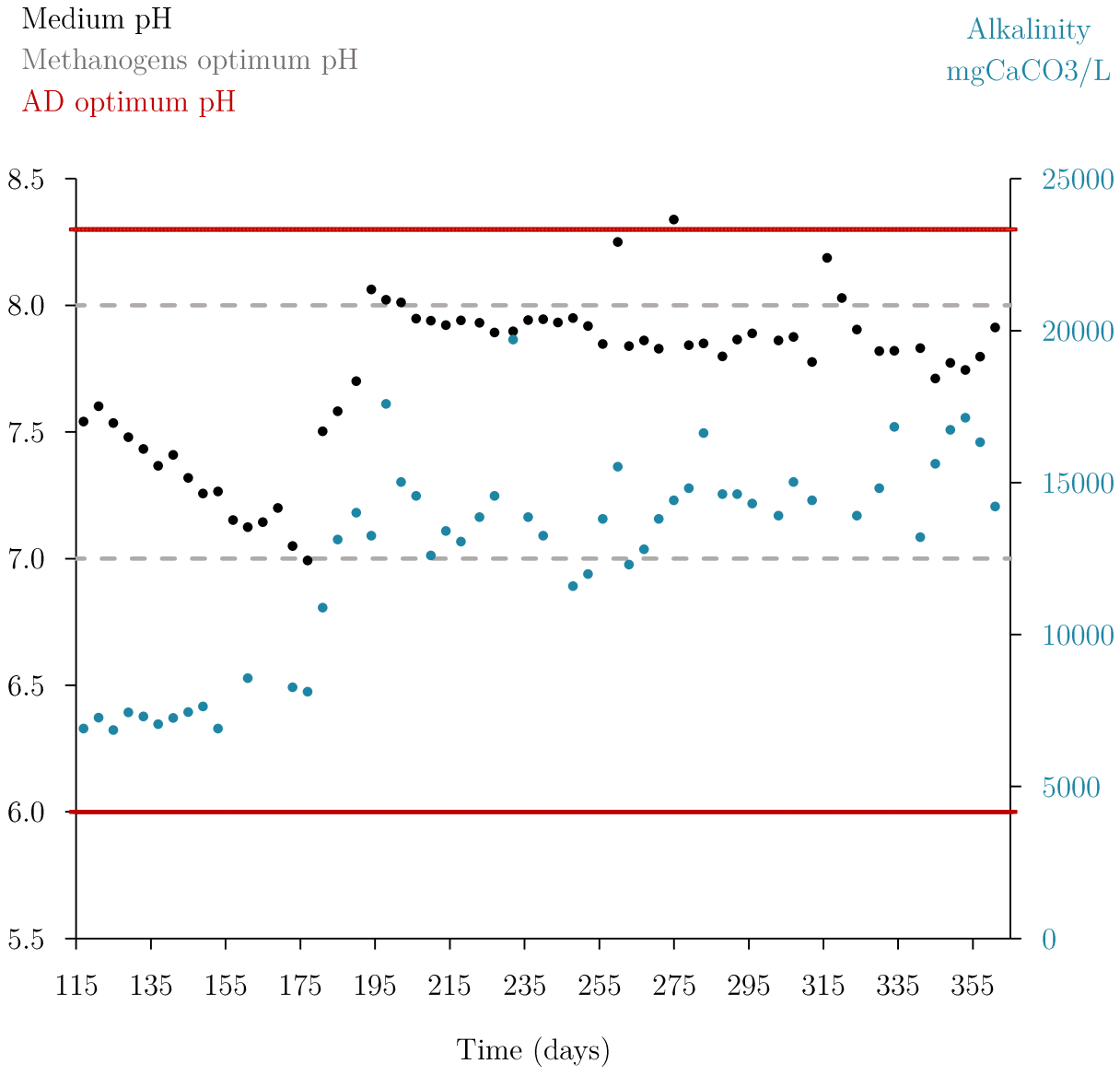

Figure 7: Evolution of the alkalinity and pH of the digestion medium

The **Figure 8** presents the biogas production in function of the alkalinity (A) and the pH in function of the VFA concentration (B). The correlation coefficients are respectively 0.61 and 0.60. First, we observe that the biogas production in higher with higher alkalinity. The result is logical because the medium alkalinity is favourable to anaerobic digestion process. Second, the pH is higher with higher VFA concentration. The average pH is around 7.4 for VFA concentration around 5 $g.L^{-1}$ and the average pH is around 7.9 for VFA concentration around 10 $g.L^{-1}$.

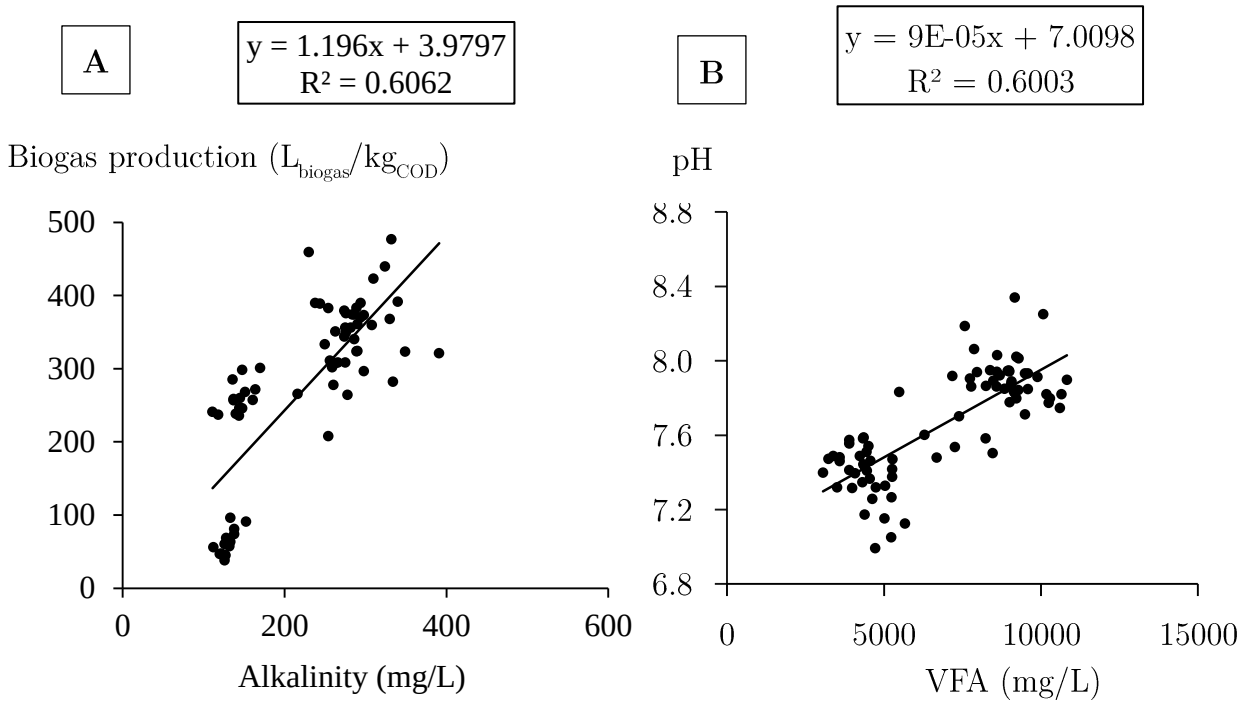

Figure 8: Biogas production in function of alkalinity (A) and pH in function of VFA concentration (B)

To conclude, the alkalinity notably increases with the stirring intensity of 30 rpm. The pH is therefore less acidic with the increase of alkalinity. For the rest of the study, the pH is stabilised around 8, while alkalinity increases gradually. The alkalinity of the medium thus seems sufficient to guarantee a stable pH, despite the increase in VFA concentration.

V-.5.3.iii. VFA to Alkalinity ratio (VFA / Alk ratio)

The VFA to alkalinity ratio is shown in the **Figure 9**. The first period corresponds to the launching of the pilot. During this period, the mixing conditions do not vary and

the loading rate is slowly increased. Thus, the variations in biogas production are due to the increase of OLR. Likewise, the variations in the VFA / Alk ratio are due to the change of OLR. The maximum ratio is observed at day 125 with a value of 1.06. This ratio value reflects a VFA accumulation at this day, resulting from the change of organic loading rate. Furthermore, peaks of the ratio are observed during the change of organic loading rate in the pilot's launch phase but also at the change of mechanical agitation.

Lossie and Pütz (2008) recommend a ratio between 0.3 and 0.4 but still emphasise that this ratio depends on the treated substrate and is therefore specific to each digester [234]. They recommend a long-term study to determine the optimal ratio for stable operation [234]. In our study, the VFA / Alk ratio stabilised a range of 0.5 to 0.7.

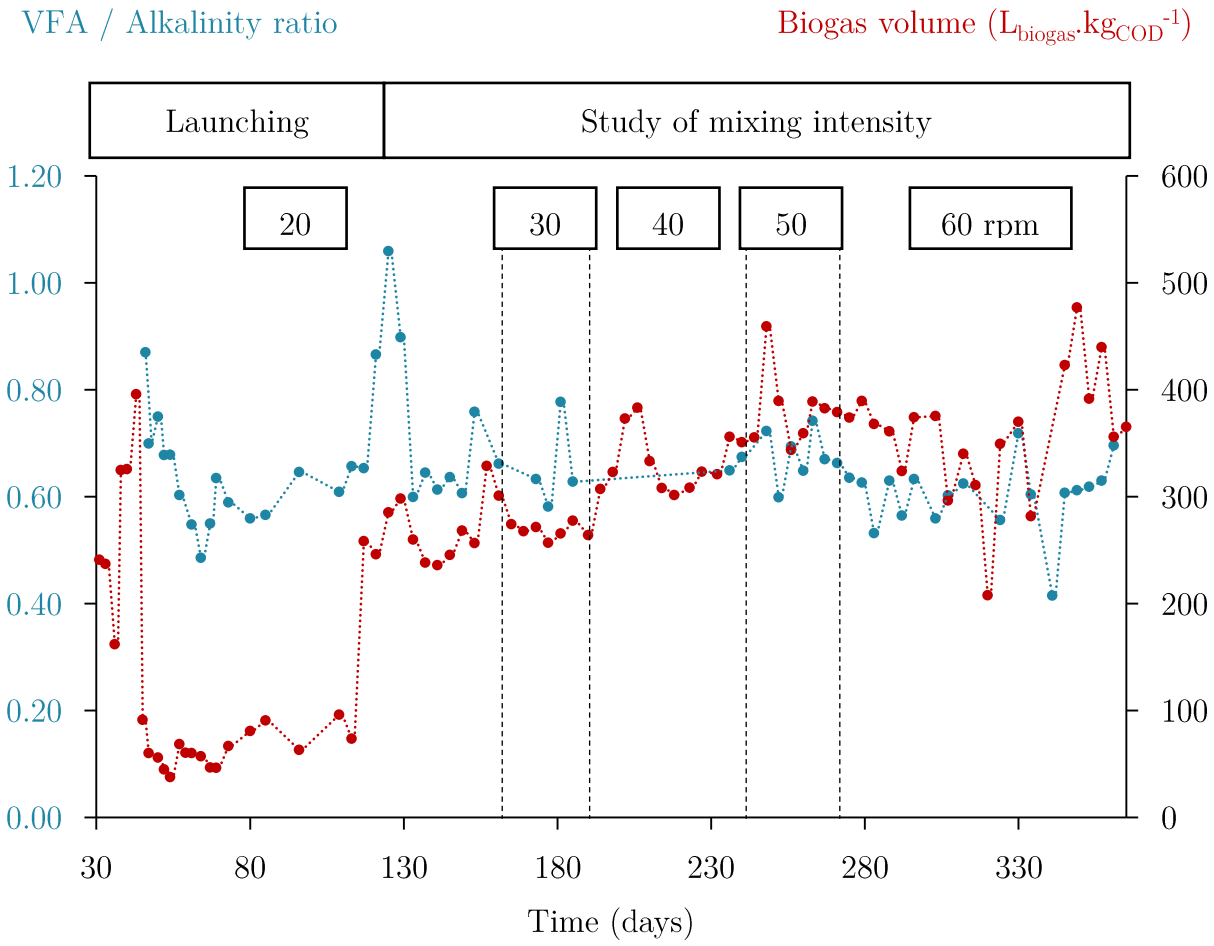

Figure 9: Evolution of VFA / Alkalinity ratio during the process

V-.5.3.iv. TS and VS contents

In the **Figure 10**, the TS and VS content are presented along the digestion process. The average TS content of the sludge and the vinasse are respectively 3.67 and 7.85 ± 0.71 %. We note that the TS content of the digestion medium is lower than the TS content of the substrates.

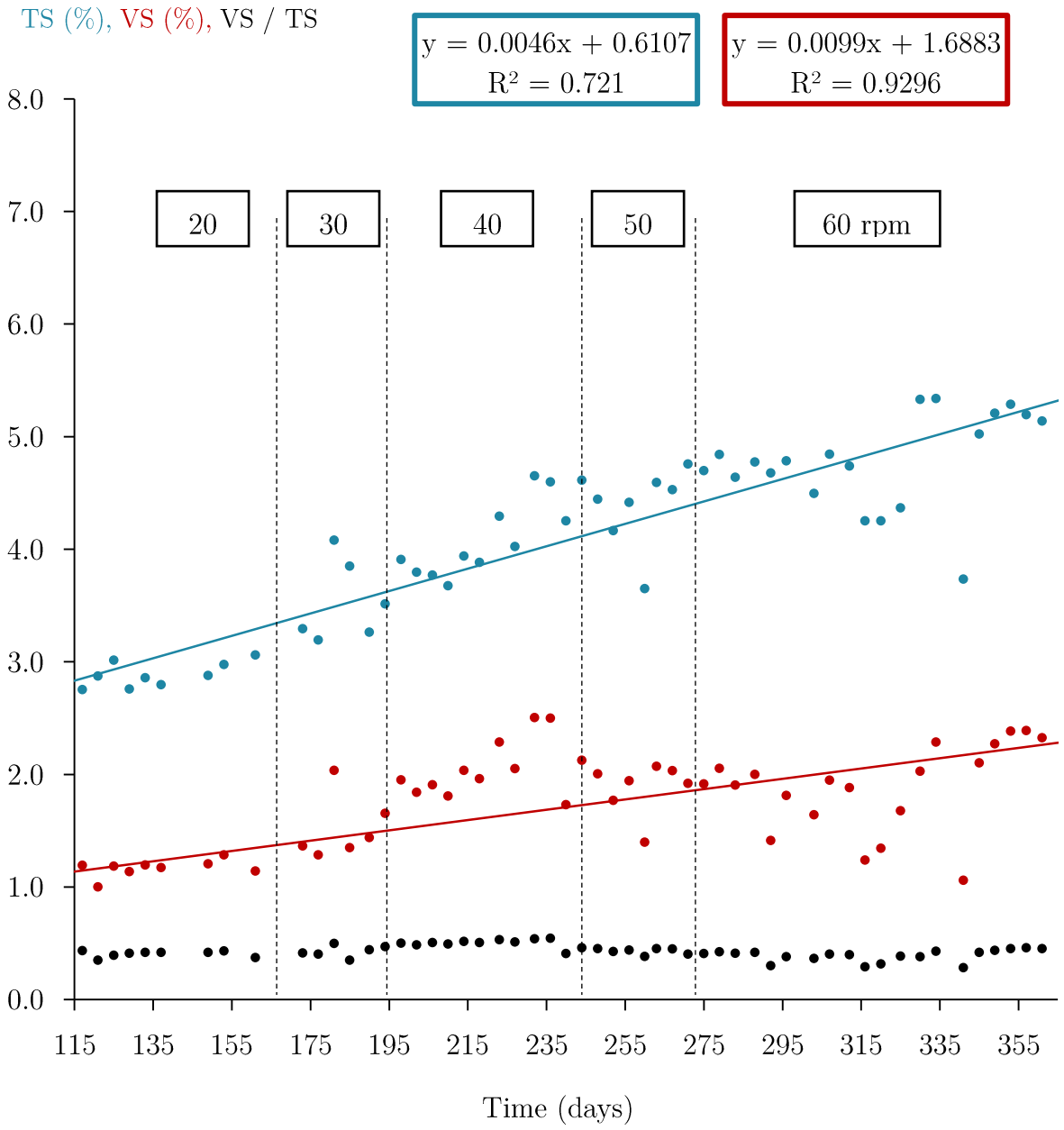

Figure 10: Evolution of TS content and VS content during the process

The TS content variation is 0.31 % the VS content variation is 0.28 % over the period during which the stirring intensity is 20 rpm. The TS content variation is 0.89 % the VS content variation is 0.75 % over the period during which the stirring intensity is 30 rpm. The TS content variation is 1.14 % the VS content variation is 0.85 % over the period during which the stirring intensity is 40 rpm. The TS content variation is 1.11 % the VS content variation is 0.73 % over the period during which the stirring intensity is 50 rpm. The TS content variation is 1.60 % the VS content variation is 1.33 % over the period during which the stirring intensity is 60 rpm. We observe that the TS and VS content are growing during the process. Globally, the TS and VS content respectively increase by 0.0099 and 0.0046 % per day. Moreover, we observe an increase of TS content with constant stirring. Therefore, this augmentation is due to the accumulation of the solid matters in the digester. In order to evaluate the influence of mixing on the TS and VS content of the digestion medium, it is necessary to compare the values before and after agitation. Indeed, the TS and VS content of the medium increase linearly despite the mixing changes.

V-.5.3.v. Summary

The **Table 6** recapitulates the maximum, minimum and average values of physicochemical analysis of the effluent for each mixing intensities.

Table 6: Maximum, minimum and average values of physicochemical analysis of the effluent at different mixing intensities

Parameters	Units	115-161 days			162-190 days			191-240 days		
		20 rpm			30 rpm			40 rpm		
		Min	Max	**A***	Min	Max	**A***	Min	Max	**A***
Ammonium	$mg.L^{-1}$	96.3	274.0	**202.36**	2.5	102.0	**46.6**	2.6	32.6	**22.0**
VFA	$g.L^{-1}$	4.38	7.26	**5.29**	4.72	8.46	**6.81**	7.87	10.83	**8.94**
Alkalinity	$g_{CaCO3}.L^{-1}$	6.85	8.57	**7.33**	8.11	14.01	**10.88**	12.60	19.70	**14.56**
VFA / Alk	-	0.60	1.06	**0.73**	0.58	0.78	**0.65**	0.65	0.67	**0.66**
pH	-	7.12	7.60	**7.37**	6.99	7.70	**7.31**	7.89	8.06	**7.95**
TS	%	2.75	3.06	**2.88**	3.19	4.08	**3.53**	3.51	4.65	**4.02**
VS	%	1.00	1.28	**1.17**	1.29	2.04	**1.49**	1.65	2.50	**2.02**
VS / TS	-	0.35	0.43	**0.41**	0.35	0.50	**0.42**	0.41	0.54	**0.50**

Parameters	Units	241-271 days 50 rpm			272-365 days 60 rpm			Average		
		Min	Max	**A***	Min	Max	**A***	Min	Max	**A***
Ammonium	$g.L^{-1}$	7.2	39.9	**19.8**	10.9	42.5	**21.4**	23.9	98.2	**64.4**
VFA	$g.L^{-1}$	7.18	10.07	**8.96**	5.48	10.65	**9.02**	5.93	9.45	**7.80**
Alkalinity	$g_{CaCO3}.L^{-1}$	11.59	15.52	**13.12**	13.20	17.14	**15.09**	10.47	14.99	**12.2**
VFA / Alk	-	0.60	0.74	**0.68**	0.42	0.72	**0.60**	0.57	0.79	**0.66**
pH	-	7.83	8.25	**7.93**	7.71	8.34	**7.88**	7.51	7.99	**7.69**
TS	%	3.65	4.61	**4.34**	3.73	5.34	**4.78**	3.37	4.35	**3.91**
VS	%	1.40	2.12	**1.91**	1.06	2.39	**1.88**	1.28	2.07	**1.69**
VS / TS	-	0.38	0.46	**0.44**	0.28	0.46	**0.39**	0.35	0.48	**0.43**

*Average value

V-5.4. Variation of physicochemical properties before and after mixing

In this part, the results on the physicochemical properties at different points of the pilot before and after stirring are presented. This study aims to identify the physicochemical parameters impacted locally during agitation. Indeed, as the properties throughout the pilot medium are not identical, the impact of mixing on the physicochemical properties of the medium is worthy of interest. This exploratory study allows us to follow the physicochemical parameters before and after the agitation period (15 min) according to the intensities carried out. In this part, we recall that the local samples were made using a syringe to better control the position of the sample.

V-.5.4.i. VFA concentrations

The VFA concentration before and after stirring is presented in the **Table 7**. On an average, we notice an increase in VFA concentration after mechanical agitation for the "Top" and "Middle" samples. Indeed, we obtain a variation of 0.47, 1.06, 1.81 and 4.11 $g.L^{-1}$ for the "Top" samples respectively for the agitations of 30, 40, 50 and 60 rpm. A slightly higher increase is observed for the "Middle" samples with values of 3.82, 2.98, 0.26 and 1.39 $g.L^{-1}$ for the agitations of 30, 40, 50 and 60 rpm. We can thus conclude that agitation causes an increase in the VFA concentration in the pilot's liquid phase. In addition, the greater the intensity of agitation, the greater the increase in VFA concentration is marked. Moreover, the increase in the VFA concentration is greater for

the "Middle" sample than for the "Top" sample, which suggests that the increase in the VFA concentration is due to the delivery in the liquid phase of the VFAs present in the sludge. Concerning the “sludge” samples, the VFA measured values show that the VFA concentration is much higher in the sludge than in the liquid phase (both Top and Middle value). The VFAs accumulate in the sludge. In addition, from the **Figure 12**, we find that the difference in concentration between the samples "Sludge" and "Middle" is much smaller after the stirring. It also appears that this gap increases with the increase in the intensity of agitation. From this we deduce that the agitation allows to homogenise the concentration of VFAs between the sludge and the lower part of the liquid phase. Moreover, the VFA concentration increases or decreases depending on the days and the standard deviations are larger. Therefore, we cannot conclude on a trend regarding the evolution of the VFA concentration in the mud. This can be explained by two reasons. First, taking the sample can affect the sludge and thus influence the VFA concentration of the next sample, especially the samples collected after agitation. Second, it could reflect the heterogeneity of the mud. As a result, for the remainder of the study, we sampled a smaller number of mud samples (from day 240). Even if the mud analyses are very heterogeneous, we can still note that it is on these samples that we obtain the largest decreases in VFA concentrations. This reinforces the hypothesis that the increase in the concentration of VFA in the liquid phase comes from the delivery into the liquid phase of the VFA present in the sludge. Similarly, we obtain decreases in the VFA concentrations that are higher for the quickest agitations.

The Figure 11 presents the difference between the VFA concentration of the “Middle” sample and the “Top” sample before and after stirring. The difference between these two measures reflects the heterogeneity of the VFA concentration. For stirring intensities of 30 and 40 rpm, we can see that the difference between these two measurements is about twice as great after stirring. The increase in this difference is due to the increase in the VFA concentration of the "Middle" sample. Thus, the stirring is not sufficiently powerful and does not allow homogenisation of the VFA concentration in the pilot's liquid phase. The latter causes a delivery of the VFA in the liquid medium without obtaining a homogeneous concentration. There is thus the creation of zones with higher concentrations of acids, where the alkalinity of the medium will have to be large enough to guarantee a stable pH. However, for the stirring intensity of 50 rpm, we observe the opposite effect, the difference in VFA concentration is lower after stirring. It is also

lower than the differences in VFA concentrations between the "Middle" and "Top" samples of lower agitation intensities. From the Table 7, we can see that the VFA concentration of the "Middle" sample after stirring varies very little when the stirring change with the mean values 11.38, 10.42, 10.99 and 10.64 $g.L^{-1}$ for stirring intensities of 30, 40, 50 and 60 rpm. While the VFA concentration of the "Top" sample after agitation increases with the average values 5.39, 6.69, 8.09 and 10.08 $g.L^{-1}$. Thus, the reduction in the difference between "Top" and "Middle" concentrations after stirring (**Figure 11**) is due to the increase of the VFA concentration at the top of the pilot. We can therefore conclude that lower agitation intensities do not suffice to homogenise the VFA concentration in the upper part of the pilot's liquid phase. In addition, the higher the intensity of the agitation, the more the VFA concentration in the pilot will be homogeneous. The pilot will thus be less subject to local inhibitions due to high concentrations of VFA in the case where the alkalinity of the pilot is not sufficiently important.

By comparing local VFA concentrations and biogas production, we find that biogas production decreases when the agitation intensity of 60 rpm is applied. Thus, this decrease could be explained by inhibitory VFA concentrations in the digestion medium. Indeed, the overall measurements of the medium show that the concentration of VFA is stable in the pilot. This shows the importance of local monitoring of VFA concentrations at the pilot scale.

Table 7: Variation of VFA concentration ($g.L^{-1}$) before and after the mixing

Days	Before agitation			After agitation			Variation		
	Top	Middle	Sludge	Top	Middle	Sludge	Top	Middle	Sludge
30 rpm (161-190 days)									
161	4.97	-	-	5.67	-	18.10	0.70	-	-
165	-	-	26.90	-	-	21.90	-	-	-5
185	4.87	7.56	19.50	5.10	11.38	22.10	0.23	3.82	2.60
A*	**4.92**	**7.56**	**19.50**	**5.39**	**11.38**	**20.10**	**0.47**	**3.82**	**-1.20**
SD**	**0.60**	**-**	**-**	**0.40**	**-**	**2.83**	**0.33**	**-**	**5.37**
40 rpm (190-240 days)									
190	5.74	5.76	17.85	6.33	8.46	23.15	0.59	2.7	5.3
194	5.43	5.89	37.35	6.43	9.30	18.60	1.00	3.41	-18.75
198	6.25	5.74	14.40	6.55	11.89	14.75	0.30	6.15	0.35
202	6.02	11.43	-	7.47	11.10	-	1.45	-0.33	-

236	4.71	-	18.75	6.65	11.34	30.60	1.94	-	11.85
A*	**5.63**	**7.03**	**22.09**	**6.69**	**10.42**	**21.78**	**1.06**	**2.98**	**-0.31**
SD**	**0.60**	**2.82**	**10.35**	**0.45**	**1.46**	**6.81**	**0.66**	**2.66**	**13.16**
50 rpm (240-271 days)									
240	7.87	9.27	68.30	6.44	11.44	23.85	-1.43	2.17	-44.45
244	5.35	12.56	-	7.74	11.94	-	2.39	-0.62	-
248	5.56	14.14	-	8.23	9.21	-	2.67	-4.93	-
267	6.32	6.97	-	9.94	11.37	-	3.62	4.40	-
A*	**6.28**	**10.74**	**68.30**	**8.09**	**10.99**	**23.85**	**1.81**	**0.26**	**-44.45**
SD**	**1.14**	**3.23**	**-**	**1.45**	**1.21**	**-**	**2.22**	**4.02**	**-**
60 rpm (271-365 days)									
271	6.25	6.67	-	10.03	10.52	-	3.78	3.85	-
361	5.70	11.82	22.90	10.13	10.75	17.85	4.43	-1.07	-5.05
A*	**5.98**	**9.25**	**22.90**	**10.08**	**10.64**	**17.85**	**4.11**	**1.39**	**-5.05**
SD**	**0.39**	**3.64**	**-**	**0.07**	**0.16**	**-**	**0.46**	**3.48**	**-**

*Average value, **Standard deviation

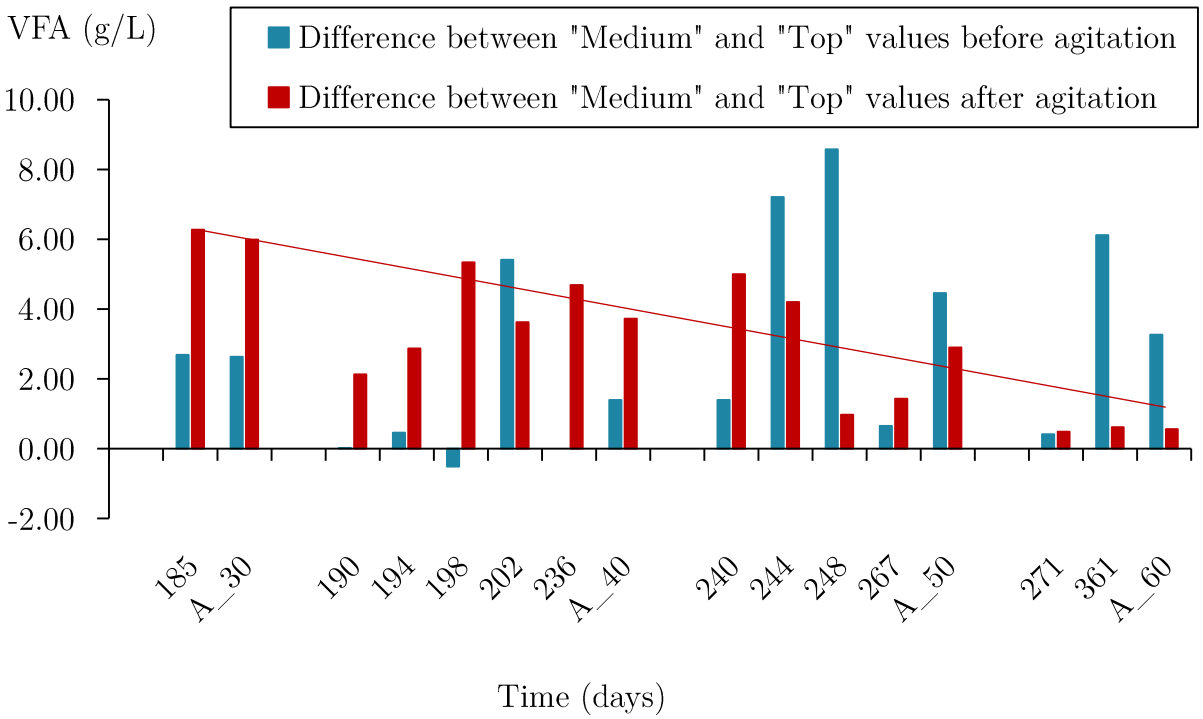

Figure 11: Difference between "Middle" and "Top" VFA concentrations before and after agitation (A_30, A_40, A_50 and A_60: differences between the average values for 30, 40, 50 and 60 rpm)

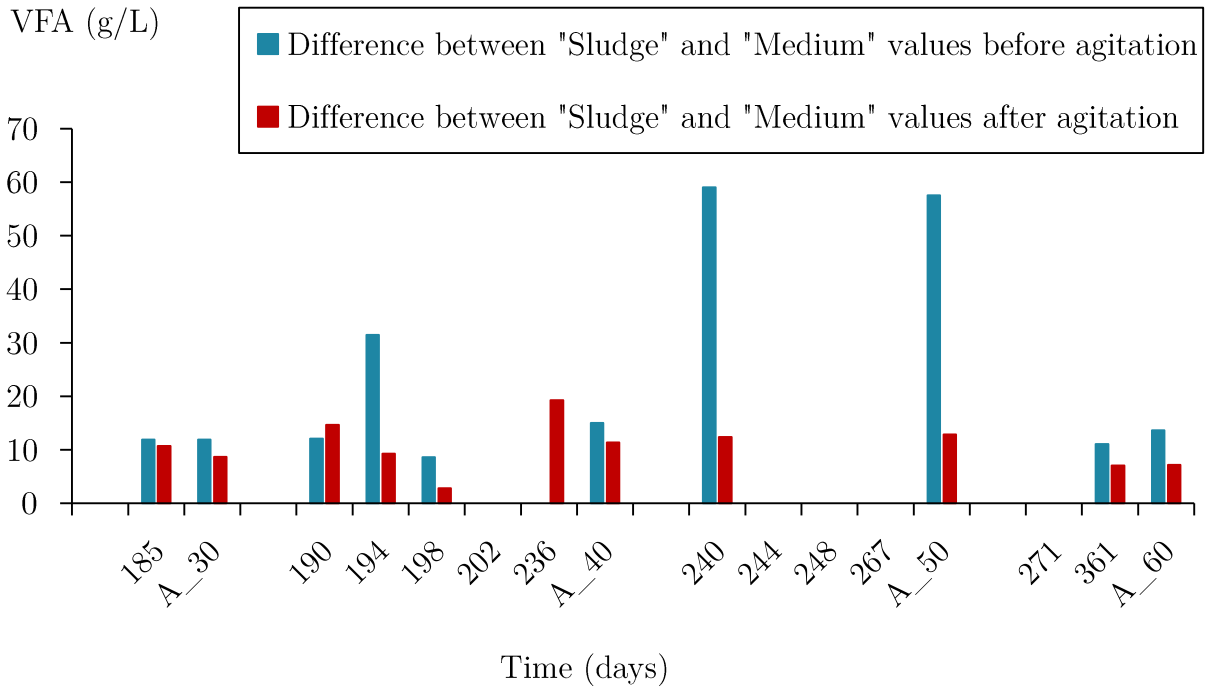

Figure 12: Difference between "Sludge" and "Middle" VFA concentrations before and after agitation (A_30, A_40, A_50 and A_60: differences between the average values for 30, 40, 50 and 60 rpm)

In conclusion, agitation influences the pilot's local VFA concentrations. The VFA concentration tends to increase in the liquid phase and decrease in the sludge. By comparing the VFA concentrations before and after stirring but also at different locations of the pilot, we can conclude that the homogenization of the VFA concentration in the pilot is favoured by a greater stirring. Furthermore, knowing the VFA cause instabilities digesters, precautions must be taken in agitating a digester wherein it is accumulated mud. Indeed, the experimental results show that the VFAs present in the sludge are being resuspended in the liquid phase during stirring. Another solution to avoid pilot intoxication by acidification would be to remove the accumulated sludge before applying agitation. It would be interesting to study this solution experimentally in order to study its impact on pilot yields.

V-.5.4.ii. Ammonium concentration

The variations of ammonium concentration before and after mixing for each stirring intensity are presented in the Table 8.

Table 8: Variation of ammonium concentration ($mg.L^{-1}$) before and after the mixing

Days	Before agitation			After agitation			Variation		
	Top	Middle	Sludge	Top	Middle	Sludge	Top	Middle	Sludge
30 rpm (161-190 days)									
161	165	-	-	223	-	100	58	-	-
165	-	-	23.8	-	-	60	-	-	36.2
185	26.5	119	24.8	140	21.7	36.1	113.5	-97.3	11.3
A*	**95.8**	**119**	**24.3**	**181.5**	**21.7**	**63.4**	**85.8**	**-97.3**	**11.3**
SD**	**97.9**	**-**	**0.70**	**58.69**	**-**	**32.59**	**39.24**	**-**	**23.75**
40 rpm (190-240 days)									
190	1.90	5.05	78.3	3.21	6.96	29.5	1.31	1.91	-48.8
194	2.36	3.00	33.7	3.84	6.61	30.6	1.48	3.61	-3.1
198	1.73	2.02	24.0	3.29	9.66	29.0	1.6	7.6	5
202	2.19	8.78	-	-	8.02	-	-	-0.8	-
236	55.3	-	17.6	4.19	16.9	59.4	-51.1	-	41.8
A*	**12.7**	**4.7**	**38.4**	**3.6**	**9.6**	**37.1**	**-11.7**	**53.9**	**-1.3**
SD**	**23.8**	**2.99**	**27.4**	**0.47**	**4.23**	**14.87**	**26.28**	**6.88**	**37.22**
50 rpm (240-271 days)									
240	33.4	14.7	41.8	75.6	39.1	16.0	42.2	24.4	-25.8
244	2.3	10.1	-	6.81	19.5	-	4.5	9.4	-
248	1.9	11.3	-	48.9	35.8	-	47	24.5	-
267	35.2	25.0	-	26.6	9.7	-	-8.6	-15.3	-
A*	**18.2**	**15.3**	**41.8**	**39.48**	**26.03**	**16**	**21.28**	**10.75**	**-25.8**
SD**	**18.6**	**6.77**	**-**	**29.59**	**13.85**	**-**	**27.53**	**18.76**	**-**
60 rpm (271-365 days)									
271	33.7	26.1	-	15.1	11.6	-	-18.6	-14.5	-
361	24.9	19.0	18.5	18.8	18.9	31.7	-6.1	-0.1	13.2
A*	**29.3**	**22.6**	**18.5**	**17.0**	**15.3**	**31.7**	**-12.4**	**-7.3**	**13.2**
SD**	**6.22**	**5.02**	**-**	**2.62**	**5.16**	**-**	**8.84**	**10.18**	**-**

*Average value, **Standard deviation

V-.5.4.iii. Alkalinity and pH

The alkalinity before and after mixing of “Top”, “Middle” and “Sludge” samples is presented in the **Table 9.** For all the agitations, the sludge has the highest alkalinity, then comes the sample "Middle" and finally the sample "Top". Therefore, the deepest areas of the digester are the most alkaline. Comparing the alkalinity values before and after stirring, we see an increase for “Top” and “Middle” samples. Concerning the

"Sludge" sample, alkalinity increases in some cases but decreases in most cases studied. We can therefore conclude that the agitation influences the homogenisation of the alkalinity within the pilot. Initially, the alkalinity of the upper zones is lower, but increases with agitation accompanied by a decrease in the alkalinity of the lower zones. Even though the alkalinity remains much higher in the mud.

Table 9: Variation of alkalinity ($g_{CaCO3}.L^{-1}$) before and after the mixing

Days	Before agitation			After agitation			Variation		
	Top	Middle	Sludge	Top	Middle	Sludge	Top	Middle	Sludge
30 rpm (161-190 days)									
161	7.95	-	-	8.57	-	14.59	0.62	-	-
165	-	-	18.07	-	-	22.13	-	-	4.06
185	9.23	11.69	19.68	9.21	17.04	23.11	-0.02	5.35	3.43
A*	**8.59**	**11.69**	**18.88**	**8.89**	**17.04**	**19.94**	**0.3**	**5.35**	**3.75**
SD**	**0.91**	**-**	**1.14**	**0.45**	**-**	**4.66**	**0.45**	**-**	**0.45**
40 rpm (190-240 days)									
190	11.79	12.80	16.71	12.90	15.12	37.04	1.11	2.32	20.33
194	12.50	13.51	56.45	12.00	14.52	24.34	-0.5	1.01	-32.11
198	12.30	15.22	29.74	15.12	20.06	27.97	2.82	4.84	-1.77
202	14.92	18.35	-	-	17.74	-	-	-0.61	-
236	9.45	-	20.39	11.29	16.43	26.21	1.84	-	5.82
A*	**12.19**	**14.97**	**30.82**	**12.83**	**16.77**	**28.89**	**1.32**	**1.89**	**-1.93**
SD**	**1.95**	**2.47**	**17.94**	**1.66**	**2.21**	**5.63**	**1.40**	**2.30**	**22.10**
50 rpm (240-271 days)									
240	10.69	11.29	27.47	12.40	14.11	22.88	1.71	2.82	-4.59
244	10.69	14.01	-	12.90	15.22	-	2.21	1.21	-
248	11.39	14.92	-	12.20	13.00	-	0.81	-1.92	-
267	11.79	15.02		15.22	14.21	-	3.43	-0.81	-
A*	**11.14**	**13.81**	**27.47**	**13.18**	**14.14**	**22.88**	**2.04**	**0.33**	**-4.59**
SD**	**0.54**	**1.74**	**-**	**1.39**	**0.91**	**-**	**1.09**	**2.11**	**-**
60 rpm (271-365 days)									
271	12.20	15.12	-	15.73	15.12	-	3.53	0	-
361	11.69	14.31	11.09	12.70	14.62	34.52	1.01	0.31	23.43
A*	**11.95**	**14.72**	**11.09**	**14.22**	**14.87**	**34.52**	**2.27**	**0.15**	**23.43**
SD**	**0.36**	**0.57**	**-**	**2.14**	**0.35**	**-**	**1.78**	**0.22**	**-**

*Average value, **Standard deviation

The variation of pH before and after agitation at different height of pilot is presented in the **Figure 13** and the **Table 10**. Globally, the pH before and after stirring

for “Middle” and “Top” samples are similar with some exceptions. Indeed, we observe a decrease in pH after stirring for both samples between days 200 and 210 and increases at days 272 and 330. The **Table 10** shows that the difference in pH between “Top” and “Middle” samples slightly increases with stirring. However, this difference is lower at 60 rpm, thus this stirring allows the homogenisation of the pH. Moreover, the difference in pH between after and before stirring is higher for “Middle” sample than “Top” sample. We also note that this difference is higher for higher mixing intensities for both samples. Therefore, the agitation impacts locally the digestion medium. An adapted stirring mode is crucial to avoid acidic zones in the pilot. These measurements also reflect the impact of mixing on the local VFA concentrations.

Table 10: Differences between the pH of “Top” and “Middle” samples before and after the mixing and differences of the pH after and before agitation of “Top” and “Middle” samples

Mixing intensity	Top pH minus Middle pH				pH after agitation minus pH before agitation			
	Before agitation		After agitation		Top		Middle	
	A*	SD**	A*	SD**	A*	SD**	A*	SD**
30 rpm	-0.01	0.03	0.12	0.01	0.02	0.00	-0.10	0.04
40 rpm	0.05	0.06	0.06	0.07	0.01	0.13	-0.01	0.16
50 rpm	0.03	0.02	0.09	0.18	0.10	0.23	0.04	0.15
60 rpm	0.04	0.05	-0.03	0.20	-0.44	1.94	-0.38	1.95
Average	**0.03**	**0.04**	**0.06**	**0.12**	**-0.08**	**0.57**	**-0.11**	**0.57**
SD**	**0.03**	**0.02**	**0.06**	**0.09**	**0.24**	**0.91**	**0.19**	**0.92**

*Average value, **Standard deviation

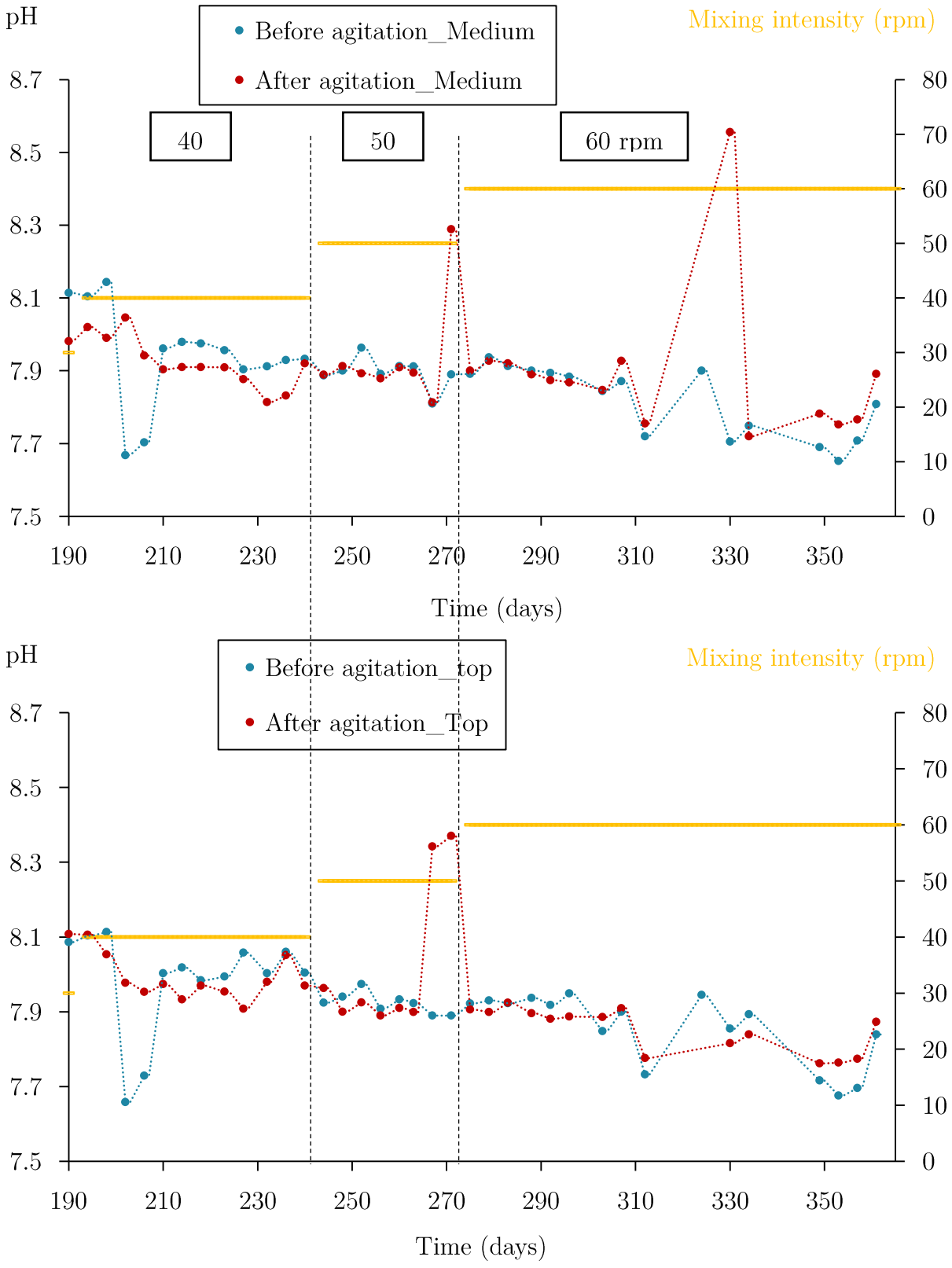

Figure 13: Variation of the pH before and after agitation of "Top" and "Middle" samples in function of time

V-.5.4.iv. TS and VS contents

The **Tables 11 and 12** outline the variation of TS and VS content before and after mixing. Both the average TS and VS content of "Top" and "Middle" samples increases after stirring. Comparing the variation in TS content for each mixing intensities, we observe and increase in variation for "Top" sample with the increase of mixing intensity. In contrary, we note a decrease for "Middle" sample with the increase of mixing intensity. We notice the same trend for the VS content of "Top" and "Middle" samples. Therefore, agitation allows to resuspension the solid matters present in the lower part of the digester. Measurements on the sludge are less numerous, so no trend is identifiable as to the impact of the agitation. Logically, the TS and VS content of the sludge should decrease but we observe an increase at days 185, 190, 198 and 361. As previously said, the sampling in mud at two identical locations affects the sludge, which explains the experimental results obtained.

Table 11: Variation of TS (%) content before and after the mixing

Days	Before agitation			After agitation			Variation		
	Top	Middle	Sludge	Top	Middle	Sludge	Top	Middle	Sludge
30 rpm (161-190 days)									
161	3.01	-	-	3.06	-	6.85	0.05	-	-
165	-	-	8.44	-	-	8.06	-	-	-0.38
185	3.32	3.90	7.86	3.45	5.24	8.67	0.13	1.34	0.81
A*	**3.17**	**3.9**	**8.15**	**3.26**	**5.24**	**7.86**	**0.09**	**1.34**	**0.81**
SD**	**0.22**	**-**	**0.41**	**0.28**	**-**	**0.93**	**0.06**	**-**	**0.84**
40 rpm (190-240 days)									
190	3.28	3.30	7.22	3.38	4.14	7.49	0.1	0.84	0.27
194	3.38	3.36	8.53	3.76	4.27	7.63	0.38	0.91	-0.9
198	3.36	3.41	7.10	3.70	5.12	8.07	0.34	1.71	0.97
202	3.45	4.80	-	3.87	4.72	-	-	-0.08	-
236	3.63	4.55	9.84	4.02	6.17	9.88	0.39	-	0.04
A*	**3.42**	**3.88**	**8.17**	**3.75**	**4.88**	**8.27**	**0.30**	**0.85**	**0.10**
SD**	**0.13**	**0.73**	**1.29**	**0.24**	**0.82**	**1.10**	**0.14**	**0.73**	**0.77**
50 rpm (240-271 days)									
240	3.63	4.55	9.84	3.97	5.54	9.27	0.34	0.99	-0.57
244	3.63	5.11	-	4.58	5.79	-	0.95	0.68	-
248	3.88	5.44	-	4.62	5.12	-	0.74	-0.32	-
267	3.72	4.27	-	4.73	5.34	-	1.01	1.07	-

A*	**3.72**	**4.84**	**9.84**	**4.48**	**5.48**	**9.27**	**0.76**	**0.61**	**-0.57**
SD**	**0.12**	**0.53**	**-**	**0.34**	**0.29**	**-**	**0.30**	**0.64**	**-**
60 rpm (271-365 days)									
271	3.71	4.03	-	5.14	4.91	-	1.43	0.88	-
361	3.74	5.62	7.86	5.21	5.44	10.50	1.47	-0.18	2.64
A*	**3.73**	**4.83**	**7.86**	**5.188**	**5.18**	**10.50**	**1.45**	**0.35**	**2.64**
SD**	**0.02**	**1.12**	**-**	**0.05**	**0.37**	**-**	**0.03**	**0.75**	**-**

*Average value, **Standard deviation

Table 12: Variation of VS (%) content before and after the mixing

Days	Before agitation			After agitation			Variation		
	Top	Middle	Sludge	Top	Middle	Sludge	Top	Middle	Sludge
30 rpm (161-190 days)									
161	0.85	-	-	1.14	-	4.29	0.29	-	-
165	-	-	5.67	-	-	5.39	-	-	-0.28
185	1.33	1.74	4.94	1.35	1.35	5.38	0.02	-0.39	0.44
A*	**1.09**	**1.74**	**5.31**	**1.25**	**1.35**	**5.02**	**0.16**	**-0.39**	**0.08**
SD**	**0.34**	**-**	**0.52**	**0.15**	**-**	**0.63**	**0.19**	**-**	**0.51**
40 rpm (190-240 days)									
190	0.94	0.55	4.32	1.14	1.74	4.35	0.2	1.19	0.03
194	1.00	0.84	5.11	1.47	1.84	4.43	0.47	1	-0.68
198	1.00	0.86	4.08	1.38	2.52	4.88	0.38	1.66	0.8
202	1.02	1.72	-	1.56	2.12	-	-	0.4	-
236	1.33	1.79	5.11	1.65	3.35	5.61	0.32	-	0.5
A*	**1.06**	**1.15**	**4.66**	**1.44**	**2.31**	**4.82**	**0.34**	**1.06**	**0.16**
SD**	**0.15**	**0.56**	**0.53**	**0.20**	**0.65**	**0.58**	**0.11**	**0.52**	**0.64**
50 rpm (240-271 days)									
240	1.33	2.04	6.04	1.61	2.85	5.61	0.28	0.81	-0.43
244	1.29	2.44	-	2.09	3.01	-	0.80	0.57	-
248	1.46	2.76	-	2.11	3.11	-	0.65	0.35	-
267	1.40	1.77	-	2.09	2.67	-	0.69	0.9	-
A*	**1.37**	**2.25**	**6.04**	**1.98**	**2.91**	**5.61**	**0.61**	**0.66**	**-0.43**
SD**	**0.08**	**0.44**	**-**	**0.24**	**0.19**	**-**	**0.23**	**0.25**	**-**
60 rpm (271-365 days)									
271	1.38	1.61	-	1.24	1.81	-	-0.14	0.2	-
361	0.96	2.34	4.35	2.38	2.51	6.17	1.42	0.17	1.82
A*	**1.17**	**1.98**	**4.35**	**1.81**	**2.16**	**6.17**	**0.64**	**0.19**	**1.82**
SD**	**0.30**	**0.52**	**-**	**0.81**	**0.49**	**-**	**1.10**	**0.02**	**-**

*Average value, **Standard deviation

V-6. Conclusion

This paper showed that the change in mixing intensity impacts the process yield and global and local physicochemical parameters. In this study, the biogas production gradually increases for stirring intensities ranging from 20 to 60 rpm, with a maximum production of 477 $L_{CH4}.kg_{COD}^{-1}$. Moreover, peaks in biogas production are observed during the stirring change. In parallel, variation in VFA and ammonium concentrations are apparent. It also appears that anaerobic digestion process is more destabilised for higher agitation intensities. However, after a stabilisation period, the process yield is improved. The monitoring of global physicochemical parameters provides information on the state of the digestion process. Nevertheless, the local study allows to understand the impact of mixing on the whole medium and to interpret the yields. Indeed, the homogenisation of the medium is known thanks to these measurements. Furthermore, the local measurements show the location of the acidic zones. The mechanical agitation on an industrial scale can be adapted with local measurements study.

In perspectives, experimental studies must be done in larger scale in order to know if similar yield variations are observed. Moreover, it could be interesting to launch pilot tests in parallel to overcome the impact of the pilot's age on outcomes. In this paper, only the mixing intensity was changed, therefore, the impact of the mixing frequency and duration are also worthy of interest. Indeed, in large scale unit, the agitation of the medium causes important energy consumptions, thus these studies will allow to choose the minimum mixing (intensity, rate, etc.) to be used to guarantee biogas yields while limiting the energy consumption of the unit.

V-7. Acknowledgments

This work was supported by the Region Reunion (France) as part of the funding of a research thesis in the PIMENT (Physics and Mathematical Engineering for Energy, Environment and Building) laboratory at the University of Reunion Island. We are also grateful to the Rivière du Mât distillery (Reunion Island) for supplying us with the sugar cane vinasse needed for this study.

Chapitre VI

CFD simulation of mechanical mixing in anaerobic digester

Les chapitres précédents ont porté sur l'étude expérimentale de la digestion anaérobie de la vinasse à l'échelle d'un pilote de 16 L. Nous avons notamment étudié l'impact de l'agitation mécanique sur les rendements du processus de digestion. Les résultats obtenus ont montré que l'intensité de l'agitation influe les rendements. Au cours des expérimentations, nous avons pu caractériser les propriétés physicochimiques du milieu. Dans ce sens, nous souhaitons apporter un niveau de description du milieu supplémentaire en utilisant des modèles numériques décrivant les écoulements.

L'objectif de ce chapitre, rédigé au format d'article scientifique, porte ainsi sur la compréhension des écoulements au sein du digesteur. Pour cela, nous avons recours à la CFD. Cet outil, appliqué aux digesteurs anaérobies, nous permet de comprendre et caractériser les écoulements selon l'agitation employée. Dans un premier temps nous mettons en exergue les inhibitions de la digestion anaérobie et l'intérêt de la CFD pour l'optimisation de la digestion anaérobie. Dans un deuxième temps, nous présentons les premiers résultats de simulations CFD d'un digesteur agité mécaniquement à différentes intensités d'agitation pour un cas Newtonien.

VI-1. Abstract

Anaerobic digestion is a widely used process for waste treatment, such as manure, sludge or biowaste. On laboratory or industrial scale, a stirring system is used in order to enhance mass and heat transfers. The stirring can be done by recirculation of gas or leachate or mechanical system. The understanding of the flows during the agitation of the medium is crucial for the optimisation of the mixing system. In this study the context of work and the Reynolds-averaged Navier-Stokes (RANS) simulations of mechanical agitation of Newtonian fluids for different mixing intensities are presented.

Keywords: Anaerobic digestion, computational fluid dynamics (CFD), Newtonian, mechanical mixing.

VI-2. Introduction

Anaerobic digestion is a widely used process for waste treatment, such as manure, sludge or biowaste. Anaerobic digestion is based on the digestion of the material by four groups of microorganisms successively. The chemical reactions and the microorganisms involved in each reaction are explained in the **Figure 1**. Therefore, the contact between the material and each group of microorganisms must be guaranteed in order to promote the production of biogas. Otherwise, an accumulation of intermediate products could lead to the failure of the process.

On laboratory or industrial scale, a stirring system is used in order to enhance mass and heat transfers. The stirring can be done by recirculation of gas or leachate or mechanical system. The understanding of the flows during the agitation of the medium is crucial for the optimisation of the mixing system. According to the agitation mode used, the medium can be well-agitated or there might be the presence of dead zones. The two main issues are the following. First, to promote the anaerobic digestion process, it is necessary to limit the volume of dead zones without stirring too vigorously. In the dead zones, the organic matter could be not digested due to the absence of contact between the substrate and each group of micro-organisms. In this sense studies are being conducted to evaluate the volume and the position of dead zones with the aim of reducing their volumes [42, 79, 167]. Second, in the case of mixed zones, the velocity field must be

chosen to prevent the destruction of the methanogenic centers and to allow the chemical reactions. Moreover, the mixing should ensure the homogenisation of the temperature and the digestion medium. As a consequence, the biogas yield depends on the chosen stirring system. In fact, there is thus optimal agitation for anaerobic digestion. It will depend in particular on the geometry of the digester, the stirring system used as well as the substrate.

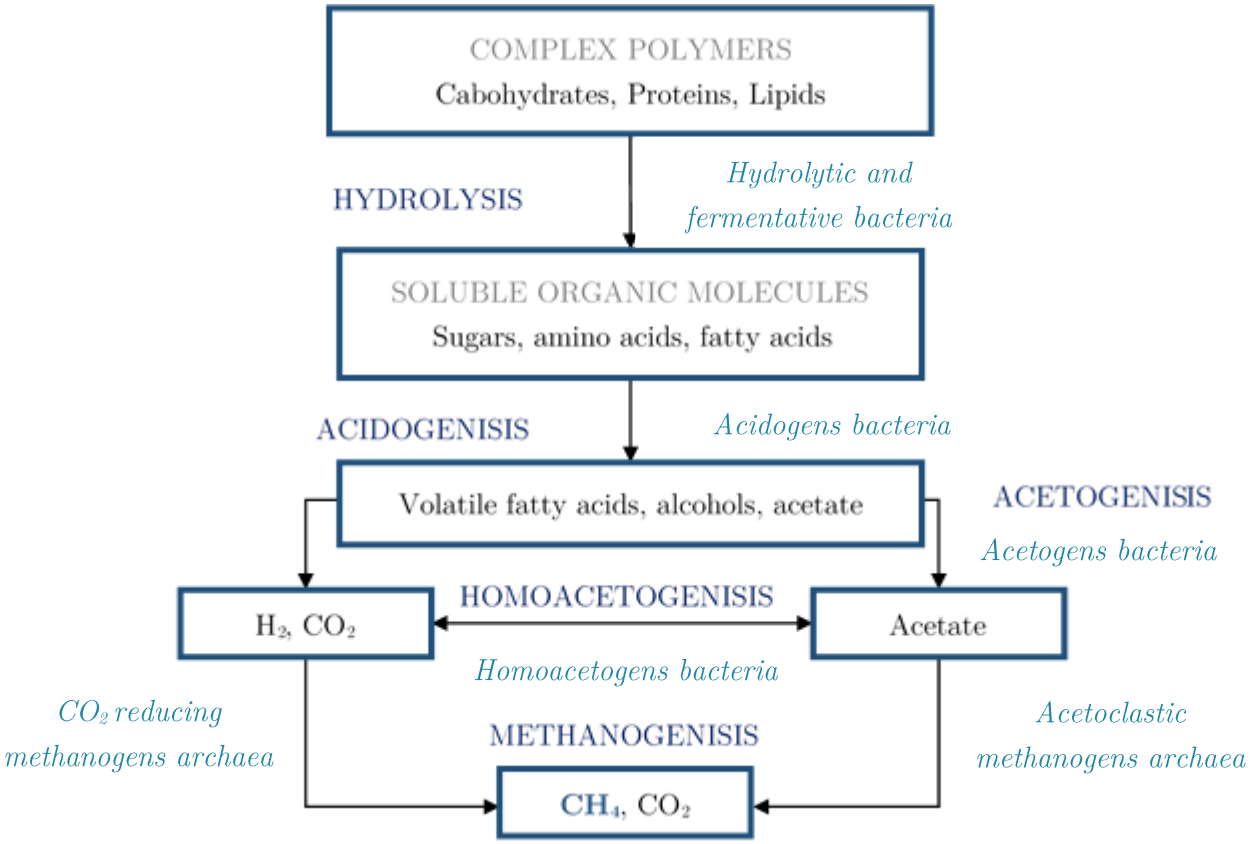

Figure 1: Anaerobic digestion process

As a matter of fact, depending on the waste or the treated waste mixture, the properties of the digestion medium will be different. Consequently, the waste characterisation is crucial. In this work, the literature data are used. In the case of liquid digestion, defined by a solids content of less than 15%, the medium may also have a Newtonian or non-Newtonian behavior. The behavior of the fluid has a direct consequence on the flows within the digester. Depending on the waste, the digestion medium will also have a different viscosity. Viscosity is the term for the resistance of a fluid to flow and motion. In order to model the flows within a digester, it is therefore

necessary to know both its technical characteristics (geometry, stirring mode) but also the rheology of the digestion medium. All these choices will have an incidence on the mechanical energy and thus on the expended electrical energy to produce methane.

The CFD simulations thus allow to analyse the flows within a digester by considering the treated waste insofar as we possess the rheological data of the latter. In the literature, the CFD models developed are based on the Reynolds-averaged Navier-Stokes (RANS) equations, the large eddy simulation (LES) as well as direct numerical simulation (DNS). DNS method provide the more precise results by solving directly the Navier-Stokes equations but it is also the most time-consuming method. RANS and LES methods are both used by many authors. LES method is more time-consuming than RANS method but provide more accurate outcomes. For example, Fan et al. used RANS method for simulating the hydrodynamic behaviours in a stirred tank [147], and Foukrach et al. employed RANS method for studying mixing performance in a gas-mixed anaerobic digester [173]. In the current work, the RANS method is used, closed with the standard k-epsilon turbulence model. Simulations for different stirring intensities are carried out in order to study the flows and the volume of dead zones in function of mixing intensity.

In perspectives, the simulations results will be confronted with experiments [235] and Wu simulations [77] in order to provide validation elements. This work constitutes a first step: the modelling of the flows of a Newtonian fluid, homogeneous and incompressible with mechanical agitation. The second step will consist in the consideration of the multiphase aspect of the digestion medium and the integration of the sedimentation phenomena. Sedimentation leads to the formation of sludge at the bottom of the digester. Furthermore, biofilms formation occurs at the walls. This raises the question of the stirring conditions inducing the accumulation / return of the sludge in the medium and the formation / detachment of the biofilm; and the effects on biogas yields.

VI-3. Context of the study carried out

VI-3.1. Inhibition and failure risks in anaerobic digestion

Various phenomena can destabilise the process of anaerobic digestion lowering it to complete failure of the biogas production. Anaerobic digestion is subjected to inhibition or failure risks due to the following reasons:

1. While the hydrolysis phase is largely considered as the rate-limiting phase for complex organic, intermediate product concentrations like free ammonia, volatile fatty acids and sulphide/sulphate can lead to inhibitions. Methanogenesis can also be considered like a rate-limiting phase [236] for easily biodegradable substrates. Total nitrogen concentration measured on the vinasse is approximately 2000 mg.L-1, which is relatively high for anaerobic digestion. Although this concentration is relatively high, anaerobic digestion is possible if the micro-organisms are acclimatised to the substrate [237].

2. For liquid anaerobic digestion (TS < 15%), inhibitions can occur because of an uneven distribution of biomass and substrates, the intensity and duration of the mixing as well as the retention time, must therefore be precisely studied to optimise the hydrodynamic behaviour of the process. Unsuitable mixing conditions can break the flocs of micro-organisms, disturbing the synergetic effects. Proper mixing conditions also must be established to control the volume of dead zones and turbulence.

3. For solid anaerobic digestion, where dry processes are concerned, i.e. if the dry solid content reaches 15% or for cases of codigestion, high viscosity leads to limited mass and heat transfer among enzymes, bacteria and substrates in the digester. Mechanical mixing is in this case, considered to be the most efficient way to optimise the diffusion processes [238]. However, few studies have been carried out on the hydrodynamics of media.

4. Anaerobic co-digestion is often recommended to optimise biogas yield. However, co-digestion can lead to solid digestion and inhibitions due to the accumulation of volatile fatty acids. In that case, the development of biofilms among the substrate can disrupt the liquid flows [239].

VI-3.2. Anaerobic digester modelling

We have seen a rise in numerical models, especially CFD models in recent years. Regarding the process modelling, the biochemical and physicochemical processes are taken into account in the ADM1 model [30]. To meet the needs related to the industrialisation of the anaerobic digestion process, the development of models taking the flows into account in a precise way, is necessary. There is experimental evidence that mixing schemes and intensities have an impact on biogas production [5]. Indeed, all the chemical reactions leading to the complete digestion of the substrates can only occur when they are in contact with the microorganisms involved in each reaction. To do this, the digestion medium must be stirred. The agitation mode and type thus influence the quality of the digestion of the substrates. In fact, vigorous mixing suppresses growth and the propagation of methanogenic centres if methanogenesis is the rate-limiting step, but also may enhance methane production and degradation if hydrolysis is the rate-limiting step [6].

In addition, anaerobic digestion can also be carried out by the dry route (TS > 15%). In this case, the medium agitation is even more significant than in the wet digestion, since the homogenisation of the medium becomes more difficult. Moreover, the waste treated by this process also has particular rheological properties which influence the flow and therefore have a role in the optimisation of the mechanical agitation. Indeed, these fluids can be viscous, Newtonian or non-Newtonian. The rheology of waste including sewage sludge, manure and biowaste, has been studied in order to model the flow of these fluids which have a Newtonian or non-Newtonian behaviour according to the content of total solid [42, 45, 47, 78, 79, 82, 111]. It has been shown that the fluid dynamics in the digester can be affected by the TS [83].

CFD provides accurate results on the flow and is therefore of great interest for anaerobic digestion modelling and optimisation. The major interest of the CFD is to characterise the flows within the digester in order to study configurations (digester, impeller) allowing optimal contact between the substrates and the microorganisms. With this in mind, we conducted a literature review of CFD models applied to anaerobic digesters to identify studies that have already been carried out using this technique.

These models are implemented to optimise the industrial process. The **Table 1** outlines the literature review of the aims of CFD in digesters.

Table 1: Objectives of CFD models

References	Objectives	Phase model	Fluid property
[167]	Study the impact of the design of the digester (diameter of the draft tube) on the flows by studying the position and the volume of the dead zones.	Liquid-gas	N
[156, 178]	Compute the flow with LES techniques.	Liquid	N
[79]	Optimise the power supply and reduce the volume of dead zones or weakly stirred area.	Liquid	N-N
[45, 148, 177]	Study the liquid homogenisation in stirred tanks and the required time for homogenisation (RANS and LES).	Liquid	N ; N-N
[172]	Reduce the percentage of poorly mixing zones in gas-lift digesters by testing configurations of the bottom of the digesters.	Liquid	N-N
[149]	Simulate the characteristics of digesters: the rates of mixing and the slug injection of tracers from the digester volume turnover time, the mixture diffusion time, and the hydraulic retention time.	Liquid	N
[142]	Study different mechanical stirring configurations.	Liquid	N ; N-N
[157]	Investigate the flow fields, power and mixing time in a fully baffled stirred vessel with mechanical agitation (LES).	Liquid	N
[150, 171]	Investigate turbulence models.	Liquid	N-N
[83]	Simulate mechanical agitation in high solid anaerobic digester.	Liquid	N-N
[77]	Model the flows with mechanical agitation.	Liquid	N-N
[44]	Describe the settling and suspension in anaerobic digester and evaluate the biomass retention physical process.	Three phases	N
[48]	Model the flows for fluids with variable rheology to study the impact on the performance of the digester.	Liquid	N-N
[152]	Study the stirring performance of gas recirculation agitation configurations, and the impact of agitation intensity on biological processes.	Liquid-gas	N
[42]	Study the hydraulic performance of an existing digester (percentage of dead zones, recirculation volume).	Liquid	N

[183]	Study the impact of the agitator on suspended particles in order to optimise the digester.	Liquid-solid	N
[160]	Study the effect of impeller rotational speed and velocity field in the mixing tank.	Liquid	N
[50]	Study the influence of the behaviour of the sludge on the flow and the consequences on the quality of the agitation.	Liquid-gas	N-N

N = Newtonian, N-N = non-Newtonian.

VI-3.3. Turbulence modelling

A point of attention is the modelling of turbulence phenomena. The interest comes from the fact that the mass transfer during the process is dependent on the turbulence phenomena in digesters [77], and the contact between micro-organisms and substrate is correlated to turbulence [37]. Moreover, studies show that flow predictions are particularly sensitive to the turbulence model implemented [180]. Thereby, the choice of the turbulence model is important in the simulations. Mainly Reynolds-average Navier-Stokes (RANS) simulations were conducted on digesters [42, 44, 48, 79, 80, 82, 83, 142, 143, 152, 167, 171, 180]. The SST k-omega model [48, 80, 143, 152, 180], the standard k-epsilon model [42, 79, 80, 83, 149, 150] and the realisable k-epsilon model [44, 82, 142, 150, 177] are recommended by many authors among the RANS models. Furthermore, other authors claim that the Reynold stress model (RSM) is the most suitable model to predict the behaviour of this bioreactor [37, 180].

VI-4. Theoretical model

VI-4.1. Assomptions

The anaerobic digestion occurs at the mesophilic regime at 37 °C. It is assumed that the sugarcane vinasse is Newtonian [39] and the slurry is a non-Newtonian power-law fluid [45, 82], and the fluid is isothermal and incompressible. The rheological properties of the medium are chosen with the total solid content of the substrates. The properties of the substrates are detailed in the following part in the **Tables 1 and 2.**

As a matter of fact, anaerobic digesters are commonly heated by the walls through a double membrane in which circulates a heated fluid, to keep the medium at a constant

temperature. Therefore, homogenisation of the temperature is also controlled by agitation of the digester. In the present study, we consider isothermal single-phase turbulent flow. We are interested in flows in a mechanically agitated digester.

VI-4.2. Geometry

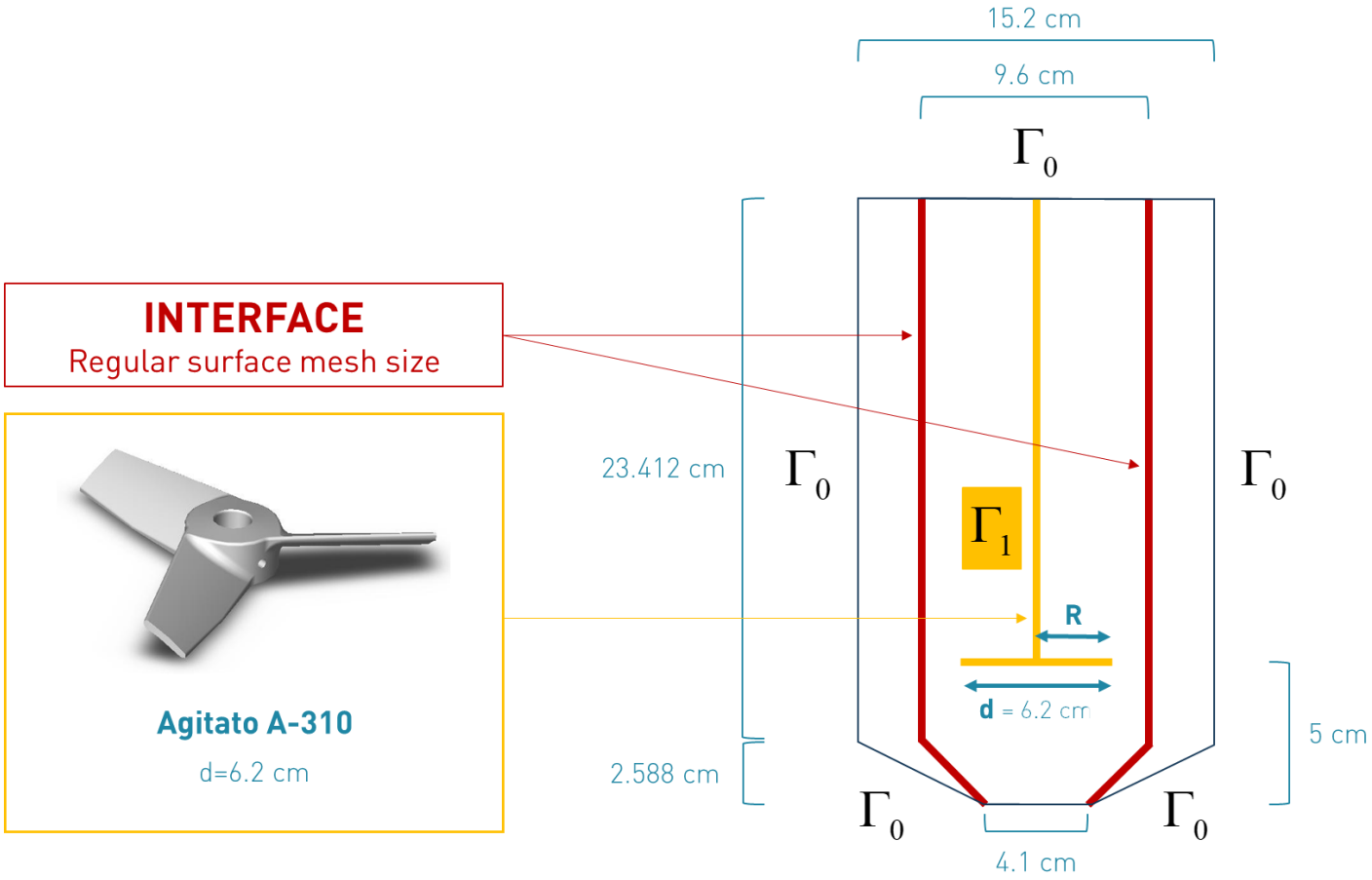

Figure 2: Cross section of the pilot geometry with the moving zone and the stationary zone (A) and the impeller geometry (B)

Based on the study carried out by Wu (2012) [77], the geometry consists in a 260 mm height tank (liquid height) with a diameter of 152 mm. The digester bottom is conical with a height of 25.88 mm and a diameter of 41 mm. The tank geometry is shown in the **Figure 2**. Wu (2012) validated his model from computer automated radioactive particle tracking (CARPT) experiment developed by Hoffmann et al. (2008) [235]. Then, Wu (2012) also confronted his results with particle image velocimetry (PIV) experiment carried out by Bugay et al. (2002) [240]. The geometry of the impeller is shown in the **Figure 2.**

VI-4.3. Governing equations

The sliding mesh (SM) method is suitable for unsteady flow [185]. In our case study, we are in the case of unsteady flow. Indeed, initially, the mechanical agitation is zero and increases gradually until the desired agitation. The flow is steady only when the intensity of the stirrer is reached. Therefore, the SM method is used in this work. In order to model the impeller rotation, the digester tank is thus divided in to domain, the rotating zone which contains the impeller and the stationary zone. The arbitrary mesh interface (AMI) is used to link the two domains. The AMI interface is a pair of detached surfaces, giving the AMI1 and AMI2 boundaries. One belongs to the mobile zone and the other to the stationary zone. These two boundaries are identical and have the same initial and boundary conditions. The rotational speed is assigned directly to the moving zone.

The mathematical model is based on Reynolds averaged Navier-Stokes (RANS) equations associated with the forces linked to the impeller rotation: the Coriolis and centrifugal forces. The governing equations for the rotating zone and the stationary zone are respectively:

$$\begin{cases} \dfrac{\partial u_R}{\partial t} + \nabla \cdot \left(u_R \otimes u_I \right) = -\nabla p + \nabla \cdot \left(\nu_{eff} \left(\nabla u_I + \left(\nabla u_I \right)^T \right) \right) \\ \nabla \cdot u_R = 0 \end{cases} \tag{62}$$

$$\begin{cases} \dfrac{\partial u_I}{\partial t} + \nabla \cdot \left(u_I \otimes u_I \right) = -\nabla p + \nabla \cdot \left(\nu_{eff} \left(\nabla u_I + \left(\nabla u_I \right)^T \right) \right) \\ \nabla \cdot u_I = 0 \end{cases} \tag{63}$$

Where u_I and u_R are the absolute velocities viewed from the stationary and the rotating frames (m.s^{-1}), t is the time (s), ν_{eff} is the effective kinematic viscosity (m^2.s^{-1}) and p is the pressure (Pa).

The system is closed with the standard $k-\varepsilon$ turbulence model, where is k turbulent kinetic energy (m^2.s^{-2}) and ε is the turbulent dissipation rate (m^2.s^{-3}). The model implemented in OpenFOAM does not include the buoyancy contribution. The two equations of this model are:

$$\frac{\partial k}{\partial t} = \nabla \cdot \left(D_k \nabla k \right) + G_k - \varepsilon + S_k \tag{64}$$

$$\frac{\partial \varepsilon}{\partial t} = \nabla \cdot \left(D_\varepsilon \nabla_\varepsilon \right) + \frac{C_1 G_k \varepsilon}{k} - C_2 \frac{\varepsilon^2}{k} + S_\varepsilon \tag{65}$$

Where u is equal to u_I or u_R, S_k is the internal source term for k, S_ε is the internal source term for ε, G_k is the production of k, C_1 and C_2 are model constants, D_k the effective diffusivity for k and D_ε is the effective diffusivity for ε. The values of the model constants used in OpenFoam, as in the standard model are: $C_\mu = 0.09$, $C_1 = 1.44$, $C_2 = 1.92$, $\sigma_k = 1$ and $\sigma_\varepsilon = 1.3$ [241].

The production term G_k is:

$$G_k = \nu_t S^2 \tag{66}$$

The assumption of the standard $k-\varepsilon$ turbulence model turbulence is the following expression of the turbulent viscosity ν_t ($m^2.s^{-1}$):

$$\nu_t = C_\mu \frac{k^2}{\varepsilon} \tag{67}$$

For the initialisation of the numerical simulations, the turbulent kinetic energy for isotropic turbulence and the turbulent dissipation rate are calculated as follows:

$$k_0 = \frac{3}{2}\left(I \left| u_{ref} \right| \right)^2 \tag{68}$$

$$\varepsilon_0 = \frac{C_\mu^{0.75} k_0^{1.5}}{L} \tag{69}$$

Where I (%) is the turbulence intensity with a default value of 0.05, u_{ref} ($m.s^{-1}$) is a reference velocity (the stirring velocity) and L (m) is the reference length scale (the digester radius).

The mesh must be refined at the walls. In fact, the standard turbulent model is derived under the assumption of a high local turbulent Reynolds number [242]. This low turbulent Reynolds number region is called the viscous sub layer. Launder and Spalding suggested the following wall function equation [241] to reduce cell number in these zones:

$$u^+ = \frac{1}{\kappa} \ln y^+ + C \tag{70}$$

Where $u^+ = |u|/u_T$ is the dimensionless velocity where u_T is the friction velocity (or shear velocity). $y^+ = u_T y/\nu$ is the dimensionless local Reynolds number where y is the width of the boundary layer (normal distance from the wall). The range of the local Reynolds number is $11.06 \leq y^+ \leq 300$ [243]. Recommends that the local Reynolds number of the first cell should be in the range of $20 \leq y^+ \leq 100$ [242]. κ is the von Karman constant and C a parameter related to the wall roughness. In the case of smooth walls, the values are respectively 0.419 and 5.24.

The boundary conditions are:

$$\begin{aligned} &\text{No slip: } u = 0 \ , && \frac{\partial}{\partial n} p = 0 \ , \quad \text{on } \Gamma_0 \text{ (digester walls)} \\ &\text{Imposed velocity fields: } v_r = \omega R \, , && \frac{\partial}{\partial n} p = 0 \, , \quad \text{on } \Gamma_1 \text{ (impeller wall)} \end{aligned} \tag{71}$$

Where the index r is the center of the elementary surfaces of each cell the agitator, ω is the angular velocity and R is the impeller radius.

The rotational speed of the agitator is defined by the speed of rotation of the mobile zone of the mesh. A sudden increase in the stirring speed at the first-time step causes a sharp increase in the CFL. Thus, a velocity ramp is necessary for the simulations starting to maintain the Courant number lower than 0.5.

VI-4.4. Rheological expressions

We refer to the pseudo-plastic model of Ostwald. It allows to express the shear stress τ (Pa) as a function of the shear rate $\dot{\gamma}$ (s^{-1}). It is calibrated by two parameters: the consistency index k (Pa.s^n) and the flow index n. It is expressed as follows:

$$\tau = k\dot{\gamma}^n \tag{72}$$

The viscosity is expressed as follows:

$$\eta = k\dot{\gamma}^{n-1} \tag{73}$$

The components of the tensor of the shear rate are:

$$\dot{\gamma}_{ij} = \left(\frac{\partial u_i}{\partial x_j} + \frac{\partial u_j}{\partial x_i} \right) \tag{74}$$

$$S_{ij} = \eta \left(\frac{\partial u_i}{\partial x_j} + \frac{\partial u_j}{\partial x_i} \right) = k\dot{\gamma}^{n-1} \left(\frac{\partial u_i}{\partial x_j} + \frac{\partial u_j}{\partial x_i} \right) \tag{75}$$

The rheological properties of the vinasse, the water and diluted dairy cow manure are shown in the **Table 2**. It can be seen that the properties of the vinasse are closed to the properties of water. The difference between these two substrates is mainly the presence of suspensions. In anaerobic digestion process, the particles settle, accumulate at the bottom of the digester and result in the formation of sludge. In the present study, as a monophasic model is considered, the suspensions are not taken in account.

Table 2: Rheological properties of Newtonian fluids

Fluid	Density ($kg.m^{-3}$)	Dynamic viscosity (Pa.s)	Sources
Vinasse	1044.69	0.0010097	[39]
Water	1000	0.001	
Screened and diluted dairy cow manure	1000	0.0009	[235]

The rheological properties of the liquid manure vary with the total solid content. There are data in the literature on the rheological properties of liquid manure for different solid content. The manure slurry exhibits pseudo-plastic fluid behaviour when TS is superior to 2.5% [82]. The rheological properties used are presented in the Table 3 [75, 77–79].

Table 3: Rheological properties of liquid manure

TS %	T °C	K Pa.s^n	n	$\dot{\gamma}$ s^{-1}	ρ kg.m^{-3}	η_{min} Pa.s	η_{max} Pa.s	C_p J.kg^{-1}.K^{-1}	λ W.m^{-1}.K^{-1}	Sources
2.5	35	0.042	0.710	226-702	1000.36	0.006	0.008	4186.78	0.6171	[75, 79]
5	35	0.103	0.639	50-702	1000.72	0.009	0.025	-	-	[77]
7.5	35	0.525	0.533	11-399	1001.00	0.03	0.17	4185.33	0.6168	[75, 79]
9.1	35	1.052	0.467	11-156	1001.31	0.07	0.29	4184.87	0.6167	[75, 79]
12.1		5.885	0.367	3-149	1001.73	0.25	2.93	4184.00	0.6165	[75, 79]
15	17-24	31.3	0.3	0.61-24.37	973	3.35	44.24	4183.17	0.6163	[78]
20	17-24	56.8	0.35	0.24-23.90	1090	34.47	172.5	-	-	[78]

VI-4.5. Flow field characterisation

The Reynolds number for mechanical agitation of Newtonian fluids is [151, 244, 245]:

$$\mathrm{Re} = \frac{\rho N d^2}{\mu} \tag{76}$$

Where N is the rotational speed (rev.s^{-1} or rps), ρ is the fluid density (kg.m^{-3}), d is the impeller diameter (m) and μ is the dynamic viscosity (Pa.s).

The generalised Reynolds number, valid for non-Newtonian fluids, is [79]:

$$\mathrm{Re}_g = \frac{\rho U_\infty^{2-n} d^n}{k\left(0.75 + \frac{0.25}{n}\right)^n 8^{n-1}} \tag{77}$$

Where U_∞ is the average velocity of the fluid (m.s^{-1}), k is the consistency index (Pa.s^n), n is the flow index and d is the reference length (m).

The evaluation of the energy consumption and consequently its economic impact is possible with the calculation of the power calculation. The power consumption P (W) calculation based on the torque of the impeller is:

$$P = 2\pi N T \tag{78}$$

Where N is the impeller rotational speed and T is the impeller torque (N.m).

The torque is defined as [142]:

$$T = \left(\int_S \left(\vec{r} \times \left(\bar{\bar{\tau}} \cdot \hat{n} \right) \right) dS \right) \cdot \hat{\alpha} \tag{79}$$

Where S represents the surfaces including the rotating parts, $\bar{\bar{\tau}}$ Is the total stress tensor, $\hat{n}$ is a unit vector normal to the surface, $\vec{r}$ is the position vector and $\hat{\alpha}$ is a unit vector parallel to the rotation axis.

The mixing energy level (MEL) ($W.m^{-3}$) is calculated by [82]:

$$MEL = \frac{P}{V} \tag{80}$$

Where P is the power consumption (W) and V is the working volume (m^3).

The flow rate through the moving zone Q ($m^3.s^{-1}$) is used for the evaluation of the fluid circulation through the digester. We create a surface for the discharge zone for computing the flow rate. The surface consists of two discs above and below the stirrer for the axial flow and a cylinder (AMI section) for the radial flow.

The power and flow (also called pumping number) numbers are two dimensionless numbers commonly used to characterise the stirred tank flows and mixing processes. The flow number is a measure of the pumping capacity of an impeller [244]. The power number is a dimensionless parameter that provides a measure of the power requirements for the operation of an impeller [244]. These two mixing parameters can be calculated from CFD results and allow to compare the results of simulations with the experimental results. In our case, the experimental values for hydrofoil impeller are N_P equal to 0.3 and N_Q equal to 0.56 [77, 246]. The power and flow numbers are respectively expressed by:

$$N_P = \frac{P}{\rho N^3 d^5} \tag{81}$$

$$N_Q = \frac{Q}{N d^3} \tag{82}$$

The spatially average characteristic velocity gradient G (s^{-1}) is used for describing the mixing intensity through the digester [247], as well as characterising the turbulent shear rate [246]. It is defined with the following expression [246, 247]:

$$G = \left(\frac{\bar{\varepsilon}}{\nu} \right)^{1/2} \tag{83}$$

Where ν is the kinematic viscosity and $\bar{\varepsilon}$ ($m^2.s^{-3}$) is the global average turbulent energy dissipation rate calculated as follow [246, 247]:

$$\bar{\varepsilon} = \left(\frac{N_P N^3 d^5}{V} \right) \tag{84}$$

The circulation time t_c is expressed by [246, 248]:

$$t_c = \frac{V}{N_Q N d^3} = \frac{V}{Q} \tag{85}$$

The vorticity ξ (s^{-1}) is a measure of the local rotation in the fluid. More specifically, it is a vector field that gives a microscopic measure of the rotation at any point in the fluid. The vorticity describes the local spinning motion. The helicity H provides indications on the alignment of the vorticity vector and the velocity vector U. It allows to illustrate the longitudinal vortices, or spiral motion, as is often found in vortex cores.

The vorticity is defined as the curl of the velocity vector:

$$\xi = \nabla \times U \tag{86}$$

The helicity is expressed as:

$$H = U \cdot \xi = U \cdot \left(\nabla \times U \right) \tag{87}$$

The angle α between the vorticity vector and the velocity vector (which is 0^o or 180^o in a vortex core) is given by:

$$\alpha = \cos^{-1} \left(\frac{H}{|\xi||U|} \right) \tag{88}$$

VI-4.6. CFD simulations

The numerical simulations are performed on OpenFOAM software. The PIMPLE algorithm is used, which is a combination of the PISO (pressure-implicit with splitting of operators) [249, 250] and SIMPLE (semi-implicit method for the pressure linked equations) [251] algorithms. The PISO algorithm is pressure implicit with splitting of operators [249] and allows the use of the sliding mesh method. The SIMPLE algorithm is the semi-implicit method for pressure linked equations [252]. The pimpleFoam solver (dynamic solver mesh) assumes incompressible, unsteady and viscous flows. The simulations are launched in parallel on 16 processors. The simulation time, for which we get a steady state flows, is a few seconds. The calculation time is about a few days.

VI-5. Results and discussions

VI-5.1. Mesh

The mixing is modelled using the sliding mesh method. The sliding mesh model is a time-dependent solution approach in which the grid surrounding the rotating component(s) physically moves during the solution [244]. Two zones are defined: the stationary zone and the moving zone, which contains the impeller. The impeller is located in the moving zone. The Lightnin A310 impeller, which is a hydrofoil impeller, is used. Hydrofoil impellers were developed for applications where axial flow is important and low shear is desired [244]. The impeller diameter is 62 mm and the axis diameter is 8 mm. The impeller axis is positioned at a height of 50 mm from the bottom of the digester. The tank geometry and mesh are done on OpenFOAM. Then, the openFOAM snappyHexMesh command is used to obtain the final mesh. The mesh is shown in the **Figure 3**.

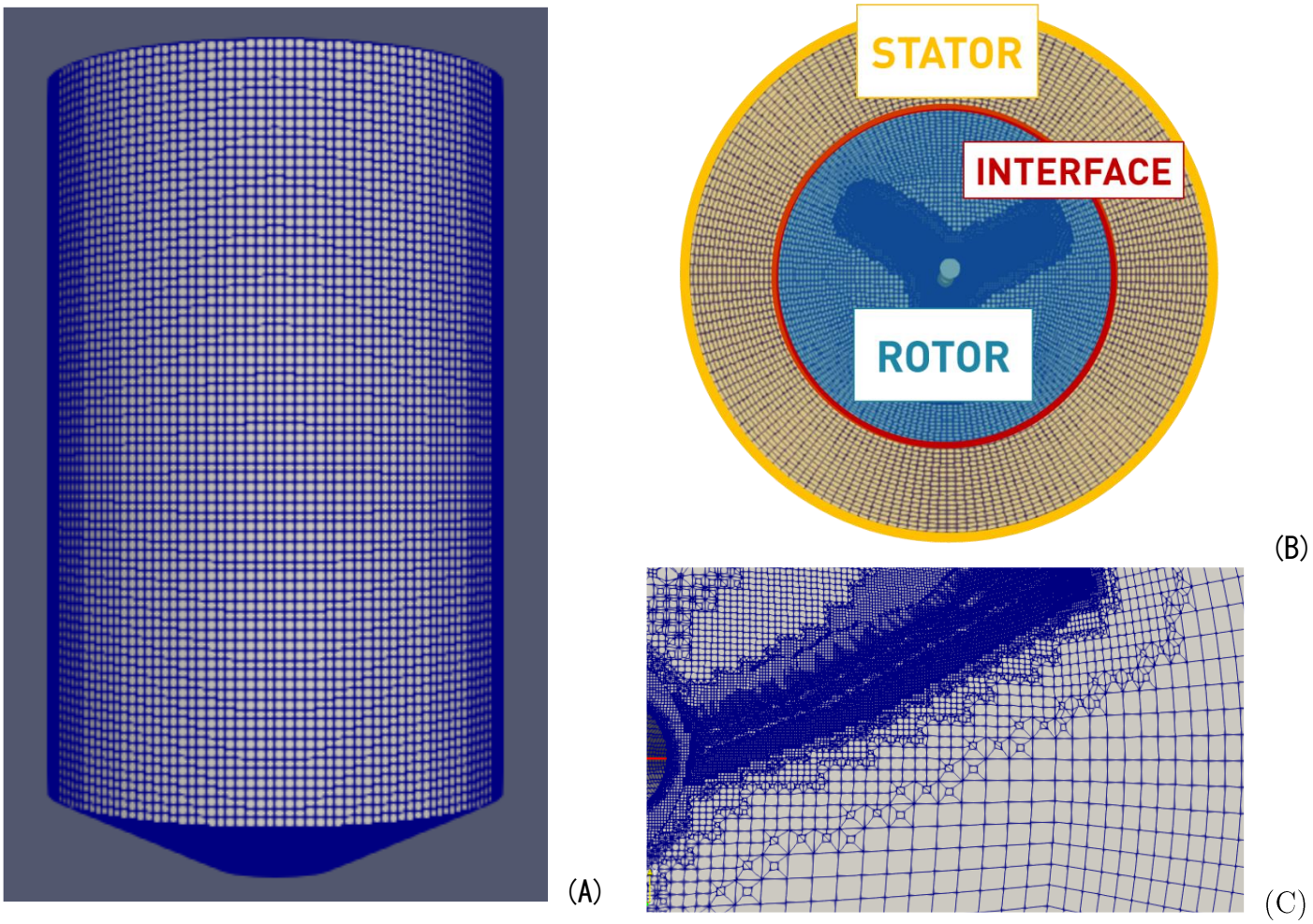

Figure 3: Digester mesh (A) and cross section of the mesh (B) and (C)

Table 4: Mesh characteristics

Characteristics	
Total mesh cells	2,841,535
Total mesh points	3,485,073
Total mesh faces	9,150,640
Total mesh internal faces	8,591,189
Number of hexahedra	2,578,249
Number of prisms	10,298
Number of wedges	3
Number of polyhedra	252,985
Maximum cell skewness	3.40025
Maximum mesh non-orthogonality	65.0182
Average mesh non-orthogonality	21.3783

Breakdown of polyhedra by number of faces		
Faces	Number of cells	
<10	216,780	
≥10	36,205	
Patch topology		
Patch	Faces	Points
Upper edge (moving zone)	5,719	5,952
Bottom edge (moving zone)	4,800	4,881
Impeller edge (moving zone)	465,732	483,277
Upper edge (stationary zone)	3,200	3,360
Bottom edge (stationary zone)	3,200	3,360
Lateral wall (stationary zone)	25,760	25,760
AMI1	25,760	25,760
AMI2	25,760	25,760

The mesh is refined to meet the quality criteria of mesh such as cell skewness and mesh non-orthogonality. To meet these criteria, we reach a very large number of cells and thus long computing times. Consequently, we do not perform grid independence tests. The characteristics of the mesh are shown in the **Table 4**. In total, this mesh is composed of 2,841,535 cells with mostly hexahedra. The total mesh faces is 9,150,640. The impeller edge has the larger amount of faces with a value of 465,732 due to its geometry. Concerning the interface between the moving zone and the stationary zone (AMI1 and AMI2), the two-surface mesh must be identical with the same faces number in order to avoid numerical errors. Globally, the maximum cell skewness is 3.4 and the maximum mesh non-orthogonality is 65.0, which reflect an acceptable mesh quality. The dimensionless local Reynolds number y^+ is below 1.

VI-5.2. Velocity profiles

In this part, we present the simulation results for various mixing intensity: 20, 40, 60 and 100 rpm. The **Figure 4** shows the cross section of the velocity field within the digester at the agitator height and the **Figure 5** extends the longitudinal section of the velocity field.

The results obtained are consistent. In fact, by increasing the rotation velocity of the stirrer, the maximum velocity increases, the volume of dead zones decreases and the volume of continuously agitated zones increases. The maximum velocity observed for

each case is the agitator velocity. The velocity decreases gradually with the distance from the agitator. For each case, we find that the velocity at the edges of the digester is zero. However, we neglected in our study the impact of temperature on the flows. Indeed, the heating of the digester at these edges would generate flows at this level. Similarly, the velocity at the axis of the agitator increases with the increase in mechanical agitation. The interest of the study of the velocity field at this level relates in particular to the influence of the agitation on the biofilm which tends to develop on the axis of the agitator. The interest is even greater in the case of intermittent agitation. This mode of agitation is particularly interesting because it leads to the reduction of energy consumption. Overall, the optimisation of the mechanical agitation must allow to properly stir the medium, so as to have the best biogas yields, while reducing the intensity and frequency of agitation.

Flow modelling of a mechanically agitated digester is the first step of our work. CFD simulations are useful for defining the volume of dead zones. We assume that the dead zones are defined by a velocity magnitude less than 0.001 $m.s^{-1}$ as [3]. Indeed, the dead zones within a digester lead to the heterogeneity of the medium. There will be areas where the substrate will not be digested or acidic areas. This can eventually lead to the failure of the digester generating significant costs on an industrial scale. CFD simulations accompanied by experimental studies allow to relate the stirring velocity, the volume of dead zones, the homogenisation of the medium (physicochemical properties) and the biogas yields. Thus, a better understanding of the physical phenomena involved in the digesters is necessary for the optimisation of anaerobic digestion on an industrial scale. Findings on optimal velocity fields will be dependent on the substrates studied. As said before, the heat transfers are not taken into account in the simulations but will have to be integrated in future studies because they influence the flows. In addition, sedimentation and movement of suspended solids should be incorporated into the model.

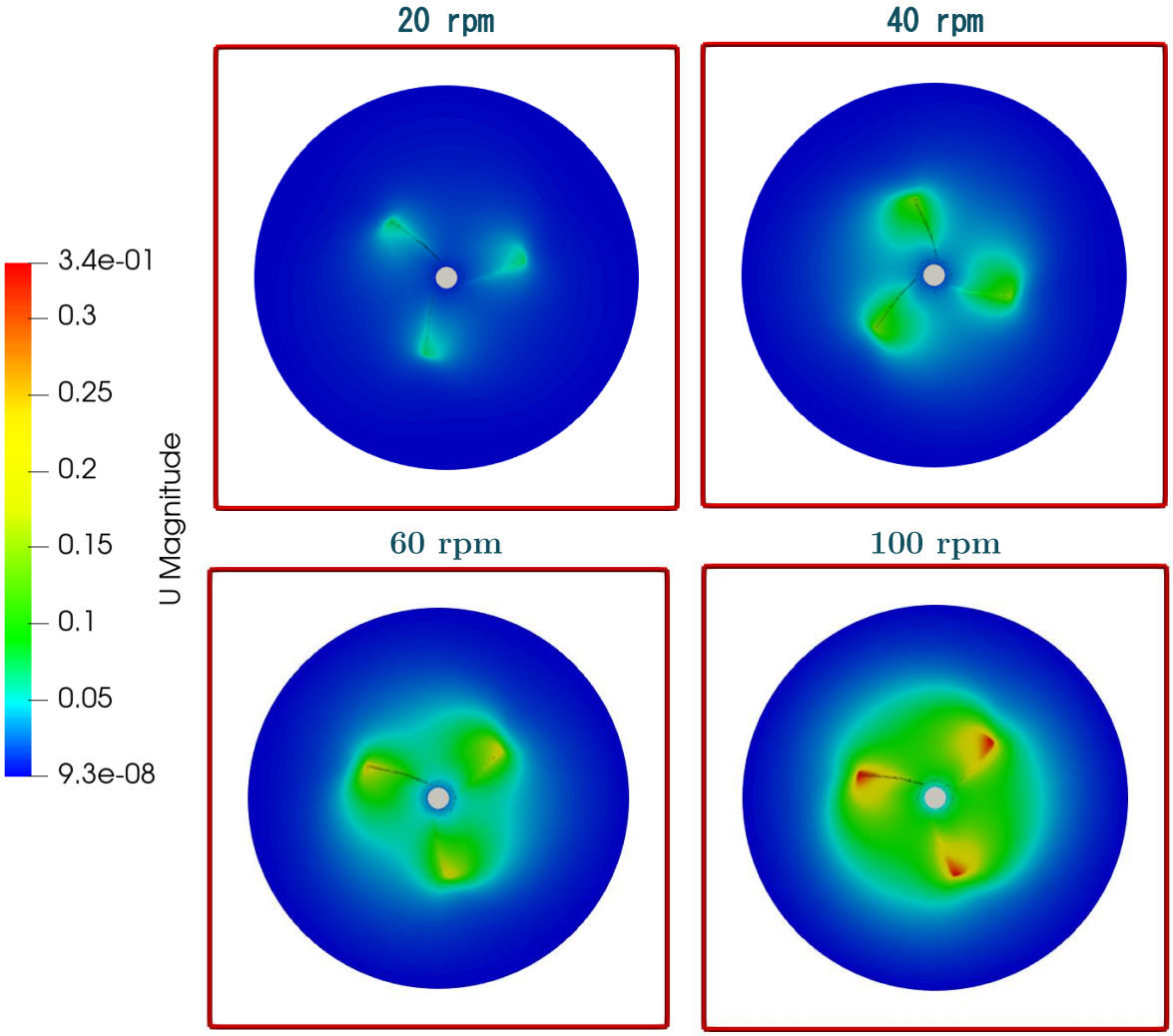

Figure 4: Cross section of the velocity field (m.s^{-1}) within the digester at the agitator height for different stirring intensities (z = 0.059 m)

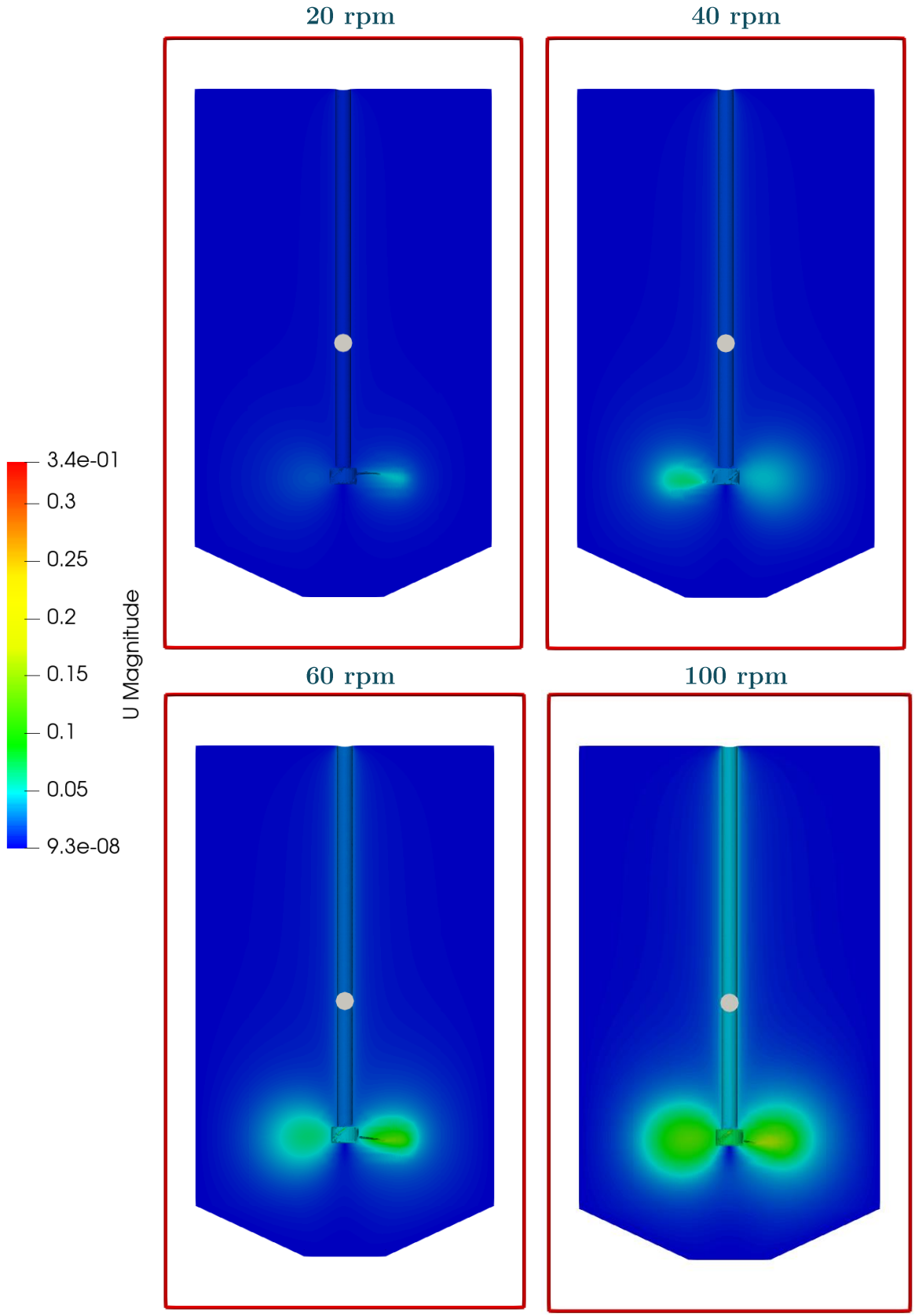

Figure 5: Longitudinal section of the velocity field ($m.s^{-1}$) within the digester

VI-6. Conclusion

VI-6.1. Mesh

The mesh produced allows to obtain coherent results. However, the local dimensionless Reynolds number y^+ is below the values recommended in the literature. Therefore, work on the mesh must be done to increase the value of y^+. For this, the mesh at the agitator must be coarser while respecting its geometry. This will also reduce the number of cells in the mesh and thus the computation time.

VI-6.2. Validation of the simulation outcomes

Simulations were performed for a Newtonian case. The experiment [235] with which we will compare the results of our model is done with the non-Newtonian fluid. Therefore, in order to provide validation elements, especially on velocity fields, we have to perform simulations for a non-Newtonian case. The results will be compared to the experimental results of Hoffmann et al. (2008) [235]. In this paper, three impeller velocities were studied with computer automated radioactive particle tracking (CARPT) and CFD simulations: 250, 500 and 1000 rpm. After bringing model validation elements, the CFD model for mechanically stirred tank will be completed. We will be able to add other physical phenomena to our model.

VI-6.3. Conclusion

Three-dimensional CFD simulations were carried out. The model was based on RANS equations and standard k-epsilon turbulence model and the fluid was Newtonian. The sliding mesh method was used for the mechanical mixing. The outcomes were the velocity field. The area of influence of the agitator is in the area of the blades. The volume of dead zones is thus important. The maximum velocity is observed at the tips of the blades. In conclusion, several rows of paddles would be required to agitate the entire digester.

VI-7. Acknowledgments

This work was supported by the Region Reunion (France) as part of the funding of a research thesis in the PIMENT (Physics and Mathematical Engineering for Energy, Environment and Building) laboratory at the University of Reunion Island.

Chapitre VII

Conclusions, discussions et perspectives générales

VII-1. Conclusions générales

Ces travaux de thèse ont porté sur l'hydrodynamique des réacteurs anaérobies avec une double approche expérimentale (cas de la vinasse) et numérique (modélisation et simulations numériques). La CFD, de par la précision des résultats, est largement utilisée pour répondre aux problématiques liées aux écoulements telles que l'homogénéisation du milieu de digestion ou encore l'optimisation des caractéristiques géométriques des digesteurs (forme du digesteur, dimensions et modèle de l'agitateur, etc.), a été utilisée pour mettre en évidence les impacts des vitesses d'agitation.

L'étude expérimentale s'est déclinée en trois étapes :

Le potentiel méthanogène de la vinasse de canne à sucre de la distillerie Rivière du Mât (Saint-Benoît, La Réunion) a été déterminé. Des protocoles spécifiques ont été adaptés, notamment en testant différents ratios I / S. Le potentiel méthanogène a été atteint pour trois valeurs de ce ratio inférieures à 1. En outre, nous obtenons une constante d'hydrolyse de 0.29 s^{-1} en utilisant le modèle de cinétique de premier ordre.

Un protocole du démarrage du pilote a été établi pour la digestion anaérobie de la vinasse, permettant ainsi d'éviter des dysfonctionnements menant à son arrêt de façon anticipée. Les analyses physicochimiques du milieu ainsi que la production de biogaz ont permis de montrer que la phase de stabilisation a duré 45 jours.

Enfin, nous avons évalué l'impact de la vitesse d'agitation sur les rendements en biogaz dans des conditions réelles. Des mesures physicochimiques ont également été effectuées sur le milieu de digestion à différentes profondeurs au moment du nourrissage du pilote, avant et après la période d'agitation. Nous avons successivement expérimenté les vitesses

d'agitation de 20, 30, 40, 50 et 60 tr/min. Nous avons constaté que la production de biogaz croît avec l'âge du pilote. En outre, des pics dans la production ont été observés lors des changements d'agitation pour les intensités de 30, 40 et 50 tr/min. La production de biogaz s'est stabilisée rapidement pour toutes ces intensités. Cependant, la période de stabilisation du processus est plus longue avec l'augmentation de la vitesse d'agitation. En parallèle des variations de production de biogaz, il a été observé des variations de concentrations des AGV et de l'ammonium. De plus, les mesures locales ont montré que l'agitation a un impact majeur sur les concentrations en AGV, en effet les AGV s'accumulent au fond du digesteur au cours du temps et retournent dans le milieu durant l'agitation. Les mesures de l'alcalinité et du pH traduisent la stabilité du processus avec une alcalinité qui tend à augmenter et un pH stable et peu sensible aux variations des concentrations en AGV. En conclusion, l'impact de l'agitation mécanique sur les rendements de la digestion anaérobie de la vinasse est confirmé.

Les résultats expérimentaux obtenus au cours de cette thèse constituent une base de données qui pourra servir de comparaison avec de futures études pilotes. Ces résultats justifient le recours à la simulation des écoulements grâce à la CFD afin de caractériser l'hydrodynamique des réacteurs. Les travaux suivants ont ainsi concerné la modélisation des écoulements au sein d'un digesteur agité mécaniquement à l'aide du logiciel libre d'accès OpenFOAM.

Nous avons modélisé les écoulements au sein d'un digesteur agité mécaniquement dans le cas d'un fluide Newtonien, pour différentes vitesses de rotation (20, 40, 60 et 100 tr/min). Les équations sont basées sur le modèle de RANS et le modèle de turbulence standard k-epsilon. En outre, il a fallu mettre un place un maillage glissant, permettant d'effectuer des simulations d'un digesteur agité mécaniquement. Les résultats obtenus sont cohérents, avec des champs de vitesse maximaux obtenus au niveau des pâles de l'agitateur et une réduction du volume de zones mortes pour des vitesses supérieures.

VII-2. Discussions

De par nos deux études expérimentales et numériques, nous avons pu mettre en évidence un ensemble de phénomènes qui sont récapitulés sur la **Figure 1** :

1. Le milieu de digestion est un milieu vivant, il est sensible aux variations des conditions physicochimiques et les réactions biochimiques sont liées aux vitesses d'écoulement.

2. Nous avons constaté une accumulation de matières non digérées et d'espèces en phase inférieure du pilote, et donc une stratification du milieu de digestion. Cette accumulation est due aux phénomènes de sédimentation pouvant être décris avec un modèle numérique basé sur la mécanique des fluides.

3. Nous avons également observé le développement d'un biofilm au niveau des parois du digesteur et de l'agitateur.

4. Les mesures expérimentales ont montré que l'agitation mécanique permet de remettre en suspension les matières et espèces accumulées au fond du digesteur. Cette remise en suspension peut être positive ou négative pour la digestion anaérobie. D'un point de vue numérique, nous avons pu décrire les écoulements au sein d'un digesteur agité mécaniquement pour différentes vitesses d'agitation. Un changement de repère et de la géométrie de l'agitateur nous permettrait d'étudier les écoulements pour ce cas d'étude. Compte tenu des premiers résultats numériques obtenus, nous avons pu observer que la zone d'influence de l'agitateur est principalement la zone proche des pâles. Dans le cas du digesteur utilisé expérimentalement, les extrémités des pâles étaient proches des parois du digesteur. Ainsi, conformément aux résultats numériques, l'agitation a eu une influence sur la partie inférieure du pilote. Les résultats numériques et expérimentaux sont donc cohérents et appuient l'intérêt d'une modélisation fine des écoulements.

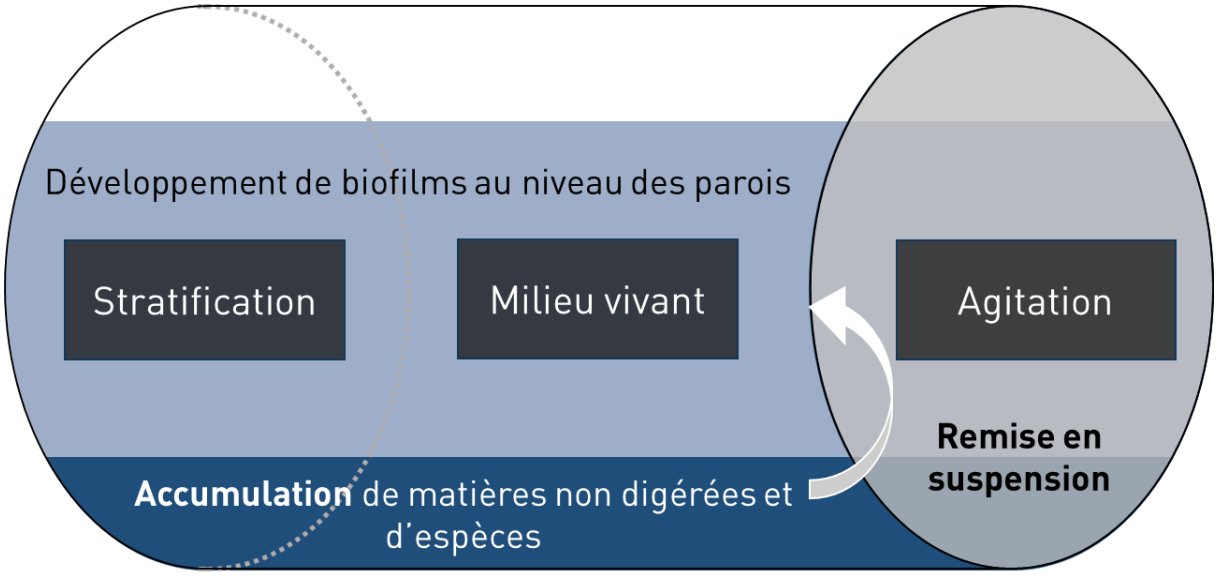

Figure 1: Phénomènes mis en évidence au cours de l'étude expérimentale

VII-3. Perspectives générales

De par la confrontation des études expérimentales et numériques, nous nous posons les questions suivantes : Quel est le champ de vitesse optimal pour la digestion anaérobie ? Quels sont les effets des écoulements sur les processus bio-physico-chimiques ? Et comment modéliser conjointement les écoulements et les processus bio-physico-chimiques de la digestion anaérobie ?

Les lignes suivantes exposent les perspectives potentielles de ce travail de thèse :

Un travail est déjà en cours sur la prise en compte de l'aspect multiphasé du milieu de digestion. En effet, de nombreux déchets, y compris la vinasse, possèdent des particules solides qui sédimentent ou restent en suspension selon le profil d'écoulement au sein du digesteur. L'objectif est ainsi de modéliser avec précision les écoulements au sein du digesteur en fonction du mode d'agitation. En effet les particules sédimentées se retrouvent au fond du digesteur et forment une boue épaisse avec le temps. Ces particules sont remises dans la phase liquide au moment de l'agitation. Or, il a été montré expérimentalement que les boues formées ont un taux de matière organique supérieur à celui de la phase liquide tout comme la concentration en AGV. L'agitation risque ainsi de déstabiliser la digestion anaérobie. Ainsi l'intégration des phénomènes de

sédimentation permettra de rendre compte de l'impact de l'agitation sur les boues accumulées au fond des digesteurs. Ces simulations pourraient aussi nous renseigner sur la fréquence et l'intensité de l'agitation à employer pour améliorer la digestion anaérobie.

Sur le plan opérationnel, nous pourrions effectuer une étude similaire avec des chargements organiques plus importants. En effet, nous nous questionnons sur la stabilité du pilote pour des chargements organiques supérieurs. Pour cela, il serait nécessaire d'augmenter la capacité de stockage du substrat. Nous nous sommes concentrés sur un mode d'agitation. Dans des travaux ultérieurs, étudier des agitations continues et intermittentes ou encore la recirculation. Nous proposons d'automatiser la mise en route et l'arrêt de l'agitation du pilote, mais aussi l'alimentation du pilote avec une pompe. Il sera envisagé de comparer les rendements.

Les expérimentations ont été menées sur la vinasse. Dans de futurs travaux, il serait intéressant d'étudier l'impact de l'agitation sur la digestion anaérobie des déchets solides. Une étude rhéologique des déchets choisis sera indispensable pour la modélisation précise des écoulements étant donné la pauvreté des données de littératures pour les déchets solides. En perspectives, nous souhaitons considérer des cas non-Newtoniens. L'objectif final est à terme de coupler le modèle CFD et à un modèle biochimique simplifié dans un premier temps, puis complet, afin de prendre en compte les effets de l'hydrodynamique sur le rendement de la digestion anaérobie de divers déchets dans un modèle unique afin d'optimiser le processus.

Le travail réalisé est une amorce vers le développement de modèles bio-physicochimiques avec la prise en compte des cinétiques de dégradation mais également l'impact de l'hydrodynamique afin d'améliorer les rendements et la stabilité de la digestion anaérobie. Toutefois, ce modèle mérite d'être complété pour une prise en compte des d'autres phénomènes et les résultats de simulations validés.

Références

1. Chuppa Tostain, G.: Traitement biologique de vinasses de distillerie en vue de la production de molécules d'intérêt et énergétiques, (2016)
2. Angelidaki, I., Alves, M., Bolzonella, D., Borzacconi, L., Campos, J.L., Guwy, A.J., Kalyuzhnyi, S., Jenicek, P., van Lier, J.B.: Defining the biomethane potential (BMP) of solid organic wastes and energy crops: a proposed protocol for batch assays. Water Science & Technology. 59, 927 (2009). https://doi.org/10.2166/wst.2009.040
3. Delfosse, P.: MICROBIOLOGIE DE LA DIGESTION ANAEROBIE. (2011)
4. Vavilin, V.A., Lokshina, L.Y., Flotats, X., Angelidaki, I.: Anaerobic digestion of solid material: Multidimensional modeling of continuous-flow reactor with non-uniform influent concentration distributions. Biotechnology and Bioengineering. 97, 354–366 (2007). https://doi.org/10.1002/bit.21239
5. Kaparaju, P., Buendia, I., Ellegaard, L., Angelidakia, I.: Effects of mixing on methane production during thermophilic anaerobic digestion of manure: Lab-scale and pilot-scale studies. Bioresource Technology. 99, 4919–4928 (2008). https://doi.org/10.1016/j.biortech.2007.09.015
6. Vavilin, V.A., Angelidaki, I.: Anaerobic degradation of solid material: Importance of initiation centers for methanogenesis, mixing intensity, and 2D distributed model. Biotechnology and Bioengineering. 89, 113–122 (2005). https://doi.org/10.1002/bit.20323
7. Sindall, R., Bridgeman, J., Carliell-Marquet, C.: Effect of mixing speed on lab-scale anaerobic digester biogas production. In: 13th world congress on anaerobic digestion (2013)
8. Van Hulle, S.W.H., Vesvikar, M., Poutiainen, H., Nopens, I.: Importance of scale and hydrodynamics for modeling anaerobic digester performance. Chemical Engineering Journal. 255, 71–77 (2014). https://doi.org/10.1016/j.cej.2014.06.041
9. Mohammadrezaei, R., Zareei, S., Behroozi- Khazaei, N.: Optimum mixing rate in biogas reactors: Energy balance calculations and computational fluid dynamics simulation. Energy. (2018). https://doi.org/10.1016/j.energy.2018.06.132
10. Zhai, X., Kariyama, I.D., Wu, B.: Investigation of the effect of intermittent minimal mixing intensity on methane production during anaerobic digestion of dairy manure. Computers and Electronics in Agriculture. 155, 121–129 (2018). https://doi.org/10.1016/j.compag.2018.10.002

11. Bollon, J.: Etude des mécanismes physiques et de leur influence sur la cinétique de méthanisation en voie sèche: essais expérimentaux et modélisation, http://www.theses.fr/2012ISAL0011, (2012)
12. Bollon, J.: Etude des mécanismes physiques et de leur influence sur la cinétique de méthanisation en voie sèche: essais expérimentaux et modélisation, http://www.theses.fr/2012ISAL0011, (2012)
13. Kerroum, D., Mossaab, B.-L., Hassen, M.A.: Production of biogas from sludge waste and organic fraction of municipal solid waste. INTECH Open Access Publisher (2012)
14. Zupančič, G.D., Grilc, V.: Anaerobic treatment and biogas production from organic waste. Management of Organic Waste. 1–28 (2012)
15. McHugh, S., Carton, M., Mahony, T., O'Flaherty, V.: Methanogenic population structure in a variety of anaerobic bioreactors. FEMS Microbiology Letters. 219, 297–304 (2003). https://doi.org/10.1016/S0378-1097(03)00055-7
16. Thiele, J.H.: Mixed-culture interactions in methanogenesis. (1991)
17. Hess, J.: Modélisation de la qualité du biogaz produit par un fermenteur méthanogène et stratégie de régulation en vue de sa valorisation. 229
18. Derbal, K.: DIGESTION ANAEROBIE DES DECHETS SOLIDES MELANGES AVEC LES BOUES DE STATION D'EPURATION, http://bu.umc.edu.dz/theses/ch-ind/DER5283.pdf, (2006)
19. Oles, J., Dichtl, N., Niehoff, H.: Full scale experience of two stage thermophilicimesophilic sludge digestion. Water Science and Technology. 36, 449–456 (1997)
20. Holliger, C., Alves, M., Andrade, D., Angelidaki, I., Astals, S., Baier, U., Bougrier, C., Buffiere, P., Carballa, M., de Wilde, V., Ebertseder, F., Fernandez, B., Ficara, E., Fotidis, I., Frigon, J.-C., de Laclos, H.F., Ghasimi, D.S.M., Hack, G., Hartel, M., Heerenklage, J., Horvath, I.S., Jenicek, P., Koch, K., Krautwald, J., Lizasoain, J., Liu, J., Mosberger, L., Nistor, M., Oechsner, H., Oliveira, J.V., Paterson, M., Pauss, A., Pommier, S., Porqueddu, I., Raposo, F., Ribeiro, T., Rusch Pfund, F., Stromberg, S., Torrijos, M., van Eekert, M., van Lier, J., Wedwitschka, H., Wierinck, I.: Towards a standardization of biomethane potential tests. Water Science and Technology. 74, 2515–2522 (2016). https://doi.org/10.2166/wst.2016.336
21. Buffière, P.: Les technologies de la méthanisation des résidus solides.pdf
22. Raposo, F., Fernández-Cegrí, V., De la Rubia, M.A., Borja, R., Béline, F., Cavinato, C., Demirer, G., Fernández, B., Fernández-Polanco, M., Frigon, J.C., Ganesh, R., Kaparaju, P., Koubova, J., Méndez, R., Menin, G., Peene, A., Scherer, P., Torrijos, M., Uellendahl, H., Wierinck, I., de Wilde, V.: Biochemical methane potential (BMP) of solid organic substrates: evaluation of anaerobic biodegradability using data from

an international interlaboratory study. Journal of Chemical Technology & Biotechnology. 86, 1088–1098 (2011). https://doi.org/10.1002/jctb.2622
23. Noguerol-Arias, J., Rodríguez-Abalde, A., Romero-Merino, E., Flotats, X.: Determination of Chemical Oxygen Demand in Heterogeneous Solid or Semisolid Samples Using a Novel Method Combining Solid Dilutions as a Preparation Step Followed by Optimized Closed Reflux and Colorimetric Measurement. Analytical Chemistry. 84, 5548–5555 (2012). https://doi.org/10.1021/ac3003566
24. Moletta, R.: Technologies du traitement des effluents par méthanisation. 20
25. Moletta, R.: Contrôle et conduite des digesteurs anaérobies. Revue des sciences de l'eau. 2, 265 (1989). https://doi.org/10.7202/705031ar
26. Yenigün, O., Demirel, B.: Ammonia inhibition in anaerobic digestion: A review. Process Biochemistry. 48, 901–911 (2013). https://doi.org/10.1016/j.procbio.2013.04.012
27. Chen, Y., Cheng, J.J., Creamer, K.S.: Inhibition of anaerobic digestion process: A review. Bioresource Technology. 99, 4044–4064 (2008). https://doi.org/10.1016/j.biortech.2007.01.057
28. Swanwick, J.D., Shurben, D.G., Jackson, S.: A survey of the performance of sewage sludge digesters in Great Britain. (1969)
29. Sterrit, R.M., Lester, J.N.: Interaction of heavy metals with bacteria. (1980)
30. Batstone, D.J., Keller, J., Angelidaki, I., Kalyuzhnyi, S.V., Pavlostathis, S.G., Rozzi, A., Sanders, W.T.M., Siegrist, H., Vavilin, V.A.: The IWA anaerobic digestion model no 1 (ADM1). Water Science and Technology. 45, 65–73 (2002)
31. Batstone, D.J., Puyol, D., Flores-Alsina, X., Rodríguez, J.: Mathematical modelling of anaerobic digestion processes: applications and future needs. Reviews in Environmental Science and Bio/Technology. 14, 595–613 (2015). https://doi.org/10.1007/s11157-015-9376-4
32. Flores Alsina, X., Solon, K., Kazadi-Mbamba, C., Tait, S., Gernaey, K.V., Jeppsson, U., Bastone, D.: Modelling phosphorus (P), sulphur (S) and iron (Fe) interactions during the simulation of anaerobic digestion processes.pdf. (2015)
33. Galera, S.: Modélisation thermique de la turbulence de proche paroi en régime hypersonique, (2005)
34. Hughes, W.F., Brighton, J.A.: Theory and problems of fluid dynamics. Shaum's outline (1999)
35. Hughes, W.F., Brighton, J.A.: Non-Newtonian fluids. In: Theory and problems of fluid dynamics (1999)
36. Zhou, H., Wen, Z.: Solid-State Anaerobic Digestion for Waste Management and Biogas Production. Presented at the , Berlin, Heidelberg (2019)

37. Koerich, D.M., Rosa, L.M.: Numerical evaluation of the low Reynolds turbulent flow behaviour in a bioreactor. International Journal of Simulation and Process Modelling. 11, 66–75 (2016)
38. Björn, A., Šafarič, L., Karlsson, A., Danielsson, Å., Ejlertsson, J., Svensson, B.H., Yekta, S.S.: Substrate and operational conditions as regulators of fluid properties in full-scale continuous stirred-tank biogas reactors – implications for rheology-driven power requirements. Water Science and Technology. 78, 814–826 (2018). https://doi.org/10.2166/wst.2018.352
39. Koerich, D.M., Rosa, L.M.: Optimization of bioreactor operating conditions using computational fluid dynamics techniques. The Canadian Journal of Chemical Engineering. 95, 199–204 (2017). https://doi.org/10.1002/cjce.22635
40. Ramos-Vaquerizo, F., Cruz-Salomón, A., Ríos-Valdovinos, E., Pola-Albores, F., Lagunas-Rivera, S.: Anaerobic Treatment of Vinasse from Sugarcane Ethanol Production in Expanded Granular Sludge Bed Bioreactor. Journal of Chemical Engineering and Process Technology. 9, 3 (2018)
41. CANTÚ-LOZANO, D., VELÁZQUEZ MACARIO, M.V., VALLEJO CANTÚ, N.A., MAURO, M.A., DEL BIANCHI, V.L., TELIS-ROMERO, J.: Rheological behaviour of vinasses from a mexican bioethanol factory. (2010)
42. López-Jiménez, P.A., Escudero-González, J., Montoya Martínez, T., Fajardo Montañana, V., Gualtieri, C.: Application of CFD methods to an anaerobic digester: The case of Ontinyent WWTP, Valencia, Spain. Journal of Water Process Engineering. 7, 131–140 (2015). https://doi.org/10.1016/j.jwpe.2015.05.006
43. Chacua, L.M., Ayala, G., Rojas, H., Agudelo, A.C.: Mathematical models for prediction of rheological parameters in vinasses derived from sugar cane. International Agrophysics. 30, (2016). https://doi.org/10.1515/intag-2015-0083
44. Yu, L., Ma, J., Frear, C., Zhao, Q., Dillon, R., Li, X., Chen, S.: Multiphase modeling of settling and suspension in anaerobic digester. Applied Energy. 111, 28–39 (2013). https://doi.org/10.1016/j.apenergy.2013.04.073
45. Terashima, M., Goel, R., Komatsu, K., Yasui, H., Takahashi, H., Li, Y., Noike, T.: CFD simulation of mixing in anaerobic digesters. Bioresource Technology. 100, 2228–2233 (2009). https://doi.org/10.1016/j.biortech.2008.07.069
46. Ratkovich, N., Horn, W., Helmus, F.P., Rosenberger, S., Naessens, W., Nopens, I., Bentzen, T.R.: Activated sludge rheology: A critical review on data collection and modelling. Water Research. 47, 463–482 (2013). https://doi.org/10.1016/j.watres.2012.11.021
47. Baudez, J.C., Slatter, P., Eshtiaghi, N.: The impact of temperature on the rheological behaviour of anaerobic digested sludge. Chemical Engineering Journal. 215–216, 182–187 (2013). https://doi.org/10.1016/j.cej.2012.10.099

48. Craig, K.J., Nieuwoudt, M.N., Niemand, L.J.: CFD simulation of anaerobic digester with variable sewage sludge rheology. Water Research. 47, 4485–4497 (2013). https://doi.org/10.1016/j.watres.2013.05.011
49. Baroutian, S., Eshtiaghi, N., Gapes, D.J.: Rheology of a primary and secondary sewage sludge mixture: Dependency on temperature and solid concentration. Bioresource Technology. 140, 227–233 (2013). https://doi.org/10.1016/j.biortech.2013.04.114
50. Dapelo, D., Bridgeman, J.: Euler-Lagrange Computational Fluid Dynamics simulation of a full-scale unconfined anaerobic digester for wastewater sludge treatment. Advances in Engineering Software. 117, 153–169 (2018). https://doi.org/10.1016/j.advengsoft.2017.08.009
51. Lotito, V., Lotito, A.M.: Rheological measurements on different types of sewage sludge for pumping design. Journal of Environmental Management. 137, 189–196 (2014). https://doi.org/10.1016/j.jenvman.2014.02.005
52. Jiang, J., Wu, J., Poncin, S., Li, H.Z.: Rheological characteristics of highly concentrated anaerobic digested sludge. Biochemical Engineering Journal. 86, 57–61 (2014). https://doi.org/10.1016/j.bej.2014.03.007
53. Dai, X., Gai, X., Dong, B.: Rheology evolution of sludge through high-solid anaerobic digestion. Bioresource Technology. 174, 6–10 (2014). https://doi.org/10.1016/j.biortech.2014.09.122
54. Kumar, S.: Biogas. InTech, Rijeka (2012)
55. Farno, E., Baudez, J.C., Parthasarathy, R., Eshtiaghi, N.: Rheological characterisation of thermally-treated anaerobic digested sludge: Impact of temperature and thermal history. Water Research. 56, 156–161 (2014). https://doi.org/10.1016/j.watres.2014.02.048
56. Farno, E., Baudez, J.C., Parthasarathy, R., Eshtiaghi, N.: Impact of temperature and duration of thermal treatment on different concentrations of anaerobic digested sludge: Kinetic similarity of organic matter solubilisation and sludge rheology. Chemical Engineering Journal. 273, 534–542 (2015). https://doi.org/10.1016/j.cej.2015.03.097
57. Hong, E., Yeneneh, A.M., Sen, T.K., Ang, H.M., Kayaalp, A., Kayaalp, M.: Rheological characteristics of mixture of raw primary and thickened excess activated sludge: impact of mixing ratio, solid concentration, temperature and sludge age. Desalination and Water Treatment. 1–12 (2015). https://doi.org/10.1080/19443994.2015.1115374
58. Seyssiecq, I., Karrabi, M., Roche, N.: In situ rheological characterisation of wastewater sludge: Comparison of stirred bioreactor and pipe flow configurations.

Chemical Engineering Journal. 259, 205–212 (2015). https://doi.org/10.1016/j.cej.2014.07.102
59. Cheng, Y., Li, H.: Rheological behavior of sewage sludge with high solid content. Water Science and Technology. 71, 1686–1693 (2015). https://doi.org/10.2166/wst.2015.152
60. Eshtiaghi, N., Markis, F., Zain, D., Mai, K.H.: Predicting the apparent viscosity and yield stress of digested and secondary sludge mixtures. Water Research. 95, 159–164 (2016). https://doi.org/10.1016/j.watres.2016.03.002
61. Feng, X., Tang, B., Bin, L., Song, H., Huang, S., Fu, F., Ding, J., Chen, C., Yu, C.: Rheological behavior of the sludge in a long-running anaerobic digestor: Essential factors to optimize the operation. Biochemical Engineering Journal. 114, 147–154 (2016). https://doi.org/10.1016/j.bej.2016.06.022
62. Al-Dawery, S.: Effects of suspended solid and polyelectrolyte on settling and rheological properties of municipal activated sludge. Journal of Environmental Chemical Engineering. 4, 4731–4743 (2016). https://doi.org/10.1016/j.jece.2016.11.009
63. Zhang, J., Haward, S.J., Wu, Z., Dai, X., Tao, W., Li, Z.: Evolution of rheological characteristics of high-solid municipal sludge during anaerobic digestion. Appl Rheol. 26, 32973 (2016)
64. Cao, X., Jiang, Z., Cui, W., Wang, Y., Yang, P.: Rheological Properties of Municipal Sewage Sludge: Dependency on Solid Concentration and Temperature. Procedia Environmental Sciences. 31, 113–121 (2016). https://doi.org/10.1016/j.proenv.2016.02.016
65. Markis, F., Baudez, J.-C., Parthasarathy, R., Slatter, P., Eshtiaghi, N.: Predicting the apparent viscosity and yield stress of mixtures of primary, secondary and anaerobically digested sewage sludge: Simulating anaerobic digesters. Water Research. 100, 568–579 (2016). https://doi.org/10.1016/j.watres.2016.05.045
66. Markis, F., Baudez, J.-C., Parthasarathy, R., Slatter, P., Eshtiaghi, N.: Rheological characterisation of primary and secondary sludge: Impact of solids concentration. Chemical Engineering Journal. 253, 526–537 (2014). https://doi.org/10.1016/j.cej.2014.05.085
67. Hong, E., Yeneneh, A.M., Sen, T.K., Ang, H.M., Kayaalp, A.: The relationship between physico-chemical and rheological characteristics of digested sludge, biosolid, centrate and the effects on dewatering performance (A case study). Journal of Water Process Engineering. 19, 193–204 (2017). https://doi.org/10.1016/j.jwpe.2017.07.022
68. Hii, K., Parthasarathy, R., Baroutian, S., Gapes, D.J., Eshtiaghi, N.: Rheological measurements as a tool for monitoring the performance of high pressure and high

temperature treatment of sewage sludge. Water Research. 114, 254–263 (2017). https://doi.org/10.1016/j.watres.2017.02.031
69. Liang, F., Sauceau, M., Dusserre, G., Arlabosse, P.: A uniaxial cyclic compression method for characterizing the rheological and textural behaviors of mechanically dewatered sewage sludge. Water Research. 113, 171–180 (2017). https://doi.org/10.1016/j.watres.2017.02.008
70. Abbà, A., Collivignarelli, M.C., Manenti, S., Pedrazzani, R., Todeschini, S., Bertanza, G.: Rheology and Microbiology of Sludge from a Thermophilic Aerobic Membrane Reactor. Journal of Chemistry. 2017, 1–19 (2017). https://doi.org/10.1155/2017/8764510
71. Bobade, V., Baudez, J.C., Evans, G., Eshtiaghi, N.: Impact of gas injection on the apparent viscosity and viscoelastic property of waste activated sewage sludge. Water Research. 114, 296–307 (2017). https://doi.org/10.1016/j.watres.2017.02.039
72. Bobade, V., Evans, G., Baudez, J.C., Eshtiaghi, N.: Impact of gas injection on physicochemical properties of waste activated sludge: A linear relationship between the change of viscoelastic properties and the change of other physiochemical properties. Water Research. 144, 246–253 (2018). https://doi.org/10.1016/j.watres.2018.07.041
73. Gienau, T., Kraume, M., Rosenberger, S.: Rheological Characterization of Anaerobic Sludge from Agricultural and Bio-Waste Biogas Plants. Chemie Ingenieur Technik. 90, 988–997 (2018). https://doi.org/10.1002/cite.201700102
74. Cao, X., Jiang, K., Wang, X., Xu, G.: Effect of total suspended solids and various treatment on rheological characteristics of municipal sludge. Research on Chemical Intermediates. 44, 5123–5138 (2018). https://doi.org/10.1007/s11164-018-3413-1
75. Achkari-Begdouri, A., Goodrich, P.R.: Rheological properties of Moroccan dairy cattle manure. Bioresource Technology. 40, 149–156 (1992)
76. Wu, B.: Advances in the use of CFD to characterize, design and optimize bioenergy systems. Computers and Electronics in Agriculture. 93, 195–208 (2013). https://doi.org/10.1016/j.compag.2012.05.008
77. Wu, B.: Large eddy simulation of mechanical mixing in anaerobic digesters. Biotechnology and Bioengineering. 109, 804–812 (2012). https://doi.org/10.1002/bit.24345
78. Landry, H., Laguë, C., Roberge, M.: Physical and rheological properties of manure products. Applied Engineering in Agriculture. 20, 277 (2004)
79. Wu, B., Chen, S.: CFD simulation of non-Newtonian fluid flow in anaerobic digesters. Biotechnology and Bioengineering. 99, 700–711 (2007). https://doi.org/10.1002/bit.21613

80. Bakker, C.W., Meyer, C.J., Deglon, D.A.: Numerical modelling of non-Newtonian slurry in a mechanical flotation cell. Minerals Engineering. 22, 944–950 (2009). https://doi.org/10.1016/j.mineng.2009.03.016
81. Thota Radhakrishnan, A.K., van Lier, J.B., Clemens, F.H.L.R.: Rheological characterisation of concentrated domestic slurry. Water Research. (2018). https://doi.org/10.1016/j.watres.2018.04.064
82. Wu, B.: CFD simulation of mixing in egg-shaped anaerobic digesters. Water Research. 44, 1507–1519 (2010). https://doi.org/10.1016/j.watres.2009.10.040
83. Yu, L., Ma, J., Chen, S.: Numerical simulation of mechanical mixing in high solid anaerobic digester. Bioresource Technology. 102, 1012–1018 (2011). https://doi.org/10.1016/j.biortech.2010.09.079
84. Elmashad, H., Vanloon, W., Zeeman, G., Bot, G.: Rheological properties of dairy cattle manure. Bioresource Technology. 96, 531–535 (2005). https://doi.org/10.1016/j.biortech.2004.06.020
85. Diamante, L., Umemoto, M.: Rheological Properties of Fruits and Vegetables: A Review. International Journal of Food Properties. 18, 1191–1210 (2015). https://doi.org/10.1080/10942912.2014.898653
86. Tonon, R.V., Alexandre, D., Hubinger, M.D., Cunha, R.L.: Steady and dynamic shear rheological properties of açai pulp (Euterpe oleraceae Mart.). Journal of Food Engineering. 92, 425–431 (2009). https://doi.org/10.1016/j.jfoodeng.2008.12.014
87. Antonio, G.C., Faria, F.R., Takeiti, C.Y., Park, K.J.: Rheological behavior of blueberry. Food Science and Technology. 29, 732–737 (2009)
88. Haminiuk, C.W.I., Sierakwoski, M.-R., Izidor, D.R., Maciel, G.M., Scheer, A. de P., Masson, M.L.: Rheological characterization of blackberry pulp. Ciência e Tecnologia de Alimentos. 29, (2009)
89. Sharoba, A.M., Ramadan, M.F.: rheological behavior and physicochemical characteristics of goldenberry (physalis peruviana) juice as affected by enzymatic treatment: rheological behavior of goldenberry juice. Journal of Food Processing and Preservation. 35, 201–219 (2011). https://doi.org/10.1111/j.1745-4549.2009.00471.x
90. Maceiras, R., Álvarez, E., Cancela, M.A.: Rheological properties of fruit purees: Effect of cooking. Journal of Food Engineering. 80, 763–769 (2007). https://doi.org/10.1016/j.jfoodeng.2006.06.028
91. Ahmed, J., Ramaswamy, H.S.: Dynamic and steady shear rheology of fruit puree based baby foods. JOURNAL OF FOOD SCIENCE AND TECHNOLOGY-MYSORE-. 44, 579 (2007)
92. Juszczak, L., Fortuna, T.: Effect of temperature and soluble solids content on the viscosity of cherry juice concentrate. International Agrophysics. 18, 17–22 (2004)

93. Bhattacharya, S., Rastogi, N.K.: Rheological properties of enzyme-treated mango pulp. Journal of food engineering. 36, 249–262 (1998)
94. Ahmed, J., Ramaswamy, H.S., Hiremath, N.: The effect of high pressure treatment on rheological characteristics and colour of mango pulp. International Journal of Food Science and Technology. 40, 885–895 (2005). https://doi.org/10.1111/j.1365-2621.2005.01026.x
95. Augusto, P.E.D., Cristianini, M., Ibarz, A.: Effect of temperature on dynamic and steady-state shear rheological properties of siriguela (Spondias purpurea L.) pulp. Journal of Food Engineering. 108, 283–289 (2012). https://doi.org/10.1016/j.jfoodeng.2011.08.015
96. Ibarz, A., Garvin, A., Costa, J.: Rheological behaviour of sloe (Prunus spinosa) fruit juices. Journal of Food Engineering. 27, 423–430 (1996)
97. Pereira, E.A., Brandão, E.M., Borges, S.V., Maia, M.C.: Influence of concentration on the steady and oscillatory shear behavior of umbu pulp. Revista Brasileira de Engenharia Agrícola e Ambiental. 12, 87–90 (2008)
98. Rudra, S.G., Sarkar, B.C., Shivhare, U.S., Basu, S.: Rheological properties of coriander and mint leaf puree, (2007)
99. Ahmed, J., Ramaswamy, H.S., Sashidhar, K.C.: Rheological characteristics of tamarind (Tamarindus indica L.) juice concentrates. LWT - Food Science and Technology. 40, 225–231 (2007). https://doi.org/10.1016/j.lwt.2005.11.002
100. Augusto, P.E.D., Ibarz, A., Cristianini, M.: Effect of high pressure homogenization (HPH) on the rheological properties of tomato juice: Time-dependent and steady-state shear. Journal of Food Engineering. 111, 570–579 (2012). https://doi.org/10.1016/j.jfoodeng.2012.03.015
101. da Mota, R.V., Lajolo, F.M., Cordenunsi, B.R., Ciacco, C.: Composition and functional properties of banana flour from different varieties. Starch-Stärke. 52, 63–68 (2000)
102. Chin, N.L., Chan, S.M., Yusof, Y.A., Chuah, T.G., Talib, R.A.: Modelling of rheological behaviour of pummelo juice concentrates using master-curve. Journal of Food Engineering. 93, 134–140 (2009). https://doi.org/10.1016/j.jfoodeng.2009.01.005
103. Falguera, V., Vélez-Ruiz, J.F., Alins, V., Ibarz, A.: Rheological behaviour of concentrated mandarin juice at low temperatures: Rheological behaviour of mandarin juice. International Journal of Food Science & Technology. 45, 2194–2200 (2010). https://doi.org/10.1111/j.1365-2621.2010.02392.x
104. Ditchfield, C., Tadini, C.C., Singh, R., Toledo, R.T.: Rheological Properties of Banana Puree at High Temperatures. International Journal of Food Properties. 7, 571–584 (2004). https://doi.org/10.1081/JFP-200032973

105. Corrêa, R.C.G., Haminiuk, C.W.I., Sora, G.T.S., Bergamasco, R., Vieira, A.M.S.: Antioxidant and rheological properties of guava jam with added concentrated grape juice: Characterization of guava jam with added grape juice. Journal of the Science of Food and Agriculture. 94, 146–152 (2014). https://doi.org/10.1002/jsfa.6233
106. Işıklı, N.D., Karababa, E.: Rheological characterization of fenugreek paste (çemen). Journal of Food Engineering. 69, 185–190 (2005). https://doi.org/10.1016/j.jfoodeng.2004.08.013
107. Koocheki, A., Ghandi, A., Razavi, S.M.A., Mortazavi, S.A., Vasiljevic, T.: The rheological properties of ketchup as a function of different hydrocolloids and temperature. International Journal of Food Science & Technology. 44, 596–602 (2009). https://doi.org/10.1111/j.1365-2621.2008.01868.x
108. Shamsudin, R., Ling, C.S., Adzahan, N.M., Daud, W.R.W.: Rheological properties of ultraviolet-irradiated and thermally pasteurized Yankee pineapple juice. Journal of Food Engineering. 116, 548–553 (2013). https://doi.org/10.1016/j.jfoodeng.2012.12.031
109. Vandresen, S., Quadri, M.G.N., Souza, J.A.R. de, Hotza, D.: Temperature effect on the rheological behavior of carrot juices. Journal of Food Engineering. 92, 269–274 (2009). https://doi.org/10.1016/j.jfoodeng.2008.11.010
110. VITALI, A.A., Rao, M.A.: Flow behavior of guava puree as a function of temperature and concentration. Journal of Texture Studies. 13, 275–289 (1982)
111. Baroutian, S., Munir, M.T., Sun, J., Eshtiaghi, N., Young, B.R.: Rheological characterisation of biologically treated and non-treated putrescible food waste. Waste Management. 71, 494–501 (2017). https://doi.org/10.1016/j.wasman.2017.10.003
112. Lyberatos, G., Skiadas, I.V.: Modelling of anaerobic digestion–a review. Global Nest Int J. 1, 63–76 (1999)
113. Hill, D.T., Barth, C.L.: A Dynamic Model for Simulation of Animal Waste Digestion. Water Environment Federation. 49, 2129–2143 (1977)
114. Andrews, J.F., Graef, S.P.: Dynamic Modeling and Simulation of the Anaerobic Digestion Process. In: Pohland, F.G. (ed.) Anaerobic Biological Treatment Processes. pp. 126–162. AMERICAN CHEMICAL SOCIETY, WASHINGTON, D. C. (1971)
115. Graef, S.P., Andrews, J.F.: Stability and Control of Anaerobic Digestion. Journal (Water Pollution Control Federation). 46, 666–683 (1974)
116. Hill, D.T.: A Comprehensive Dynamic Model for Animal Waste Methanogenesis. Transactions of the ASAF. 25, 1374–2143 (1982)
117. Kleinstreuer, C., Poweigha, T.: Dynamic simulator for anaerobic digestion processes. Biotechnology and Bioengineering. 24, 1941–1951 (1982)

118. Bryers, J.D.: Structured modeling of the anaerobic digestion of biomass particulates. Biotechnol. Bioeng. 27, 638–649 (1985). https://doi.org/10.1002/bit.260270514
119. Moletta, R., Verrier, D., Albagnac, G.: DYNAMIC MODELLING OF ANAEROBIC DIGESTION. Water Research. 20, 427–434 (1986)
120. Mosey, F.E.: Mathematical modelling of the anaerobic digestion process: regulatory mechanisms for the formation of short-chain volatile acids from glucose. Water Science and Technology. 15, 209–232 (1983)
121. Costello, D.J., Greenfield, P.F., Lee, P.L.: Dynamic modelling of a single-stage high-rate anaerobic reactor—I. Model derivation. Water Research. 25, 847–858 (1991). https://doi.org/10.1016/0043-1354(91)90166-N
122. Angelidaki, I., Ellegaard, L., Ahring, B.K. er: A mathematical model for dynamic simulation of anaerobic digestion of complex substrates: focusing on ammonia inhibition. Biotechnology and bioengineering. 42, 159–166 (1993)
123. Siegrist, H., Renggli, D., Gujer, W.: Mathematical Modelling of Anaerobic Mesophilic Sewage Sludge Treatment. Water Science and Technology. 27, 25–36 (1993). https://doi.org/10.2166/wst.1993.0070
124. Keshtkar, A., Meyssami, B., Abolhamd, G., Ghaforian, H., Asadi, M.K.: Mathematical modeling of non-ideal mixing continuous flow reactors for anaerobic digestion of cattle manure. Bioresource Technology. 87, 113–124 (2003)
125. Wu, B., Bibeau, E.L., Gebremedhin, K.G.: Three-dimensional numerical simulation model of biogas production for anaerobic digesters. In: 2006 ASAE Annual Meeting. p. 1. American Society of Agricultural and Biological Engineers (2006)
126. Lübken, M., Wichern, M., Schlattmann, M., Gronauer, A., Horn, H.: Modelling the energy balance of an anaerobic digester fed with cattle manure and renewable energy crops. Water Research. 41, 4085–4096 (2007). https://doi.org/10.1016/j.watres.2007.05.061
127. Yasui, H., Goel, R., Li, Y.Y., Noike, T.: Modified ADM1 structure for modelling municipal primary sludge hydrolysis. Water Research. 42, 249–259 (2008). https://doi.org/10.1016/j.watres.2007.07.004
128. Contois, D.E.: Kinetics of Bacterial Growth: Relationship between Population Density and Specific Growth Rate of Continuous Cultures. Journal of General Microbiology. 21, 40–50 (1959). https://doi.org/10.1099/00221287-21-1-40
129. Ramirez, I., Mottet, A., Carrère, H., Déléris, S., Vedrenne, F., Steyer, J.-P.: Modified ADM1 disintegration/hydrolysis structures for modeling batch thermophilic anaerobic digestion of thermally pretreated waste activated sludge. Water Research. 43, 3479–3492 (2009). https://doi.org/10.1016/j.watres.2009.05.023

130. Fezzani, B., Ben Cheikh, R.: Extension of the anaerobic digestion model No. 1 (ADM1) to include phenol compounds biodegradation processes for simulating the anaerobic co-digestion of olive mill wastes at mesophilic temperature. Journal of Hazardous Materials. 172, 1430–1438 (2009). https://doi.org/10.1016/j.jhazmat.2009.08.017
131. Galí, A., Benabdallah, T., Astals, S., Mata-Alvarez, J.: Modified version of ADM1 model for agro-waste application. Bioresource Technology. 100, 2783–2790 (2009). https://doi.org/10.1016/j.biortech.2008.12.052
132. Astals, S., Ariso, M., Galí, A., Mata-Alvarez, J.: Co-digestion of pig manure and glycerine: Experimental and modelling study. Journal of Environmental Management. 92, 1091–1096 (2011). https://doi.org/10.1016/j.jenvman.2010.11.014
133. Soda, S.: Application of modified ADM1 to long-term experiments for methane/hydrogen production from model organic waste. Water Practice & Technology. 6, 1–1 (2011). https://doi.org/10.2166/WPT.2011.009
134. Antonopoulou, G., Gavala, H.N., Skiadas, I.V., Lyberatos, G.: Modeling of fermentative hydrogen production from sweet sorghum extract based on modified ADM1. International Journal of Hydrogen Energy. 37, 191–208 (2012). https://doi.org/10.1016/j.ijhydene.2011.09.081
135. Abbassi-Guendouz, A., Brockmann, D., Trably, E., Dumas, C., Delgenès, J.-P., Steyer, J.-P., Escudié, R.: Total solids content drives high solid anaerobic digestion via mass transfer limitation. Bioresource Technology. 111, 55–61 (2012). https://doi.org/10.1016/j.biortech.2012.01.174
136. Mottet, A., Ramirez, I., Carrère, H., Déléris, S., Vedrenne, F., Jimenez, J., Steyer, J.P.: New fractionation for a better bioaccessibility description of particulate organic matter in a modified ADM1 model. Chemical Engineering Journal. 228, 871–881 (2013). https://doi.org/10.1016/j.cej.2013.05.082
137. Hinken, L., Huber, M., Weichgrebe, D., Rosenwinkel, K.-H.: Modified ADM1 for modelling an UASB reactor laboratory plant treating starch wastewater and synthetic substrate load tests. Water Research. 64, 82–93 (2014). https://doi.org/10.1016/j.watres.2014.06.044
138. Barrera, E.L., Spanjers, H., Solon, K., Amerlinck, Y., Nopens, I., Dewulf, J.: Modeling the anaerobic digestion of cane-molasses vinasse: Extension of the Anaerobic Digestion Model No. 1 (ADM1) with sulfate reduction for a very high strength and sulfate rich wastewater. Water Research. 71, 42–54 (2015). https://doi.org/10.1016/j.watres.2014.12.026
139. Bai, J., Liu, H., Yin, B., Ma, H.: Modeling of enhanced VFAs production from waste activated sludge by modified ADM1 with improved particle swarm

optimization for parameters estimation. Biochemical Engineering Journal. 103, 22–31 (2015). https://doi.org/10.1016/j.bej.2015.06.015

140. Xie, S., Hai, F.I., Zhan, X., Guo, W., Ngo, H.H., Price, W.E., Nghiem, L.D.: Anaerobic co-digestion: A critical review of mathematical modelling for performance optimization. Bioresource Technology. 222, 498–512 (2016). https://doi.org/10.1016/j.biortech.2016.10.015
141. Bai, J., Liu, H., Yin, B., Ma, H., Chen, X.: Modified ADM1 for modeling free ammonia inhibition in anaerobic acidogenic fermentation with high-solid sludge. Journal of Environmental Sciences. 52, 58–65 (2017)
142. Wu, B.: CFD analysis of mechanical mixing in anaerobic digesters. Transactions of the ASABE. 52, 1371–1382 (2009)
143. Wu, B.: CFD simulation of gas and non-Newtonian fluid two-phase flow in anaerobic digesters. Water Research. 44, 3861–3874 (2010). https://doi.org/10.1016/j.watres.2010.04.043
144. Trad, Z., Vial, C., Fontaine, J.-P., Larroche, C.: Modeling of hydrodynamics and mixing in a submerged membrane bioreactor. Chemical Engineering Journal. 282, 77–90 (2015). https://doi.org/10.1016/j.cej.2015.04.119
145. Dapelo, D., Alberini, F., Bridgeman, J.: Euler-Lagrange CFD modelling of unconfined gas mixing in anaerobic digestion. Water Research. 85, 497–511 (2015). https://doi.org/10.1016/j.watres.2015.08.042
146. Meister, M., Rezavand, M., Ebner, C., Pümpel, T., Rauch, W.: Mixing non-Newtonian flows in anaerobic digesters by impellers and pumped recirculation. Advances in Engineering Software. 115, 194–203 (2018). https://doi.org/10.1016/j.advengsoft.2017.09.015
147. Fan, W., Yuan, L., Qu, X.: CFD simulation of hydrodynamic behaviors and aerobic sludge granulation in a stirred tank with lower ratio of height to diameter. Biochemical Engineering Journal. 137, 78–94 (2018). https://doi.org/10.1016/j.bej.2018.05.012
148. Jahoda, M., Moštěk, M., Kukuková, A., Machoň, V.: CFD Modelling of Liquid Homogenization in Stirred Tanks with One and Two Impellers Using Large Eddy Simulation. Chemical Engineering Research and Design. 85, 616–625 (2007). https://doi.org/10.1205/cherd06183
149. Meroney, R.N., Colorado, P.E.: CFD simulation of mechanical draft tube mixing in anaerobic digester tanks. Water Research. 43, 1040–1050 (2009). https://doi.org/10.1016/j.watres.2008.11.035
150. Wu, B.: CFD investigation of turbulence models for mechanical agitation of non-Newtonian fluids in anaerobic digesters. Water Research. 45, 2082–2094 (2011). https://doi.org/10.1016/j.watres.2010.12.020

151. Wu, B.: Computational Fluid Dynamics Study of Large-Scale Mixing Systems with Side-Entering Impellers. Engineering Applications of Computational Fluid Mechanics. 6, 123–133 (2012). https://doi.org/10.1080/19942060.2012.11015408
152. Wu, B.: CFD simulation of gas mixing in anaerobic digesters. Computers and Electronics in Agriculture. 109, 278–286 (2014). https://doi.org/10.1016/j.compag.2014.10.007
153. Mohammadrezaei, R., Zareei, S., Behroozi-Khazaei, N.: Improving the performance of mechanical stirring in biogas plant by computational fluid dynamics (CFD), (2017)
154. Zhang, J., Chen, X., Liu, J., Huang, B., Xu, M.: Structural characteristics of a spiral symmetry stream anaerobic bioreactor based on CFD. Biochemical Engineering Journal. 137, 50–61 (2018). https://doi.org/10.1016/j.bej.2018.05.016
155. Wiedemann, L., Conti, F., Saidi, A., Sonnleitner, M., Goldbrunner, M.: Modeling Mixing in Anaerobic Digesters with Computational Fluid Dynamics Validated by Experiments. Chemical Engineering & Technology. 41, 2101–2110 (2018). https://doi.org/10.1002/ceat.201800083
156. Jian, M.I.N., Zhengming, G.A.O.: Large eddy simulations of mixing time in a stirred tank. Chinese Journal of Chemical Engineering. 14, 1–7 (2006)
157. Zadghaffari, R., Moghaddas, J.S., Revstedt, J.: A mixing study in a double-Rushton stirred tank. Computers & Chemical Engineering. 33, 1240–1246 (2009). https://doi.org/10.1016/j.compchemeng.2009.01.017
158. Bridgeman, J.: Computational fluid dynamics modelling of sewage sludge mixing in an anaerobic digester. Advances in Engineering Software. 44, 54–62 (2012). https://doi.org/10.1016/j.advengsoft.2011.05.037
159. Wang, F., Zhang, C., Huo, S.: Influence of fluid dynamics on anaerobic digestion of food waste for biogas production. Environmental Technology. 38, 1160–1168 (2017). https://doi.org/10.1080/09593330.2016.1220429
160. Rasool, A.A.A., Ahmad, S., Hamad, F.A.: effect of impeller rotational speed on flow behavior in fully baffled mixing tank. International Journal of Advanced Research. 5, 1566–1576 (2017). https://doi.org/10.21474/IJAR01/3665
161. Mishra, P., Ein-Mozaffari, F.: Using computational fluid dynamics to analyze the performance of the Maxblend impeller in solid-liquid mixing operations. International Journal of Multiphase Flow. 91, 194–207 (2017). https://doi.org/10.1016/j.ijmultiphaseflow.2017.01.009
162. Cheng, D., Wang, S., Yang, C., Mao, Z.-S.: Numerical Simulation of Turbulent Flow and Mixing in Gas–Liquid–Liquid Stirred Tanks, (2017)
163. Lebranchu, A., Delaunay, S., Marchal, P., Blanchard, F., Pacaud, S., Fick, M., Olmos, E.: Impact of shear stress and impeller design on the production of biogas in

anaerobic digesters. Bioresource Technology. 245, 1139–1147 (2017). https://doi.org/10.1016/j.biortech.2017.07.113

164. Xinxin, L., Yadong, C., Zhenfeng, H., Jingfu, L., Gang, C., Rui, P.: Study on Side-entering Agitator Flow Field Simulation in Large Scale Biogas Digester. MATEC Web of Conferences. 153, 05003 (2018). https://doi.org/10.1051/matecconf/201815305003
165. Rasouli, M., Mousavi, S.M., Azargoshasb, H., Jamialahmadi, O., Ajabshirchi, Y.: CFD simulation of fluid flow in a novel prototype radial mixed plug-flow reactor. Journal of Industrial and Engineering Chemistry. 64, 124–133 (2018). https://doi.org/10.1016/j.jiec.2018.03.008
166. Xie, L., Wang, Q.-A., Luo, X.-J., Luo, Z.-H.: CFD Simulation of the Particle Dispersion Behavior and Mass Transfer–Reaction Kinetics in non-Newton Fluid with High Viscosity. International Journal of Chemical Reactor Engineering. 0, (2019). https://doi.org/10.1515/ijcre-2018-0293
167. Vesvikar, M.S., Al-Dahhan, M.: Flow pattern visualization in a mimic anaerobic digester using CFD. Biotechnology and Bioengineering. 89, 719–732 (2005). https://doi.org/10.1002/bit.20388
168. Wei, P., Mudde, R.F., Uijttewaal, W., Spanjers, H., van Lier, J.B., de Kreuk, M.: Characterising the two-phase flow and mixing performance in a gas-mixed anaerobic digester: Importance for scaled-up applications. Water Research. 149, 86–97 (2019). https://doi.org/10.1016/j.watres.2018.10.077
169. Leonzio, G.: Study of mixing systems and geometric configurations for anaerobic digesters using CFD analysis. Renewable Energy. 123, 578–589 (2018). https://doi.org/10.1016/j.renene.2018.02.071
170. Sajjadi, B., Raman, A.A.A., Parthasarathy, R.: Fluid dynamic analysis of non-Newtonian flow behavior of municipal sludge simulant in anaerobic digesters using submerged, recirculating jets. Chemical Engineering Journal. 298, 259–270 (2016). https://doi.org/10.1016/j.cej.2016.03.069
171. Wu, B.: Computational Fluid Dynamics Investigation of Turbulence Models for Non-Newtonian Fluid Flow in Anaerobic Digesters. Environmental Science & Technology. 44, 8989–8995 (2010). https://doi.org/10.1021/es1010016
172. Karim, K., Thoma, G.J., Al-Dahhan, M.H.: Gas-lift digester configuration effects on mixing effectiveness. Water Research. 41, 3051–3060 (2007). https://doi.org/10.1016/j.watres.2007.03.042
173. Foukrach, M., Bouzit, M., Ameur, H., Kamla, Y.: Influence of the vessel shape on the performance of a mechanically agitated system. Chemical Papers. 73, 469–480 (2019). https://doi.org/10.1007/s11696-018-0606-4

174. Vesvikar, M.S., Al-Dahhan, M.: Effect of Scale on Hydrodynamics of Internal Gas-Lift Loop Reactor-Type Anaerobic Digester Using CFD. Chemical Product and Process Modeling. 10, (2015). https://doi.org/10.1515/cppm-2015-0009
175. Mendoza, A.M., Martínez, T.M., Montañana, V.F., Jiménez, P.A.L.: Modeling flow inside an anaerobic digester by CFD techniques. In: International Journal of Energy and Environment. pp. 963–974. International Energy and Environment Foundation (2011)
176. Zhang, Y., Yu, G., Yu, L., Siddhu, M.A.H., Gao, M., Abdeltawab, A.A., Al-Deyab, S.S., Chen, X.: Computational fluid dynamics study on mixing mode and power consumption in anaerobic mono- and co-digestion. Bioresource Technology. 203, 166–172 (2016). https://doi.org/10.1016/j.biortech.2015.12.023
177. Wu, B.: CFD prediction of mixing time in anaerobic digesters. Transactions of the ASABE. 53, 553–563 (2010)
178. Alcamo, R., Micale, G., Grisafi, F., Brucato, A., Ciofalo, M.: Large-eddy simulation of turbulent flow in an unbaffled stirred tank driven by a Rushton turbine. Chemical Engineering Science. 60, 2303–2316 (2005). https://doi.org/10.1016/j.ces.2004.11.017
179. Zadghaffari, R., Moghaddas, J.S., Revstedt, J.: Large-eddy simulation of turbulent flow in a stirred tank driven by a Rushton turbine. Computers & Fluids. 39, 1183–1190 (2010). https://doi.org/10.1016/j.compfluid.2010.03.001
180. Coughtrie, A.R., Borman, D.J., Sleigh, P.A.: Effects of turbulence modelling on prediction of flow characteristics in a bench-scale anaerobic gas-lift digester. Bioresource Technology. 138, 297–306 (2013). https://doi.org/10.1016/j.biortech.2013.03.162
181. Madhania, S., Cahyani, A.B., Nurtono, T., Muharam, Y., Winardi, S., Purwanto, W.W.: CFD study of mixing miscible liquid with high viscosity difference in a stirred tank. IOP Conference Series: Materials Science and Engineering. 316, 012014 (2018). https://doi.org/10.1088/1757-899X/316/1/012014
182. Ryma, A., Dhaouadi, H., Mhiri, H., Bournot, P.: CFD Study of the Fluid Viscosity Variation and Effect on the Flow in a StirredTank. World Academy of Science, Engineering and Technology, International Journal of Mechanical, Aerospace, Industrial, Mechatronic and Manufacturing Engineering. 7, 470–478 (2013)
183. Zhang, Y., Yu, G., Siddhu, M.A.H., Masroor, A., Ali, M.F., Abdeltawab, A.A., Chen, X.: Effect of impeller on sinking and floating behavior of suspending particle materials in stirred tank: A computational fluid dynamics and factorial design study. Advanced Powder Technology. 28, 1159–1169 (2017). https://doi.org/10.1016/j.apt.2017.02.002

184. Okiyama, D.C.G., Rabi, J.A., Ribeiro, R., Ferraz, A.D.N., Zaiat, M.: CFD Simulations of Fluid Dynamics Inside a Fixed-Bed Bioreactor for Sugarcane Vinasse Treatment. In: Mannina, G. (ed.) Frontiers in Wastewater Treatment and Modelling. pp. 684–690. Springer International Publishing, Cham (2017)
185. Cortada-Garcia, M., Dore, V., Mazzei, L., Angeli, P.: Experimental and CFD studies of power consumption in the agitation of highly viscous shear thinning fluids. Chemical Engineering Research and Design. 119, 171–182 (2017). https://doi.org/10.1016/j.cherd.2017.01.018
186. Ri, P.-C., Ren, N.-Q., Ding, J., Kim, J.-S., Guo, W.-Q.: CFD optimization of horizontal continuous stirred-tank (HCSTR) reactor for bio-hydrogen production. International Journal of Hydrogen Energy. 42, 9630–9640 (2017). https://doi.org/10.1016/j.ijhydene.2017.02.035
187. Hartmann, H., Derksen, J.J., Montavon, C., Pearson, J., Hamill, I.S., van den Akker, H.E.A.: Assessment of large eddy and RANS stirred tank simulations by means of LDA. Chemical Engineering Science. 59, 2419–2432 (2004). https://doi.org/10.1016/j.ces.2004.01.065
188. Wu, B.: Integration of mixing, heat transfer, and biochemical reaction kinetics in anaerobic methane fermentation. Biotechnology and Bioengineering. 109, 2864–2874 (2012). https://doi.org/10.1002/bit.24551
189. Karpinska, A.M., Bridgeman, J.: CFD-aided modelling of activated sludge systems – A critical review. Water Research. 88, 861–879 (2016). https://doi.org/10.1016/j.watres.2015.11.008
190. Gebremedhin, K.G., Wu, B., Gooch, C., Wright, P.: Simulation of heat transfer for biogas production. In: 2004 ASAE Annual Meeting. p. 1. American Society of Agricultural and Biological Engineers (2004)
191. Gomez, J., de Gracia, M., Ayesa, E., Garcia-Heras, J.L.: Mathematical modelling of autothermal thermophilic aerobic digesters. Water Research. 41, 959–968 (2007). https://doi.org/10.1016/j.watres.2006.11.042
192. Perrigault, T., Weatherford, V., Martí-Herrero, J., Poggio, D.: Towards thermal design optimization of tubular digesters in cold climates: A heat transfer model. Bioresource Technology. 124, 259–268 (2012). https://doi.org/10.1016/j.biortech.2012.08.019
193. Merlin, G., Kohler, F., Bouvier, M., Lissolo, T., Boileau, H.: Importance of heat transfer in an anaerobic digestion plant in a continental climate context. Bioresource Technology. 124, 59–67 (2012). https://doi.org/10.1016/j.biortech.2012.08.018
194. Terradas-Ill, G., Pham, C.H., Triolo, J.M., Martí-Herrero, J., Sommer, S.G.: Thermic Model to Predict Biogas Production in Unheated Fixed-Dome Digesters

Buried in the Ground. Environmental Science & Technology. 48, 3253–3262 (2014). https://doi.org/10.1021/es403215w
195. Hreiz, R., Adouani, N., Jannot, Y., Pons, M.-N.: Modeling and simulation of heat transfer phenomena in a semi-buried anaerobic digester. Chemical Engineering Research and Design. 119, 101–116 (2017). https://doi.org/10.1016/j.cherd.2017.01.007
196. Singh, T.S., Verma, T.N., Nashine, P.: Analysis of an Anaerobic Digester using Numerical and Experimental Method for Biogas Production, (2017)
197. Lindmark, J., Thorin, E., Bel Fdhila, R., Dahlquist, E.: Effects of mixing on the result of anaerobic digestion: Review. Renewable and Sustainable Energy Reviews. 40, 1030–1047 (2014). https://doi.org/10.1016/j.rser.2014.07.182
198. Holliger, C., Alves, M., Andrade, D., Angelidaki, I., Astals, S., Baier, U., Bougrier, C., Buffiere, P., Carballa, M., de Wilde, V., Ebertseder, F., Fernandez, B., Ficara, E., Fotidis, I., Frigon, J.-C., de Laclos, H.F., Ghasimi, D.S.M., Hack, G., Hartel, M., Heerenklage, J., Horvath, I.S., Jenicek, P., Koch, K., Krautwald, J., Lizasoain, J., Liu, J., Mosberger, L., Nistor, M., Oechsner, H., Oliveira, J.V., Paterson, M., Pauss, A., Pommier, S., Porqueddu, I., Raposo, F., Ribeiro, T., Rusch Pfund, F., Stromberg, S., Torrijos, M., van Eekert, M., van Lier, J., Wedwitschka, H., Wierinck, I.: Towards a standardization of biomethane potential tests. Water Science and Technology. 74, 2515–2522 (2016). https://doi.org/10.2166/wst.2016.336
199. Alzate, M.E., Muñoz, R., Rogalla, F., Fdz-Polanco, F., Pérez-Elvira, S.I.: Biochemical methane potential of microalgae: Influence of substrate to inoculum ratio, biomass concentration and pretreatment. Bioresource Technology. 123, 488–494 (2012). https://doi.org/10.1016/j.biortech.2012.06.113
200. Raposo, F., Banks, C.J., Siegert, I., Heaven, S., Borja, R.: Influence of inoculum to substrate ratio on the biochemical methane potential of maize in batch tests. Process Biochemistry. 41, 1444–1450 (2006). https://doi.org/10.1016/j.procbio.2006.01.012
201. Zhou, Y., Zhang, Z., Nakamoto, T., Li, Y., Yang, Y., Utsumi, M., Sugiura, N.: Influence of substrate-to-inoculum ratio on the batch anaerobic digestion of bean curd refuse-okara under mesophilic conditions. Biomass and Bioenergy. 35, 3251–3256 (2011). https://doi.org/10.1016/j.biombioe.2011.04.002
202. Yoon, Y.-M., Kim, S.-H., Shin, K.-S., Kim, C.-H.: Effects of Substrate to Inoculum Ratio on the Biochemical Methane Potential of Piggery Slaughterhouse Wastes. Asian-Australasian Journal of Animal Sciences. 27, 600–607 (2014). https://doi.org/10.5713/ajas.2013.13537

203. Kim, H.-W., Han, S.-K., Shin, H.-S.: The optimisation of food waste addition as a co-substrate in anaerobic digestion of sewage sludge. Waste management & research. 21, 515–526 (2003)
204. Yadvika, Santosh, Sreekrishnan, T.R., Kohli, S., Rana, V.: Enhancement of biogas production from solid substrates using different techniques—a review. Bioresource Technology. 95, 1–10 (2004). https://doi.org/10.1016/j.biortech.2004.02.010
205. Moraes, B.S., Triolo, J.M., Lecona, V.P., Zaiat, M., Sommer, S.G.: Biogas production within the bioethanol production chain: Use of co-substrates for anaerobic digestion of sugar beet vinasse. Bioresource Technology. 190, 227–234 (2015). https://doi.org/10.1016/j.biortech.2015.04.089
206. Llabres-Luengo, P., Mata-Alvarez, J.: Kinetic study of the anaerobic digestion straw-pig manure mixtures. Biomass 14. 129–142 (1987)
207. Lay, J.-J., Li, Y.-Y., Noike, T.: Influences of pH and moisture content on the methane production in high-solids sludge digestion. Water Research. 31, 1518–1524 (1997)
208. López González, L.M., Pereda Reyes, I., Romero Romero, O.: Anaerobic co-digestion of sugarcane press mud with vinasse on methane yield. Waste Management. 68, 139–145 (2017). https://doi.org/10.1016/j.wasman.2017.07.016
209. Peixoto, G., Pantoja-Filho, J.L.R., Agnelli, J.A.B., Barboza, M., Zaiat, M.: Hydrogen and Methane Production, Energy Recovery, and Organic Matter Removal from Effluents in a Two-Stage Fermentative Process. Applied Biochemistry and Biotechnology. 168, 651–671 (2012). https://doi.org/10.1007/s12010-012-9807-4
210. Siles, J.A., García-García, I., Martín, A., Martín, M.A.: Integrated ozonation and biomethanization treatments of vinasse derived from ethanol manufacturing. Journal of Hazardous Materials. 188, 247–253 (2011). https://doi.org/10.1016/j.jhazmat.2011.01.096
211. Henze, M., Loosdrecht, M.C.M. van, Ekama, G.A., Brdjanovic, D. eds: Biological wastewater treatment: principles, modelling and design. IWA Publishing, London (2008)
212. Bastide, G.: Fiche technique-méthanisation. Service Prévention et Gestion des Déchets Direction Consommation Durable et Déchets. ADEME Angers, (2015)
213. Farinet, J.-L.: La méthanisation à la Réunion. Compte rendu de mission du 15 au 23 septembre 2010: perspectives et enjeux de recherche. Appui technique au programme PILMO. (2010)
214. Chowdhury, Z.Z., Hamid, S.B.A.: Preparation and Characterization of Nanocrystalline Cellulose using Ultrasonication Combined with a Microwave-assisted Pretreatment Process. BioResources. 11, 3397–3415 (2016). https://doi.org/10.15376/biores.11.2.3397-3415

215. Chowdhury, Z.Z., Chandran, R.R.R., Jahan, A., Khalid, K., Rahman, M.M., Al-Amin, M., Akbarzadeh, O., Badruddin, I.A., Khan, T.M.Y., Kamangar, S., Hamizi, N.A.B., Wahab, Y.A., Johan, R.B., Adebisi, G.A.: Extraction of Cellulose Nano-Whiskers Using Ionic Liquid-Assisted Ultra-Sonication: Optimization and Mathematical Modelling Using Box–Behnken Design. Symmetry. 11, 1148 (2019). https://doi.org/10.3390/sym11091148
216. Abd Hamid, S.B., Chowdhury, Z.Z., Karim, Md.Z., Ali, Md.E.: Catalytic Isolation and Physicochemical Properties of Nanocrystalline Cellulose (NCC) using HCl-FeCl3 System Combined with Ultrasonication. BioResources. 11, 3840–3855 (2016). https://doi.org/10.15376/biores.11.2.3840-3855
217. Cruz-Salomón, A., Ríos-Valdovinos, E., Pola-Albores, F., Meza-Gordillo, R., Lagunas-Rivera, S., Ruíz-Valdiviezo, V.M.: Anaerobic treatment of agro-industrial wastewaters for COD removal in expanded granular sludge bed bioreactor. Biofuel Research Journal. 4, 715–720 (2017). https://doi.org/10.18331/BRJ2017.4.4.3
218. Janke, L., Leite, A.F., Nikolausz, M., Radetski, C.M., Nelles, M., Stinner, W.: Comparison of start-up strategies and process performance during semi-continuous anaerobic digestion of sugarcane filter cake co-digested with bagasse. Waste Management. 48, 199–208 (2016). https://doi.org/10.1016/j.wasman.2015.11.007
219. Budiyono, Syaichurrozi, I., Sumardiono, S.: Effect of Total Solid Content to Biogas Production Rate from Vinasse. International Journal of Engineering. 27, (2014). https://doi.org/10.5829/idosi.ije.2014.27.02b.02
220. Barros, V.G. de, Duda, R.M., Oliveira, R.A. de: Biomethane production from vinasse in upflow anaerobic sludge blanket reactors inoculated with granular sludge. Brazilian Journal of Microbiology. 47, 628–639 (2016). https://doi.org/10.1016/j.bjm.2016.04.021
221. Caillet, H., Lebon, E., Akinlabi, E., Madyira, D., Adelard, L.: Influence of inoculum to substrate ratio on methane production in Biochemical Methane Potential (BMP) tests of sugarcane distillery waste water. Procedia Manufacturing. 35, 259–264 (2019). https://doi.org/10.1016/j.promfg.2019.05.037
222. Nielfa, A., Cano, R., Fdz-Polanco, M.: Theoretical methane production generated by the co-digestion of organic fraction municipal solid waste and biological sludge. Biotechnology Reports. 5, 14–21 (2015). https://doi.org/10.1016/j.btre.2014.10.005
223. Jiménez, A.M., Borja, R., Martín, A.: Aerobic–anaerobic biodegradation of beet molasses alcoholic fermentation wastewater. Process Biochemistry. 38, 1275–1284 (2003). https://doi.org/10.1016/S0032-9592(02)00325-4
224. Iqbal Syaichurrozi, B., Sumardiono, S.: Kinetic Model of Biogas Yield Production from Vinasse at Various Initial pH: Comparison between Modified Gompertz Model

and First Order Kinetic Model. Research Journal of Applied Sciences, Engineering and Technology. 7, 2798–2805 (2014). https://doi.org/10.19026/rjaset.7.602

225. Zhao, H.: Analysis of the performance of an anaerobic digestion system at the Regina wastewater treatment plant. Bioresource Technology. 95, 301–307 (2004). https://doi.org/10.1016/j.biortech.2004.02.023

226. Angelidaki, I., Ahring, B.K.: Anaerobic thermophilic digestion of manure at different ammonia loads: effect of temperature. Water Research. 28, 727–731 (1994)

227. Gosme, M.: Agro-épuration des vinasses de distillerie sur l'île de la Réunion, (2002)

228. Janke, L., Leite, A., Nikolausz, M., Schmidt, T., Liebetrau, J., Nelles, M., Stinner, W.: Biogas Production from Sugarcane Waste: Assessment on Kinetic Challenges for Process Designing. International Journal of Molecular Sciences. 16, 20685–20703 (2015). https://doi.org/10.3390/ijms160920685

229. Cabrera-Díaz, A., Pereda-Reyes, I., Oliva-Merencio, D., Lebrero, R., Zaiat, M.: Anaerobic Digestion of Sugarcane Vinasse Through a Methanogenic UASB Reactor Followed by a Packed Bed Reactor. Applied Biochemistry and Biotechnology. 183, 1127–1145 (2017). https://doi.org/10.1007/s12010-017-2488-2

230. Stroot, P.G., McMahon, K.D., Mackie, R.I., Raskin, L.: Anaerobic codigestion of municipal solid waste and biosolids under various mixing conditions—I. Digester performance. Water research. 35, 1804–1816 (2001)

231. Karim, K., Thomasklasson, K., Hoffmann, R., Drescher, S., Depaoli, D., Aldahhan, M.: Anaerobic digestion of animal waste: Effect of mixing. Bioresource Technology. 96, 1607–1612 (2005). https://doi.org/10.1016/j.biortech.2004.12.021

232. Nguyen, L.N., Johir, M.A.H., Commault, A., Bustamante, H., Aurisch, R., Lowrie, R., Nghiem, L.D.: Impacts of mixing on foaming, methane production, stratification and microbial community in full-scale anaerobic co-digestion process. Bioresource Technology. 281, 226–233 (2019). https://doi.org/10.1016/j.biortech.2019.02.077

233. Souza, M.E., Fuzaro, G., Polegato, A.R.: Thermophilic Anaerobic Digestion of Vinasse in Pilot Plant UASB Reactor. Water Science and Technology. 25, 213–222 (1992). https://doi.org/10.2166/wst.1992.0153

234. Lossie, U., Pütz, P.: Targeted control of biogas plants with the help of FOS/TAC. Practice Report Hach-Lange. (2008)

235. Hoffmann, R.A., Garcia, M.L., Veskivar, M., Karim, K., Al-Dahhan, M.H., Angenent, L.T.: Effect of shear on performance and microbial ecology of continuously stirred anaerobic digesters treating animal manure. Biotechnology and Bioengineering. 100, 38–48 (2008). https://doi.org/10.1002/bit.21730

236. Yuan, H., Zhu, N.: Progress in inhibition mechanisms and process control of intermediates and by-products in sewage sludge anaerobic digestion. Renewable and Sustainable Energy Reviews. 58, 429–438 (2016). https://doi.org/10.1016/j.rser.2015.12.261
237. Rozzi, A., Remigi, E.: Methods of assessing microbial activity and inhibition under anaerobic conditions: a literature review. Re/Views in Environmental Science & Bio/Technology. 3, 93–115 (2004)
238. Karim, K., Hoffmann, R., Klasson, T., Aldahhan, M.: Anaerobic digestion of animal waste: Waste strength versus impact of mixing. Bioresource Technology. 96, 1771–1781 (2005). https://doi.org/10.1016/j.biortech.2005.01.020
239. André, L., Pauss, A., Ribeiro, T.: Solid anaerobic digestion: State-of-art, scientific and technological hurdles. Bioresource Technology. 247, 1027–1037 (2018). https://doi.org/10.1016/j.biortech.2017.09.003
240. Bugay, S., Escudié, R., Liné, A.: Experimental analysis of hydrodynamics in axially agitated tank. AIChE journal. 48, 463–475 (2002)
241. Launder, B.E., Spalding, D.B.: The numerical computation of turbulent flows. 21
242. Platteeuw, P.D.A., Loeven, G.J.A., Bijl, H.: Uncertainty Quantification Applied to the k-epsilon Model of Turbulence Using the Probabilistic Collocation Method. In: 49th AIAA/ASME/ASCE/AHS/ASC Structures, Structural Dynamics, and Materials Conference
 16th AIAA/ASME/AHS Adaptive Structures Conference
 10t. American Institute of Aeronautics and Astronautics, Schaumburg, IL (2008)
243. Kuzmin, D., Mierka, O., Turek, S.: On the implementation of the k − ε turbulence model in incompressible flow solvers based on a finite element discretization. 8
244. Paul, E.L., Atiemo-Obeng, V.A., Kresta, S.M., American Institute of Chemical Engineers eds: Handbook of industrial mixing: science and practice. Wiley-Interscience, Hoboken, NJ (2004)
245. Marshall, E.M., Bakker, A.: Computational Fluid Mixing. In: Paul, E.L., Atiemo-Obeng, V.A., and Kresta, S.M. (eds.) Handbook of Industrial Mixing. pp. 257–343. John Wiley & Sons, Inc., Hoboken, NJ, USA (2003)
246. Spicer, P.T., Keller, W., Pratsinis, S.E.: The effect of impeller type on floc size and structure during shear-induced flocculation. Journal of Colloid and Interface Science. 184, 112–122 (1996)
247. Clark, M.M., Flora, J.R.: Floc restructuring in varied turbulent mixing. Journal of Colloid and Interface Science. 147, 407–421 (1991)
248. Alliet-Gaubert, M., Sardeing, R., Xuereb, C., Hobbes, P., Letellier, B., Swaels, P.: CFD analysis of industrial multi-staged stirred vessels. Chemical Engineering and Processing: Process Intensification. 45, 415–427 (2006)

249. Issa, R.I.: Solution of the implicitly discretised fluid flow equations by operator-splitting. Journal of computational physics. 62, 40–65 (1986)
250. Issa, R.I., Gosman, A.D., Watkins, A.P.: The computation of compressible and incompressible recirculating flows by a non-iterative implicit scheme. Journal of Computational Physics. 62, 66–82 (1986). https://doi.org/10.1016/0021-9991(86)90100-2
251. Patankar, S.V., Spalding, D.B.: A calculation procedure for heat, mass and momentum transfer in three-dimensional parabolic flows. In: Numerical Prediction of Flow, Heat Transfer, Turbulence and Combustion. pp. 54–73. Elsevier (1983)
252. Caretto, L.S., Gosman, A.D., Patankar, S.V., Spalding, D.B.: Two calculation procedures for steady, three-dimensional flows with recirculation. In: Proceedings of the third international conference on numerical methods in fluid mechanics. pp. 60–68. Springer (1973)

UNIVERSITÉ DE LA RÉUNION

Pôle Recherche
Ecoles doctorales

LETTRE D'ENGAGEMENT DE NON-PLAGIAT

Je, soussigné(e) Hélène Corinne Caillet en ma qualité de doctorant(e) de l'Université de La Réunion, déclare être conscient(e) que le plagiat est un acte délictueux passible de sanctions disciplinaires. Aussi, dans le respect de la propriété intellectuelle et du droit d'auteur, je m'engage à systématiquement citer mes sources, quelle qu'en soit la forme (textes, images, audiovisuel, internet), dans le cadre de la rédaction de ma thèse et de toute autre production scientifique, sachant que l'établissement est susceptible de soumettre le texte de ma thèse à un logiciel anti-plagiat.

Fait à Saint-Denis le : 29/11/2019

Signature :

Extrait du Règlement intérieur de l'Université de La Réunion
(validé par le Conseil d'Administration en date du 11 décembre 2014)

Article 9. Protection de la propriété intellectuelle – Faux et usage de faux, contrefaçon, plagiat

L'utilisation des ressources informatiques de l'Université implique le respect de ses droits de propriété intellectuelle ainsi que ceux de ses partenaires et plus généralement, de tous tiers titulaires de tes droits.
En conséquence, chaque utilisateur doit :
- utiliser les logiciels dans les conditions de licences souscrites ;
- ne pas reproduire, copier, diffuser, modifier ou utiliser des logiciels, bases de données, pages Web, textes, images, photographies ou autres créations protégées par le droit d'auteur ou un droit privatif, sans avoir obtenu préalablement l'autorisation des titulaires de ces droits.

La contrefaçon et le faux
Conformément aux dispositions du code de la propriété intellectuelle, toute représentation ou reproduction intégrale ou partielle d'une œuvre de l'esprit faite ans le consentement de son auteur est illicite et constitue un délit pénal.
L'article 444-1 du code pénal dispose : « Constitue un faux toute altération frauduleuse de la vérité, de nature à cause un préjudice et accomplie par quelque moyen que ce soit, dans un écrit ou tout autre support d'expression de la pensée qui a pour objet ou qui peut avoir pour effet d'établir la preuve d'un droit ou d'un fait ayant des conséquences juridiques ».
L'article L335_3 du code de la propriété intellectuelle précise que : « Est également un délit de contrefaçon toute reproduction, représentation ou diffusion, par quelque moyen que ce soit, d'une œuvre de l'esprit en violation des droits de l'auteur, tels qu'ils sont définis et réglementés par la loi. Est également un délit de contrefaçon la violation de l'un des droits de l'auteur d'un logiciel (…) ».

Le plagiat est constitué par la copie, totale ou partielle d'un travail réalisé par autrui, lorsque la source empruntée n'est pas citée, quel que soit le moyen utilisé. Le plagiat constitue une violation du droit d'auteur (au sens des articles L 335-2 et L 335-3 du code de la propriété intellectuelle). Il peut être assimilé à un délit de contrefaçon. C'est aussi une faute disciplinaire, susceptible d'entraîner une sanction.
Les sources et les références utilisées dans le cadre des travaux (préparations, devoirs, mémoires, thèses, rapports de stage…) doivent être clairement citées. Des citations intégrales peuvent figurer dans les documents rendus, si elles sont assorties de leur référence (nom d'auteur, publication, date, éditeur…) et identifiées comme telles par des guillemets ou des italiques.

Les délits de contrefaçon, de plagiat et d'usage de faux peuvent donner lieu à une sanction disciplinaire indépendante de la mise en œuvre de poursuites pénales.